1999

AN ARTIFICIAL INTELLIGENCE APPROACH TO THE PROCESSING OF RADAR RETURN SIGNALS FOR TARGET DETECTION

Li, Vincent Yiu Fai

AN ARTIFICIAL INTELLIGENCE APPROACH TO THE PROCESSING OF RADAR RETURN SIGNALS FOR TARGET DETECTION

by

Vincent Yiu Fai Li

A thesis submitted to the University of Plymouth for the degree of

DOCTOR OF PHILOSOPHY

Institute of Marine Studies
University of Plymouth

December 1999

An Artificial Intelligence Approach to the Processing of Radar Return Signals For Target Detection

Vincent Yiu Fai Li

ABSTRACT

Most of the operating vessel traffic management systems experience problems, such as track loss and track swap, which may cause confusion to the traffic regulators and lead to potential hazards in the harbour operation. The reason is mainly due to the limited adaptive capabilities of the algorithms used in the detection process. The decision on whether a target is present is usually based on the magnitude of the returning echoes. Such a method has a low efficiency in discriminating between the target and clutter, especially when the signal to noise ratio is low. The performance of radar target detection depends on the features, which can be used to discriminate between clutter and targets. To have a significant improvement in the detection of weak targets, more obvious discriminating features must be identified and extracted.

This research investigates conventional Constant False Alarm Rate (CFAR) algorithms and introduces the approach of applying artificial intelligence methods to the target detection problems. Previous research has been undertaken to improve the detection capability of the radar system in the heavy clutter environment and many new CFAR algorithms, which are based on amplitude information only, have been developed. This research studies these algorithms and proposes that it is feasible to design and develop an advanced target detection system that is capable of discriminating targets from clutters by learning the different features extracted from radar returns.

The approach adopted for this further work into target detection was the use of neural networks. Results presented show that such a network is able to learn particular features of specific radar return signals, e.g. rain clutter, sea clutter, target, and to decide if a target is present in a finite window of data. The work includes a study of the characteristics of radar signals and identification of the features that can be used in the process of effective detection. The use of a general purpose marine radar has allowed the collection of live signals from the Plymouth harbour for analysis, training and validation. The approach of using data from the real environment has enabled the developed detection system to be exposed to real clutter conditions that cannot be obtained when using simulated data.

The performance of the neural network detection system is evaluated with further recorded data and the results obtained are compared with the conventional CFAR algorithms. It is shown that the neural system can learn the features of specific radar signals and provide a superior performance in detecting targets from clutters. Areas for further research and development are presented; these include the use of a sophisticated recording system, high speed processors and the potential for target classification.

CONTENTS

Contents **Page No.**

Contents i

List of figures v

List of tables xi

Acknowledgements xii

Declaration xiii

Chapter 1 Introduction

1.1 Preface 1

1.2 Introduction 2

1.3 Constant False Alarm Rate (CFAR) Algorithms 3

1.4 Intelligent Methods in Radar Detection 9

1.5 Specific Aims and Objective 14

1.6 Organisation of the Thesis 15

Chapter 2 Analysis of CFAR Detection Algorithms

2.1 Introduction 18

2.2 Description of the Theoretical Model 19

2.3 Analysis of Mean-Level CFAR Algorithms 23

2.3.1. Cell Averaging CFAR Processor 24

2.3.2. The Greatest Of and Smallest Of CFAR Algorithm 25

2.3.3. Ordered Statistics (OS) CFAR Algorithm 27

2.3.4. The Trimmed-Mean ™ CFAR Algorithm 30

2.4 Application of CFAR Algorithms 31

2.5 Conclusion 36

Chapter 3 Characteristic of radar signal and feature extraction

3.1 Introduction 39

3.2 Radar Cross Section 40

3.3 Statistical Characteristics 46

3.4 Correlation 53

3.5 Spectral Characteristics 56

3.6 Conclusion 60

Chapter 4 Data fusion techniques in radar signal processing

4.1 Introduction 66

4.2 Fuzzy approach to data fusion 67

4.2.1 Fuzzy set theory 67

4.2.2 Fuzzy algorithms for data fusion in radar signal processing 69

4.3 Data fusion in neural networks 73

4.3.1 Neural network theory 74

4.3.2 Neural networks for data fusion of radar signal 77

4.4 Conclusion 87

Chapter 5 The radar system and data acquisition

5.1 Introduction 90

5.2 The radar equipment 90

5.3 Parameters affecting the radar signal and maximum range 91

5.3.1. Beam width 91

5.3.2. Pulse repetition frequency 93

5.3.3. Transmission power 93

5.3.4. Receiver noise 97

5.4 Data acquisition system 98

5.4.1 Sampling rate 99

5.4.2 Resolution and range 100

5.5 Conclusion 100

Chapter 6 The integrated radar detection system

6.1 Introduction 102

6.2 System hardware 102

6.3 Selection of features to be extracted from radar signals 104

6.4 Methods of extracting statistical signal characteristics 108

6.5 Neural target detection 109

6.6 Conclusion 120

Chapter 7 Training, testing and verification of the radar detection system

7.1 Introduction 122

7.2 Features extracted from radar sweeps 122

7.3 Size of moving windows 128

7.4 Formulation of the neural detection system 128

7.4.1. Setting up the initial network 129

7.4.2. Application of the training algorithm 141

7.4.3. Testing the trained network 148

7.5 Investigation of applying the network to a trace of radar waveform 154

7.6 Investigation of parameters required for target classification 166

7.7 Conclusion 176

Chapter 8 Conclusion and further work

8.1 Introduction 178

8.2 Approach to the solution of problems in target detection 179

8.2.1 Drawback of commonly used detection algorithms 179

8.2.2 Extraction of features from radar signals 180

8.2.3 Data acquisition of radar signals 181

8.3 The application of neural networks to radar detection 182

8.4 Contribution of this study to radar detection system 184

8.5 Future developments 185

8.5.1 Additional inputs and outputs to the system 186

8.5.2 The use of sophisticated data recording system 186

8.5.3 Using high speed parallel processor 187

8.5.4 The implementation of alternative artificial intelligence methods... 188

8.5.5 The use of additional features in the classification of radar targets.. 189

8.6 Conclusion 190

References

Appendix A Published Papers

LIST OF FIGURES

Figure		Page No.
2.1	Block diagram of a typical CFAR processor	19
2.2	Mean-level CFAR processor	20
2.3	OS-CFAR processor	20
2.4	TM-CFAR processor	21
2.5	Plot of the sea target scenario for testing the CFAR algorithms	32
2.6	Sea target signal with CA-CFAR threshold	33
2.7	Sea target signal with GO-CFAR threshold	33
2.8	Sea target signal with SO-CFAR threshold	34
2.9	Sea target signal with OS-CFAR threshold	34
2.10	Sea target signal with TM-CFAR threshold, T1=40, T2=40	35
3.1a	Random noise of a typical radar return	62
3.1b	Statistical distribution of random noise	62
3.2a	Radar return of a marine vessel	62
3.2b	Statistical distribution of a radar target	62
3.3a	Sea clutter signal	62
3.3b	Statistical distribution of sea clutter signal	62
3.4a	Rain clutter in a radar return	63
3.4b	Statistical distribution of rain clutter	63
3.5a	A typical radar return with signal being embedded in noise	63
3.5b	The radar return after correlating with a square pulse	63

3.6a Return in N sweep 63

3.6b Radar return in N+1 sweep 63

3.6c Radar return in N+2 sweep 64

3.7a Correlation of N and N+1 sweeps 64

3.7b Correlation of N+1 and N+2 sweeps 64

3.8 Correlation of N/N+1 and N+1/N+2 sweeps 64

3.9 Frequency spectrum for a window with noise only 64

3.10 Frequency spectrum for a typical target 64

3.11 Frequency spectrum for a window with landclutter 65

3.12 Immediate frequency for a typical sweep 65

3.13 Immediate frequency for a typical sweep with noise only 65

4.1 Graphical representation of rule no.5 72

4.2 Determination of the output from a set of rules 72

4.3a A typical neural network architecture 78

4.3b A perceptron with two inputs 81

4.4 Classification of radar signals using perceptrons 81

4.5 A three layer back propagation network 85

5.1 Heading markers for 4 revolutions 92

5.2 Pulse repetition frequency for short pulse 94

5.3 Pulse repetition frequency for long pulse 94

5.4 Six sweeps of radar video for short pulse 95

5.5 Three sweeps of radar video for long pulse 95

6.1 Block diagram of the experimental set up 103

6.2 The time delay circuit for the heading marker 107

6.3 Waveform of a target in a 50 samples window 107

6.4a Waveform of target A in a 50 samples window 110

6.4b Waveform of target B in a 50 samples window 110

6.4c Waveform of target C in a 50 samples window 111

6.4d Waveform of target D in a 50 samples window 111

6.4e Waveform of target E in a 50 samples window 112

6.4f Waveform of target F in a 50 samples window 112

6.4g Waveform of target G in a 50 samples window 113

6.4h Waveform of target H in a 50 samples window 113

6.5a Waveform of noise A in a 50 samples window 114

6.5b Waveform of noise B in a 50 samples window 114

6.5c Waveform of noise C in a 50 samples window 115

6.5d Waveform of noise D in a 50 samples window 115

6.5e Waveform of noise E in a 50 samples window 116

6.5f Waveform of noise F in a 50 samples window 116

6.5g Waveform of noise B in a 50 samples window 117

6.5h Waveform of noise A in a 50 samples window 117

7.1 Distribution of mean amplitude 125

7.2 Distribution of amplitude deviation 125

7.3 Distribution of mean period 126

7.4 Distribution of period deviation 126

7.5 Distribution of maximum period 127

7.6 Spread of the five parameters 127

7.7a Large target with window size of 1.6 microseconds 131

7.7b Large target with window size of 2.0 microseconds 131

7.7c Large target with window size of 2.4 microseconds 131

7.7d Large target with window size of 2.8 microseconds 132

7.8 Spread with different window size (large target) 132

7.9a Small target with window size of 1.6 microseconds 133

7.9b Small target with window size of 2.0 microseconds 133

7.9c Small target with window size of 2.4 microseconds 133

7.9d Small target with window size of 2.8 microseconds 134

7.10 Spread with different window size (small target) 134

7.11a Performance of training with learning rate =0.001, SSE=3.7596 135

7.11b Performance of training with learning rate =0.005, SSE=3.7606 135

7.11c Performance of training with learning rate =0.01, SSE=3.7845 136

7.11d Performance of training with learning rate =0.05, SSE=3.6720 136

7.11e Performance of training with learning rate =0.1, SSE=3.7314 137

7.11f Performance of training with learning rate =0.3, SSE=3.7445 137

7.12a Performance of training with momentum=0.1, SSE=7.8479 138

7.12b Performance of training with momentum=0.5, SSE=4.97838 138

7.12c Performance of training with momentum=1, SSE=100 139

7.12d Performance of training with momentum=0.9, SSE=3.9437 139

7.12e Performance of training with momentum=0.98, SSE=4.5261 140

7.12f Performance of training with momentum=0.95, SSE=3.6789 140

7.13a Network with a single layer, SSE=4.009 143

7.13b Network with one neuron in hidden layer, SSE=4.0675..... 143

7.13c Network with two neurons in hidden layer, SSE=3.5629..... 144

7.13d Network with three neurons in hidden layer, SSE=4.4272 144

7.13e Network with 2 hidden layers, each with 2 neurons, SSE=4.4288 145

7.13f Network with 2 hidden layers, each with 1 neuron, SSE=4.0626 145

7.14a 2-layer backpropagation with adaptive LR & momentum,first 300,000runs 146

7.14b 2-layer backpropagation with adaptive LR & momentum, last 300,000runs 146

7.15 Distribution of trained data 147

7.16a Plot of test data 1, S/N=3.7db, output value=0.9986 149

7.16b Plot of test data 2, S/N=12.6db, output value=0.9964 149

7.16c Plot of test data 3, S/N=6.6db, output value=0.7732 150

7.16d Plot of test data 4, S/N=10db, output value=0.9745 150

7.17a Plot of test data 5 (noise), output value=0 151

7.17b Plot of test data 6 (noise), output value=0 151

7.17c Plot of test data 7 (noise), output value=0 152

7.17d Plot of test data 8 (noise), output value=0 152

7.18 Output values for target and noise 153

7.19 Distribution of S/N ratio 153

7.20a Trace of radar return with 100 samples 157

7.20b Output of the network for the trace in Fig.7.20a 157

7.20c Output of the detection system with a shift of one sample 158

7.20d Output of the detection system with an overlapping of 20 samples 158

7.20e A trace of radar return with 100 samples (large target) 159

7.20f Output of the detection system with an overlapping of 20 samples 159

7.21a A radar trace with 2000 samples 160

7.21b Output of the detection system 160

7.21c Sea target signal with TM-CFAR threshold, T1=40, T2=40 161

7.21d Signals accepted by TM-CFAR 161

7.22a Radar trace with rain clutters 162

7.22b Output of the detection system 162

7.22c Sea target signal with TM-CFAR threshold, T1=40, T2=40 163

7.22d Signals accepted by TM-CFAR 163

7.23a Radar trace with sea clutters 164

7.23b Output of the detection system 164

7.23c Sea target signal with TM-CFAR threshold, T1=40, T2=40 165

7.23d Signals accepted by TM-CFAR 165

7.24a Discrimination in mean amplitude 169

7.24b Discrimination in amplitude deviation 170

7.24c Discrimination in mean period..... 170

7.24d Discrimination in maximum period 171

7.24e Discrimination in period deviation 171

7.24f Discrimination in instant frequency 172

7.25a Radar return sequence of large target 173

7.25b Radar return sequence of small target 173

7.26 A three layer backpropagation network with fuzzifier 174

7.27a Membership function of amplitude deviation 175

7.27b Membership function of immediate frequency 175

LIST OF TABLES

Table		Page No.
2.1	Quality of CFAR algorithms	36
3.1	Typical RCS values for some common targets	42
3.2	Statistical data of target, sea clutter, rain clutter and noise	53
4.1	Membership matrix table	70
4.2	Testing sets for fuzzy network	73
4.3	Training sets for neural network	86
4.4	Testing sets for neural network	86
6.1	Statistical characteristics of target	118
6.1	Statistical characteristics of noise	118
7.1	Training errors of the network after 30,000 iterations	141
7.2	Variation of immediate frequency and amplitude deviation between 5 scans	168
7.3	Testing set for the neural network	169

ACKNOWLEDGEMENTS

I would like to thank the following people for their help and support during the preparation of this thesis:

- Dr. Keith Miller for acting as Director of Studies and providing continuous support and encouragement.
- Dr. Neil Witt and Dr. G. Zhu for acting as supervisors and their advice and assistance.
- The staff of Marine Technology Division and the Navigation and Hydrography Division at the University of Plymouth for their assistance and encouragement.
- The technical staff at the Institute of Marine Studies who always provided assistance to my practical work, and allowed me to use their workshop and equipment.
- My mother for her continual support and encouragement.
- My brother, Stephen, for his arrangement for me to undertake my research at the University of Plymouth.
- My wife, Wandy, who always gives me support and assistance during the course of my studies.

DECLARATION

No part of this thesis has been submitted for any award or degree at any institute.

While registered as a candidate for the degree of Doctor of Philosophy, the author has not been a registered candidate for another university.

Publications by the author, in connection with this research, are included at the end of the thesis in Appendix A.

The author was one of the project engineers to design, install and commission the Vessel Traffic Management System for the Hong Kong Government from 1987 to 1990.

The author has attended the International Radar Symposium in Munich, Germany from 15 September to 17 September 1998, and presented the paper "Radar Target Detection Using Feature Extraction".

Signed .....

Date 20.10.1999

CHAPTER 1

INTRODUCTION

1.1 Preface

Vessel traffic management systems extract data from the raster of the incoming radar signal. These data are further processed to generate target tracks that are then displayed for traffic control. In a dense harbour situation where vessels are usually manoeuvring in very close proximity to each other, targets may be swapped giving the controller a false impression of ships manoeuvres and their masters' intentions. Furthermore, reflections from land based objects such as buildings increase the level of interference to the received signals and provide further confusion to the tracking algorithms employed. When the weather is bad, clutter due to sea waves and fog will also affect the quality of the signals. All these restrictions limit the detection/tracking capability of the vessel traffic management system and hence the information provided to the operator. Any resulting target loss or swap that may occur will cause burden to the safety operation of managing traffic in the harbour. It was stated by Ming Po (1994) that statistics in 1993 showed there were over five thousand general type vessels and forty high speed ferries manoeuvuring at the same time in Hong Kong harbour. It is important that an efficient radar system with good detection capability is required to reduce the possibility of collision between these vessels in the area. As such, there is a need to review the radar signal processing techniques that are currently employed and possible alternatives with the objective of making the processing more adaptive to dynamic changes of the environment.

1.2 Introduction

Radar is an electronics device for the detection and location of objects. It operates by transmitting an electromagnetic wave at a given frequency, which may be up to several GHz, and detects the nature of the reflected signal from an object. Usually the echo is the result of the reflected wave when the objects are hit by the transmitted wave. The electromagnetic waves travel at the speed of light, nearly 3×10^8 meters per second, which is dependent on atmospheric conditions. The distance between the object and the radar can be calculated by measuring the time required between transmission of radar pulse and reception of the returning echo. Since the time includes both the transmission and the reception, the result will be divided by two. It transpires that a two way travel time of 1 microsecond corresponds to a distance of approximately 150 meters.

The initial step in radar signal processing can be regarded as the task of removing all the non-useful data. The returned radar information from the receiver must be reduced to a few signals that represent the known and new targets. The key operation to achieve this data reduction is the thresholding process, where the data sets acquired are compared with a reference level. Only those signals with magnitudes exceeding some threshold levels are processed further. However, the radar signal from a target is usually embedded in both thermal noise and clutter. The magnitude of the noise and clutter will vary in different sweeps, ranges and scans. To achieve a low false alarm rate and a high probability of detection, the setting of a threshold with constant amplitude is not feasible.

1.3 Constant False Alarm Rate (CFAR) Algorithms

The constant false alarm rate (CFAR) processing technique has been developed to adjust the threshold value according to the noise power of the return signal at specific times. The threshold of individual cells is decided based on the signal strength of a group of reference cells nearby. In the conventional cell averaging constant false alarm rate (CA-CFAR) detector (Barkat, 1989), digitized radar video is clocked through a moving window (delay line). For each range cell, which corresponds to a given range on some bearing, the mean video levels of the 'N' preceding cells and of the 'N' following cells are calculated. The threshold comparator calculates the average of these two mean levels, and the resulting threshold is compared with the radar signal. For those that are above the threshold level, they will be processed as a target for the following stages. Otherwise, they are treated as noise. The probability of detection of the CA-CFAR detector depends on the threshold multiplier (which is a function of the probability of false alarm), the signal to noise ratio and the number of range cells in the window (Steenson, 1968).

CA-CFAR provides optimum detection in a homogeneous environment where the noise power in the range cells is such that the observations are independent and identically distributed (Kassam, 1988). However, this assumption is frequently false due to the environment in which the radar system is operating. A reference window may contain cells with large sudden changes in the noise power due to some other phenomena providing a reflection that appears as clutter on the system. If the target is embedded in the test cell, this transition will unnecessarily increase the threshold to a high level and lower the detection probability. Yet, if the test cell contains the clutter, the threshold value is not high enough to reject the clutter because cells with

low noise level will have also contributed to the calculation of mean value. As a result, an excessive false alarm rate will occur. Also, when multiple targets are very close in range and appear in the same window, the noise associated with these targets may cause the threshold to increase. Such an effect will allow only the strongest target in the window to be detected.

In view of the above drawbacks of CA-CFAR, alternative solutions have been proposed to improve the effect of nonhomogeneous noise backgrounds to the CFAR detector. A 'greatest of' logic selection (GO-CFAR) was proposed by Hansen and Sawyers (1980) to reduce the number of excessive false alarms at clutter transitions. Two reference windows are formed in the leading and lagging sides of the test cell and a target is declared if the amplitude of the test cell exceeds the greater of the two windows. A slight reduction in detection probability may be expected when the leading window contains signals with low noise power while the lagging window contains clutter with large magnitude. However, the use of greatest selection will not allow the CFAR detector to efficiently detect closely spaced targets. Also, the detection probability will be greatly affected when interfering targets appear in the leading and lagging windows (Al-Hussaini, 1988 and Weiss, 1982).

It has been shown (Trunk, 1983) that the use of the 'smallest of' (SO-CFAR) selection method is able to resolve targets which are closely spaced in range. The smaller value of the leading or the lagging windows is used to estimate the noise power. Again, the performance of the SO-CFAR detector will be degraded if interfering targets are found in the leading and lagging windows. The SO-CFAR detector is not able to limit the false alarm rates during the clutter transitions. For

example, if there is a clutter transition in the window then the clear background will contribute to a low magnitude of estimated noise level. This will cause the threshold to go low and increase the false alarm rate.

Research has been performed to provide adaptive CFAR algorithms, which are able to handle radar detection in a non-homogeneous environment. Ordered statistics (OS) CFAR has been developed to reject transient noise (Rohling, 1983). In this algorithm, the range cells (c(1)...c(N)) in a window are first ordered according to their magnitudes to yield the ordered samples, i.e. $c(1) < c(2) < ....c(N)$, where N is the window size. The noise power is then estimated by selecting the magnitude of a cell with a specific order to work out the threshold. The performance of OS CFAR in clutter edges is good when the clutter returns have constant/slow varying amplitude characteristics. However, OS CFAR suffers serious degradation during the clutter power transitions.

Trimmed mean filtering has been used in signal and image restoration processes (Bovik, Huang, and Munson , 1983). The noise power of the trimmed mean CFAR (Wilson, 1993) is estimated by combining the ordered samples linearly. It firstly ranks the samples according to their magnitude and then filters T1 samples from the lower end and T2 samples from the higher end. The remaining samples are summed to work out the threshold. Optimization of such an algorithm is then a matter of fine tuning these parameters and is dependent on the amount of clutter and number of targets.

Rickard and Dillard (1971) proposed the censored mean level (CML) CFAR to deal

with interfering targets. The outputs from the range cells are ranked according to their magnitude and the largest n samples are censored. The remaining N-n samples are used to estimate the noise level (c) of the cell under test. This estimate (c) is multiplied by a threshold multiplier (M), which is based on the desired false alarm rate (Fa). If the magnitude of the strength of the signal return in a cell exceeds Mc then a target is assumed to be present. Ideally, if the samples to be censored are equal to the number of the interfering targets in the window, the performance of CML will be optimal. However, it will be degraded if the censorship does not include all the interfering targets. This may be the case when the number of interfering targets is unknown. Thus, if an interfering target is included in the process of noise estimation, the threshold will be unnecessarily high and lower the probability of detection. However, if the number of interfering targets is underestimated, this will cause the threshold to be low and increase the false alarm rate.

The generalized censored mean-level (GCML) CFAR does not require the exact knowledge of numbers of interfering targets (Rickard and Dillard, 1971). The samples of both the leading and the lagging windows are ordered independently. The returning signals in the cells, which are considered as interfering targets, will be censored. To decide whether the cell should be censored or not, the higher ordered samples are compared with the lower ones in sequence. A scaling multiplier (M), which is a function of the desired false alarm rate, will be introduced to the lower ordered samples. If c(k) is greater than Mc(k-1), then samples c(k) (k, k+1, ...N) are regarded as echoes from interfering targets and they will be censored. The noise estimate is processed based on the magnitude of the remaining samples. The performance of the GCML CFAR is optimum when the interfering targets appear in

both the leading and lagging window. The performance will be slightly degraded when the interfering targets fall in one of the windows only. The number of range cells in a window will also affect the performance, the higher the number the better the performance.

The greatest of order statistics estimator CFAR (GOOSE-CFAR) (Wilson, 1993) takes the nth ordered samples from both the leading and the lagging windows. It compares these two samples and takes the larger one to estimate the threshold. Since n is less than N/2 (the number of samples in each window), GOOSE-CFAR can handle interfering targets in both windows and such targets will normally appear in samples from n+1 to N/2. When a clutter boundary appears in the window, the worst case occurs when the cell under test is in the heavy clutter. With the larger of the two ordered samples being taken for threshold estimation, the threshold will be high enough to prevent excessive false alarms. GO-CFAR has demonstrated its good performance in clutter boundaries when interfering targets are not present. However, with GOOSE-CFAR, targets with magnitude larger than the nth sample in both windows will be filtered. This will prevent the masking of multiple targets in the window and improve the detection capability in the clutter boundary.

Censored greater-of (CGO) CFAR (Al-Hussaini, 1988) filters n largest range cell from both leading and the lagging windows. The remaining samples of each window are summed. A threshold multiplier to give the required threshold will multiply the larger of the two. The choice of numbers of cells to be censored depends on the likelihood of the number of interfering targets in the windows. When the number of interfering targets exceeds the number of samples to be censored, the performance of

CGO CFAR will be degraded. However, the detection loss of CGO CFAR will be less than the OS and GOOSE CFAR because CGO CFAR takes the mean of the magnitude of the interfering targets and the noise samples, while OS and GOOSE CFAR will use the ordered magnitude alone. Both GOOSE and CGO CFAR have the greatest-of logic which is able to reduce the sharp rise of false alarm rate at the clutter boundary.

MEMO CFAR (Al-Hussaini, 1988) combines both median and morphological filtering (Vassilis and Lampropoulos, 1992) to decide the threshold level. The first median filter transforms the input into a new series of samples in which those samples less than the mean power of the clutter will be replaced by this mean value. As such, it changes the smaller values of clutter to the estimate of the mean noise power. Also, any samples with a magnitude greater than a fixed multiple of the mean power will also be replaced by the mean value. The objective is to reduce the effect caused by interfering targets. The second median filter will be used to smooth out the samples from the first filter and gives an unbiased estimate of the original samples. The output from the second filter is then processed by a morphological filter that uses an open-closing technique (Jain, 1989; and Stevenson and Arce, 1987). 'Open' breaks small targets and smoothes boundary while 'close' fills up narrow gaps between targets. MEMO CFAR detectors have superior performance in the presence of interfering targets since it gives a mean estimate of noise power with minimum bias and smaller variance. It is able to overcome problems due to masking of targets by clutter boundaries. However, it requires much more computer execution time to process the samples than other CFAR detectors.

1.4 Intelligent Methods in Radar Detection

Fuzzy logic has become a valuable tool in practical engineering applications; it is capable of addressing the imprecise information from a physical system by applying rule-based algorithms that resemble the flexibility of human decision making. Successful applications of fuzzy logic in various fields have been reported (Kosko, 1992; and Li and Lau, 1989). Recently, fuzzy approach to signal detection has also been addressed (Russo, 1992; Son, Song and Kim, 1991, Boston, 1995). Radar detection has been using probability theory to correctly decide the presence of a target. A two state binary logic is usually used to define the state of the signal, i.e. a threshold is applied to the signal. A signal above the threshold level will be accepted as a target and others will be rejected. Since the targets in a radar return are not always clearly defined (e.g. embedded in clutter or noise), uncertainty can appear in every task of the detection stage. Any premature decision based on limited information made at an early task of the radar processing will have a large impact on the following stages, such as tracking and feature extraction. Processing techniques that use binary logic to quantify the input signal rely on threshold values and may provide false information. With the aid of fuzzy logic, radar detection will not be solely limited to the likelihood of detection/false alarm, it can also be expressed in degrees to which an event will happen. Instead of offering a combination on conditional probabilities, the membership functions used in fuzzy logic theory combines inexact information. The fuzzy associative memory function defines the degree of likelihood of the returned signal to be a target and its exact value is of no absolute importance. When the magnitude of the returned signal is increasing, it is more likely that the signal would be detected as a target and the false alarm rate will be reduced. Such a model provides an explicit feature to represent uncertainty in the

radar detection process.

In binary hypothesis testing, Bayes Theory (Zadeh, 1965) formulates the minimization of the expected cost, called the Bayes risk, and leads to the likelihood ratio test (LRT). Assuming that the *priori* probabilities of the two hypotheses H_1 and H_0 are 0.5, the test can be formulated as follows:-

$$LR = \exp\{0.5[R^2 - (R - X)^2]\} > 1 \quad (H_1)$$

$$LR = \exp\{0.5[R^2 - (R - X)^2]\} < 1 \quad (H_0)$$

where LR is the likelihood ratio

R is the observed data

X is a positive mean of the signal amplitude

To model the uncertainties of the received radar signals, the binary hypothesis testing can be reformulated using fuzzy set theory (Zadeh, 1965).

$H1 : R = X + N$

$H0 : R = N$

where N is the standardised Gaussian noise.

Now, X is a fuzzy parameter and $\mu_x(X)$ is the membership function of X. For convenience, a triangular membership function centered about a nominal amplitude value and extending between X_1 and X_2 is used, such that $\mu_x(X_0)=1$. The likelihood ratio (LR) becomes a fuzzy set. As shown by Saade (1990), the fuzzy threshold of the likelihood ratio can be determined from prior probabilities and cost functions, which are again fuzzy or uncertain in nature. The computation of the fuzzy decision on the optimum threshold of detection requires the ordering of the fuzzy sets over the real line to obtain the expression for the utility ranking index of LR, which has

been described by Saade (1992). The performance of the fuzzy algorithms is evaluated on the basis of the probability of error technique (Saade, 1994). It was shown that the fuzzy logic method provided a better result than binary logic in treating the false alarms and misses in decision making process for radar detection.

The detection of ship wake signatures against sea clutters have been adopted to reject false targets. It produces fuzzy decisions which associate with a confidence level for each entity based on suitable fuzzification functions (Benelli, Garzelli and Mecocci, 1994). To define a membership function for a fuzzy set of radar echoes for vessels, features that will not be critically affected by speckled noise, such as mean gray level and elongation, need to be selected. Ship classes are selected according to the area of the target, e.g. class 1 for area less than 60 pixels, class 2 for area less than 120 pixels and so on. Each potential ship echo is compared with prototypes of true ships and a weighting for distance applied. The classifier associates a true ship to a high fuzzy index (approx. 1) and a false ship to a low fuzzy index (less than 0.5). Information with respect to the ship/wake relation is processed to give a coupling coefficient that is a function of the distance between the centroid of the ship and its closest extreme of wake. This coefficient, between 0 and 1, defines the position of a ship with respect to its wake in the radar image. The coefficient will finally be multiplied by the fuzzy index from the classifier to give a global value that measures the reliability of the detected ship-wake couple. It was demonstrated by Benelli (1994) that this method presented advantages with respect to the classical method of wake detection using conventional signal processing techniques on noisy images.

The detection of amplitude transitions (edge detection) has been used as a means of classification for radar images. However, the decision on whether a point in the return is an edge or not possesses ambiguity. The fuzzy reasoning technique, as proposed by Cho (1994), detects the transition on intensity changes of the radar signal. Both the brightness and contrast measures of the pixel intensity are processed as fuzzy inputs. 'If' and 'Then' fuzzy rules are used to determine the threshold decision, which will be in the form of membership function. To defuzzify the threshold decision, the centroid of the calculated membership function is evaluated by summing the confidence level of the function multiplied by the individual measurement value. This technique extracts edge features effectively because various types of objects and regions have different gray level range within a single image which makes a global threshold method difficult to deal with.

In recent years, with the improvement of methods in signal processing, more attention has been paid to the waveform recognition of the radar returns as a detection technique. The amplitude information of radar videos will no longer be the only component for processing a threshold decision. Valuable information is contained in a radar return that can be processed to provide effective detection. These include symmetry/spread and width of waveform, correlation of special features, shape and gradient of waveform and so on. To extract features from ship radar returns, Guo (1989) proposed to use a ship target recognition algorithm using multiple transform techniques.

$$F(X) = F3(F2(F1(X))),$$

where F1 is the Fourier transformation or maximum entropy spectral transformation

F2 is the Mellin transformation

F3 is coding transformation and selection of the events

X is an one dimensional digitized waveform

To enable the transformation to be done effectively, a suitable width and shift for the calculation window should be selected for sampling. The width should be slightly larger than the radar pulse width and the shift should be smaller than half the radar pulse width. It was shown by Guo (1989) that most sea clutter spiky signals have narrower and sharper features than general weak targets. A threshold in the width will be able to remove obvious sea spikes.

Radar detection in a dynamic processing environment can be achieved by extracting and combining different features in a complex waveform system. However, an intelligent radar detection system should not only rely on the features themselves and the interrelationships between them, but also on the *a priori* information about the ship targets, such as speed and course of a ship, wind situation, distance of the ship from radar centre and so on. Rules that incorporate this information are stored in a database. This method of detection requires high-speed signal processing hardware to cater for the needs of target detection in real time and will be able to detect weak targets under strong sea clutter (Guo, 1992).

Neural networks have been used for pattern recognition in very noisy environments. Lippmann (1989) has shown an example of character recognition using a Hopfield network in which the input to the network is corrupted by noise and is unrecognizable. The capability of extracting desired patterns from noisy backgrounds makes neural networks suitable to be extended to the application of

detecting weak targets in heavy clutters. The use of feed-forward and graded-response Hopfield networks can implement the optimum post-detection target track receiver. Khotanzad (1989) developed a neural network for the detection of signals in underwater acoustic fields. The input to the network is the magnitude of the received signal and noise at different frequencies as time varies. The output is a multi-layer perceptron classifier trained using the back propagation algorithm, which decides the presence and absence of the target with high classification accuracy.

1.5 Specific Aims and Objective

Radar target detection in heavy clutter environments has been a challenging task. In undertaking this research, all the commonly used CFAR algorithms have been reviewed and analyzed. Most of the research in the field of radar detection concentrates on the development of advanced algorithms to decide on the threshold to be applied to the signals based on their amplitude information. To improve the detection probability and reduce the false alarm rates, this research will study the detailed characteristics of the radar waveforms and to identify features that can be used for differentiation between targets and clutters. The objective is to develop an intelligent detection system that can extract the essential features from the radar signals and detect targets in heavy clutter environment with the help of these extracted features.

All results provided in this thesis are based on the observations made by the author using the radar system in the University of Plymouth. The author designed and

developed all the necessary hardware and software to record the radar targets and clutter in the harbour.

1.6 Organization of the Thesis

The research is divided into three specific areas:

1.6.1 The review of different CFAR algorithms and their performances.

1.6.2 The construction of a set of tools, both hardware and software, for feature extraction and implementation of the intelligent detection system.

1.6.3 The training, testing and verification of the intelligent detection system.

The contents of the succeeding chapters of this thesis have been organized as follows:

Chapter 2: Analysis of CFAR detection algorithms

Five commonly used CFAR algorithms are analyzed, with their performance being tested with live radar videos. The chapter concludes that more obvious discriminating features must be identified and extracted in order to have significant improvement in the detection of weak targets.

Chapter 3: Characteristic of radar signals and feature extraction

This chapter studies the characteristics of radar signals, and identifies features and extraction algorithms to improve the detection capability. These features can then be fed into an information fusion process for making the final decision. The detection process is not based solely on the amplitude of the radar signals and provides a more reliable method for discrimination in target identification and tracking algorithms.

Chapter 4: Data fusion techniques in radar signal processing

Methods are identified to relate the extracted features to a final decision on whether a target is present. Both fuzzy and neural network approaches are discussed and compared. The chapter concludes that neural networks are more suitable in this application as large amounts of sample data from simulated/live signals can be obtained and used as training sets for the network.

Chapter 5: The radar system and data acquisition

The radar system and the effect of its characteristics in signal processing are discussed, followed by describing the development of the data acquisition system to match the characteristics of the radar waveforms.

Chapter 6: The integrated radar detection system

This chapter describes the implementation of a data acquisition system to record the radar video signal for analysis purposes. Features are extracted from windows of signals containing targets and clutter and the criteria for selecting these features is also discussed. The chapter then describes the training procedures of the neural network and the algorithms for the final detection system.

Chapter 7: Training, testing and verification of the radar detection system

The neural network based radar detection system is presented and samples from live radar video data are used in the training process. The subsequent sections in this chapter detail the construction, testing and verification of the detection systems. The trained system is verified by trials with test scenarios that have not been used in the

training. Comparison on the performances with CFAR algorithms is also discussed. The approach that is finally adopted is then extended by combining the techniques employed with fuzzy logic to classify targets into large and small vessels.

Chapter 8. Conclusion and further work

This final chapter presents the conclusions on the tasks described in the thesis and proposes further research in this area.

CHAPTER TWO

ANALYSIS OF CFAR DETECTION ALGORITHMS

2.1 Introduction

Various CFAR algorithms and their purposes have been briefly described in chapter one. In considering these CFAR detection schemes, there are two major problems that need careful studies. These are regions of clutter power transition and multiple target environments. The clutter power transition occurs when the total noise power received within single reference window changes sharply. Depending on whether the cell under test is a sample from a clutter background or from a clear background, the presence of this transition will severely degrade the performance of this adaptive threshold scheme. This leads to either excessive false alarms or serious target masking. The multiple target environments are encountered when there are two or more closely spaced targets in the same reference window. The interfering targets may raise the threshold unnecessarily. As a result, only the stronger targets are detected by the CFAR detector.

Modifications of the CFAR schemes have been proposed to overcome the problems associated with nonhomogeneous noise backgrounds. These algorithms split the reference window into leading and lagging parts symmetrically about the cell under test. The noise power is no longer estimated efficiently, and therefore, some loss of detection in the homogeneous reference window is experienced when compared with scheme using a non-splitting window. In this section, the basic assumptions that have been used to analyze the performance of the CA-CFAR processors are discussed. The exact expressions for the GO-CFAR and the SO-CFAR processor performance are derived for

both regions of clutter transitions and multiple target environments. Both the OS-CFAR and TM-CFAR processors are defined and analyzed. Simulation results of the false alarms are given in the region of Gaussian noise, rain clutter transitions and multi-target environment by using recorded signals from the radar at the University of Plymouth.

2.2 Description of the Theoretical Model

Figure 2.1 shows the block diagram of a typical CFAR processor. The detected video range samples are sent serially into a shift register of length 2n+1. The statistic Z is proportional to the estimate of the total noise power. It is evaluated by processing the contents of the reference cells surrounding the test cell whose value is Y. A target is declared to be present if Y exceeds the threshold TZ. T is a scaling factor to achieve the desired constant false alarm rate for a given window of size N. The processor configuration varies with different CFAR algorithms.

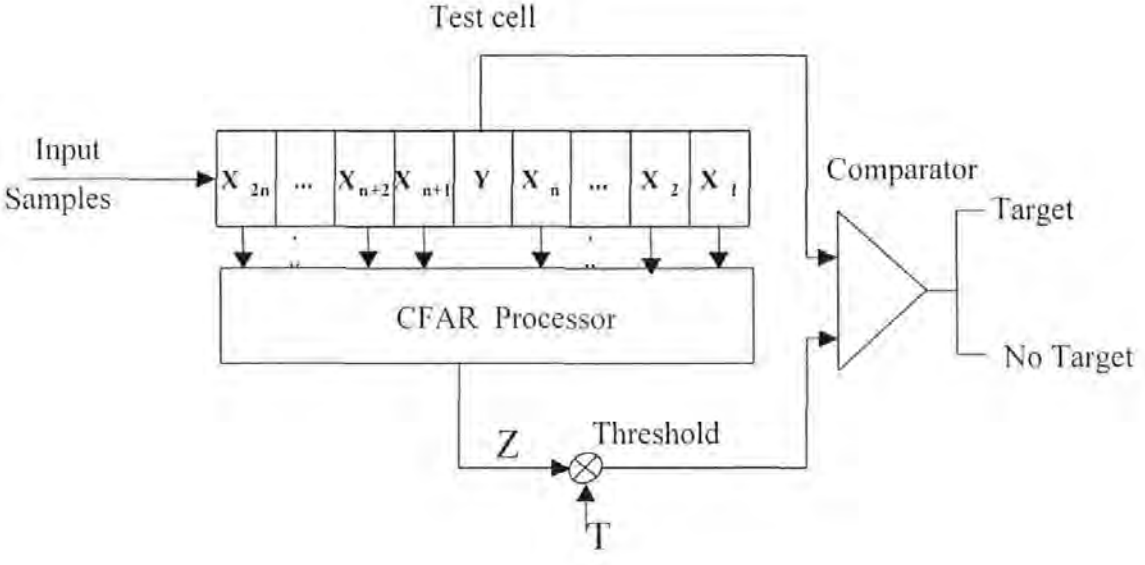

Fig. 2.1 Block diagram of a typical CFAR processor

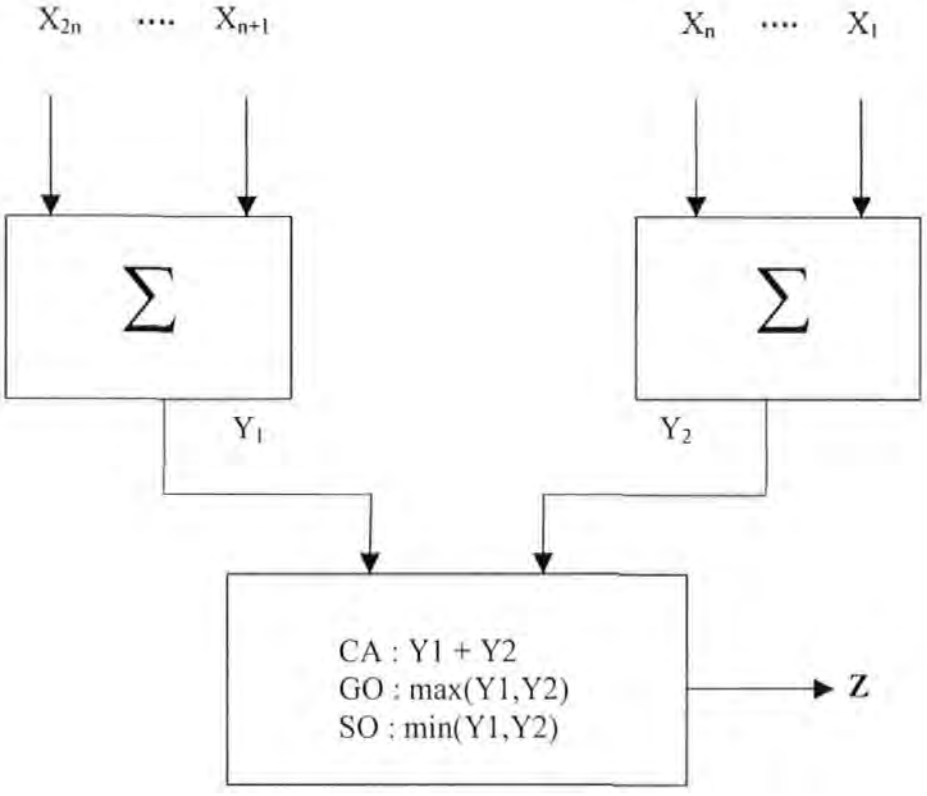

Fig.2.2 Mean-level CFAR Processor

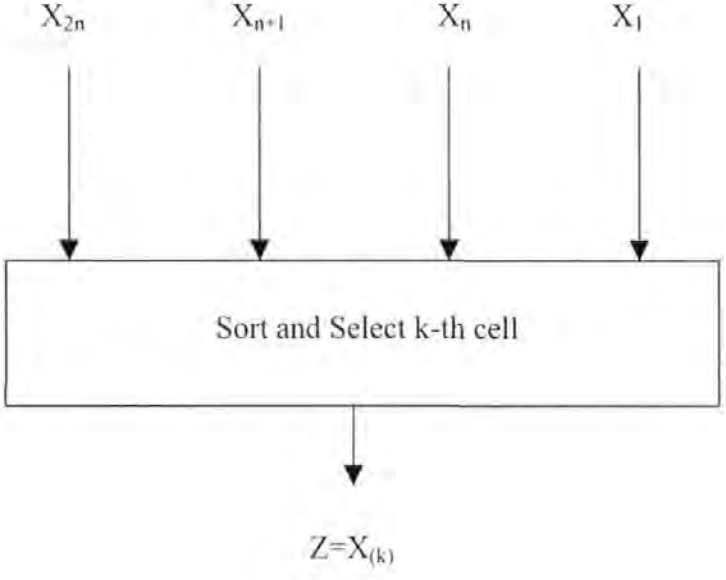

Fig. 2.3 OS-CFAR Processor

For example, figure 2.2 shows the mean level CFAR detection schemes. The processor sums Y_1 and Y_2 of the leading and lagging windows. In the CA-CFAR processor Z is simply the sum of Y1 and Y2, and in the GO- and the SO-CFAR processor, it is the larger or smaller of the outputs Y1 and Y2 respectively. The OS-CFAR processor, which involves a sort routine, is shown in figure 2.3. The kth largest range cell is selected to determine the threshold. The TM_CFAR processor includes censoring circuitry and a summing circuit along with the sort routine as show in fig.2.4. In this scheme T1 samples are trimmed from the lower end and T2 samples from the upper end of the ordered range samples. The statistic Z is formed by summing the N – T1 – T2 remaining samples.

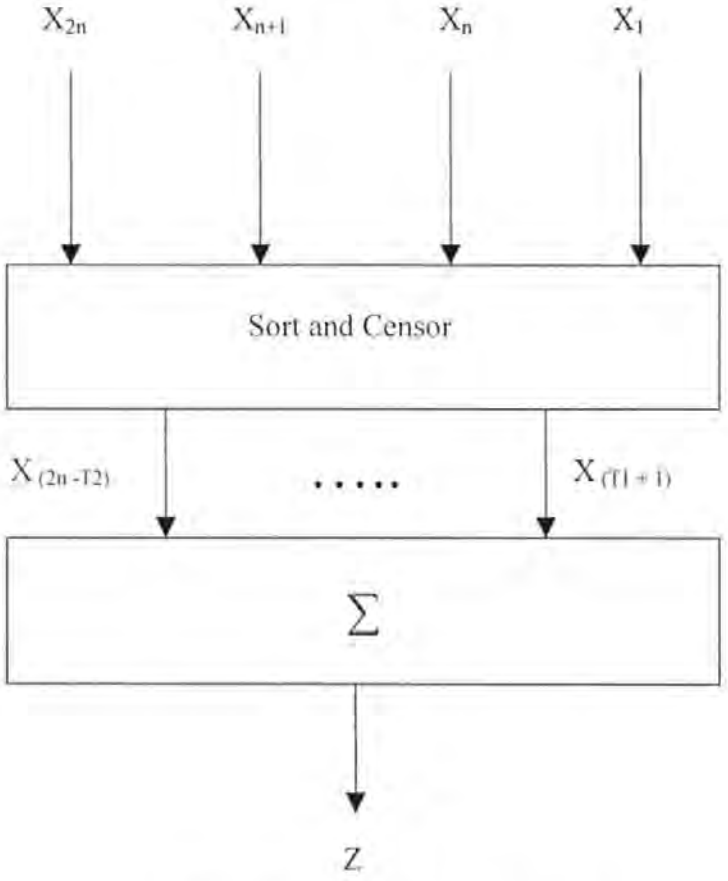

Fig. 2.4. TM-CFAR Processor

In a homogeneous environment, it is assumed that the detected output for any range cell is exponentially distributed, with probability density function (pdf) as given by Van Trees (1968).

$$f(x) = \frac{1}{2\lambda} e^{\left(\frac{-x}{2\lambda}\right)}, x \geq 0.$$

Under the null hypothesis H_0 of no target in a range cell and homogeneous background, λ is the total background clutter-plus-thermal noise power, which is denoted by μ. Under hypothesis H1 (presence of a target), λ is $\mu(1+S)$, where S is the average signal to total noise ratio (SNR) of a target.

In a nonhomogeneous background, the reference cells do not follow a single common pdf. During a single transition from a lower total noise background power level to a higher level, the initial portion of the reference cells have thermal noise only with $\lambda = \mu = \mu_0$, and that the remaining reference cells arise from a clutter background with thermal noise so that here $\lambda = \mu = \mu_0(1+C)$, with C being the clutter-to-thermal noise ratio (CNR). The optimum detector sets a fixed threshold to determine the presence of a target under the assumption that the total homogeneous noise power μ is known. The false alarm probability P_{fa} is given by:

$$P_{fa} = P[Y > Y_0 \mid H_0] = e^{\left(\frac{-Y_0}{2\mu}\right)}$$

where Y_0 denotes the fixed optimum threshold. Similarly, the optimum detection probability P_d is given by:

$$P_d = P[Y > Y_0 \mid H_1] = e^{\frac{-Y_0}{2\mu(1+S)}} = [P_{fa}]^{\frac{1}{1+S}}$$

Therefore, the statistic Z is a random variable whose distribution depends upon the particular CFAR scheme chosen and the underlying distribution of each of the reference range samples. Thus the processor performance is determined by average detection and false alarm probabilities. As shown by Kassam (1988), P_{fa} can be expressed by:

$$P_{fa} = E_Z\{\int_{TZ}^{\infty} \frac{1}{2\mu} e^{\frac{-y}{2\mu}} dy\} = E_Z\{e^{\frac{-TZ}{2\mu}}\} = M_Z(\frac{T}{2\mu})$$

Where $M_Z(.)$ denotes the moment generating function (mgf) of the random variable Z. Similarly, the detection probability Pd is given by:

$$P_d = M_Z[\frac{T}{2\mu(1+S)}]$$

There is an inherent loss of detection probability in a CFAR processor compared with the optimum processor detection performance in homogeneous noise background. This is because the CFAR processor sets the threshold by estimating the total noise power within a finite reference window. The optimum processor, on the other hand, sets a fixed threshold under the assumption that the total noise power is known.

2.3 Analysis of Mean-Level CFAR Algorithms

Mean-level CFAR algorithms incorporate arithmetic averaging to estimate the total noise power. In this section, three such types of CFAR algorithms namely, CA-,GO-, and SO-CFAR algorithms are analysed. Their performance in homogeneous backgrounds as well as in regions of clutter transition and multiple target environments are studied.

2.3.1. Cell Averaging CFAR Processor

In the CA-CFAR processor, total noise power is estimated by the sum of N range cells of the reference window (Barkat, 1990):

$$Z = \sum_{i=1}^{N} X_i$$

Where Xi's are range cells surrounding the cell under test. The probability of detection can be found as:

$$P_d = [1 + T/(1+S)]^{-N}$$

The constant scale factor T is computed by S=0:

$$T = (P_{fa})^{-1/N} - 1$$

In cases where the reference window no longer contains radar returns from a homogeneous background, e.g. in the clutter edge, the statistical characteristics of the reference cell is assumed to be independent. When the reference window contains r cells from clutter background with noise power $\mu_0(1+C)$ and N – r cells from clear background with noise power μ_0. Then, the estimated total noise power is:

$$Z = \sum_{i=1}^{r} X_i + \sum_{i=r+1}^{N} X_i \approx Z_1 + Z_2$$

Since Z_1 and Z_2 are independent, the moment generating function of Z is simply the product of the individual moment generating functions of Z_1 and Z_2 (Rohling, 1983). When the test cell is from clear background, the false alarm probability is:

$$P_{fa} = (1 + T/(1 + C))^{-r}(1 + T)^{r-N}$$

When the test cell comes under a clutter background, the false alarm probability becomes:

$$P_{fa} = (1 + T)^{-r}(1 + T/(1 + C))^{r-N}$$

In cases when the reference window contains two or more closely spaced targets, the detection probability is given by Steenson (1968) as:

$$P_d = [1 + (1 + I)T/(1 + S)]^{-r}[1 + T/(1 + S)]^{r-N}$$

Where r represents the cells in the reference window that contains the interfering targets. C and I are assumed to be different noise conditions (thermal noise for C and clutter-plus-thermal noise for I).

2.3.2 The Greatest Of and Smallest Of CFAR Algorithms

The greatest of (GO) CFAR is specifically developed to reduce the false alarms at clutter edges. The total noise power is estimated from the larger of the two separate sums computed for the leading and lagging window (Hansen and Sawyers, 1980), i.e.

$$Z = \max(Y_1, Y_2); Y_1 = \sum_{i=1}^{n} X_i; Y_2 = \sum_{i=n+1}^{N} X_i$$

$$P_{fa} = 2(1 + T)^{-n} - 2\sum_{i=0}^{n-1} \frac{(n + i - 1)!}{i!(n + 1)!}(2 + T)^{-(n+i)}$$

The false alarm rate is found by computing the moment generating function of Z. The detection probability P_d is found by simply replacing T with T/(1+S). The GO

modification introduces additional loss of detection compared with the CA-CFAR processor loss when the background is uniform.

The smallest of (SO) CFAR is introduced to solve problems associated with closely spaced targets leading to two or more targets appearing in the reference window. The algorithm estimates the smaller of the sums Y_1 and Y_2, i.e. $Z = \min(Y_1, Y_2)$ and the false alarm probability is (Trunk, 1983):-

$$P_{fa} = M_{Y1}(T/2\mu) + M_{Y2}(T/2\mu) - P_{fa}^{GO}$$

$M_{Y1}(T)$ and $M_{Y2}(T)$ are the moment generating functions of Y1 and Y2 respectively. This expression gives a very simple relationship between the performance of SO-CFAR and GO-CFAR. The GO-CFAR processor exhibits minor additional degradation in performance compared with the CA-CFAR processor. On the other hand, performance of the SO-CFAR processor is highly dependent on the value of N. For small N the loss is quite large compared with the other CFAR schemes, but decreases considerably for increasing N. Weiss (1982) has shown that the additional detection loss in the SO-CFAR scheme at P_{fa} is 10^{-6} is 11dB for N = 4 but is only 0.7 dB at N=32.

Consider the special case where the lagging window has noise values from clear background and the leading window has noise samples from the clutter region. If the test cell contains a sample from the clear background, the false alarm probability is (Gandhi and Kassam,1988):-

$$P_{fa} = (1+T)^{-n} + (1+(1+C)T)^{-n} - \sum_{j=0}^{n-1} \frac{(n+j-1)!}{j!(n+1)!} \times (1+T+\frac{1}{1+C})^{-(n+j)} \times [(1+C)^{-n} + (1+C)^{-j}]$$

As the reference window sweeps over the clutter edge, the detection rate of the GO-CFAR is superior to that of both the CA and SO-CFAR.

In the presence of interfering targets, intolerable masking of a primary target occurs in the CA- and GO-CFAR and this gets worse as the interference to signal ratio increases. The effect is greater in the GO-CFAR than in the CA-CFAR. Trunk (1978) shows that the SO-CFAR has better performance in resolving multiple targets in the reference window as long as all the interfering targets appear either in the leading or lagging window. Suppose there is one interfering target in each of the leading and lagging windows. The detection performance of the SO-CFAR will be degraded significantly. This is due to the fact that there is one interfering target in each of the half window, the noise power estimate includes power of the interfering target regardless of the specific half window chosen. This results in an increased threshold leading to a decrease in the overall detection probability.

2.3.3 Ordered Statistics (OS) CFAR Algorithm

The threshold of the OS-CFAR is obtained from one of the ordered samples of the reference window. The range samples are first ordered according to their magnitudes, and the statistic A is taken to be the kth largest sample, X(k). The detection probability Pd can now be expressed as (Rohling, 1983):

$$P_d(S) = k\binom{N}{k}\int_0^{\infty}(1-e^{-z})^{k-1}\times e^{(-(N-k+1+\frac{T}{(1+S)})z)}dz = \prod_{i=0}^{k-1}\frac{N-i}{N-i+\frac{T}{1+S}}$$

The constant T is now a function of k. As k increases, T decreases accordingly. For higher k values the noise estimate Z is one of the reference range samples that has

relatively large magnitude. Thus T decreases to compensate for this increase in Z to maintain the design false alarm rate at a constant value. As reported by Gandhi and Kassam (1988), the OS-CFAR is performing better than the SO-CFAR especially for smaller window lengths, although the OS-CFAR processor performance is inferior to that of both the CA and GO-CFAR.

Consider the situation where the reference window contains r clutter-plus thermal noise cells each with power level (1+C)/2, the remaining N – r cells have the thermal-noise-only with a power level of ½. The following expression shows the false alarm probability for the case when the cell under test is from the clutter-free region (Peterson, Lee and Kassam, 1988):

$$P_{fa} = T\sum_{i=k}^{N}\sum_{L=\max(0,i-r)}^{\min(i,N-r)}\left(\frac{(N-r)!}{L!(N-r-L)!}\right)\left(\frac{r!}{(i-L)!(r-i+L)!}\right)\sum_{j_1=0}^{L}\sum_{j_2=0}^{i-L}\frac{\left(\frac{L!}{j_1!(L-j_1)!}\right)\left(\frac{(i-L)!}{j_2!(i-L-j_2)}\right)(-1)^{j_1+j_2}}{N-r-L+T+j_1+\frac{j_2+r-i+L}{1+C}}$$

When the test cell is from the clutter region, the P_{fa} is obtained from the above results by replacing T with T/(1+C). The k = N value cannot be used in practice due to suppression of targets. Therefore, for k = N the noise estimate Z will be the highest ordered sample which may contain the interfering target with high probability. The false alarm probability will worsen in the clutter region, just after the transition, for decreasing k. This is due to lower thresholds which in turn increases the false alarm rate.

Consider the OS-CFAR of window size 24 with k=21. In the worst case, there are 12 clutter plus thermal noise samples in the lagging window and 12 clutter free samples in the leading window. The clutter samples occupy the top 12 positions of the ordered

range samples and the total noise power estimate tends to be selected as the 9^{th} largest sample among the 12 clutter samples. Suppose the test cell contains a sample from clear background. Then the threshold will be unnecessarily high, leading to a much lower false alarm rate. If the test cell is from a clutter background, the processor acts as if it were an OS(9) processor of window size 12 in a homogeneous situation. The false alarm rate increases significantly.

In case of the presence of interfering targets in a reference window, the performance of the OS-CFAR processor is highly dependent upon the values for k. If a single interfering target appears in the reference window of appreciable magnitude, it occupies the highest ranked cell with high probability. If k is chosen to be 24, the estimate will set the threshold based on the value of the interfering target. This results in an increase in the overall threshold and leads to a target miss. If k is chosen to be less than the maximum value, the OS-CFAR processor will be influenced only slightly for up to N – k interfering targets. For example, if k is chosen to be 21, then the processor is able to discriminate the primary target from, at the most, three interfering targets with little degradation in detection performance.

Though the OS-CFAR exhibits some loss of detection power in homogeneous noise background compared with the CA and GO CFARs, its performance in a multiple target environment is clearly superior. By selecting k to be near the maximum, a false alarm rate performance close to that of the GO-CFAR is obtained. The detection performance of the OS-CFAR is independent of the location of the interfering targets in the reference window while the SO-CFAR suppresses the primary target if the interfering targets are located in both the leading and lagging window. In addition, the detection performance

of the OS-CFAR in homogeneous background noise is superior compared with the SO-CFAR with k values approaching maximum.

2.3.4 The Trimmed-Mean ™ CFAR Algorithm

The TM-CFAR scheme is similar to OS-CFAR in which the noise power is estimated by a linear combination of the ordered range samples. It first orders the range cells according to their magnitude and then trims T_1 cells form lower end and T_2 cells form the upper end before summing the rest. The TM filter with symmetric trimming has been used in signal and image restoration (Bovik, Huang and Munson, 1983). The statistic Z of the TM-CFAR is given by:-

$$Z = \sum_{i=1}^{N-T_1-T_2} V_i$$

The OS-CFAR and the CA-CFAR are special cases of the TM-CFAR with $(T_1,T_2) = (k - 1, N - k)$ and (0,0), respectively. The false alarm rate is given by Bednar and Watt (1984) as:

$$P_{fa} = \prod_{i=1}^{N-T_1-T_2} M_{V_i}(T)$$

$$M_{V_1}(T) = \frac{N!}{T_1!(N-T_1-1)!(N-T_1-T_2)} \times \sum_{j=0}^{T_1} \frac{\frac{T_1!}{j!(T_1-j)!}(-1)^{T_1-j}}{\frac{N-j}{(N-T_1-T_2)}+T}$$

$$M_{V_i}(T) = \frac{a_i}{a_i + T}, i = 2,\ldots, N - T_1 - T_2$$

$$a_i = (N - T_1 - i + 1) / (N - T_1 - T_2 - i + 1)$$

The detection probability P_d is obtained by replacing T with T/(1 + S). As the trimming increases, T increases. Symmetric trimming can not offer advantages in performance over the other CFAR schemes in regions of clutter transitions. With symmetric trimming, Z is given by the sum of the middle $N - T_1 - T_2$ range cells of the ordered window. Consider the situation where the leading half of the reference window contains cells from clutter-plus-noise background and the lagging half from clear background. The noise power estimate Z will include samples from both the clear and clutter-plus-noise background. The corresponding threshold will not be high enough to regulate the false alarm rate if the test cell contains a return from the clutter-plus-noise background. As the upper trimming is increased with no lower trimming, the value of T increases. On the other hand, if the lower trimming is increased with no upper trimming, the value of T increases slowly and approaches the corresponding values for the OS-CFAR. In order to be less sensitive to interfering targets, T_2 should be different from zero. The actual value of T_2 depends on the maximum number of interfering targets present in the reference window. The value of T_1 should be small to attain good detection performance in a homogeneous background. However, if the primary concern is to follow clutter edges, T_1 should be large and T_2 should be small.

2.4 Application of CFAR Algorithms

In this section, the quality of the CFAR algorithms is compared. For this purpose, two 40 microsecond sweeps of radar returns (containing both sea clutter and rain clutter region) at Plymouth harbour were combined to form a 80 microsecond sea target scenario in the video domain. The objective was to use this specific scenario to test

the performance of the CFAR algorithms. The signal consists of 11 targets (including multiple targets) and clutter transitions. The length of the radar sweep is 80 microseconds, which corresponds to a range of 12 Km. The video signal is sampled at 25 MHz, i.e. a range cell of 40ns corresponding to a range resolution cell of 6 m. Figure 2.5 shows a plot of the sea target scenario with 11 targets identified.

Fig.2.5. Plot of the Sea Target Scenario for Testing the CFAR Algorithms

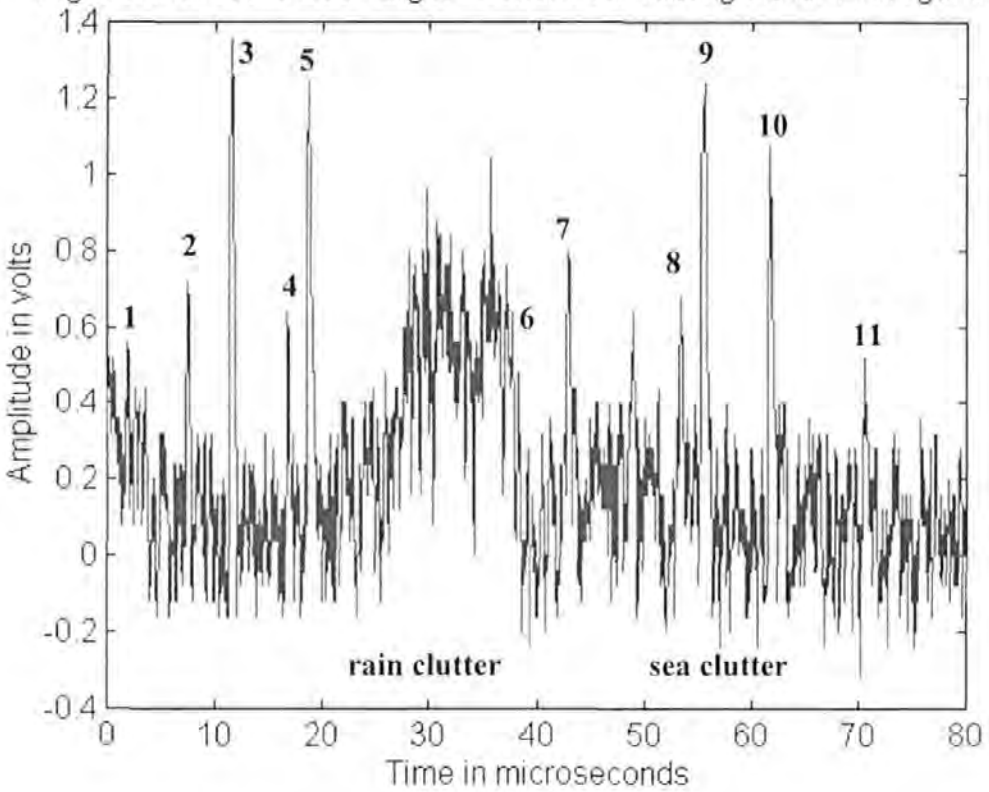

Figures 2.6 to 2.10 show the CFAR thresholds for CA, GO, SO, OS and TM algorithms. For the given sampling rate and range resolution cell size, the optimum length of the CFAR window is chosen to be 120 (Holfele, 1998). To have a reasonable comparison between these algorithms, the threshold of individual CFAR algorithms have no false alarms, i.e. the signal amplitudes in the scenario exceed the CFAR threshold only for targets. The scaling factor T is set to 1.

Fig.2.6. Sea Target Signal with CA-CFAR Threshold

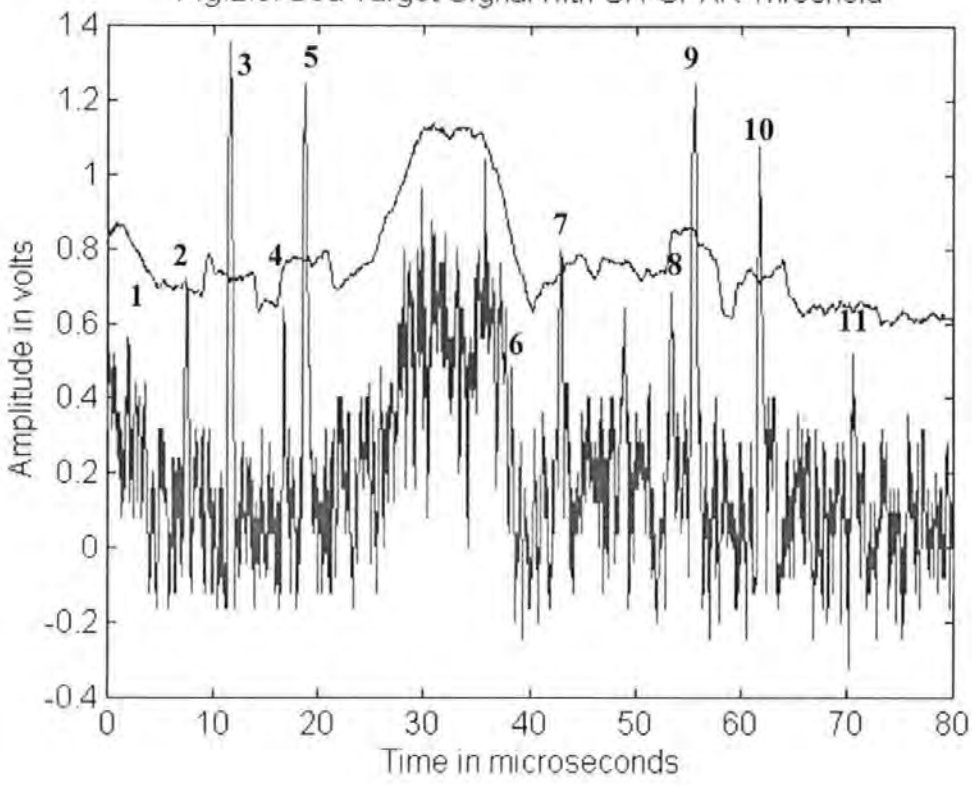

Fig.2.7 Sea Target Signal with GO-CFAR Threshold)

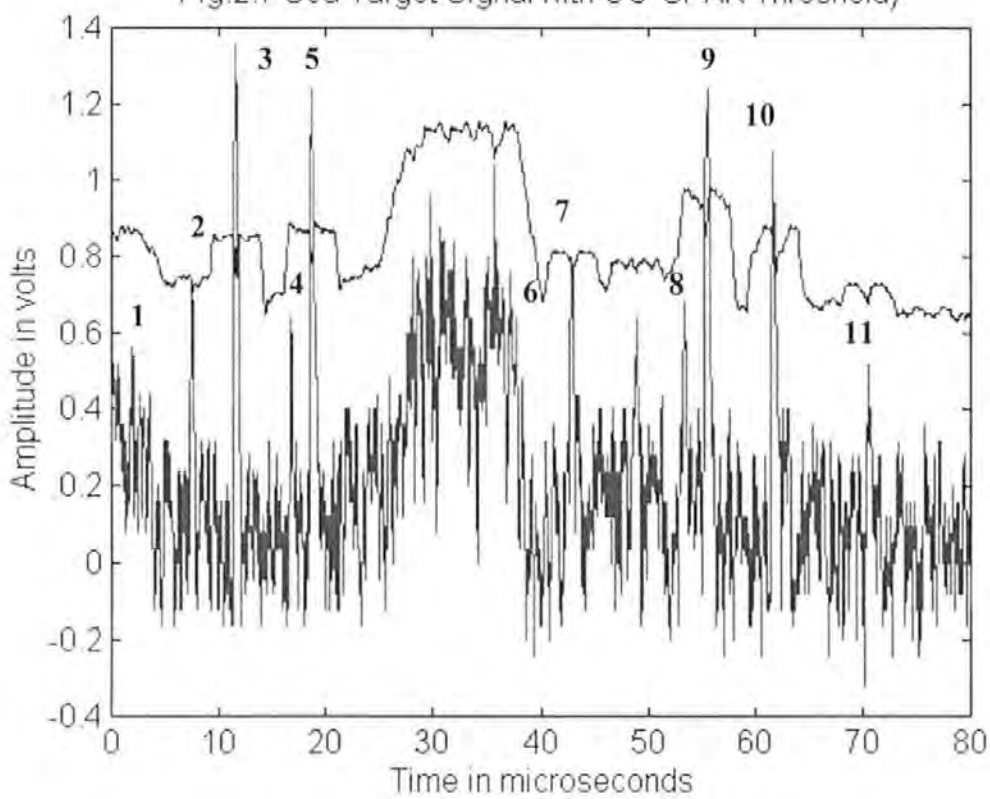

Fig.2.8. Sea Target Signal with SO-CFAR Threshold

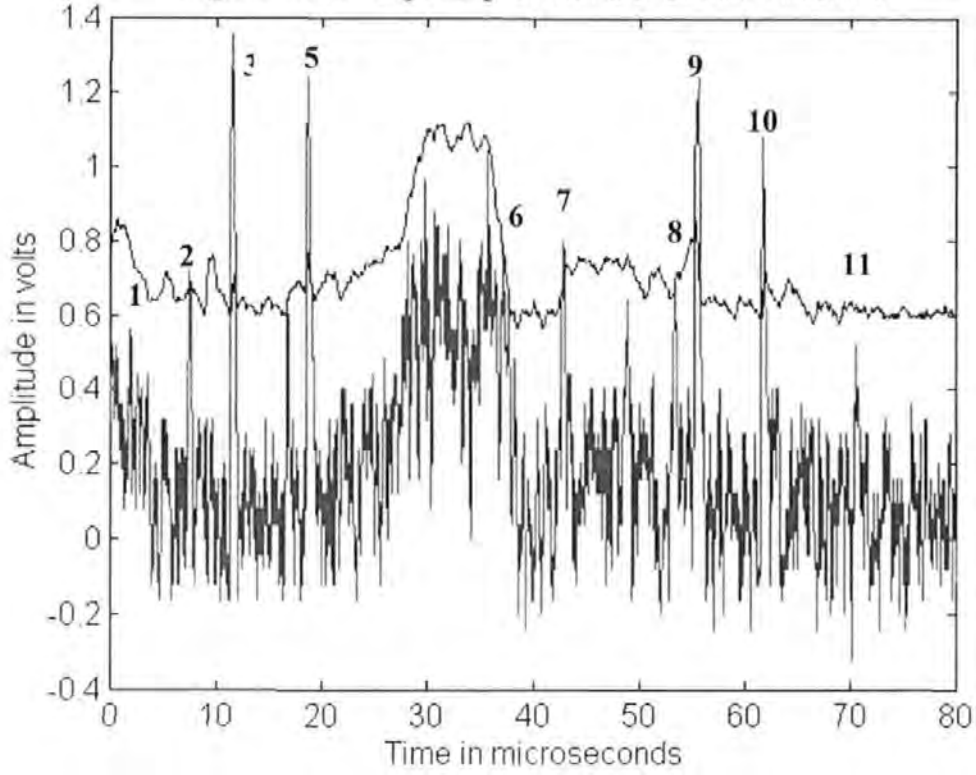

Fig.2.9. Sea Target Signal with OS-CFAR Threshold, k=80

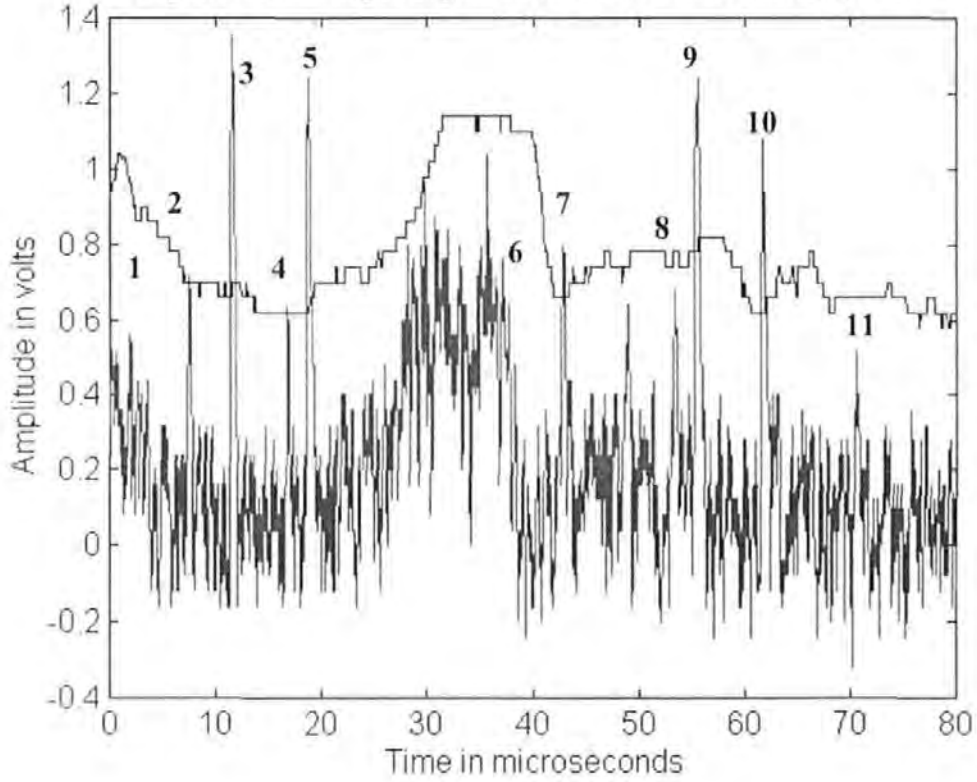

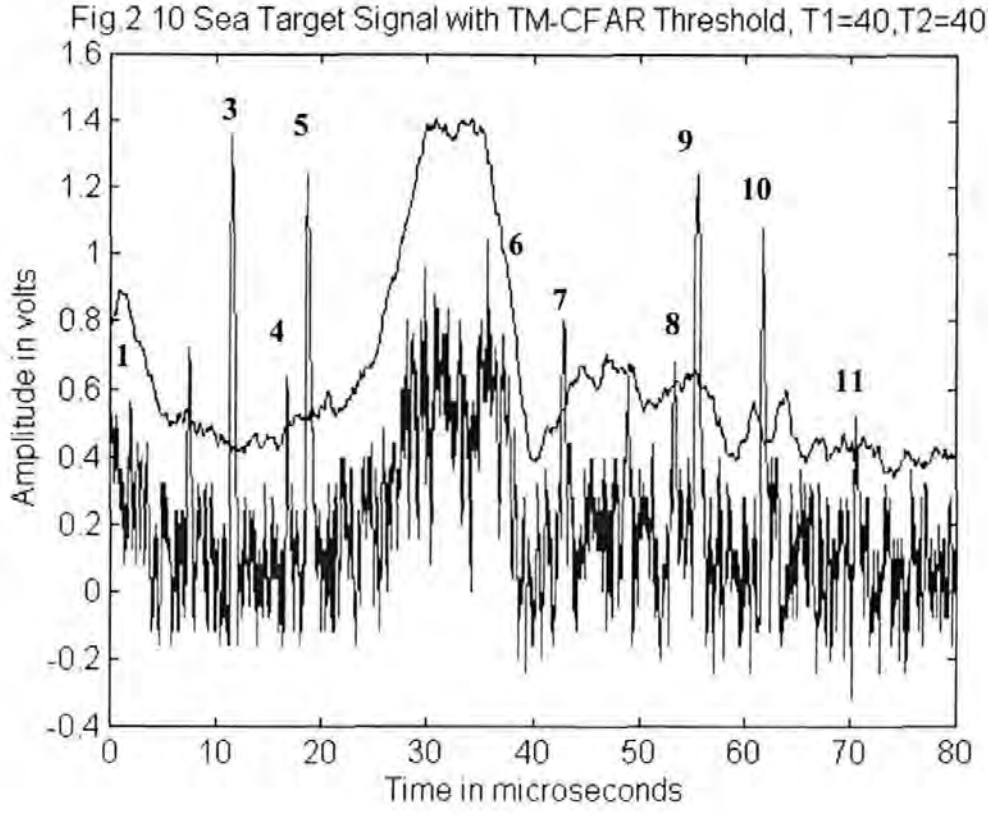

To determine the quality of a CFAR threshold, a criterion is established to calculate the fitness of the threshold to the clutter and target environment. The criterion is based on the assumption that there is no false alarm in the detection. This is performed by summing the threshold crossings, i.e.

$$q = \sum [Y(i) - Z(i)]$$

for all i with Y(i)>Z(i), where Y is the magnitude of the range cell and Z is the threshold. The following results are obtained for the five CFAR algorithms.

Table 2.1 Quality of the CFAR Algorithms

CFAR Type	Quality q
TM	17.0497
OS	16.0247
SO	15.2160
CA	12.0613
GO	10.6400

TM-CFAR has the best quality. However, two targets that are embedded in clutters are still missed. GO-CFAR has a worse quality than CA-CFAR. This is due to its poor performance in the region of multiple targets.

2.5 Conclusion

The performances of five different CFAR processing algorithms in both homogeneous and nonhomogeneous backgrounds have been analysed. The multiple target environment and regions of clutter are used as examples for nonhomogeneous backgrounds. A sea target scenario is used to indicate the variation of performance between the algorithms in a specific environment, i.e. multiple targets and clutter edges.

The detection performance of the CA- and GO-CFAR processors is superior in homogenous background. However, the performance of CA-CFAR degrades significantly in nonhomogeneous background. The false alarm rate increases considerably at the clutter edges, and target masking is experienced in multiple targets. Although the false alarm rate performance of the GO-CFAR in regions of clutter transition is better than that of any other mean-level CFARs, the detection performance

in a multiple target environment is quite poor. The SO-CFAR does not appear to offer any advantage over the CA and GO CFAR. In addition to exhibiting high loss of detection power in homogeneous background, the SO-CFAR is unable to resolve multiple targets and to control the false alarm rate at clutter edges. Yet, it has good performance in the multiple target environment when a clutter of radar targets appear in the reference window.

The CFAR algorithms based on ordered range cells have in general better overall performance than the mean-level CFAR schemes (Kassam, 1988). The TM-CFAR may have a slightly better performance in a homogeneous background for isolated targets compared with the OS-CFAR. The performance of the OS-CFAR processor is relatively unaffected if the clutter area is less than the window length as long as r, the number of clutter samples present in the reference window, is greater than $N - k$. The false alarm rate does not suffer considerably at the clutter edges if $r \leq N - k$. On the other hand, the CA and GO-CFAR exhibit further false alarm rate degradation if the extent of clutter area is smaller than the window size. This is because the noise power estimate consists of samples from clutter background as well as from clear background leading to overall decrease in threshold. However, the performance of the OS-CFAR is highly dependent upon the values of k. If k is chosen to be a high value, the noise estimate will set a large threshold and it will result in target misses. Also, a low value of k will give excessive false alarms. With regard to the TM-CFAR, again the choice of trimming factor T affects the overall false alarm rate as well as the detection probability.

The experiment using the sea target scenario showed that the five CFAR algorithms were unable to detect targets embedded in strong clutter. TM-CFAR with a good choice

of trimming factor could have a better performance in this specific case. However, two targets were still missed. It is important to note that each algorithm aims to tackle a specific problem in detection and it is obvious that no single CFAR algorithm is adequate to solve problems in a complex detection environment, such as that in which a VTS system is likely to be operated. A drawback on the CFAR algorithms is that the decision is made only from the magnitude of the return echoes (Li and Miller, 1997). To have significant improvement in the detection of weak targets, more obvious discriminating features must be identified and extracted. The following chapter will look at the other characteristics of the radar signals for improvement in detection.

CHAPTER THREE

CHARACTERISTIC OF RADAR SIGNALS AND FEATURE EXTRACTION

3.1 Introduction

The limitations of the CFAR algorithms in radar detection are mainly caused by their static processing structures that they rely only on the amplitude information of the return signal from targets and clutters. These algorithms are not suitable for a complex dynamic environment such as the Hong Kong harbour. It is quite evident that the detection capability of CFAR is very limited under strong clutter background, as the signal is embedded in the clutter which itself has a large amplitude. To provide a significant improvement in the detection of weak targets, more obvious discriminating features must be identified and extracted (Li and Miller, 1998). The radar detection system may perform better when the characteristics of target and clutter are in line with their predicted values. A wide range of targets and clutters will be received by the radar systems and it is necessary to formulate descriptions about these signals at specific times. In deciding whether a target is present, there are factors other than the magnitude of signal to be considered. The echo from the reflecting objects may consist of many components of energy scattered from points over the surface. Their spatial and correlation characteristics will vary as a function of time, angle of incident and transmitting frequency. Radar returns of weak targets will have a closer temporal correlation than those of a fairly strong sea clutter. Also, in the spatial domain, the targets have some different features when compared with spiky clutter signals. An effective approach to solve the problems in target detection is to develop algorithms which are able to extract these discriminating features of signals in the radar return. With

the recent development in the processing speed of computers, more radar information can be handled in real time. This chapter will study the characteristics from radar return signals in order to identify the features and extraction algorithms that can improve the detection capability of a radar system.

3.2 Radar Cross Section

When a radar illuminates a target, the power that is backscattered or reflected back to the radar is defined in terms of a measurable quantity, the target cross section. Since there is substantial variation of the reflected power about the target for any given illumination angle, an equivalent hypothetical target which re-radiates isotropically, is used as the basis for measurement. The radar cross section (RCS), σ, implies an area of an isotropic reflecting body which creates at the radar the same power density as does the actual target.

$$\sigma = 4\pi R^2 P_s / P_i$$

Where P_s is the backscattered power at the target and P_i is the incident or transmitted power measured at the radar, and R is radar-to-target range. The RCS depends on the characteristics of the target, namely the permittivity and the permeability of the target material, the target aspect angle relative to the radar, the shape and dimensions of the target structural elements relative to wavelength, and on the polarization of the radar receiving and transmitting antennas.

Some of the electromagnetic energy intercepted by the target is absorbed as heat and the rest is scattered. Portions of the energy scattered in the direction of the receiving antenna are received by the antenna and subsequently processed in the target detection system.

Since radar targets such as ships, aircraft, missiles, and ground terrain have a variety of forms and shapes, the use of mathematical models for smooth surfaces would lead to incorrect calculations. As such, experimental measurements with the use of the target itself or of smaller scale models form the basis of radar cross section calculations. Measurement errors caused by parasitic reflections can be reduced by placing the model in an anechoic chamber.

The target cross section fluctuates as a function of time. This is due to the scattering effects that intercept the transmitted electromagnetic energy. A complex scintillating target to a first approximation can be represented by an exponential distribution (Hovanessian, 1972). The radar illuminates the target once every revolution of the radar antenna, with the duration of illumination proportional to the rotational speed of the antenna, which is in terms of milliseconds. The target cross section used in the radar equation is the average value of the cross section and the target scintillation is incorporated in the probability of detection calculation.

The cross section of vessel type targets, as presented to the radar, is also a function of aspect angle. It can be seen initially that a vessel presents a larger physical area when viewed from both sides rather than from the bow or the stern. A target viewed from the sides may have an average cross section of 5 times larger than the same target in the bow aspect.

A single value of RCS cannot be assigned to a target, e.g. a ship, as it will depend on the aspect at which the target is viewed, both in azimuth and elevation, and also on the polarization angle of the radar. These factors, combined with interference from different

scattering surfaces on the target, would mean that the RCS of the ship will fluctuate. These fluctuations can be treated by finding the mean value of the RCS σ_{av} and a probability density function (PDF) $p(\sigma)$ to describe the variations about the mean. A commonly used density function for random variables is the chi-squared variable with two or four degrees of freedom, in the forms of:

$$p(\sigma) = \frac{1}{\sigma_{av}} e^{(-\frac{\sigma}{\sigma_{av}})}$$

$$p(\sigma) = \frac{4\sigma}{\sigma^2_{av}} e^{(-\frac{2\sigma}{\sigma_{av}})}$$

$\sigma \geq 0$

For most of the surveillance radar, typical values of RCS (σ_{av}) that might be expected are given in table 1 (Kingsley and Quegan, 1992).

Table 3.1 Typical RCS values for some common targets

Target	RCS on Linear Scale	RCS on Log Scale
Bird	$0.001m^2$	$-30dBm^2$
Cruise missile	$0.010m^2$	$-20dBm^2$
Small boat	$1.000m^2$	$0dBm^2$
Cargo ship	$10.000m^2$	$10dBm^2$
Large aircraft	100.000m2	20dBm2
Large tanker	$1000.000m^2$	$30dBm^2$

3.3 Clutter

Clutter is hard to quantify, and in many ground based systems it varies dramatically with azimuth. The clutter seen by a marine radar depends on the sea-state and wind direction.

Weather clutter is inherently variable and unpredictable. In spite of these difficulties, it is important to have an overall appreciation of clutter cross sections for target detection.

Sea clutter is often distributed over a considerable area, unlike the point targets. Its backscattering effect may be described in terms of a radar cross section density, σ_0. If a clutter area A_c produces an effective radar cross section σ_c, then

$$\sigma_0 = \frac{\sigma_c}{A_c}$$

If the radar energy strikes the surface at an angle ϕ, a clutter area corresponding to one resolution cell of the radar can then be specified. The cell's extent in the range direction is determined by the pulse length. A pulse duration of τ seconds corresponds to a transmit and return path of $c\tau/2$ metres. The equivalent distance along the clutter surface is $c\tau\sec\phi/2$ metres. The surface area lying within one resolution cell is therefore

$$A_c = \frac{c\tau \sec\phi}{2}(R\theta_B)$$

The effective radar cross-section of the clutter area is

$$\sigma_c = \sigma_0 A_c = \sigma_0 \frac{c\tau \sec\phi}{2}(R\theta_B)$$

Suppose that a point target of area σ competes with clutter of effective area σ_c in the same resolution cell. If the power of the return signals are represented by S and C respectively, then the signal to clutter ratio is:

$$\frac{S}{C} = \frac{\sigma}{\sigma_c} = \frac{2\sigma}{\sigma_0 c\tau \sec\phi R\theta_B}$$

When the clutter is heavy, the clutter power will be much greater than the receiver noise power. Hence the maximum range at which a target is detectable depends on the signal to clutter ratio rather than the signal to noise ratio. If the minimum acceptable signal to clutter ratio at the receiver input is (S/C)min, then

$$(\frac{S}{C})_{\min} = \frac{2\sigma}{\sigma_0 c\tau \sec\phi\ R_{\max}\theta_B}$$

From the above equation, it can be concluded that an effective way of improving the signal to clutter ratio is to reduce the size of the radar resolution cell. This may be achieved by reducing the pulse length, the antenna beamwidth or both. However, the actual values of the clutter cross-section density σ_0 depend heavily on the type of surface, or terrain, and on the grazing angle ϕ. It is also affected by the choice or radar frequency and the polarization. By taking a small grazing angles ($\phi<10^o$) which are widely used in marine radar, typical values of σ_0 for city in X band, cultivated land and sea are shown in the following table (Lynn, 1987).

Table 3.2 Typical values of clutter cross-section density

	Horizontal	Vertical
City	-18dB	-15dB
Cultivated land	-25dB	-22dB
Sea	-40dB	-30dB

The above quoted sea clutter values are typical of average sea conditions, in wind speed of around 15 knots.

Rain or other atmospheric conditions also produce clutters to radars. Such clutter is usually quantified in terms of an effective cross-section η per unit volume. Thus, if a clutter volume V_c produces an effective radar cross-section σ_c, then

$$\eta = \frac{\sigma_c}{V_c}, or \quad \sigma_c = \eta V_c$$

Now the radar resolution cell corresponds to a volume in space rather than a surface area. Its extent is defined in range by the pulse length, in azimuth by the horizontal beamwidth θ_B, and in elevation by the vertical beamwidth ϕ_B. The approximate volume of a resolution cell is:

$$V_c = \frac{c\tau}{2}(R\theta_B)(R\phi_B)$$

Such types of volume clutter usually come from rain and cloud droplets. They are small compared with the radar wavelength, and the cross-section presented by an individual droplet is proportional to the sixth power of its diameter. Heavy rain produces stronger clutter than light rain or cloud, not only because there are more droplets per unit volume, but also because they tend to be larger in size. Droplet cross-section is also proportional to the fourth power of the transmitter frequency. Therefore, the systems operating at lower frequencies are much less susceptible to weather clutter. A typical relationship to describe the effects of rain clutter on radar performance is,

$$\eta \approx 7 f_0^4 r^{1.6} x 10^{-12} m^{-1}$$

Where f_0 is the transmitter frequency in GHz and r is the rainfall rate in mm/h. Given a light rainfall of 1 mm/h, their cross sections as presented by two different wavelengths (23 cm and 3 cm) at a range of 50nm (τ = 2μs, θ_B = 1.5°, ϕ_B =12°) are found to be 0.2m^2 at λ=23cm and about 800m^2 at λ=3cm.

3.3 Statistical Characteristics

Most of the random noise arises in the initial stages of the radar receiver. Their behaviours during the target arrival period cannot be predicted. However, the statistical distribution of random noise at the input to the intermediate amplifier can be assumed as Gaussian, with zero mean value, which is mainly due to the thermal motion of electrons in the early amplification stages. The probability density function of Gaussian noise with zero mean is given by:

$$p(v) = \frac{1}{(2\pi\psi_0)^{1/2}} \exp(\frac{-v^2}{2\psi_0})$$

where ψ_0 is the variance and $\psi_0^{1/2}$ is the standard deviation. The random noise will have a mean value close to zero. There is small chance that at a particular time the noise level will be several standard deviations above or below the mean (Barton, 1988).

Most targets and clutters have a very complicated relationship to the cross section area. and it is difficult to format equations based on the physical dimensions. A complex radar target (e.g. a ship) has many reflecting surfaces, such as the hull, accommodation, masts and stern. Each of these contributes to the overall return signal, including the relative phase as well as magnitude. It is important to note that a specific target will not always have the same cross section area as 'looked at' by the radar for a given incidence angle.

Small changes in the direction of the incident wave can cause dramatic changes in the effective cross section area of the target and these are very unpredictable. Also, clutter is very difficult to define accurately, and it usually changes with environment and factors such as wind and weather. Measurement of radar cross section of complex targets requires readings to be taken at many frequencies, and with different polarisation. This would lead to a massive database for a single radar band and limit the usefulness of these data in radar performance analysis. These targets can be summarised in statistical form and four statistical models were established based on probability density function (Lynn, 1987). It was reported that classes 1 and 2 are of Rayleigh type model and correspond to targets to which many scattering sources are added. Basically, all complex targets having many comparable echo areas are very close to this model. For a target of average radar cross section of σ_{av}, the probability density function is of the form:

$$p_{\sigma}(\sigma) = \frac{1}{\sigma_{av}} \exp(-\frac{\sigma}{\sigma_{av}}), \qquad \sigma \geq 0$$

Classes 3 and 4 are more appropriate for targets having one dominant reflector, plus a number of other, smaller reflectors. The probability density function is of the form:

$$p_{\sigma}(\sigma) = \frac{4\sigma}{\sigma^{2}_{av}} \exp(-\frac{2\sigma}{\sigma_{av}}), \qquad \sigma \geq 0$$

The intensity of the target echo depends on the aspect angle at which the target is observed, the transmitter frequency and radar polarization. The target cross section area changes with time, i.e. it varies between different sweeps due to aspect variation. These variations will be present even when the vessel approaches the radar at constant bearing, with the radar polarization and frequency remaining constant. This is caused by the random movement of the vessel, the different propagation characteristics of the atmosphere, performance of the electronic circuits in the radar equipment, and the

variation in the transmission pattern of the radar antenna.

The Rayleigh scattering model can also apply to sea clutter if the sea is calm and the range cells are fairly large. However, the range cells are relatively small in a short pulse and high resolution radar. The size of individual sea waves may often be comparable with a range cell, especially in a rough sea condition. Under these circumstances, the distribution departs from the Rayleigh, with sharp peaks at the larger wave tops. Other forms of distributions have been used to model sea clutter received by marine radars. These types of function have a longer 'tail' than the Rayleigh distribution. One of which is the Weibull model with the form

$$p(v) = \alpha \ln 2(\frac{v}{\beta})^{\alpha-1} \exp(-\ln 2(\frac{v}{\beta})^{\alpha})$$

where α and β are constants

Alternatively, the Log-normal, which has a longer 'tail', has the distribution

$$p(v) = \frac{\gamma}{v} \exp(-\delta\{\ln[\frac{v}{\beta}]\}^2)$$

where β,γ and δ are constants.

The decision on which distribution is to be used depends on the sea state at that specific moment. Yet, the Log-normal distributions are best suited to rough seas. Moreau (1993) has developed a model for sea clutter, which is a Rayleigh distribution modulated by a Gamma distribution. The amplitude is represented by a compound K-distribution model:

$$p(v) = \frac{2b}{\Gamma(v)}(bx/2)^{v} K_{v-1}(bx)$$

where $K_v(x)$: v - order modified Bessel function

$\Gamma(x)$: Gamma function

x : clutter amplitude

v : shape parameter (function of sea-state, speed and direction of wind)

b : scale parameter

The shape parameter v is a function of transverse resolution R, grazing angle ϕ, wind direction σ and a coefficient k (k depends on polarisation) in the form of:

$$\log v = \frac{2}{3}\log\phi + \frac{5}{8}\log R + \sigma - k$$

Moreau (1993) had made simulations with this sea clutter model using a correlated Gamma process. By estimating the high order statistics, he found out that, with $v > 0.4$, simulated results fit well to the theoretical definition.

The volume clutter is usually caused by weather conditions such as rain and cloud droplets. The reflectivity of volume clutter is quantified in effective radar cross-section per unit volume. The rain and cloud droplets are usually very small compared with the radar wavelength. They can normally be described by means of Rayleigh modelling. However, the radar cross section of droplets for cloud and rain is proportional to the fourth power of the transmitter frequency. This causes the high frequency radars to have more effects from the weather clutter. For shorter wavelength, the scattering properties may depart from the pure Rayleigh distribution.

Figures 3.1 to 3.4 show the recorded noise, target, sea clutter and rain clutter, and their statistical distribution in a 2 microsecond time window. The window contains 50 samples of the radar return signal, which corresponds to a distance of 300 meters.

Despite the fact that the magnitude of the random noise, sea clutter, rain clutter of these signals are close to each other, it can be observed from their distribution that each type of return echo has its unique features. The random noise resembles a zero mean Gaussian function, with a maximum number of occurrences at 0 volts. The target is characterised by the long tail which extends by up to 1 volt. The majority of the sea clutter returns lie between 0 and 0.5 volt. The rain clutter has similar characteristics to the random noise, except that the maximum is shifted to around 0.5 volt.

To characterize the differences between these signals, the amplitude and period parameters in the 4 microsecond windows are extracted. The waveforms contain a combination of several frequency components and they exhibit a series of extremes over the time interval. A segment boundary is declared each time that the waveform passes through a zero slope condition. The segment amplitude is the absolute amplitude differences between the bounding extreme of the segments, i.e.

$$A_n = |a_n - a_{n-1}|$$

where A_n = segment amplitude of the nth segment

a_n = waveform amplitude at the highest extreme of the segment

a_{n-1} = waveform amplitude at the lowest extreme of the segment

The segment periods are the time differences between the lowest extremes of the segments. This can be expressed as

$$T_n = t_n - t_{n-1}$$

where T_n = segment period of the nth segment

t_n = waveform elapsed time at the first lowest extreme of the segment

t_{n-1} = waveform elapsed time at the next lowest extreme of the segment

To sample the waveforms, a trigger signal is activated whenever the waveform exhibits a zero slope condition, indicating an extreme position. As such, direct extraction of the waveform amplitudes (a_0, a_1, ... a_n) as the amplitude outputs of the monitoring circuit can be achieved. The segment amplitude (A1, A2, ...An) can then be calculated simply by subtracting consecutive waveform amplitudes and taking the absolute values of the differences. The triggered sampling technique can also provide trigger signals at waveform extremes, which are the segment boundaries. These signals may be used to stimulate an electronic counter to retain its present count as an elapsed time measurement. Consecutive elapsed time measurements (t0, t1, ……..,tn) are then subtracted to obtain the segment periods (T1, T2, ……Tn).

The absolute differences in amplitude between these extremes are then accumulated, and their mean and mean deviation are also calculated. The four waveform parameters, ie. the amplitude mean, amplitude deviation, period mean and period deviation are the primary measures by which the waveform can be characterized statistically. The mean is the standard sample mean, in the conventional statistical sense, and is simply the sum of the sample values divided by the number of samples. The mean deviation, however, is neither the statistically conventional variance nor standard deviation. As only a measure of the average sample deviation from the sample set mean is required, the statistically

standard quantities, which involve the calculations of squares and square roots, can be avoided to achieve the computational simplicity. The mean deviation is the average of the absolute differences between each sample and the sample mean. These parameters can be expressed mathematically as follows:

$$D_a = \sum_{i=1}^{N_s} |A_i - M_a| N_s$$

$$M_t = \sum_{i=1}^{N_s} (T_i) / N_s$$

$$M_a = \sum_{i=1}^{N_s} (A_i) / N_s$$

$$D_t = \sum_{i=1}^{N_s} |T_i - M_t| / N_s$$

where,

Ma = amplitude mean,

Mt = period mean,

Da = amplitude mean deviation

Dt = period mean deviation

Ai = amplitude of the ith segment

Ti = period of the ith segment

Ns = number of samples (segments)

The period quantities are in temporal units of microseconds and amplitude units are in quantities of volts. The statistical data of target, sea clutter, rain clutter and noise, as calculated by the author using the waveforms recorded at the Plymouth harbour, are given in the following table:

Table 3.2 Statistical data of target, sea clutter, rain clutter and noise

	Target	Sea Clutter	Rain Clutter	Noise
Mean (amplitude in volts)	0.1952	0.2340	0.5880	0.0584
Deviation (amplitude)	0.2296	0.2014	0.1960	0.1060
Maximum (period in microseconds)	0.8	0.44	0.36	0.48
Mean (period in microseconds)	0.1704	0.1508	0.1584	0.1523
S. Deviation (period)	0.1550	0.1026	0.0905	0.0979

The noise has a comparatively low mean amplitude. This can be explained that the noise is fluctuating randomly around zero and the sum of these amplitudes will be close to zero. The rain clutter has a comparatively high mean amplitude giving high peaks in the radar receiver. The negative values of the amplitudes are due to the bias and offsets of the amplifiers in the radar equipment. The amplitude deviation of sea clutter is small as most of the amplitudes are varying along the means value. The mean period of the window containing target(s) is large, which signifies that targets have a wider pulse width when compared with noise and clutters. Such statistical characterization forms the basis for a discrimination system for target detection.

3.4 Correlation

The ability to detect targets from signals coming from the receiver is largely depending on the signal to noise ratio (SNR). Hence, it is important that the SNR is maximized. The noise power is dependent only on the gain of the receiver, not on the shape of its impulse response function. For fixed gain, the best SNR is obtained by maximizing the response to the signal term. This is achieved by correlating the return echo with the transmitted pulse. The receiver can be regarded as a linear filter with impulse function

h(t) , and the output from the receiver, y(t) is therefore given by a convolution operation:

$$y(t) = u(t) * h(t) = \int_{-\infty}^{\infty} u(\tau)h(t-\tau)d\tau$$

where τ is a time variable and u is the input

According to the Cauchy-Schwartz Inequality (Kingsley and Quegan, 1992), the maximum value of signal to noise ratio can be obtained by choosing $h(\tau)$ proportional to $u(\tau + (\tau_d - t))$ and $h(\tau)$ is a reversed and shifted copy of $u(\tau)$ where τ_d is the time delay. Hence,

$$y(t) = \int_{t-\tau_d}^{\tau} u(\tau)u(\tau + \tau_d - t)d\tau$$

where $u(\tau)$ is the incoming signal

$u(\tau + \tau_d - t)$ is a copy of u shifted to a duration of $t - \tau_d$.

The product of the signal and its shifted version is integrated over the ranges for which the integral is not equal to zero. y(t) has the same shape as the autocorrelation function of u(t). As t varies, the shifted $u(t)$ will come to align with the incoming signal and then out of alignment again. When they are fully aligned, i.e. $t = \tau_d$, the maximum signal to noise ratio will occur and the amplitude is given by,

$$y(t) = \int_{0}^{\tau} u^2(\tau)d\tau$$

As such, the amplitude of the target after correlating with the transmitting pulse will be greatly enhanced. The signal to noise ratio is much improved and this will facilitate the target to be detected more easily.

Fig. 3.5a shows a radar return with a target (at 18 microsecond) being contaminated by noise. Since the transmitted pulse is rectangular in shape with a pulse width of 0.05 microseconds, the return echo will be stretched. The width of the integrating pulse can be determined by trials. It is found that the best result can be obtained when it is around 10 times the transmitting pulse. Fig. 3.5b shows the result of integrating the product of a 0.4 micro second rectangular pulse by the radar return. It is obvious that the signal to noise ratio is much improved and this will facilitate the target to be detected more easily.

New motion estimation algorithms in image processing which exploit the motion correlation of neighbour blocks in temporal and spatial directions have been presented (Hsieh, Lu and Shyn 1990 and Loui and Azimi-Sadjadi 1991). Winston, Yu, Meyer and Byrne (1995) and Chen, Deng and Zhuan (1995) have reported techniques for automatic tracking and identification of moving targets using correlation algorithms. The targets from the radar return will normally appear in more than 1 sweep in the same scan. The same target will also appear in next scan within a certain limit of distance, depending on the speed of the target. The degree of correlation will depend on the size and type of targets. Large sized targets will be correlated in a greater number of consecutive sweeps than those small sized ones. The speed of a vessel is relatively slow when compared with the time between sweeps and it can be ignored in calculating the correlation. For example, the vessel is moving at a speed of 15 nm/hr (27.78 km/hr) and the Pulse Repetition Frequency (PRF) is 1300Hz (short/medium pulse)., i.e. one sweep takes 769.2 microsecond. The vessel only travels 0.463 mm. Also, taking the rotational speed of the radar antenna is 20 rpm, one complete scan takes 3 seconds. The vessel travels 23.15 mm in one scan period. The correlation between the targets within consecutive sweeps can be determined by:-

$$C_{S_n S_{n+1}}(v) = \sum_{m=0}^{m=l} V_{S_n t_m} V_{S_{n+1} t_{m+v}}$$

where $C_{S_n S_{n-1}}(v)$ is the correlation of target points between n, and n+1 sweeps

$V_{S_n t_m}$ is the amplitude of nth sweep at time m

l is the size of the correlation window

Random noise is usually uncorrelated and thus can be removed after the first order correlation process. Despite the fact that most of the uncorrelated noise is removed, there is still some correlated noise appearing which may affect the target detection process. The use of high order correlation method (Liou, 1991, 1992 and 1993) can provide a better discrimination capability between clutter and noise. This is achieved by correlating the correlated results of N/N+1 and N+1/N+2 to generate a new sequence of radar signals.

Figures 3.6a, 3.6b and 3.6c show three consecutive sweeps of a radar return with a time frame of 10 microseconds. The correlation of N/N+1 and N+1/N+2 are shown in figures 3.7a and 3.7b respectively. Figure 3.8 shows the effect of using high order correlation. The noise is suppressed and the targets can be discriminated from the trace easily.

3.5 Spectral Characteristics

Target motion in range introduces a doppler shift of $2v/\lambda$ relative to the transmitted carrier frequency. As the target changes its velocity and heading, the spectral components are shifted. The movement of the target and its elements, as well as yaw, pitch, and roll, cause the spectrum of the received signal to fluctuate. The spectrum does not depend much on target dimension and is determined by the rate at which the range to different reflecting

elements varies. Various techniques have been reported in detecting signals using their frequency characteristics, e.g. low pass filtering, integration and matched filtering (Van Trees, 1968). It appears that radar targets have distinct features in the frequency domain compared with clutter and noise. Targets appear at some specific time of the radar sweep and the corresponding changes in the immediate frequencies throughout the time sweep may be of use in the detection of targets. Armstrong and Ahmed (1989) have modelled the immediate frequency function for a broadband signal by considering an input of n frequency varying spectral components.

By taking the square of the time derivative of the signal x(t), we have

$$[x'(t)]^2 = \sum_{i=1}^{n} \frac{1}{2} A_i^2 \omega_i^2(t)\{1 - \cos[2\phi_i(t)]\}$$

+ other cross-multiplied terms

$$x(t) = \sum_{i=1}^{n} A_i \cos[\phi_i(t)]$$

where $\omega_i(t)$ denotes the immediate frequency function $\phi_i'(t)$

If a low pass filter is applied to the signal $[x'(t)]^2$, it will suppress the terms associated with $\cos[2\phi_i(t)]$ and the other cross multiplied terms, so:

$$[x'(t)]^2 \mid_{LPF} = \sum_{i=1}^{n} \frac{1}{2} A_i^2 \omega_i^2(t)$$

The low pass filter output of the square of the input is also calculated as follows:

$$[x(t)]^2 \mid_{LPF} = \sum_{i=1}^{n} \frac{1}{2} A_i^2$$

The immediate frequency function ω(t) can then be estimated as:

$$[\omega(t)^2] = [x'(t)^2]/[x(t)^2] = \sum_{i=1}^{n} A_i^2 \omega_i^2(t) / \sum_{i=1}^{n} A_i^2$$

The normalisation element provides the weights of the individual spectral components to calculate a reasonable estimate of the immediate frequency.

The detection of radar targets in the frequency domain requires the immediate frequency at each time slot to be estimated. A moving window of a fixed number of range cells is shifted through the entire sweep. The immediate frequency for each window is calculated using the normalization technique as described. If the window size is made too large, frequency changes for small targets may be missed. However, a window that is too small will involve additional computation time as well as producing unwanted fluctuation of the frequency function due to random noise.

The slope of the distribution of the immediate frequency (i.e. the rate of change) may also be significant in detecting targets. A large slope will imply that there is a target embedded in the high frequency noise, or that there has been an abrupt change in the frequency of the noise. To remove any sharp slopes caused by random noise, the immediate frequency is averaged over several samples so that short duration changes of slope can be filtered out. So, in addition to considering the frequency response of returned signals the presence of a target may be confirmed by examining the rate of change of the immediate frequency. This can be achieved by differentiating the immediate frequency function and detecting

the slope change. Differentiation of a signal in the time domain is equivalent to multiplication of the signal's Fourier transform by an imaginary ramp function, i.e. passing the signal through a filter that has a response $H(\omega)=j\omega$.

The respective spatial and temporal characteristics of radar target signal and clutter are different to some extent on the return sweep. The targets have a lower frequency spectral component. The width of the distribution of clutter and noise is usually narrow and sharp, and this characteristic can easily be identified in the immediate frequency distribution. To detect these distinct features, thresholds on both frequency and width are applied to the incoming signal. The threshold for the frequency must be chosen so that the majority of the noise components are filtered, thus reducing the computation effort of the width detection in the next stage. As for the width threshold, the number of samples in the moving window contributes a crucial part in the value chosen. Further observation and analysis is required in order to optimize this process. This would compare returns obtained under various clutter, noise and target characteristics with respect to their width in the immediate frequency function.

By looking at the amplitude alone, it may be difficult to discriminate the targets from the noise and clutter. The signal can be converted into the frequency domain by taking the discrete Fourier transform of the sweep. New architectures of high throughput and real time Fast Fourier Transform processors have been developed for radar signal processing (Bungard, Lau and Rorabaugh 1989). A trace of the Fourier transform for a window that contains noise alone is plotted in Fig. 3.9, this will be used as a benchmark against which to compare the frequency spectrum for traces which contain signals of targets. It can be observed that the frequency distribution for the noise alone is fairly constant at all

frequencies. It was thought that targets would have some different features in the frequency domain when compared with noise. Figures 3.10 and 3.11 show the frequency characteristics of the window containing target and land clutter respectively. It has a smooth frequency distribution and is similar to the Fourier transform of a triangular wave, while that of the land clutter resembles a sync function, i.e. the Fourier transform for a square wave. The peak frequency components of the noise are equally distributed along the whole frequency spectrum. Using these features for discrimination, it is possible to develop the immediate frequencies of the radar return, which are able to extract the targets from the noise and clutter in the background. Observation windows are established and the magnitude of individual spectral components within each window is obtained by taking the fast Fourier Transform. The immediate frequency is estimated by means of the normalization technique. Figure 3.12 shows a plot of the immediate frequency of the return echo at various time frames during a sweep. The landclutter has distinct characteristics of low variation in frequency and low frequency components. The target has a constant slope in its falling and rising edges and a lower frequency. To determine the threshold for the frequency and width of the detection algorithms, the immediate frequency function for a frequency for a sweep with only random noise is used for comparison and this is shown in fig. 3.13. To compromise in allowing for weak targets against time spent processing data, and thus provide efficient detection, upper and lower thresholds are set.

3.6 Conclusion

The characteristics of radar signals and methods for the extraction of features in the time domain have been discussed in this chapter. During a full rotation of the radar antenna, a variety of return characteristics may be observed. For example, when operating in coastal

regions, very low clutter may be seen in the seaward sector and significant clutters due to the land sea interface and reflections may be received in other sectors. Targets and clutters have unique features in their statistical characterization over a finite window. These can be extracted for discrimination purposes. Radar return signals, which have been reflected by different objects, possess unique features when correlated with other waveforms. When the received signal is correlated with a square pules of similar pulse width, the signal to noise ratio is much improved. Radar pulses are transmitted at fixed time intervals and correlation of the targets between different sweeps reduces the amplitude of random noise. This is easily removed by the sweep to sweep correlation process. The use of high order correlation, which performs the correlation between correlated results of two consecutive sweeps, further suppresses the partially correlated clutters. The time frequency characteristics can also be used to achieve effective target detection. To study such characteristics, the instant frequency value of the signal at any specific time of the sweep is estimated using a normalization technique.

The statistical characterization, correlation, and time-frequency characteristics can be extracted from radar waveforms to determine if a target is present. In a very complicated environment, e.g. boundaries between the sea and land, the sea clutter may have certain similar characteristics when compared with the targets. However, it is unlikely to have similarities in all these parameters, i.e. in a multi-dimensional space. These parameters themselves are extracted from moving windows along the radar return and can be fed into an information fusion process for making the final decision. Thus, the detection process is not based solely on the magnitude of the radar echoes and will provide a more reliable technique for discrimination in target identification and tracking algorithms.

Fig 3 1a Random Noise of a Typical Radar Return

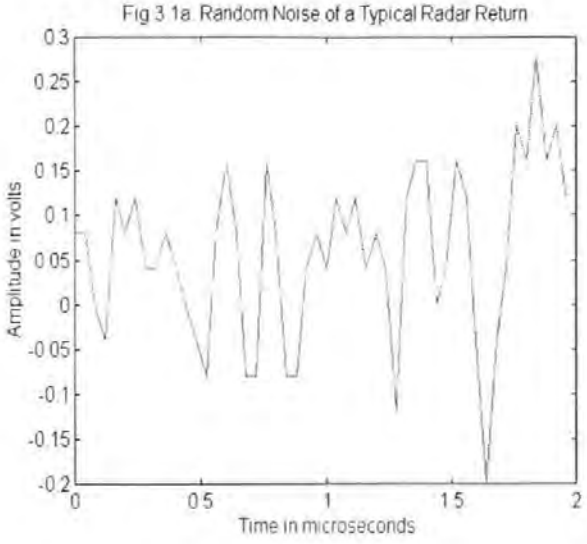

Fig. 3.1b Statistical Distribution of Random Noise

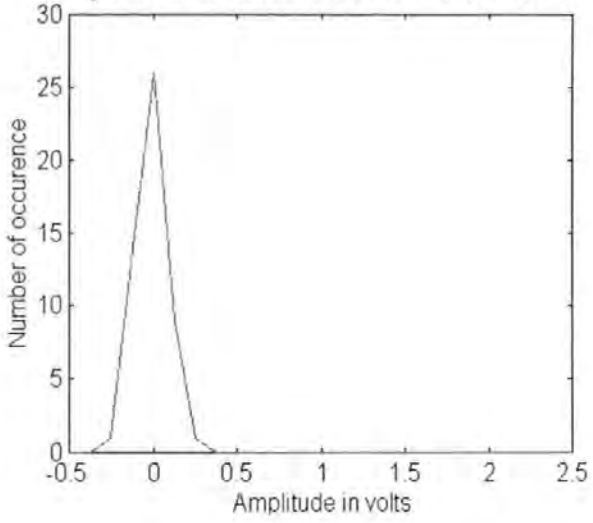

Fig 3 2a Radar Return of a Marine Vessel

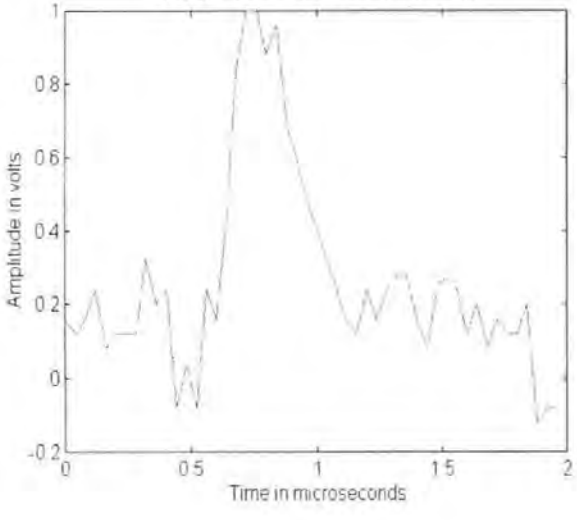

Fig 3 2b Statistical Distribution of a Radar Target

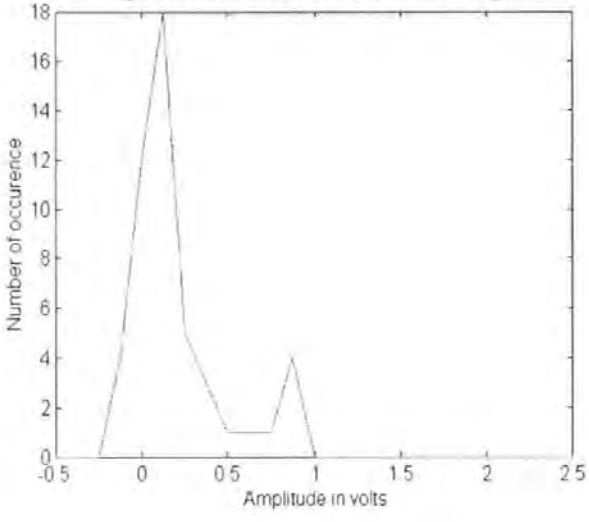

Fig 3 3a Sea Clutter Signal

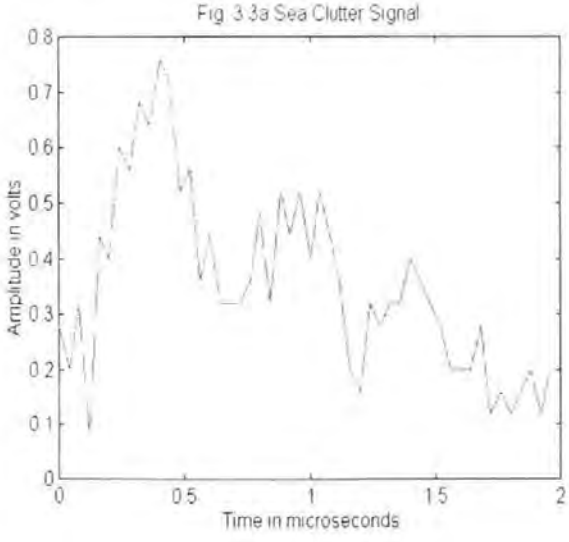

Fig 3 3b Statistical Distribution of Sea Clutter

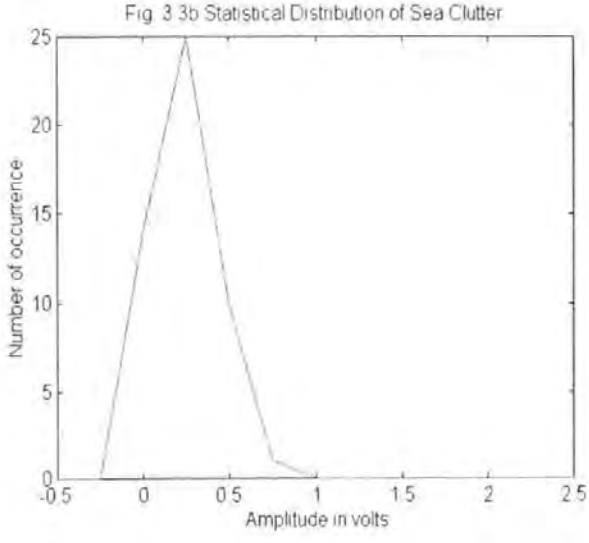

Fig 3 4a Rain Clutter in a Radar Return

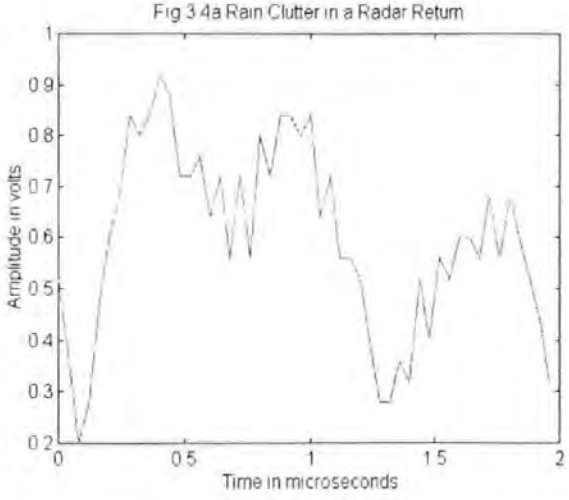

Fig. 3 4b Statistical Distribution of Rain Clutter

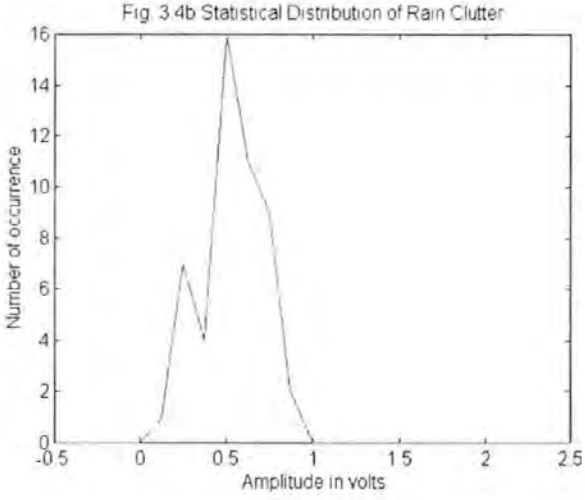

Fig 3 5a A typical Radar Return with Signal Being Embedded in Noise

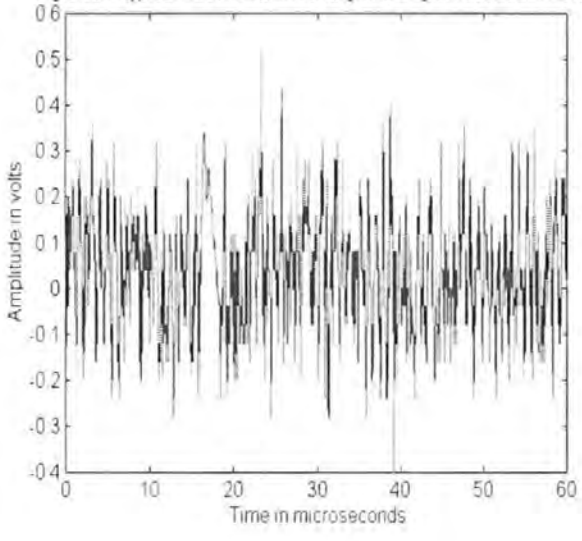

Fig 3 5b The Radar Return after correlating with a square pulse

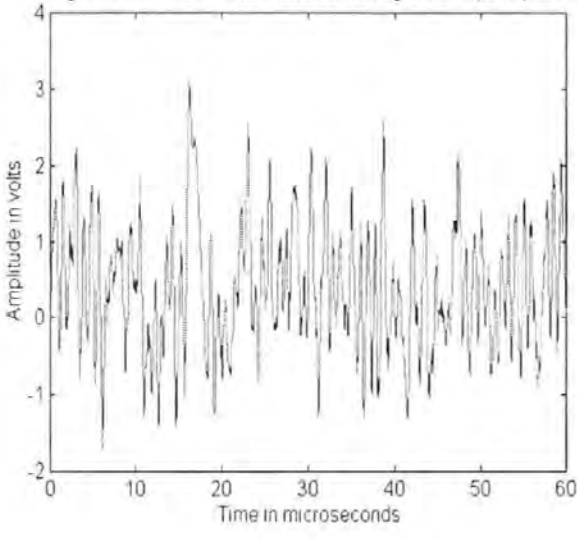

Fig 3 6a Radar Return in N Sweep

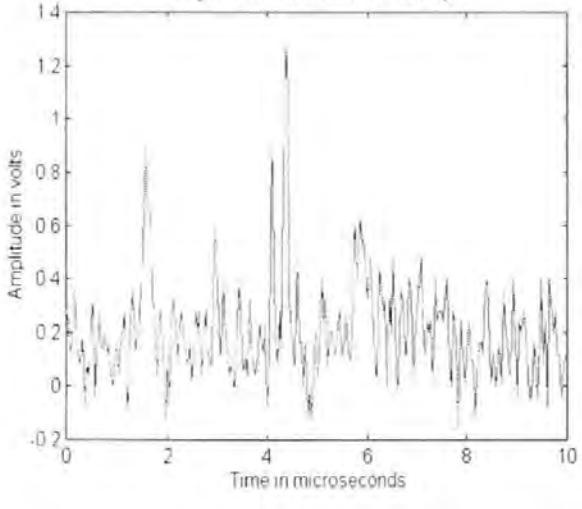

Fig 3 6b Radar Return in N+1 Sweep

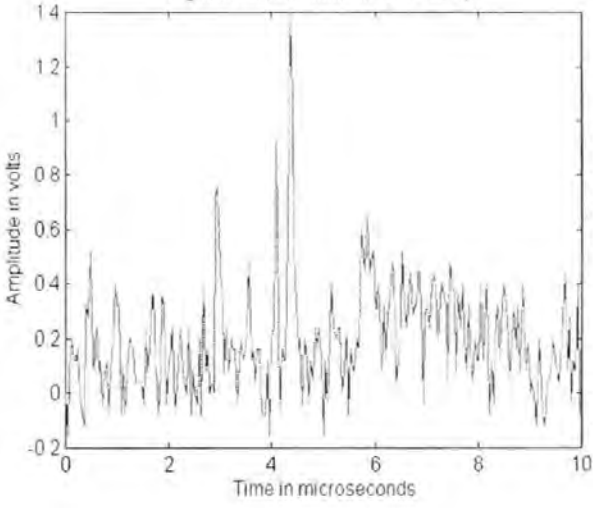

Fig 3.6c Radar Return in N+2 Sweep

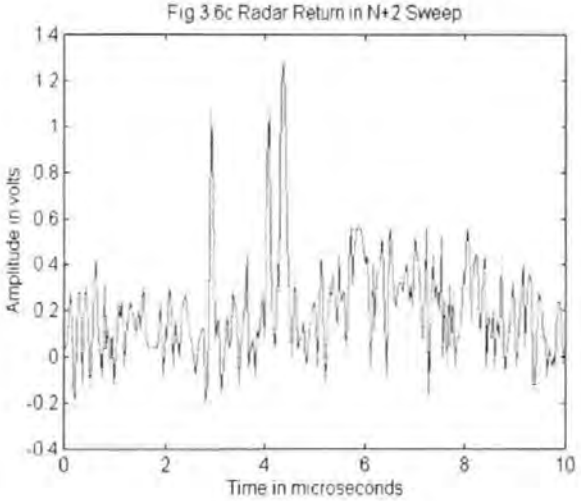

Fig 3.7a Correlation of N and N+1 Sweeps

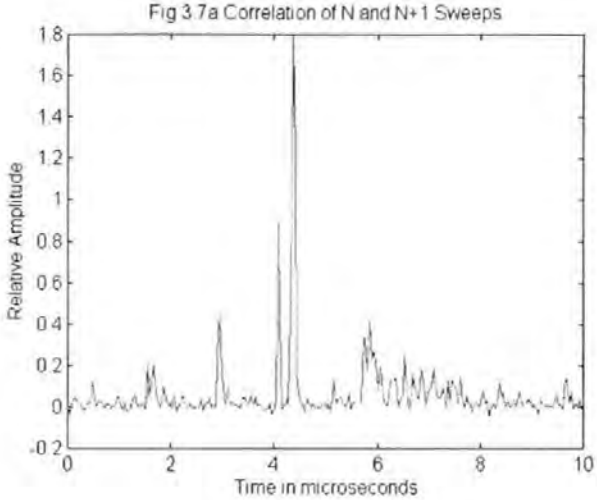

Fig 3.7b Correlation of N+1 and N+2 Sweeps

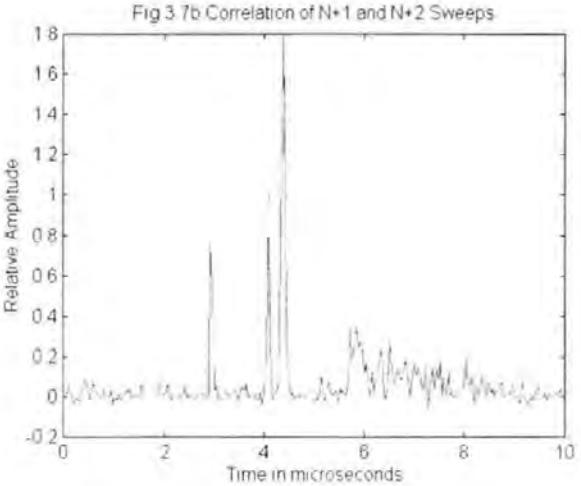

Fig 3.8 Correlation of N/N+1 and N+1/N+2 Sweeps

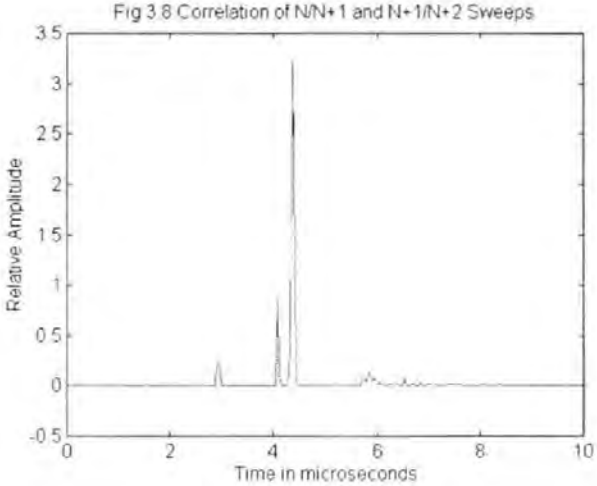

Fig 3.9 Frequency Spectrum for a Window with Noise Only

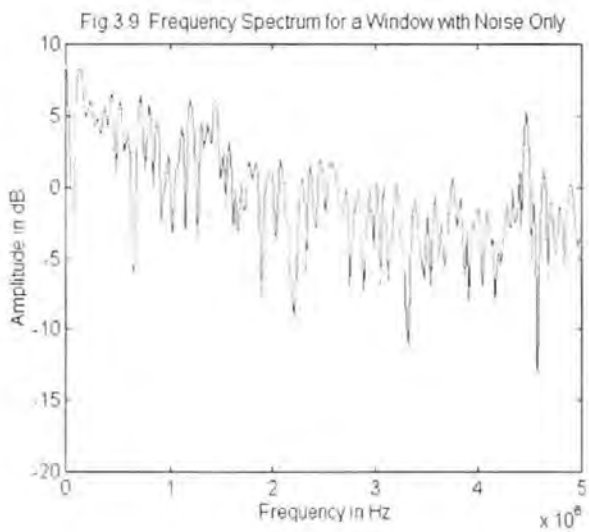

Fig 3.10 Frequency Spectrum for a Typical Target

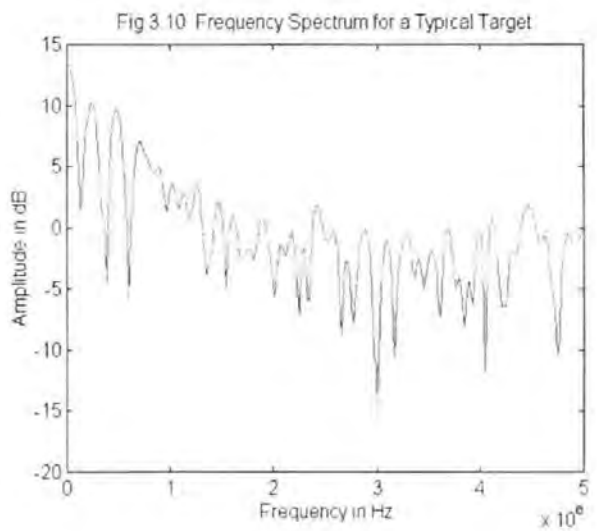

Fig 3.11 Frequency Spectrum for a Window with Landclutter Target

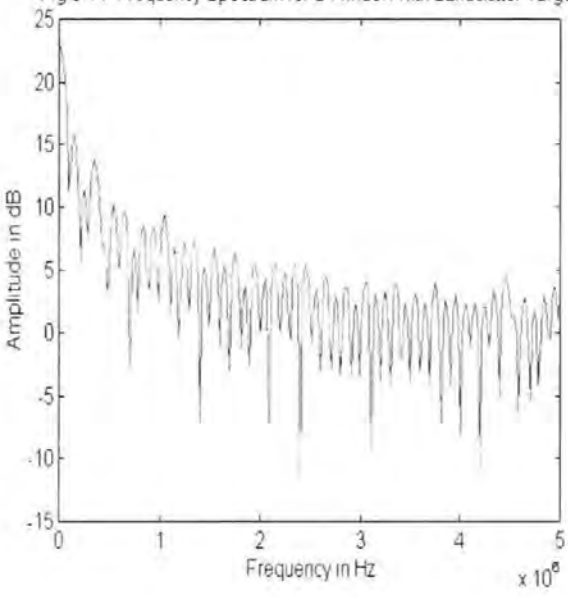

Fig 3.12 Immediate Frequencies for a Typical Sweep

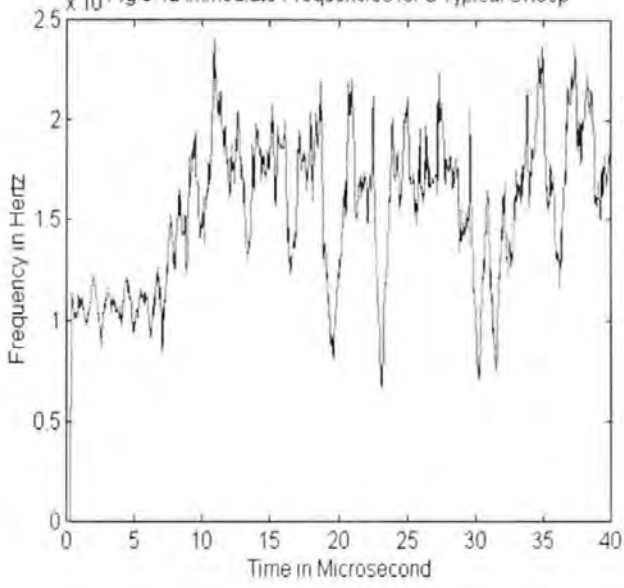

Fig 3.13 Immediate Frequencies for a Typical Sweep with noise only

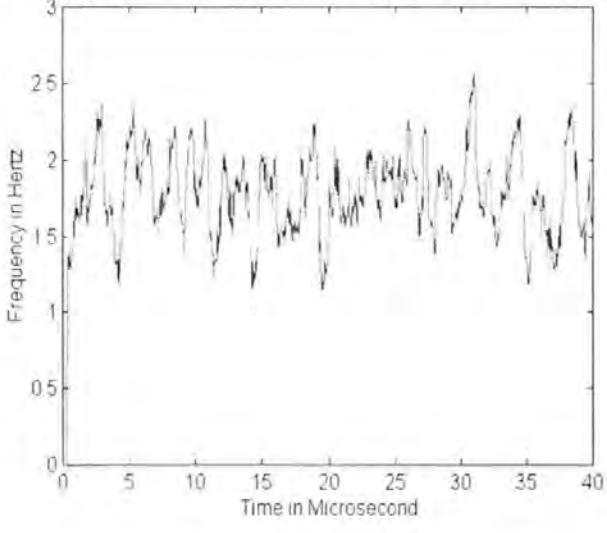

CHAPTER FOUR

DATA FUSION TECHNIQUES IN RADAR SIGNAL PROCESSING

4.1 Introduction

Methods for the extraction of useful information from the radar signal were developed and discussed in the last chapter. The next step is to identify methods which can relate the extracted information to a final decision on whether a target is present. Data fusion has been a new strategic research field which deals with the incomplete and sometimes incoherent information derived from different sources. This is the case of many important application areas such as target acquisition (Luperman, 1994), image processing (Zhou, 1994), feature extraction (Abdulghafour, Chandra and Abidi, 1993), computer vision (Tahani and Keller, 1990), and defense systems (Maloney, 1989). Processing extracted data requires a technique capable of addressing a very demanding issue, i.e. making decisions in uncertain conditions. Since the individual information extracted from the radar signals can be distorted, noisy and vague, adequate data fusion techniques must be developed in order extract the essential information which is not recognisable in any of the single sets of data. Hall (1992) provides an extensive overview and a description of classical data fusion techniques. These focus on the identity fusion algorithms based on feature extraction and identity declaration. One method of dealing with such task requires ideas from the advanced research in machine intelligence. Knowledge-based approaches are able to perform data fusion in intelligent multisensor instrumentation. However, imprecision represents a very critical issue for such knowledge-based systems as they are generally inadequate for dealing with the intrinsic vagueness of input sensor data and very poorly suited to directly process input sensor data (Russo, 1994). On the other hand, fuzzy systems and neural networks offer the best solutions

to this type of applications (Kosko, 1992). Both fuzzy and neural network approaches, which numerically process knowledge, are particularly well suited to manage uncertainty and are becoming powerful technologies with a growing range of applications. This chapter describes how these two techniques are used in the data fusion of the extracted features from the radar signal and their comparison is also discussed.

4.2 Fuzzy Approach to Data Fusion

The concept of fuzzy sets addresses problems in which imprecision is an inherent aspect of a reasoning process. Fuzzy reasoning allows the processing of problems to be expressed in the form of rules which resemble the mechanism of human decision making. Indeed, one of the key features of fuzzy logic is its ability to deal with the typical uncertainty which characterizes any physical system (Zadeh, 1965). This is a very critical task because the information acquired from different sources can be incomplete and even conflicting. Fuzzy networks are usually structured in the form of rules that permit a clear understanding of their operation. Russo (1994) has reported the fuzzy techniques represent a comprehensive framework for intelligent instrumentation that deals with multisensory input data. One of this author's papers describes the development of fuzzy algorithms for a microprocessor based servomotor controller (Li and Lau, 1989).

4.2.1 Fuzzy Set Theory

A fuzzy set A with an element x has a membership function of $\mu_A(x)$ and is in the interval between 0 and 1. If $\mu_A(x)$ is 1, then the element is a member of the set. Alternatively, if $\mu_A(x)$ is 0, then it is not. Consider a fuzzy set A with five elements, which have the membership function of 0.7, 0.9,1, 0.9,0.7. The element with a membership function of 1 is a full member of A, whereas

the other are only part members. The membership function determines the degree to which the element belongs to the subset. If a fuzzy set A is defined as "around 10 volts" on a scale from 9 to 12, it can then be described by the following:-

A = (0.7/8, 0.9/9, 1/10, 0.9/11, 0.7/12)

Where 0.7,0.9 and 1 are the membership functions and 8, 9, 10, 11 and 12 are the universe of discourse. The following three definitions form the basis of the fuzzy algorithms.

1. The union of two sets, $A \cup B$, corresponds to the OR function and is defined by

   $\mu(A \text{ OR } B) = \max(\mu_A(x), \mu_B(x))$

2. The intersection of two sets, $A \cap B$, corresponds to the AND function and is defined by

   $\mu(A \text{ AND } B) = \min(\mu_A(x), \mu_B(x))$

3. The complement of a set A corresponds to the NOT function and is defined by

   $\mu(\text{NOT } A) = 1 - \mu_A(x)$

To establish the fuzzy algorithms, it is necessary to interpret rules that are based on experience so as to give the output values that corresponding to situations of interest. A fuzzy rule consists of situation and action pairs, and they are expressed in IF and THEN statements. For example, if the signal has a high amplitude and its pulse width is wide, then it is likely to be a target. Such a rule has to be converted into a more general statement for application to fuzzy algorithms. First, the qualitative statements must be quantized into linguistic sets such as, large, medium, small and zero. The statement can then be converted into, 'If the signal amplitude is large and the pulse width is large, then the possibility that this is a target is high'.

Having formulated the rule in fuzzy terms, the next step is to define the membership functions of the linguistic sets. The shape of the fuzzy set is quite arbitrary and depends on the user's preference. Trapezoidal and triangular shapes are usually used because of simplicity. The membership functions representing the decisions are weighted according to the corresponding input statements. A pair of input parameters may fire more than one rule. To determine the value of the final decision from these contributions, the centre of the summed area, which is contributed by individual rules, is evaluated. This can be expressed in mathematical terms as follows:-

$$O = \sum_{1}^{n} (\mu_n \times U_n) / \sum_{1}^{n} \mu_n$$

where μ is the membership function, U the universe of discourse, n the number of contributions and O the output.

4.2.2. Fuzzy Algorithms for Data Fusion in Radar Signal Processing

A radar signal at specific time frames can be identified as a member of a class of signals on the basis of M different features of the waveform. Suppose that all the available information is acquired from N sweeps of the same scan. A fuzzy statement is formulated, which yields the degree of membership m of the input data.

$$m = \{(F_{11}) or (F_{21}) or \ldots\ldots\ldots (F_{N1})\} AND \{(F_{12}) or (F_{22}) or \ldots\ldots\ldots (F_{N2})\} \ldots\ldots AND \{(F_{13}) or (F_{23}) or \ldots\ldots (F_{NM})\}$$

Where $F_{ij}(1 \leq i \leq N,\ 1 \leq j \leq M)$ is the jth feature extracted from the signal from the ith sweep. The fuzzy connective logic OR is used to combine all the available information about the same feature. It maximises all the information about the same feature coming from different sweeps. On the

other hand, the choice of fuzzy connective logic AND is used for linking information about all the features makes the identification of a target. Then a fusion of information related to the same feature but derived from different sources can be performed.

$$m_j = \{(F_{1j})OR(F_{2j}).....OR(F_{Nj})\}$$

The membership function of all contributions $m_j(1 \leq j \leq M)$ can then be fused together to obtain the final degree of membership.

$$m = AND\{m_j : j = 1,.....,M\}$$

Consider the task of identifying targets from a number of radar return signals recorded at the Plymouth Harbour, each consists of 50 samples. It is necessary to write a set of fuzzy rules based on the features of the input signals. To recognise the presence of the target, the features of mean pulse width (w) and mean amplitude (v) from each signal are extracted using the method as discussed in the previous chapter. The output is the membership function which shows the possibility of the signal being a target. Table 4.1 shows the membership matrix table for the membership functions.

Table 4.1. Membership Matrix Table

Linguistic sets	**Quantized levels**							
w (microseconds)	**0.5**	**1**	**1.5**	**2**	**2.5**	**3**	**3.5**	**4**
v (volts)	**0.5**	**1**	**1.5**	**2**	**2.5**	**3**	**3.5**	**4**
output	**0**	**1**	**2**	**3**	**4**	**5**	**6**	**7**
Large	0	0	0	0	0	0	0.6	1
Medium	0	0	0	0	0.6	1	0.6	0
Small	0	0	0.6	1	0.6	0	0	0
Zero	0.6	1	0.6	0	0	0	0	0

The quantized levels for v and w are from 0 to 0.4 volts and 0 to 4 microseconds.

Nine fuzzy rules are formulated for this application.

1. If v is large and w is large then the possibility of signal being the target is large.
2. If v is large and w is medium then the possibility of signal being the target is medium.
3. If v is large and w is small then the possibility of signal being the target is small.
4. If v is medium and w is large then the possibility of signal being the target is medium.
5. If v is medium and w is medium then the possibility of signal being the target is small.
6. If v is medium and w is small then the possibility of signal being the target is zero.
7. If v is small and w is small then the possibility of signal being the target is zero.
8. If v is small and w is medium then the possibility of signal being the target is small.
9. If v is small and w is large then the possibility of signal being the target is medium.

Rule 1 implies the ideal condition where a signal with both large amplitude and large pulse width is received. The signal is likely to be the target. Rule 7 shows a condition where signal amplitude and pulse width are both small. There is high possibility that the signal is noise. These rules are developed based on the experience of observing the waveforms from detected targets. Suppose a radar signal with a mean amplitude of 0.34 and a mean pulse width of 3.4 is applied to the fuzzy network. According to the range specified, only rules 1, 2, 4 and 5 will be fired, and the output would be contributed by these four rules as follows:-

$$O = \frac{0.5 \times 7 + 0.75 \times 5 + 0.5 \times 5 + 0.75 \times 3}{0.5 + 0.75 + 0.5 + 0.75} = 4.8$$

It is important to note that in this specific input, no contribution is given by rules 3, 6 and 7. Figures 4.1 and 4.2 show the graphical representation of rule no. 5 and the output respectively.

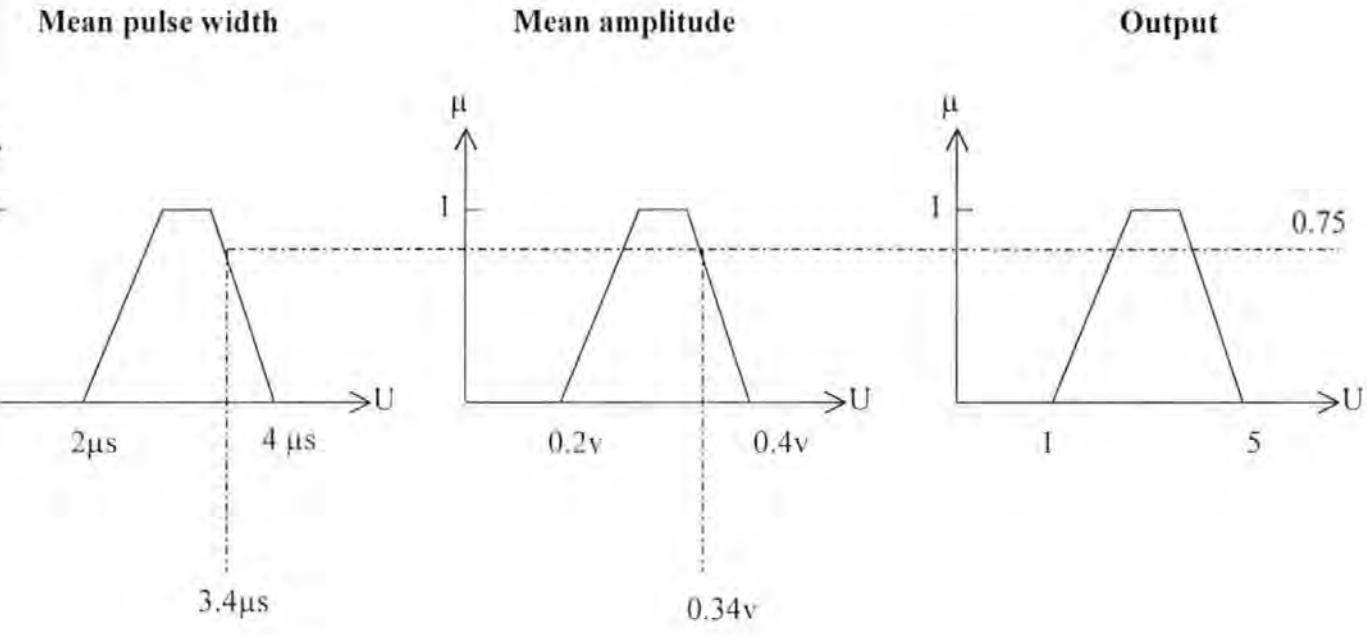

Fig.4.1 Graphical representation of rule no.5

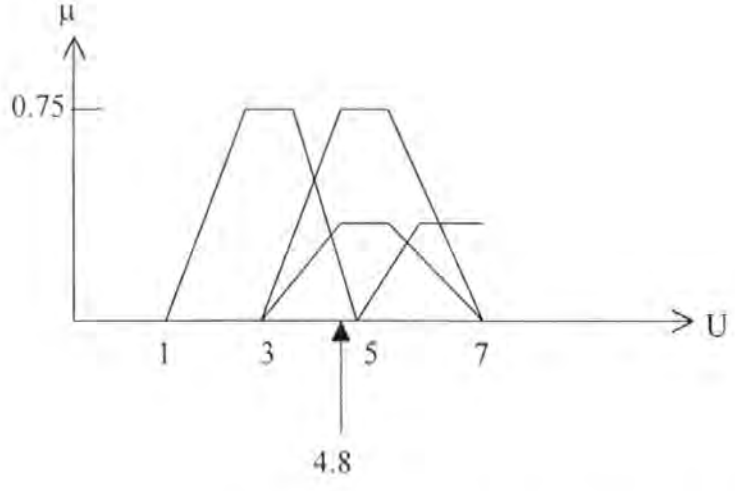

Fig. 4.2 Determination of the output from a set of rules

Since the maximum quantized level is 7, the normalised value of the output is 0.68, which indicates that the signal is likely to a target. A similar calculation is done on 6 signals that consist of four targets and two noise data. The targets have a relatively low amplitude when compared with the two noise signals. This makes the detection using amplitude information extremely difficult. One of the noise data is having a wide pulse width. The objective is trying to test the integrity of the fuzzy algorithms in these extreme conditions and the result is shown in table 4.2.

Table 4.2 Testing Sets for Fuzzy Network

Features of input signals		Desired Output	Normalized Output
Mean Amplitude	**Mean Pulse Width**		
0.40	3.2	target	0.76
0.28	4.0	target	0.71
0.34	3.4	target	0.68
0.37	4.0	target	0.64
0.38	1.8	noise	0.37
0.28	3.4	noise	0.55

It can be seen from the table that the targets have a high membership function at the output. By applying a corresponding threshold to such membership value, the targets can be extracted from these radar signals.

4.3 Data Fusion in Neural Networks

Data fusion combines information from several sources, typically sensors, towards a representational estimate. For example, the different information extracted from a single sensor

can be combined to give a more reliable output. The fusion of various information can reduce overall uncertainty and thus increase the accuracy with which the features are perceived by the system. The information provided by different sources can also serve to increase reliability in the case of error or failure of one information source. The complementary information from multiple sources allows different features in the system to be perceived (Luo and Kay, 1989).

An artificial neural network can be defined by a set of processing elements called neurons, a specific topology of weighted interconnections between these elements, and a learning law which updates the connection weights. Neurons provide non-linear input/output transfer functions. Data fusion techniques that adopt neural networks have a number of advantages. The first is adaptive fusion inference in which neural networks can infer the relationship between the desired fusion output and the multi-source input. The second is generalisation from an incomplete set of information. This is useful when the information from an individual source is noisy or distorted. The third is non-linear filtering of noise. Neural networks are nonlinear so they can perform more complex functions than linear filters. The fourth is parallel computing, since the neurons in neural network function in parallel and they can process information from multiple sources simultaneously.

4.3.1 **Neural Network Theory**

A neural network is an information processing system that operates in an intensely parallel mode. It consists of highly interconnected neurodes that are connected by a large number of weighted links, over which signal passes. A neurode receives input stimuli along its input connections and translates those stimuli into an output response, which is transmitted along the

neurode's output connection (Caudill, 1992). The output signal transmits over the neurode's outgoing connection and splits into a very large number of smaller connections, each of which terminates at a different destination. Most of these outgoing branches terminate at the incoming connection of some other neurode in the network, others may terminate outside the network and generate control or response patterns. The mathematical expression that describes the translation of the input pattern of signals at specific time frame to the output response signal consists of a three-step process. First, the neurode computes the net weighted input that it receives along its input connections. It computes the value of I_j as shown below:

$$I_i = \sum_{j=1}^{n} w_{ij} x_j$$

In this expression, I_i is the net weighted input received by neurode i from a total of n neurodes in the network. The incoming signal from the jth neurode is designated by x_j, and the weight on the connection directed from neurode j to neurode i is designated by w_{ij} (Caudill, 1992). Once the input signal pattern I is computed, all information about the amplitude of the input signal will be lost. Depending on the values of the weights, a strong input signal arriving over a weakly weighted connection may have less effect than a weaker signal arriving over a strongly weighted connection. A negative weight will reduce the overall stimulation of the receiving neurode.

The translation represented by the neurode's transfer function consists of converting the input signal pattern to an activation level for the neurode. The activation level of the neurode is equivalent to the level of excitement of a biological neuron. In most cases, the activation

function is a sigmoid function, i.e. the activation is expressed by an S-shape curve. The commonly used sigmoid function is:

$$f(I) = \frac{1}{1 + e^{-I}}$$

With a derivative of :

$$\frac{df(I)}{dI} = f(I)(1 - f(I))$$

The exact form of the sigmoid function is not particularly important, however, the function should be monotonically increasing and bounded with both lower and upper limits. In the case of f(I), the minimum value of f(I) as I approaches negative infinity is 0, and the maximum value of f(I) as I approaches positive infinity is 1.

The final step accomplished by the transfer function is to convert the neurode's activation level to an output signal. Most commonly, this is achieved by setting the output signal to the following expression:

$$y_i = \{ \begin{matrix} f(I), & if[f(i) > T] \\ 0, & otherwise \end{matrix} \}$$

T is a threshold value. The neurode's output is its activation level as long as that activation value exceeds a given threshold.

When a neural network is presented with a signal pattern, each neurode in the input layer of the network receives a small piece of the pattern. Each of the middle-layer neurodes thus receives

the entire input pattern, but the pattern is modified by its passage through the weighted connections leading to the middle layer. Since the weights on the connections are typically different for each middle-layer neurode, each of these neurodes sees a somewhat different version of the input pattern than its neighbours do, i.e. it sees a projection. This results in a variety of output reponses from the middle-layer neurodes, ranging from no output at all to one, possibly with an extremely strong output. Figure 4.3a illustrates the physical connections of a typical neural network.

Learning of the neural network is achieved not by modifying the neurodes in the network but by modifying the weights on the interconnections in the network. The output of each neurode is determined by a function of the incoming signals and the weights on the input connections to the neurode. Learning consists of making systematic changes to the weights in order to improve the network's response performance to acceptable levels. The network is provided with an input stimulus pattern along with the corresponding desired output pattern. The common learning law typically computes an error, i.e. how far from the desired output the network's actual output really is. This error is then used to modify the weights on the interconnections between the neurodes (Demuth and Beale, 1993).

4.3.2 Neural Networks for Data Fusion of Radar Signal

Neural network consists of parallel distributed processing elements that are interconnected by links. By defining the associated weights for each of the interconnections, it is possible to process data in a very rapid manner. This technique provides the potential to process radar information in real time. The difficulty of choosing an appropriate neural network architecture

Fig. 4.3a A typical neural network architecture

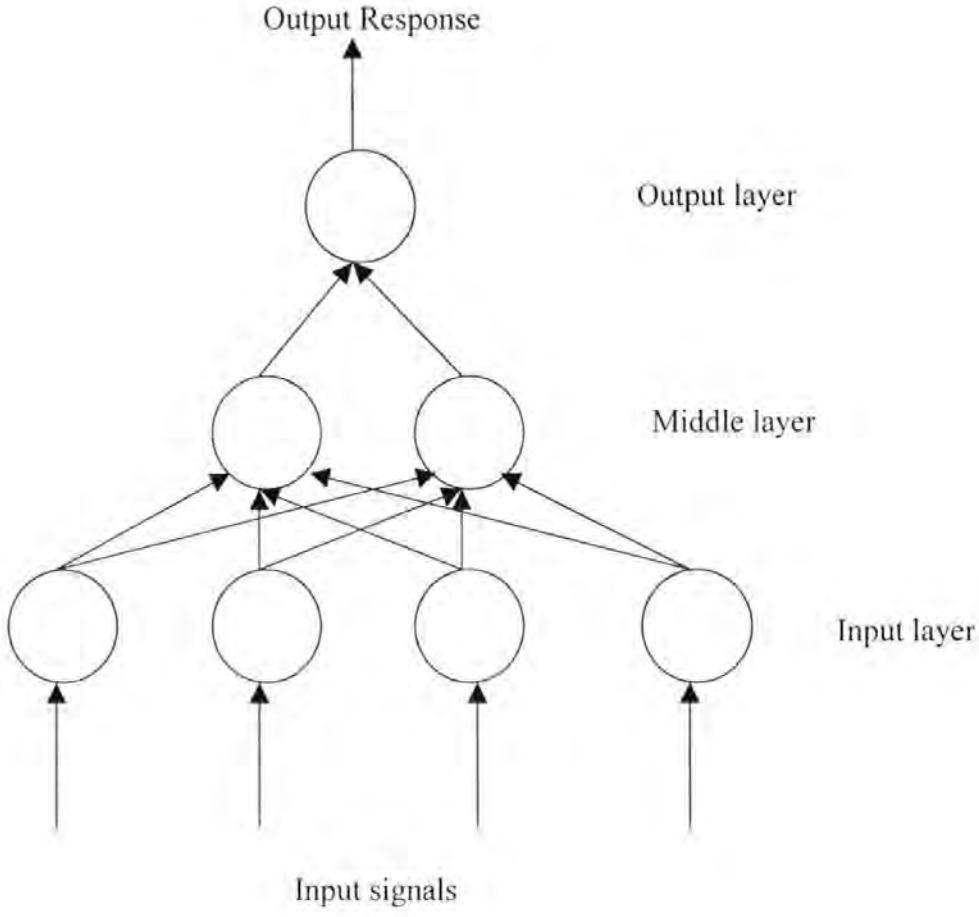

for data fusion of radar signal processing is one of matching the problem domain with the network features. This includes the problem size (i.e. number of input features and processing elements, number of outputs), the form of data (continuous, time-varying, uncertain), and incomplete knowledge about the system parameters.

The simplest format which can be applied to information fusion is a single layer network (figure 4.3b) whose weights and biases could be trained to produce a correct target vector when presented with the corresponding input vector. The perceptron has a hard limit transfer function (Caudill, 1992). Each external input is weighted with an appropriate W, and the sum of the weighted inputs is sent to the hard limit transfer function, which also has a bias input. The transfer function classifies the input vectors by dividing the input space into two regions. Output vectors will be either 0 or 1. The learning rule is applied to each neuron in order to calculate the new row of the weight matrix and a new neuron bias. The learning rule will converge to a solution in finite time if a solution exists. Vectors from a training set are presented to the network one after the other. If the network's output is correct no change is made. Otherwise the weights and biases are updated using the learning rule. When an entire pass of the training set has occurred without error, training is complete. At this time any input training vector may be presented to the network and it will respond with the correct output target vector. If a vector is not in the training set and is presented to the network, the network will tend to exhibit generalisation by responding with an output similar to target vectors for input vectors close to the previously unseen input vector.

The network first presents the matrix of input vectors and calculates the network's matrix of output vectors. Then it will check to see if each output vector is equal to the target vector associated with each input vector. The training process will stop if all input vectors have generated the correct output vectors for a specific set of weights and biases, or after a maximum number of epochs. If not, it will adjust the weights and biases and then return to the presentation phase. The mathematical model can be expressed as:

$W_{new} = W_{old} + \beta yx$

where $\beta = 0$ if the perceptron's answer is correct

$\beta = -1$ if the perceptron's answer is wrong

y = the perceptron's answer

Consider a simple information fusion problem of 24 radar signals that are recorded by the author using the radar at the University of Plymouth. The objective is to classify these signals into targets and noise. To achieve this, both the amplitude mean and maximum pulse width have already been extracted from the radar signals and these are served as input vectors to the network. In the training process, a 1 is assigned to targets and 0 to noise. The input vectors for the problem are plotted in fig. 4.4. The targets are marked with an 'o' and the noise is marked with a '+'. A network with two inputs, i.e. amplitude and pulse width, and one neuron is trained to distinguish between targets and noise. The initial conditions for the weights and bias are generated from a random numbers. The result of the training is shown in fig. 4.4 where the network adjusts its weights and bias to classify the input space into targets and noise. A boundary line separates the two regions. The final values of weights and bias were obtained after training for 1700 epochs (W = [219.5580 7.5843]; B=[-51.0778]).

Fig. 4.3b A perceptron with two inputs

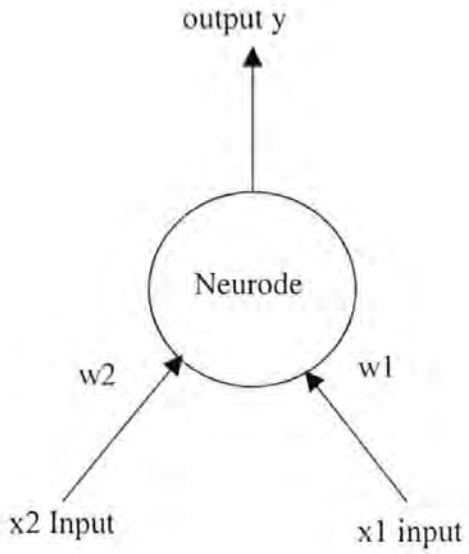

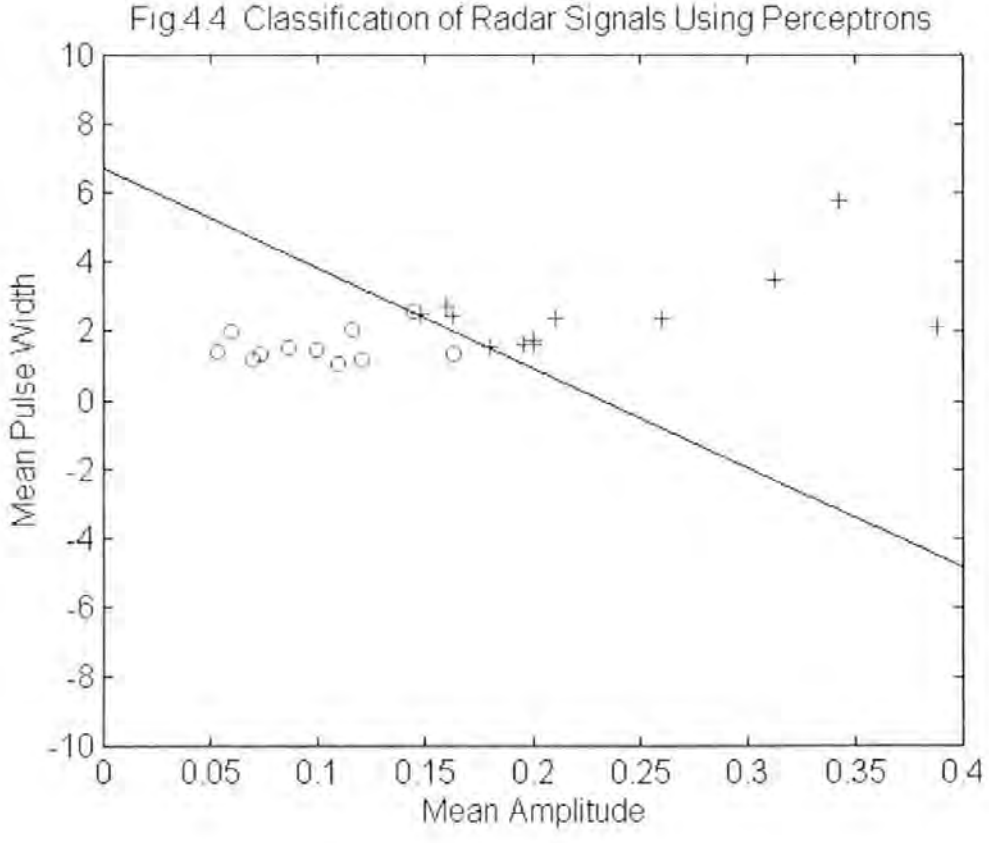

Perceptrons are only good for solving real world problems when data is linearly separable. However, it is seldom the case. The development of the backpropagation training algorithm in the 1970s and early 1980s demonstrated that training procedure was possible for a network of three or more layers. A backpropagation network operates in a two-step sequence during training. First, an input pattern is presented to the network's input layer. The resulting activity flows through the network from layer to layer until the network's response is generated at the output layer. Then, the network's output is compared to the desired output for that particular input pattern. If it is not correct, an error is generated, which is propagated backward through the network to the input layer. The weights on the interlayer connections are modified as the error passes backward based on the learning rules. Changes in each weight and bias are proportional to the pattern of the network's sum squared error. When the network is well trained, a new input will lead to an output similar to the correct output for input vectors used in the training. Such characteristic facilitates the training of a network on a representative set of input/target pairs as well as obtaining good results for new inputs, without training the network on all possible input/output pairs (Fincher, 1990).

Backpropagation networks often use the sigmoid transfer function, which generates outputs between 0 and 1 as the neuron's net input goes from negative to positive infinity. The use of the bias tends to increase the chances that the network can find an acceptable solution and also tends to decrease the number of training epochs required. It is quite usual that the backpropagation networks have one or more hidden layers of sigmoid neurons followed by an output layer of linear neurons. Multiple layers of neurons with nonlinear transfer functions allow the network to learn nonlinear and linear relationships between input and output vectors.

Derivatives of error are calculated for the network's output layer and then backpropagated through the network until the errors are available for each hidden layer. The change to be made in a layer's weights and bias are calculated using the layer's error vectors and the layer's input vector according to the backpropagation rule. Before starting the training process, all the weights and bias must be initialised to small random numbers to ensures that the network is not saturated by large values. Training the backpropagation network requires the selection of the training parameter and application of input vector to the network input. Then both the output of the network and the error are calculated. The weights of the network are adjusted to minimise the error. The generalised rule specifies the change in a given connection weight as:

$$W_i = \beta E f(I)$$

E is the error for this neurode, β is the learning constant (between zero and one), and f(I) is the input to the neurode. The process is then repeated until the error or the convergence of the entire network is to an acceptable level as specified.

Consider the same fusion problem in which a group of 6 radar signals (4 targets and 2 noise signals) are input to the network for target detection. The backpropagation network is designed and trained to discriminate the target from clutters. The network consists of one input layer with 2 elements, one hidden layer with 2 neurons and one output layer as shown in figure 4.5. Both the mean amplitude and mean pulse width are extracted from these 6 radar signals and used in training the network. It will then be required to identify the target by responding a 1-element output vector. The network should output a 1 if there is target presented in the signal

and output a 0 otherwise. The maximum error of 0.05 is used as the limit for the training. The network completes the training after 1220 iterations. Once the network is trained, a testing set is used to evaluate the performance of the network. The set consists of mean amplitudes and mean periods extracted from 6 radar signals (4 targets and 2 noise signals) which are not used in the training. Table 4.3 and table 4.4 show the training data and the testing result respectively. From the table, it can be observed that the normalised outputs of the network are 0.9702 to 0.9788 for target, and 0.0154 to 0.0378 for noise signals respectively. As such, a significant discrimination is achieved and the network is able to detect the targets from the radar returns effectively in this example.

Fig. 4.5 A three layer backpropagation network

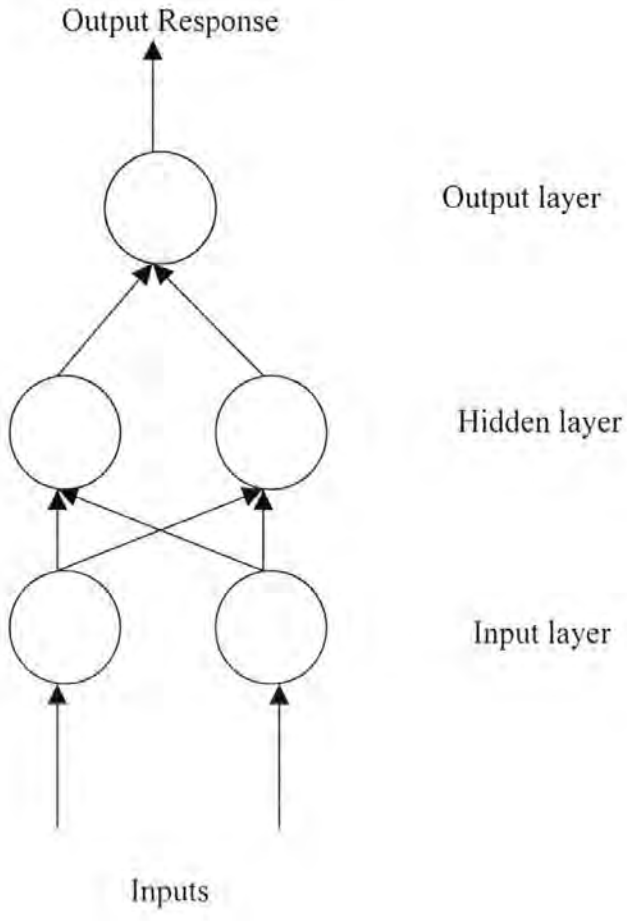

Table 4.3 Training Sets for the Neural Network

Features of input signals		Desired Output
Mean Amplitude	**Mean Pulse Width**	
0.40	3.2	target
0.28	4.0	target
0.34	3.4	target
0.37	4.0	target
0.38	1.8	noise
0.28	2.4	noise

Table 4.4 Testing Sets for the Neural Network

Features of input signals		Desired Output	Normalized Output
Mean Amplitude	**Mean Pulse Width**		
0.34	3.4	target	0.9767
0.33	3.0	target	0.9702
0.24	3.0	target	0.9755
0.28	4.0	target	0.9788
0.4	1.7	noise	0.0378
0.29	2.0	noise	0.0154

4.4 Conclusion

Data fusion techniques in radar signal processing using both fuzzy logic and a neural network have been discussed in this chapter. The performance of these methods is verified by applying signals from live radar videos to the network and observing the results. Fuzzy and neural systems do not require mathematical models to estimate functions from sample data. Neural network theory includes the mathematical fields of dynamical systems, adaptive control as well as statistics. Fuzzy theory adds probability, logic and knowledge base into these fields.

The architectures of neural networks are parallel and consist of many simple nonlinear summing junctions connected together by weights of varying strength. It has been shown in this chapter that even a simple network can perform interesting and useful computations in data fusion of radar signals for target detection. Perceptrons can classify linearly separable input vectors very well. However, the output values of a perceptron can take on only one of two values due to the hard limit transfer function. If the vectors are not linearly separable, learning will never reach a point where all vectors are classified properly. Backpropagation is slow because of small learning rates and there are a large number of variables in multi-layered networks. Yet, the multi-layer perceptron can perform linear or nonlinear computations. In the example, a three layered backpropagation network can successfully identify the targets from clutters as shown in table 4.4.

Fuzzy systems generally offer the advantage of a clear understanding of the operation as they can structure the knowledge in a way that resembles human thinking. The objective of the example is to recognise the presence of targets in radar signal. The pattern is composed of two

features (mean amplitude and mean pulse width for each radar signal) whose relative strengths are characterized by the corresponding membership function. The strength of each feature in the signals is obtained to calculate the overall degree of membership of the available information to the defined class of target. From these numerical values, the presence of the pattern of targets is more clearly defined.

There are significant differences, as well as similarities, between neural networks and fuzzy systems. Neural networks learn from the training data to recognise future patterns or fuse future data to arrive at decisions based on knowledge or solve future computational problems. Fuzzy systems start from highly formalised insights about the behaviour of the systems and they learn from the associative rules to estimate functions or formulate control strategies. Learning from examples requires the formulation of a knowledge base with a collection of input-output pairs. In neural networks, a multilayer network is used as an approximation framework and both weights and bias are modified in according to the selected algorithms. As for fuzzy systems, fuzzy if-then rules are used to relate the linguistic or fuzzy variable, which allows an approximated match between the input and the antecedents of the rules.

Fuzzy systems are suitable to be applied to areas where we can use people's experience or knowledge to develop the fuzzy if-then rules. Since there is no mature guidance in fuzzy set theory for the determination of the best shapes for fuzzy sets, different shapes for different set points need to be studied to obtain an optimum solution for various input vectors. The amount of overlap with the fuzzy sets affects the efficiency of the fuzzy controller. In the case of too much overlap, many rules will be applied for a single set of input vectors, and the situation will

not be represented accurately. If there is too little overlap, it will be difficult to derive the fuzzy decisions. In addition, it is extremely difficult to formulate universal rules for a complex radar target detection problem as the complexity changes at different periods. Therefore, neural networks are more commonly used in this type of problem where a large amount of sample data from simulated/live signals can be obtained and used as training sets for the network.

CHAPTER FIVE

THE RADAR SYSTEM AND DATA ACQUISITION

5.1 Introduction

The radar system selected for the implementation is a Racal-Decca 'Series 70' installed at the roof of Fitzroy Building (University of Plymouth). The radar is located about 3.7 km from the sea front and is 'looking at' the Harbour of Plymouth. It picks up targets of ocean going vessels, as well as pleasure crafts. Both sea clutter and rain clutter are detected by the radar under adverse weather conditions. The data acquisition system was set up to record the raw radar video for analysis purposes. The recorded videos are then imported into the computer where processing takes place. This chapter describes the radar system and the effect of its characteristics in signal processing, as well as the development of the data acquisition system to match the characteristics of the radar waveforms.

5.2 The Radar Equipment

As stated in the service manual of the radar equipment, it includes an X-band transmitter (9380-9440 MHz) with a nominal power output of 10 KW. The top unit is fitted with 4 feet end-fed slotted waveguide aerial and the rotational speed is 25 rpm. The horizontal beamwidth and vertical beamwidth are 2 degrees and 23 degrees respectively. The sidelobes within 10 degrees of the main beam are better than –23 dB. The aerial gain is approximately 28 dB with horizontal polarization. The pulse repetition frequency and pulse widths are 2400Hz at 0.08 microsecond (short pulse), 1200 Hz at 0.3 microseconds (medium pulse)

and 600 Hz at 1.0 microseconds (long pulse). The receiver is equipped with a low noise front end with a noise factor of better than 7 dB. The intermediate frequency is centred on 60 MHz with I.F. bandwidths of 25 MHz (short pulse) and 4 MHz (medium and long pulse). The viewing unit uses a raster scan format with 625 line/60 field per second and 2:1 interlaced. There are 4 planes of 512 x 512 pixels for the radar picture memory and 1 plane of 768 x 576 pixels for the synthetic data memory [Racal-Decca 'Series 70' service manual].

5.3 Parameters Affecting the Radar Signal and Maximum Range

The radar transmits a train of narrow pulses modulating a high frequency sine wave carrier and detects the nature of the reflected signal when hitting an object. The parameters which affect the reflected signal and the maximum range is discussed as follows:-

5.3.1 Beam Width

The vertical beam width indicates the height of the beam effect within the vertical plane. This parameter determines the minimum range which the target is 'seen' by the radar. The horizontal beam width is measured in degrees and indicates the width of the radar beam in the horizontal direction. In this case, the horizontal beam width is 2 degrees measured at the half power point. This is not a particularly fine beam as beam width can go down to 0.5 degree for some sophisticated radar equipment. The horizontal beam width of the radar signal transmitted from the antenna has a decisive meaning in the bearing accuracy. Incorrect information will be indicated in cases where the distance between the two objects is smaller than the width of the beam at that range. The targets would be seen by the radar as

one unique target instead of two objects and the radar is said to have a low bearing discrimination. The zero degree in bearing is represented by the heading marker which is normally aligned with the ship's head. A reed relay is used to provide a closure signal to the control unit whenever the antenna passes this point. Figure 5.1 shows the heading marker signal for 4 complete revolutions of the antenna.

Fig. 5.1 Heading Markers for 4 Revolutions

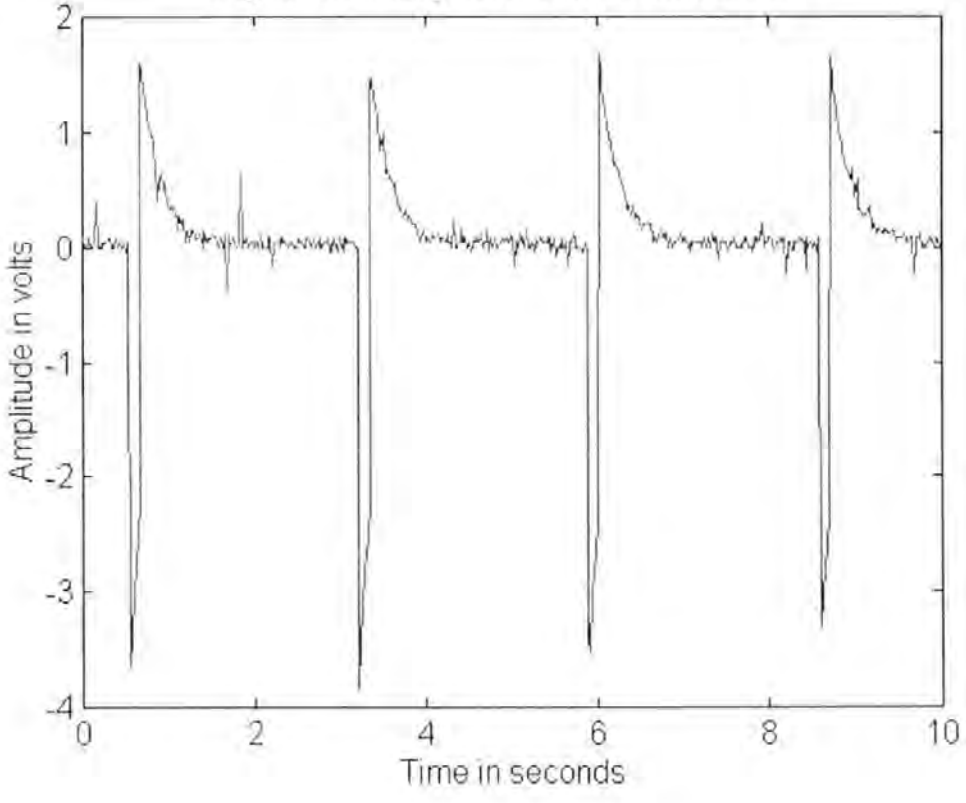

5.3.2. Pulse Repetition Frequency

The pulse repetition frequency (PRF) is the number of pulses transmitted from the radar per second and it will limit the maximum detectable range. Figures 5.2 and 5.3 show the PRF for short pulse and long pulse. In the short pulse, the PRF is 2400 Hz (416.67 microsecond) which corresponds to a range of 62.5 km. For the long pulse, the PRF is 600 Hz (1667 microsecond) which corresponds to a range of 250 km. The pulse width will affect the range resolution of the radar. It is the time that the magnetron is active. In the radar used within this work, the pulse width for short pulse is 0.08 microsecond, which corresponds to a distance of 12 meters, and the pulse width for long pulse is 1 microsecond which corresponds to a distance of 150 meters. The pulse width affects the radar range; longer pulse width tends to achieve a greater range due to the average power being higher. However, it will have less range resolution, that is, it is unable to discriminate targets which are less than 150 meters apart. For the same reason, the shorter pulse width can achieve better range resolution. Thus, short pulse is usually used for close ranges and long pulse for larger distance. Digitized radar video returns for both short pulse and long pulse are shown in figures 5.4 and 5.5.

5.3.3 Transmission Power

During transmission, the peak power of the radar is 10 KW and the transmitter is idle after this pulse period. The average power of the radar pulse in watts is given by:

(Peak power (in KW) x Pulse Repetition Frequency x Pulse Width)/1000

The average power is 1.92 watts for short pulse and 6 watts for long pulse. Apart from the transmitted power, there are a number of factors which will affect the maximum radar

Fig. 5.2. Pulse Repetition Frequency for Short Pulse

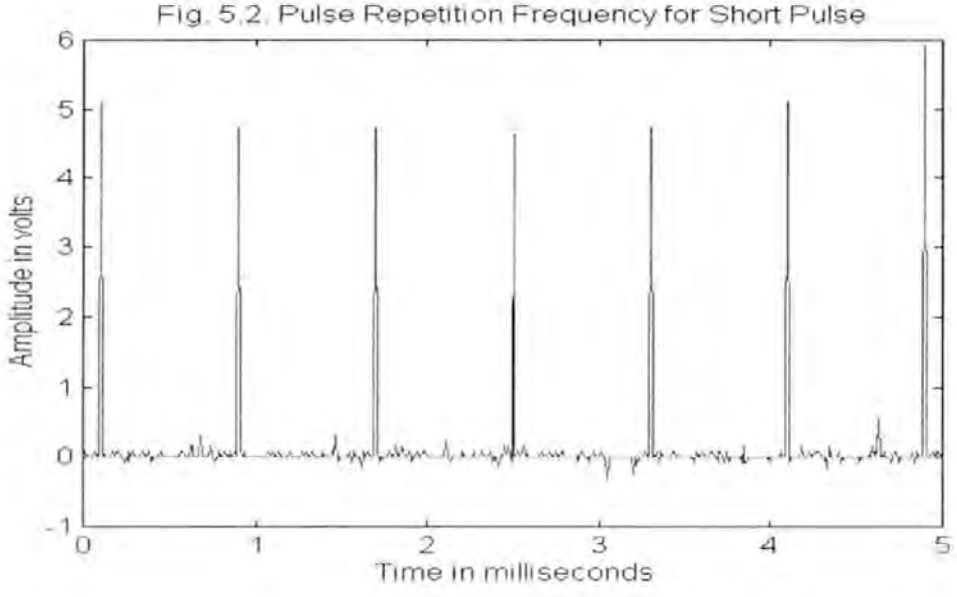

Fig. 5.3. Pulse Repetition Frequency for Long Pulse

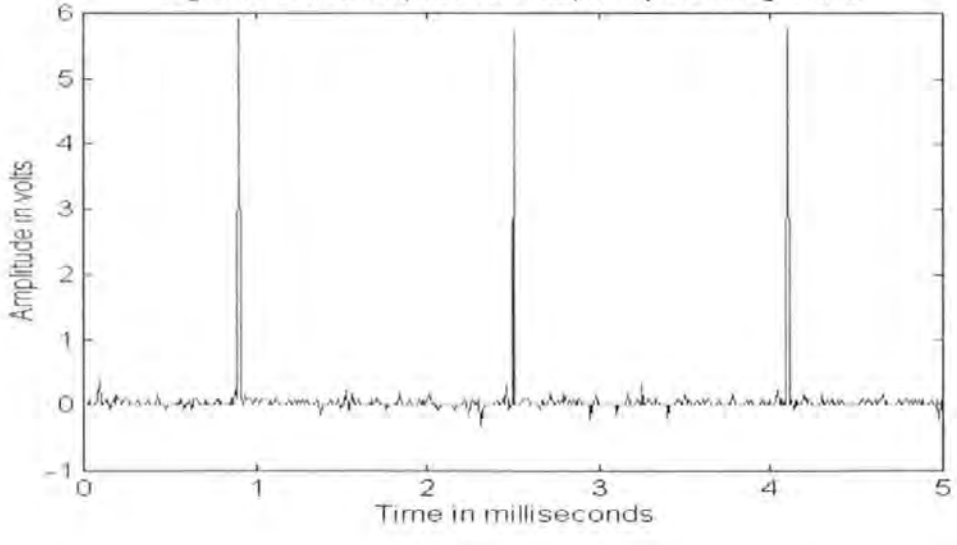

Fig. 5.4 Six Sweeps of Radar Video for Short Pulse

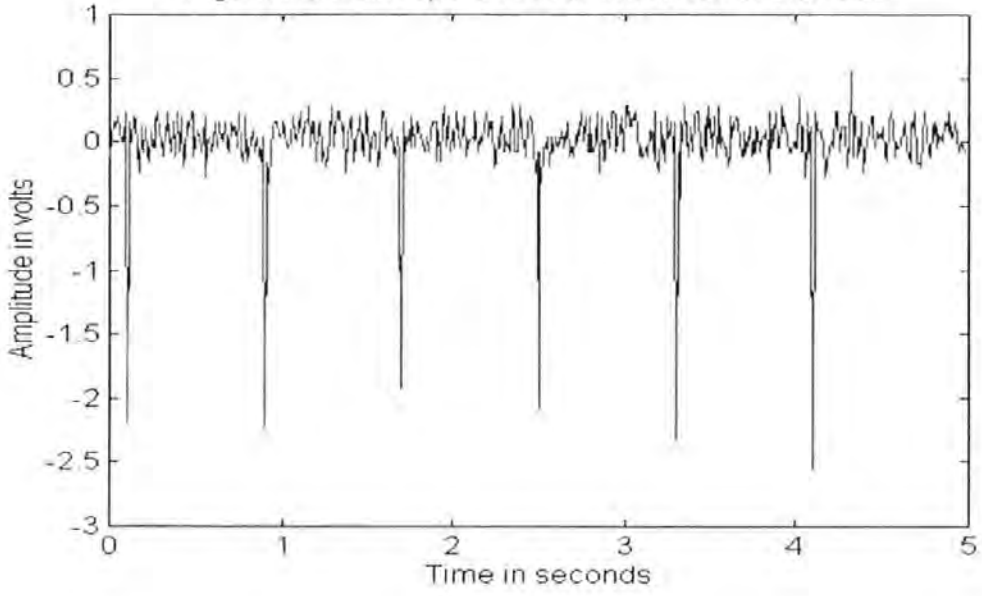

Fig. 5.5 Three Sweeps of Radar Video for Long Pulse

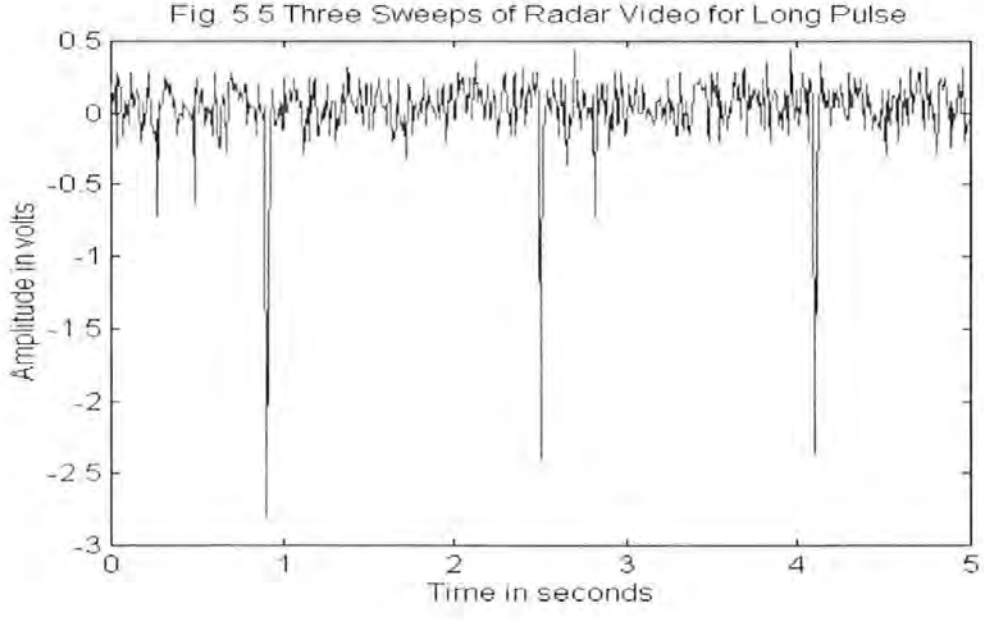

detection range. If the power of an omni-directional radar transmitter is denoted by P, the power density at a distance R from the radar is equal to the transmitter power divided by the spherical surface area of an imaginary sphere of radius R, i.e. $P/4\pi R^2$. The gain G of an antenna is a measure of the increased power radiated in the direction of the target as compared with the power that would have been radiated from an isotropic source. The power density at the target from an antenna with a transmitting gain G would then be, $PG/4\pi R^2$. The target intercepts a portion of the radiated power and re-radiates it in the direction or the radar and the re-radiated power is $PG\sigma/4\pi R^2$ where σ is the radar cross sectional area of the target. The power density of the echo at the radar receiving antenna is then, $PG\sigma/(4\pi R^2)^2$. The radar antenna captures a portion of the echo power. If the effective capture area of the receiving antenna is A, the echo power received at the radar is, $PGA\sigma/(4\pi R^2)^2$. Antenna theory gives the ralationship between antenna gain and effective area as, $G = 4\pi A/\lambda 2$. If the minimum signal that can be detected by a radar is:

$$S_{min} = \frac{PG^2\lambda^2\sigma^2}{(4\pi)^3(R_{max})^4}$$

then the maximum range for detection is

$$(R_{max})^4 = \frac{PG^2\lambda^2\sigma^2}{(4\pi)^3 S_{min}}$$

The above equation shows that if longer ranges are desired, the transmitted power must be increased. This can be achieved by concentrating the radiated energy into a narrow beam (high transmitting antenna gain), the received echo energy must be collected with a large antenna aperture, and the receiver must be sensitive to weak signal (small S_{min} value).

However, the minimum detectable signal and the target cross section area are both statistical in nature and should therefore be expressed in statistical terms. Other statistical factors are the meteorological conditions (rain, fog, sea clutter) along the propagation path. The statistical nature of these several parameters does not allow the maximum radar range to be described by a single number and a statement of probability that the radar will detect certain type of target at a particular range must be specified.

5.3.4 Receiver Noise

Noise may originate within the receiver itself, or it may enter via the receiving antenna along with the desired signal. If the radar is operating in a perfectly noise-free environment so that no external sources of noise accompanies the desired signal, and if the receiver itself were so perfect that it did not generate any excess noise, then there would still exist an unavoidable component of noise generated by the thermal motion of the electrons in the receiver input stages. The available thermal-noise power generated by a receiver of bandwidth B_n at a temperature T (degrees Kelvin) is equal to, KTB_n, where K=Boltzmann's constant = 1.38 x 10^{-23} joule/degree. Kingsley and Quegan (1992) and Barton (1988) state that the total noise at the output of the receiver is equal to the thermal noise power obtained from an receiver multiplied by a factor called the noise figure. The noise figure F of a receiver is given by:

$$F = \frac{N_o}{K * T_o * B_n * G_a} = \frac{noise\ \ out\ \ of\ \ practical\ \ receiver}{noise\ \ out\ \ of\ \ ideal\ \ receiver\ \ std\ \ temp\ \ T_o}$$

where N_o is the noise generated from receiver and G_a is the available gain. B_n is the bandwidth of the IF amplifier in the receiver. The available gain G_a is the ratio of the output signal to the input signal of the receiver and Kt_oB_n is the input noise level N_i in an ideal receiver. Since the minimum detectable signal S_{min} is the value of S_i corresponding to the minimum signal to noise ratio $(S_o/N_o)_{min}$ necessary for detection, and

$$S_{min} = KT_0 B_n F(S_o / N_o)_{min}$$

Then F becomes:

$$F = \frac{S_i / N_i}{S_o / N_o}$$

Practical systems are designed such that the radar pulse width t is approximately equal to the reciprocal of the receiver bandwidth B_n. By considering the total loss L, which include the loss occurred throughout the system, the radar equation becomes:

$$R_{max} = \frac{PG^2 \lambda^2 \sigma t}{(4\pi)^3 KTF(S/N)_{min}}$$

This shows that the maximum detectable range of a radar depends on the peak power, the antenna gain, the wavelength, the target cross sectional area, the pulse width, the thermal noise power, the noise figure, the total loss and the minimum signal to noise ratio (Hovanessian, 1972).

5.4 Data Acquisition System

To develop a suitable algorithm for the detection of target return signals that exist within the noise, it is necessary that these signals can be imported into the computer for analysis.

This requires a data acquisition system which can record the radar video with minimum distortion, as well as identify the bearing of each sweep so the both sweep to sweep and scan to scan correlation can be performed. To cope with the wide band width of the signals, a system with fast analogue to digital conversion rate is needed.

5.4.1 Sampling Rate

This parameter specifies how frequently conversions take place. A faster sampling rate can acquire more points in a given time, thus providing a better representation of the original signal. If the signal is changing faster than the sampling rate, errors will be introduced into the measured data. When the data sampling rate is too slow, the signal may appear to be at a completely different frequency due to aliasing. According to Nyquist theorem, the sample frequency must be at least twice the rate of the maximum frequency components. The frequency at one-half the sampling frequency is referred to as the Nyquist frequency. Theoretically, it is possible to recover information about signals with frequencies at or below the Nyquist frequency (Kuc, 1982). To sample the radar signals when operating in short pulse (which has a bandwidth of 12.5 MHz), a sampling frequency of 25 MHz is needed. Video cassette recorders have been used to record the raw radar videos. However, due to the limited bandwidth available (only around 3 MHz), the video signal has to be compressed before being recorded. As such, a lot of detailed information will be lost in the compression.

5.4.2 Resolution and Range

Resolution is the number of bits that the analogue to digital converter uses to represent the analog signal. The higher the resolution, the higher the number of divisions the voltage range is broken into, and therefore the smaller the detectable voltage change. For example, if a 3 bit converter is used, it will divide the analog range into 2^3, or 8 divisions. Each division is represented by a binary code between 000 and 111. It is obvious that the digital representation is not a good representation of the original analog signal because information has been lost in the conversion. If the number of bits is increased to 16 bits, the codes for the converter will be increased from 8 to 65,536 which can represent the analogue signal very accurately. However, this will also require a larger space in the random access memory of a digital system for storage. Taking the sampling rate as 25MHz, i.e. the interval is 0.04 microsecond per sample, then in short pulse, the period for 1 sweep is 1/PRF, i.e. 417 microsecond. As such, there are 417/0.04=10,417 samples in one sweep and this would require 10,417x16=166,666 bits. The antenna rotates at 25 rpm, i.e. 2.4 seconds in one revolution. There are 5759 sweeps in one revolution and this would require 960 M bits or120 M Bytes of storage media. As such, the radar recording system needs a large memory size as well as a fast data transfer rate to digitize the waveform data into the computer for analysis.

5.5 Conclusion

The radar equipment that is available for use in this research is a general purpose marine radar used in small commercial vessels. Selective sampling allows various weather conditions including Plymouth rain clutters and sea clutters to be observed and recorded.

The reflections from extraneous targets, such as those from nearby buildings, are detected by the radar in addition to those from vessels. It is the returns from vessels however, that form the database for the analysis and implementing the feature extraction techniques. It has been shown that the system requires a very special data logging system for recording the waveforms, i.e. a high sampling rate and a large storage media. Also, the instrumentation must be able to identify the bearing of each sweep so that analysis on sweep to sweep and scan to scan correlation can be performed. One method is to divide one revolution of the radar antenna into 4096 steps and encode each sweep with a sync word at the zero range. A market survey has been undertaken by the author done and no data acquisition system, which is suitable for this application, is available from manufacturers. One company, Transas, has been developing a similar system using signal processing chips from Texas Instrument. The equipment is still under development and much of the processing will be undertaken by dedicated hardware. To overcome this problem, a Tektronix TDS410 digitize oscilloscope is used as a data recording system. The scope has a bandwidth of 100MHz and is able to provide the sampling rate as required by the radar signal. The internal memory in the scope is limited so only a few sweeps can be recorded in one time. The number of sweeps will depend on the sampling rate used. The recorded waveform is then input to a IBM PC via a GPIB interface. Software from Tektronix, called the 'Wavestar' is used to acquire the data for further analysis. The details of the complete system are discussed in the next section.

CHAPTER SIX

THE INTEGRATED RADAR DETECTION SYSTEM

6.1 Introduction

The radar system described in Chapter Five provides the raw radar videos from the environment in the vicinity of the antenna. A data acquisition system is then implemented to record the video signal for analysis purposes. In order to identity the targets and clutters, the recording is done at a specific bearing only. This is to ensure that the data can be compared with the visual scene and the observation on the radar display. Windows of signals containing targets and clutter would be extracted for feature identification. The features include amplitude mean and deviation, period mean and deviation, as well as the maximum pulse width. The criteria for selecting these features are also discussed in this chapter. Results presented in tables 4.3 and 4.4 indicated that neural networks may be suitable for target detection and this work is now expanded. The training procedure and the detection algorithms are discussed in detail in this chapter.

6.2 System Hardware

To record the waveforms of radar signals, the raw video, trigger signal and the heading marker from the radar transceiver are input to the Tektronix TDS410 digitised oscilloscope, which has a maximum sampling rate of 100 MHz. The recording length is 50 points per division with a maximum of 15000 points. For example, at the 2 microsecond per division range the time interval for each sample will be 0.04 microsecond. Therefore, the total recorded length is 0.04 x 15000 = 600 microseconds. This corresponds to around 1.3 sweeps of raw video in short pulse, 0.3 sweep in long pulse. To increase the number of recorded sweeps in 15000 points, the sampling rate must be reduced. For example, at the 20 microsecond per division range, the time interval for each sample will be 0.4 microseconds. Therefore, the total recorded length will be

0.4 x 15000 = 6000 microseconds. This corresponds to around 13 sweeps of raw video in short pulse, 3 sweeps in long pulse. The data is transferred from the oscilloscope to the IBM personal computer via a GPIB bus. The configuration is shown in fig. 6.1.

Fig. 6.1 Block Diagram of the Experimental Set Up

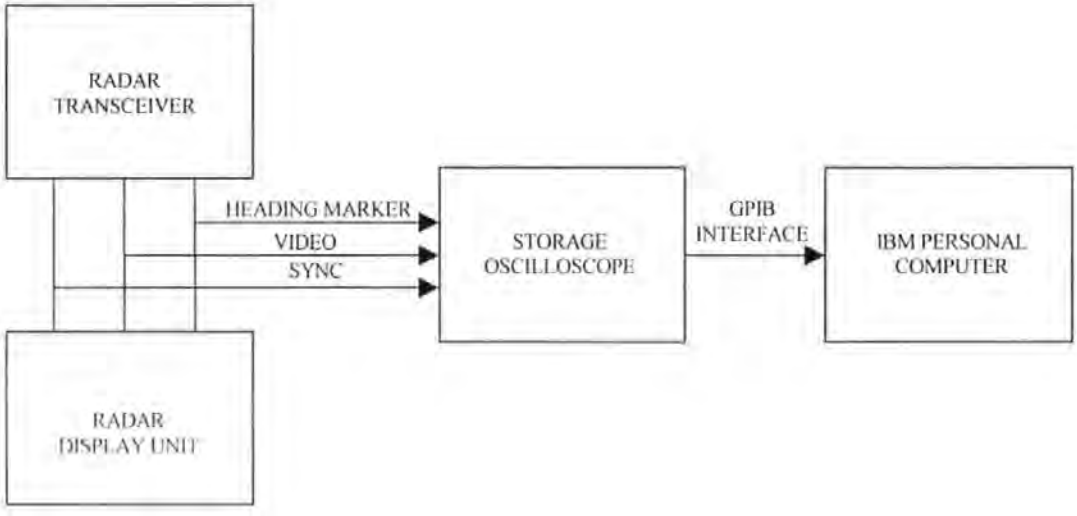

To compare the recorded radar signal with the actual targets and environment, it is necessary to identify the bearing of each recorded sweep. One way is to use the electronic bearing marker as a trigger signal for the acquisition process of the oscilloscope. As such, the acquired waveform corresponds to the video shown on the display unit as marked by the electronic bearing marker. However, it was observed that the output signal from the electronic bearing marker was embedded in the electronic circuitry of the display unit. A considerable amount of effort would be required to trace the circuit diagram and build interface circuit to extract the signal. It was decided that the heading marker signal, instead of the electronic bearing marker, would be used as the trigger signal. The heading marker signal can easily be taken from the transceiver output. It was observed however that the heading marker is pointing south and there is a large radar shadow in that direction due to the nearby buildings. No targets can be seen in that sector to around 4 degrees either side of it. To enable the bearing of the marker signal to be adjusted, the

author designed and added a time delay circuit at the output of the transceiver. The objective is to introduce a variable time delay to the arrival of the heading marker signal. Since the antenna rotates at 25 rpm, one revolution will take 2.4 seconds. An RC time delay circuit with a resistor of 1k ohm and a capacitor of 1000 microfarad is used. This contributes a delay of 1second and it corresponds to a bearing of 360 x 1/2.4 = 150 degrees. By adjusting the 100k ohm resistor, a delay of 0 to 150 degrees on the heading marker can be achieved. The arrangement is shown in fig. 6.2. Adjustment of the resistor allows digitisation of targets that can be seen visually and observed on the radar display.

6.3 Selection of Features to be Extracted from Radar Signals

In Chapter 3, the characteristics of radar signal have been discussed and features can be extracted from the signals for detection purpose. However, it is impossible to extract all these features for detection due to the computational time involved in the process. As such, it is necessary to identify the features that are just sufficient for discriminating targets from clutters with the minimum computational time required. Discrete Fourier transform (DFT) or fast Fourier transform (FFT) technique is commonly used to assess the relative contributions of the frequency components in a radar waveform and convert them into the frequency domain. The waveform can then be characterised according to the relative amplitude of the components. While this method is effective and accurate, it is also computationally intense. Consider a waveform that consists of a fixed frequency component and a variable frequency component. The objective is to identify when one of the possible combinations of frequencies occurs in a particular sample. The mathematical representation is as follows:

$$A(t,n) = A_1 \sin[(2\pi t f_n) + \phi_n] + A_2 \sin[(2\pi t f_n) + \phi_n]$$

where A_1 = peak amplitude of the fixed-frequency component,

A_2 = peak amplitude of the variable-frequency component

f_0 = frequency of the fixed frequency component

f_n = frequency of the variable frequency component

ϕ_1 = initial phase of the fixed frequency component

ϕ_2 = initial phase of the variable frequency component

t = elapsed time

The Fourier Transform can be used to identify the frequency components of the samples. Despite the fact that both Discrete Fourier Transform and Fast Fourier Transform can solve the problem, the FFT takes advantage of powers of 2 relationships to achieve a transform with reduced computational complexity, compared to DFT. In either case, the number of basic mathematical computational operations (add, subtract, multiply and divide) is a direct function of the number of samples. Hirsch (1991) stated this relationship as:

$$N_o = N_s^2 \quad (for \ \ the \ \ DFT) \qquad\qquad N_o = 5N_s \log(N_s) \quad (for \ \ the \ \ FFT)$$

where N_o is the number of operations required and N_s is the number of samples.

In view of the computational complexity of Fourier Transform, it is necessary to find an alternative means to characterise the frequency domain similarities and differences of waveforms without actually performing the transform. The process must use simple computational methods to extract the frequency domain significance of the waveform without actually transforming the signals into the frequency domain. The statistical signal characterisation method characterises the radar waveform not only as a function of the frequency components but also as a function of the relative phases of its frequency components. The characterisation method is used to associate waveforms to different types in a high signal density and real time environment. The characteristics of radar waveforms can be manipulated with

simple statistical mathematics to produce a set of numerical parameters for a given waveform. It involves the division of a waveform into segments which are bounded by the extremes of the waveform. As shown in chapter 3, the absolute differences in amplitude between these extremes are then accumulated and their mean and mean deviation are calculated. Similarly, the mean and mean deviation of the times between the extremes are also calculated. The five waveform parameters, amplitude mean, amplitude deviation, period mean and period deviation are the primary measures which are used for characterisation purpose. In order to extract the special features of individual targets, the maximum period between extremes is also evaluated. The parameters on periods are numerically very close to the reciprocal of the frequencies of the components presented in the waveform. Therefore, the characterisation technique can determine the frequency indirectly, which is significantly simpler than a Fourier Transform. Computationally, this technique offers a considerable reduction in the number of operations as compared to the more classical methods such as Fourier Transform and Correlation. It simply sums consecutive time segments and is divided by the number of segments. Hirsch (1992) worked out the number of operations required as follows:

N_s subtractions + N_s additions + 1 division to calculate the amplitude mean

+ 1 subtraction + 1 division to calculate the period mean

+ N_s subtractions + N_s additions + 1 division to calculate the amplitude mean deviation

+ N_s subtractions + N_s additions + 1 division to calculate the period mean deviation

which gives a total of approximately 6 N_s +5 operations. When continuous sampling is required, another N_s operations would be needed to accomplish the detection of maximum and minimum. The technique requires fewer computational operations in comparison to Fourier Transform or correlation (both auto correlation and cross correlation).

Fig. 6.2 The Time Delay Circuit for the Heading Marker

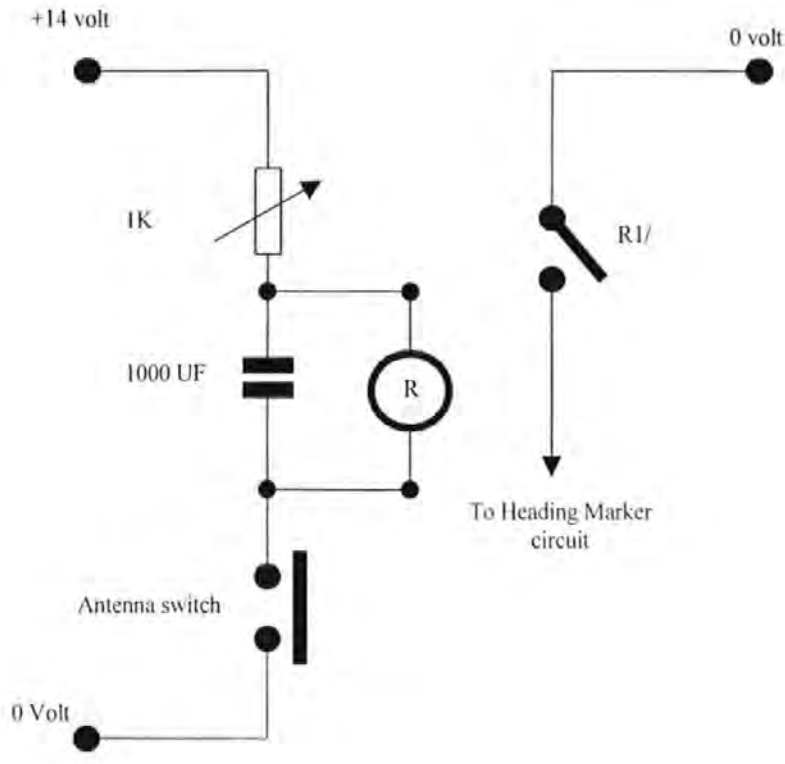

Fig. 6.3 Waveform of a Target in a 50 Samples Window

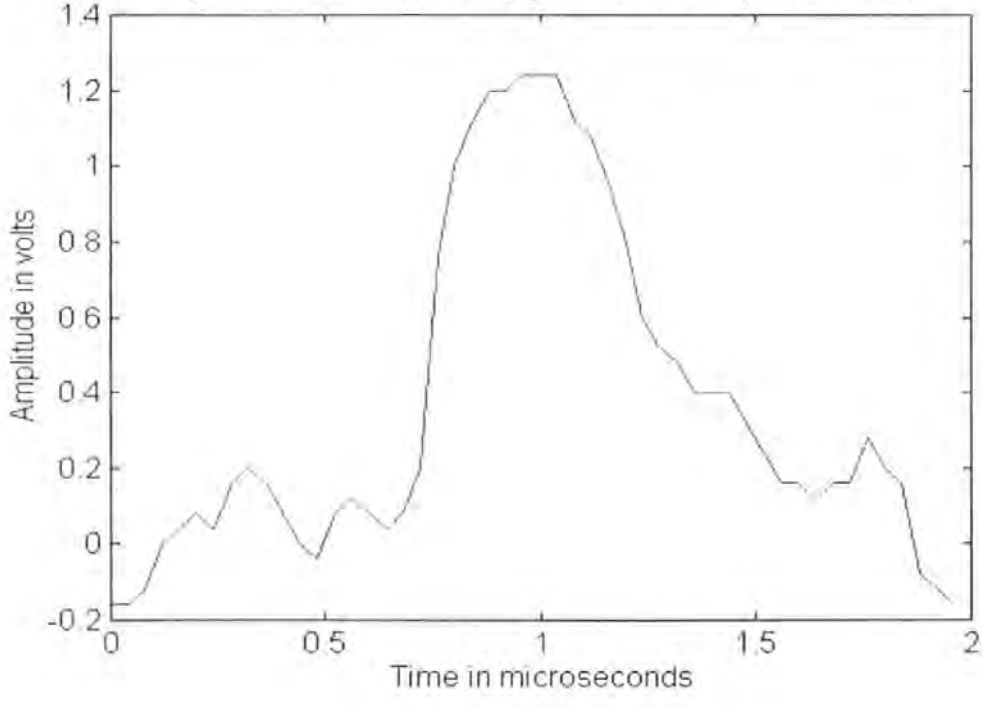

6.4 Methods of Extracting Statistical Signal Characteristics

The statistical signal characteristics are extracted from the radar signal at each time slot. A moving window of a fixed number of range cells is shifted through the entire sweep. As such, the size of the moving window has to be determined. If the window size is made too large, then the extracted characteristics will be comprised of a large number of samples and the accuracy of the detection algorithms will be reduced. However, too small a window will involve extra computational time as well as not truly representing the situation due to the limited amount of samples available. The window size used for the initial testing is 50 samples. Taking the sampling rate of 25M samples per second, the window corresponds to a time slot of 2 microsecond and a distance of 300 meters. The slot approximates the size of nominal targets. Figure 6.3 shows the waveform of a target that is contained in a window of 50 samples. The maximum extreme is declared when the magnitudes of the previous and subsequent samples are both less than the present sample, i.e. $A(n-1) < A(n) > A(n+1)$, where A is the amplitude and n is the sample number. Consideration is also given to conditions where the amplitude maximum extreme may be constant for a number of samples. Similarly, the minimum extreme is determined when, $A(n-1)>A(n)<A(n+1)$

From the figure, it can be observed that the maximum extremes occur at 5 points. These are 0.08 volt at 0.2 microsecond, 0.2 volt at 0.32 microsecond, 0.12 volt at 0.56 microsecond, 1.24 volt at 1 microsecond and 0.28 volt at 0.18 microsecond. Similarly, the minimum extremes occur at 4 points. These are 0.04 volt at 0.24 microsecond, -0.04 at 0.48 microsecond, 0.04 at 0.64 microseconds and 0.12 at 1.64 microsecond. The statistical characteristics are then calculated out as follows:

Amplitude Mean = (0.08 + 0.2 +0.12 + 1.24 +0.28)/5 = 0.384 volts

Amplitude Deviation = (|0.08-0.384| + |0.2-0.384| + |0.12-0.384| + |1.24-0.384| + |0.28-0.384|)/5 = 0.3424 volts

Period Mean = (0.6 + 0.4 + 1)/3 = 0.667 microseconds

Period Deviation = (|0.667-0.6| + |0.667-0.4| + |0.667-1|)/3 = 0.222 microseconds

Maximum Period = 1 microsecond

Similarly, the statistical characteristics of eight sets of waveforms for targets (figures 6.4a to 6.4h) and eight sets of waveform for noise (figures 6.5a to 6.5h) are shown in tables 6.1 and 6.2 respectively. The targets are returns from vessels in the vicinity of the radar and the noise consists of both rain and sea clutters. The figures on the table show that each set of waveform parameters is unique to a particular type of radar signals. Although there are similarities spread across more than one parameter, the similarities seldom spread across all five parameters. From these figures, different types of targets and noise can be extracted.

6.5 Neural Target Detection

The neural network's ability to learn, the fast on line processing ability and robustness of the system indicates that it is appropriate to be applied in radar target detection. The method chosen for the implementation of target detection is supervised learning using the backpropagation learning rules. This particular methodology is chosen because they are simple to implement and allow great flexibility in the structure of the system. The number of network inputs and the number of neurons in the output layer are constrained by the information available and requirements of the application. The number of neurons in the hidden layer(s) depend on the designer. The more neurons, the more likely solution will be found. However, more neurons

Fig. 6.4a Waveform of Target A in a 50 Samples Window

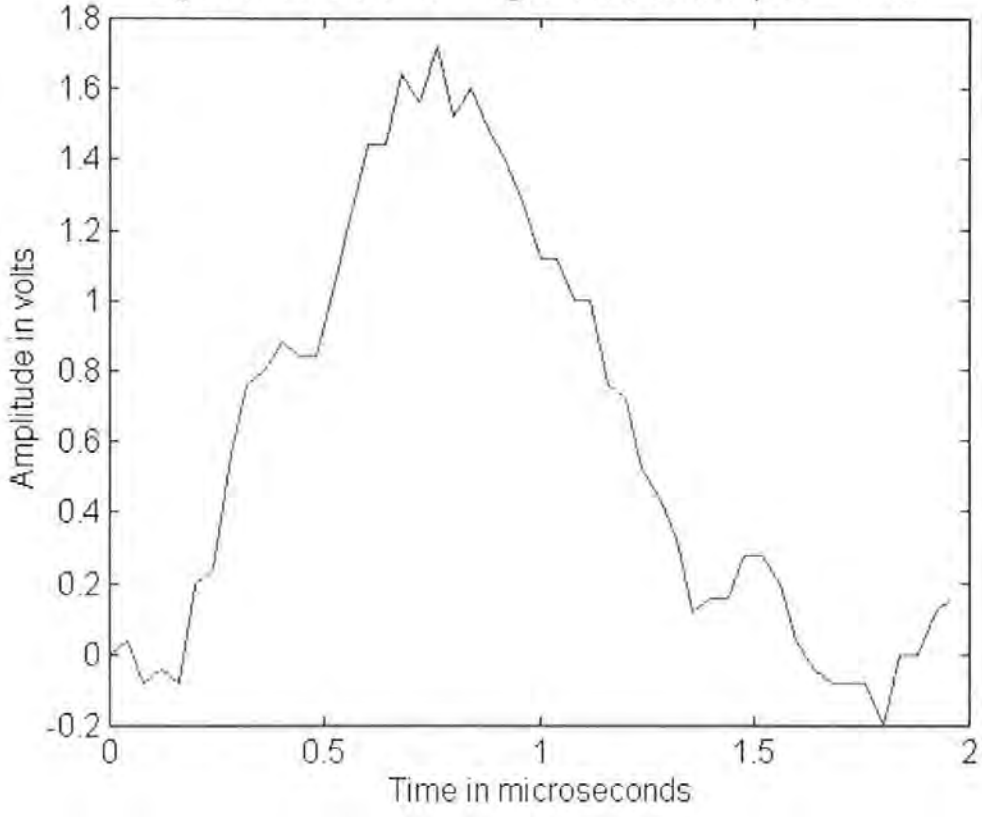

Fig. 6.4b Waveform of Target B in a 50 Samples Window

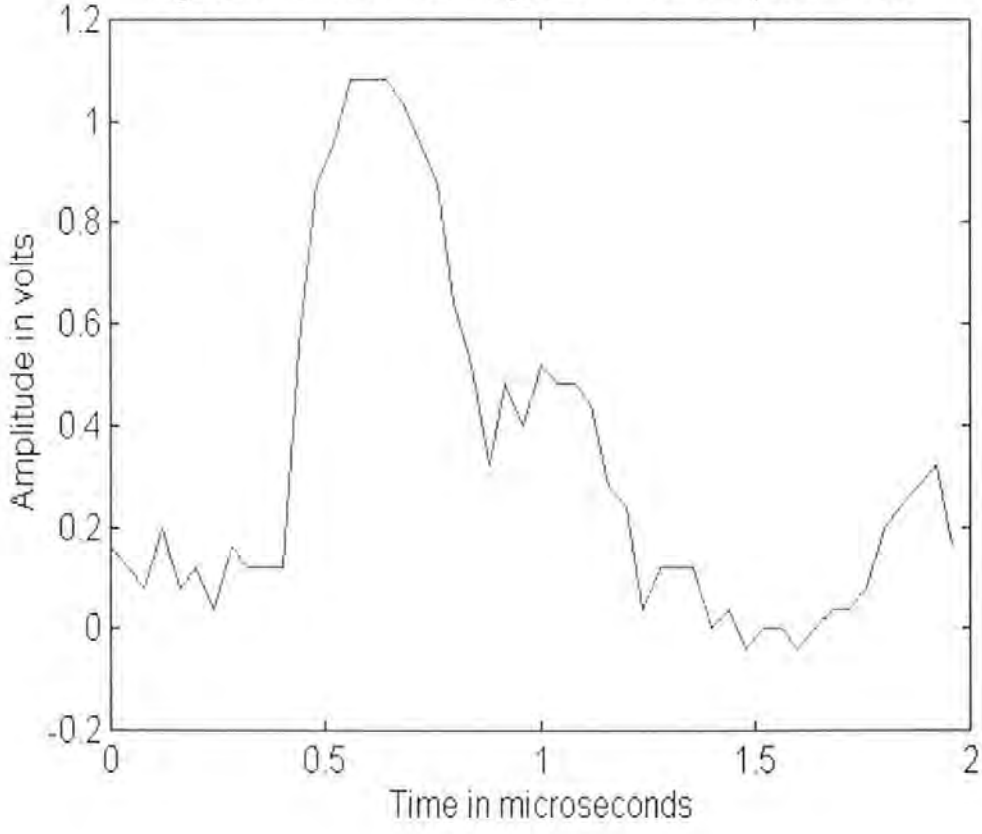

Fig. 6.4c Waveform of Target C in a 50 Samples Window

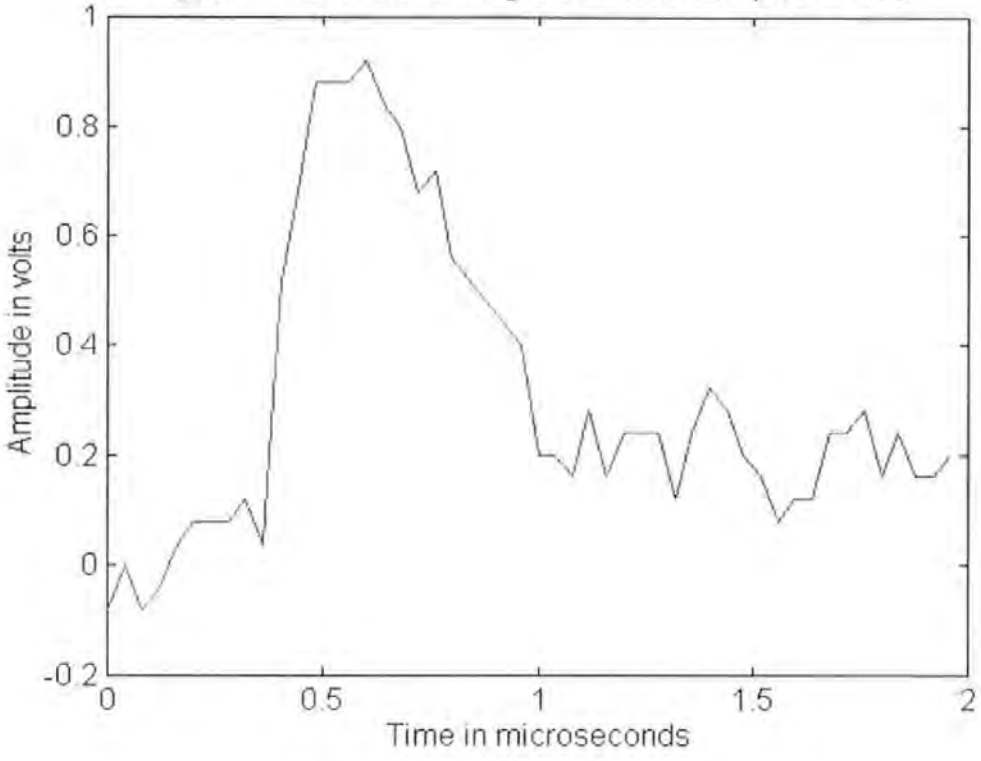

Fig. 6.4d Waveform of Target D in a 50 Samples Window

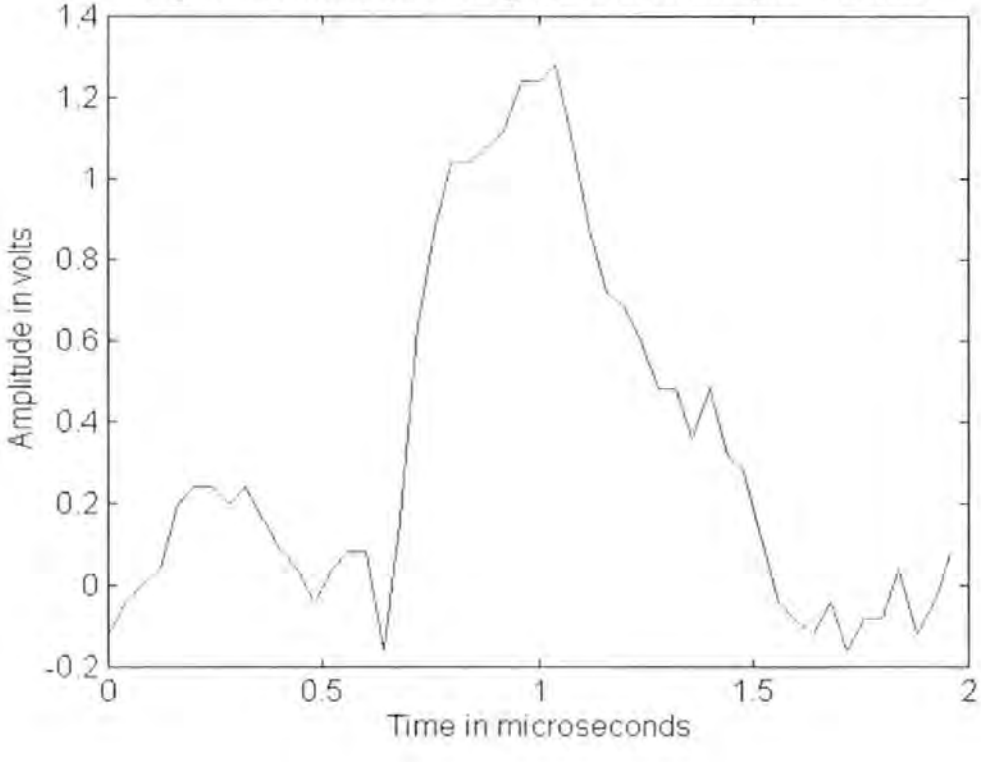

Fig. 6.4e Waveform of Target E in a 50 Samples Window

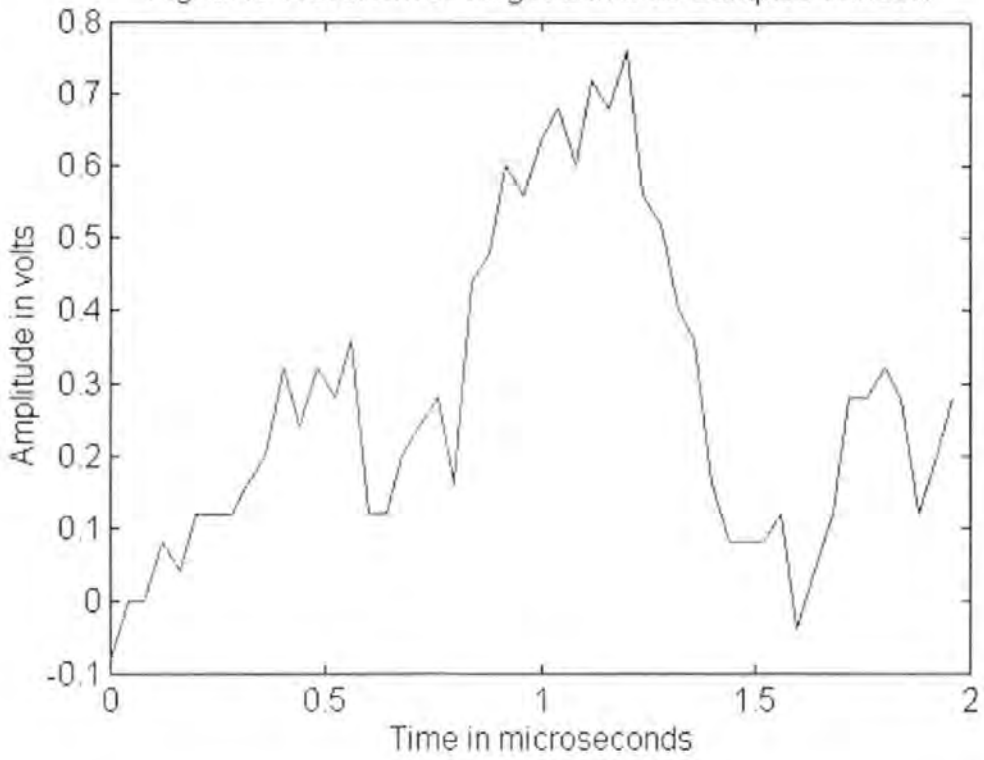

Fig. 6.4f Waveform of Target F in a 50 Samples Window

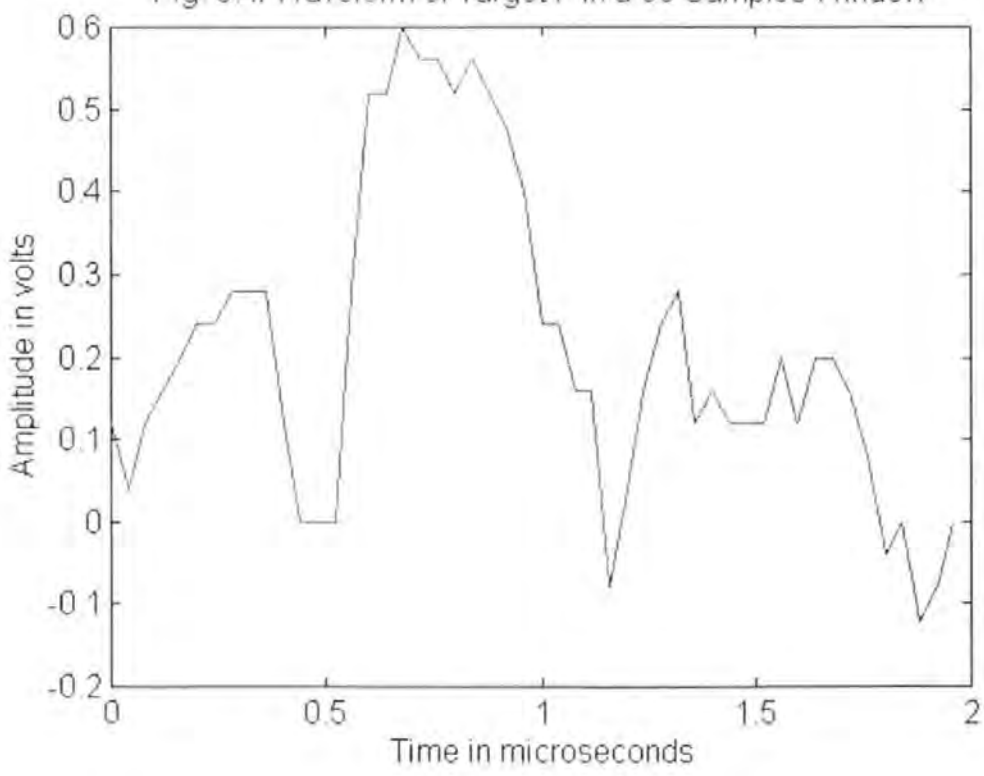

Fig. 6.4g Waveform of Target G in a 50 Samples Window

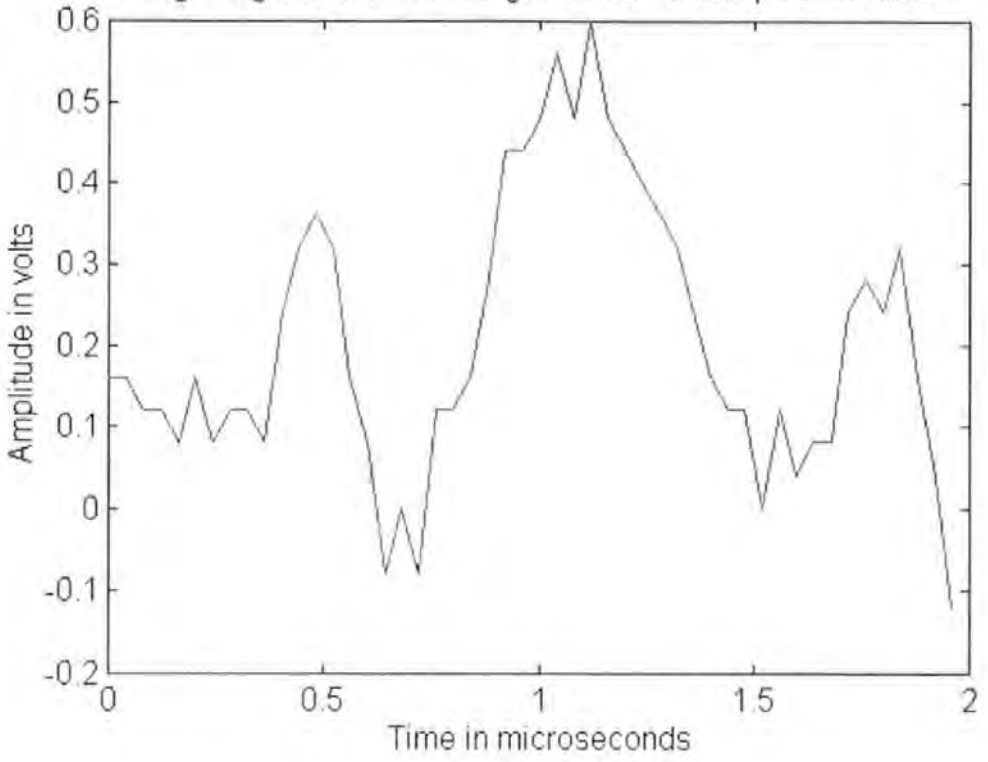

Fig. 6.4h Waveform of Target H in a 50 Samples Window

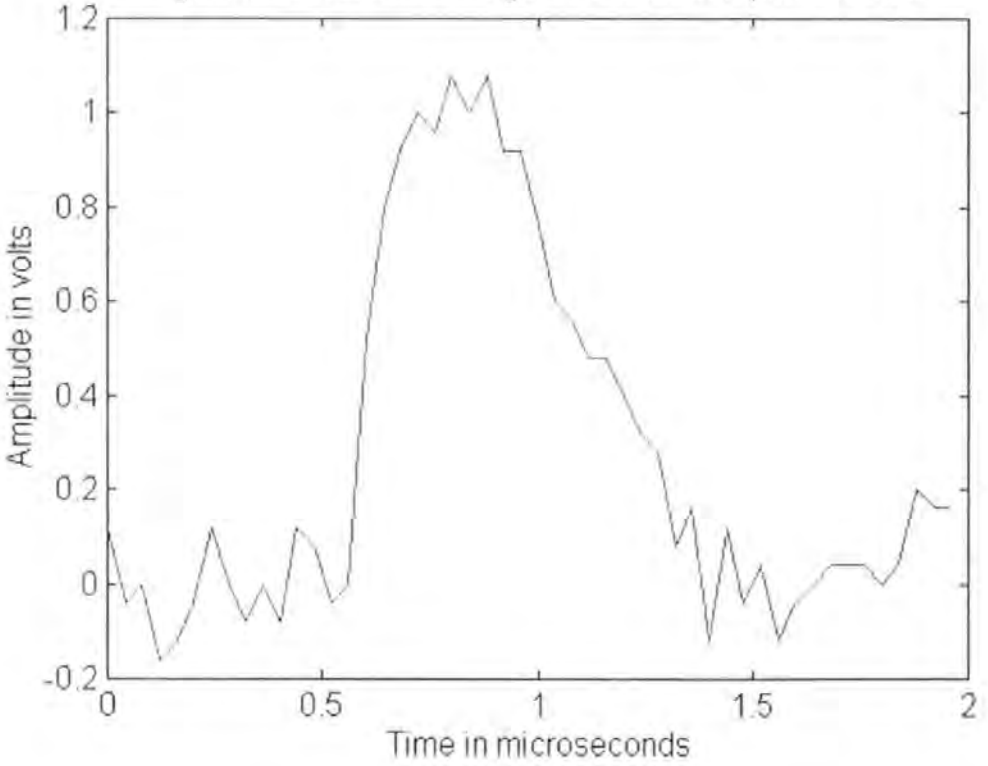

Fig. 6.5a Waveform of Noise A in a 50 Samples Window

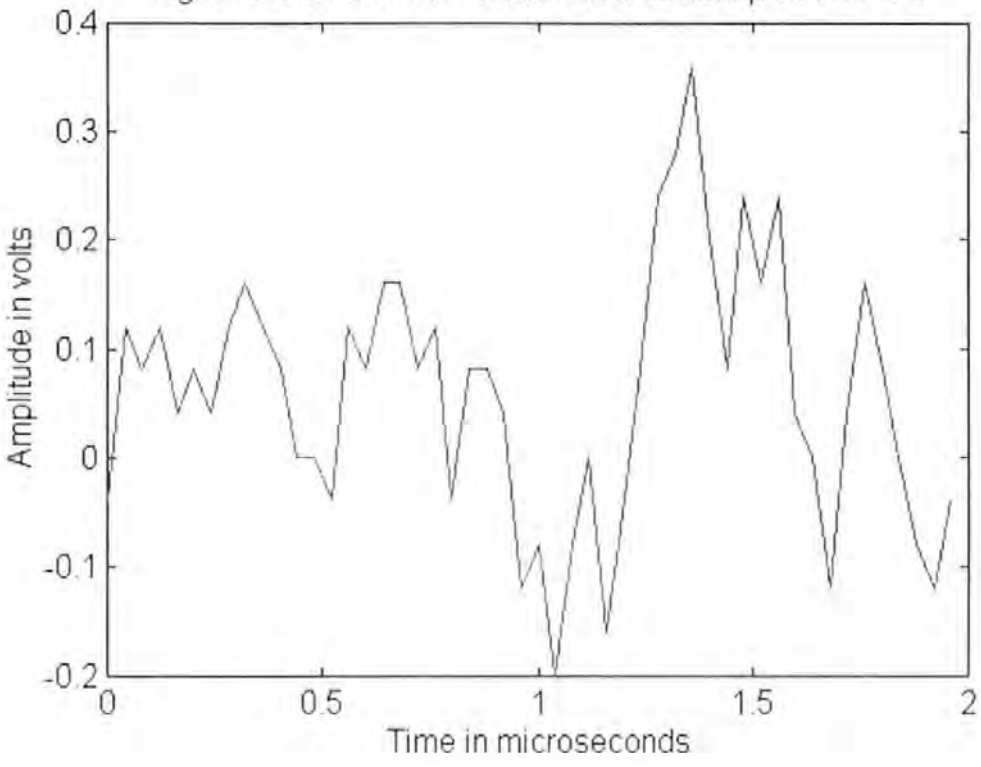

Fig. 6.5b Waveform of Noise B in a 50 Samples Window

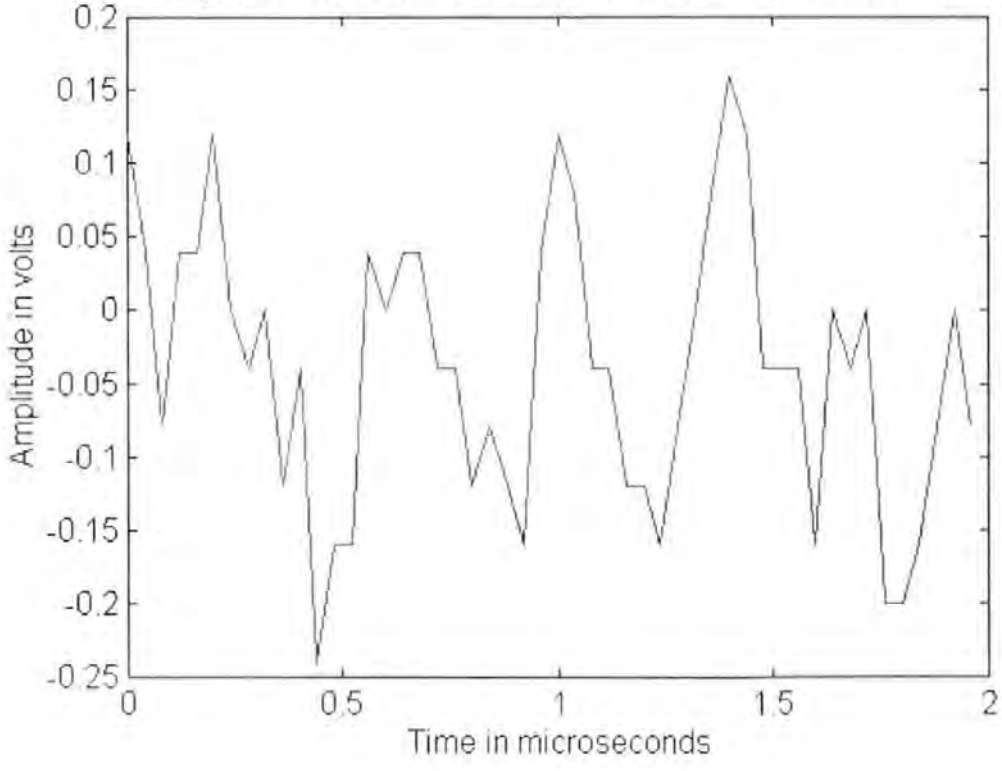

Fig. 6.5c Waveform of Noise C in a 50 Samples Window

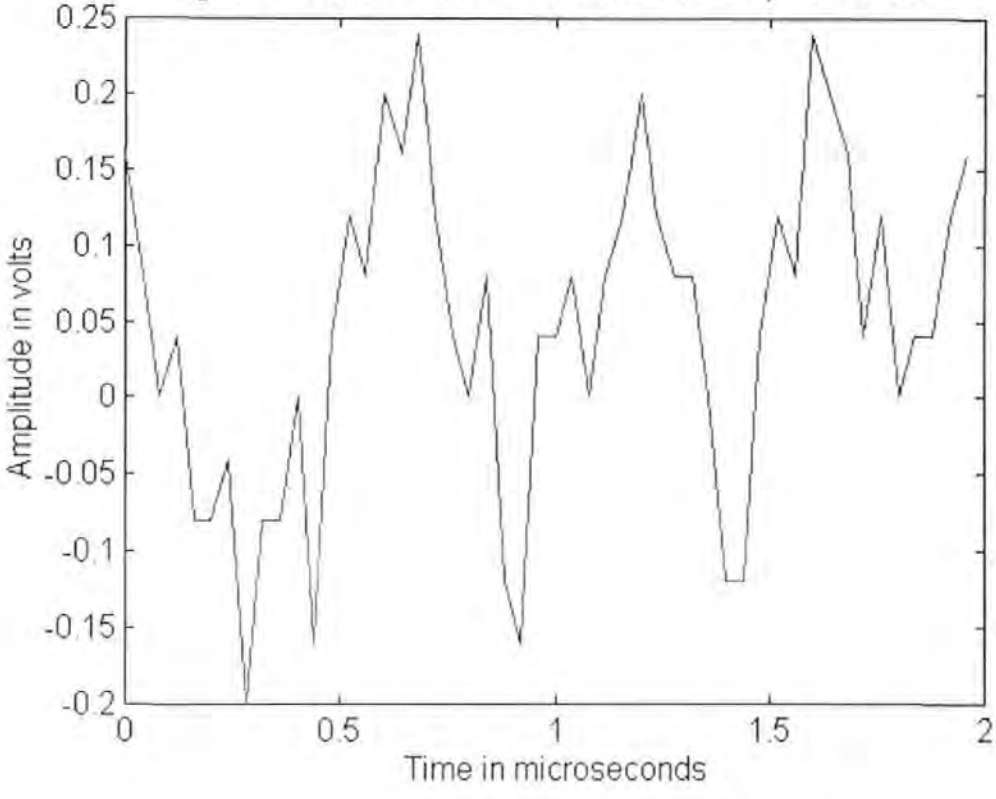

Fig. 6.5d Waveform of Noise D in a 50 Samples Window

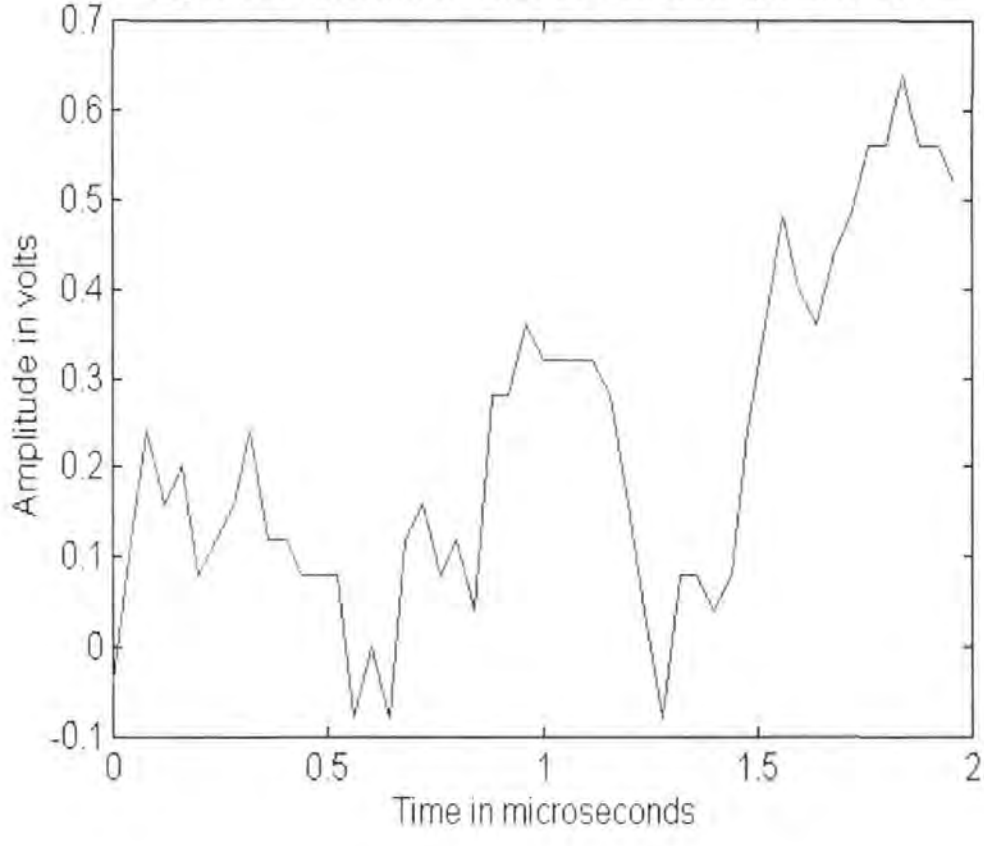

Fig. 6.5e Waveform of Noise E in a 50 Samples Window

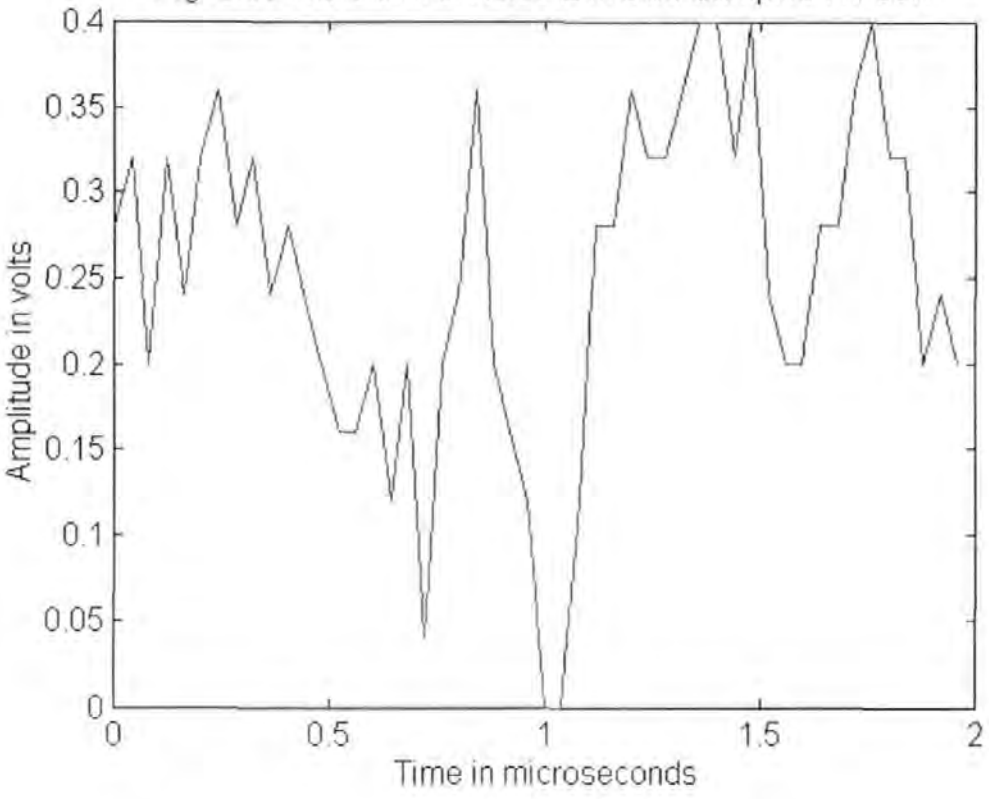

Fig. 6.5f Waveform of Noise F in a 50 Samples Window

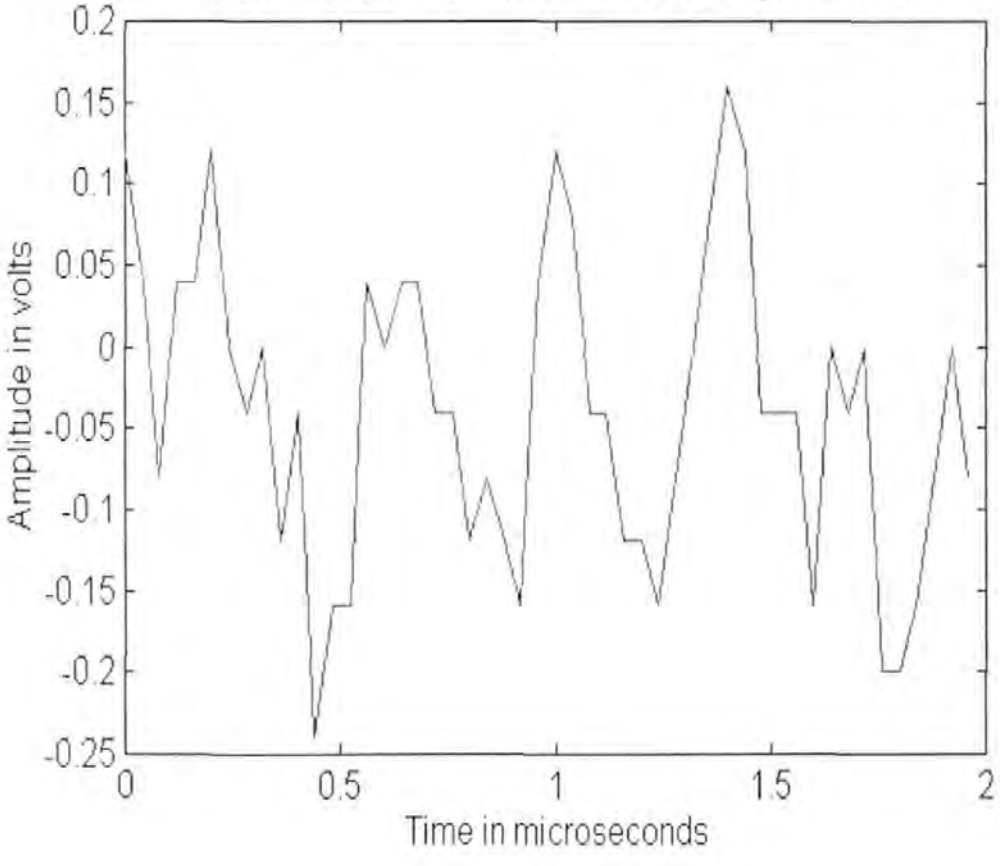

Fig. 6.5g Waveform of Noise G in a 50 Samples Window

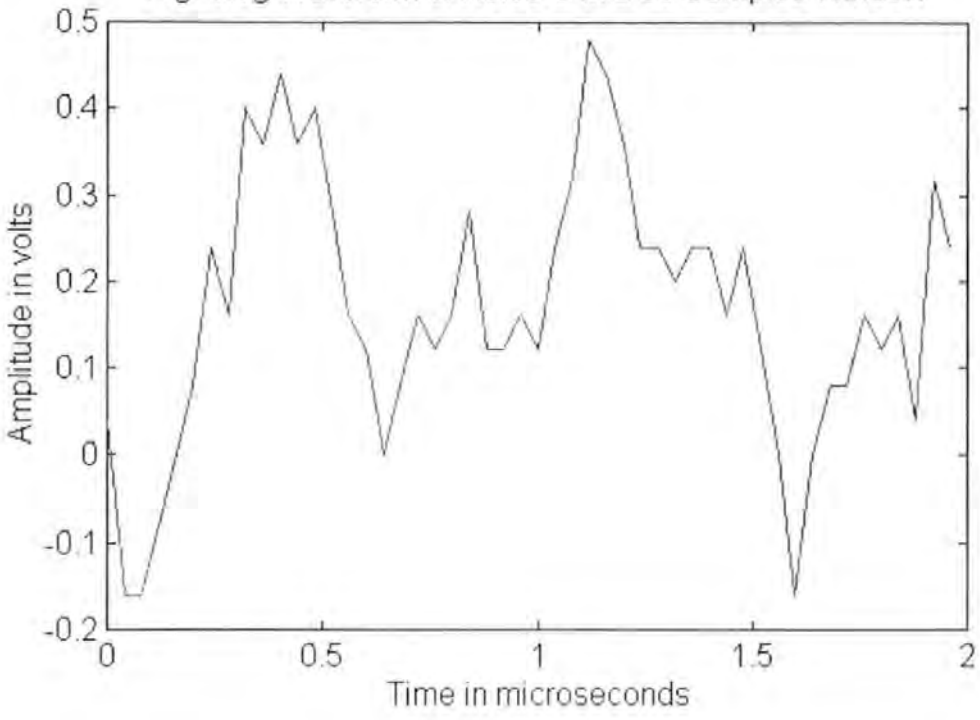

Fig. 6.5h Waveform of Noise H in a 50 Samples Window

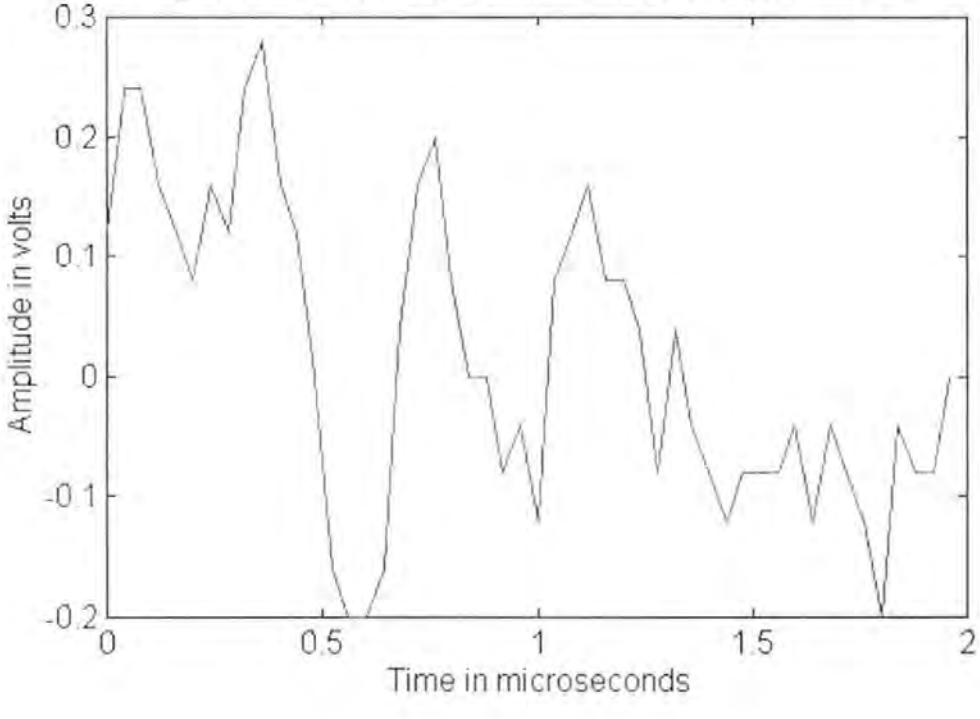

Table 6.1. Statistical Characteristics of Targets

Targets	A	B	C	D	E	F	G	H	mean
Mean Amplitude	0.8743	0.3022	0.3467	0.3314	0.4145	0.2850	0.2800	0.3418	0.3970
Amp. Deviation	0.6694	0.2607	0.2104	0.3135	0.2003	0.1475	0.1600	0.3881	0.2925
Period Mean	0.2150	0.1382	0.1911	0.2057	0.1309	0.1956	0.1640	0.1354	0.1720
Period Deviation	0.1481	0.0939	0.0953	0.1388	0.0655	0.0988	0.1084	0.0847	0.1042
Maximum Period	0.5600	0.5600	0.3600	0.7200	0.2800	0.4000	0.4400	0.4800	0.4750

Table 6.2. Statistical Characteristics of Noise

Noise	A	B	C	D	E	F	G	H	Mean
Mean Amplitude	0.1343	0.0360	0.1167	0.2520	0.3267	0.0360	0.2800	0.0920	0.1592
Amp. Deviation	0.1333	0.0735	0.0600	0.0706	0.1448	0.0533	0.0600	0.1000	0.0869
Period Mean	0.1143	0.1400	0.1229	0.1520	0.1233	0.1400	0.1354	0.1600	0.1360
Period Deviation	0.0539	0.0783	0.0459	0.1016	0.0542	0.0783	0.0577	0.0800	0.0687
Maximum Period	0.2800	0.3600	0.3200	0.4400	0.2800	0.3600	0.3200	0.3600	0.3400

means longer training times with larger weight matrices and bias vectors in the solution. Initially, the test network consists of one input layer with 5 elements, one middle layer with two neurons and one output layer. The five inputs are the amplitude mean, amplitude deviation, period mean, period deviation and maximum period. These parameters for targets and clutter are extracted from different radar returns for training purpose. In the initial training process, targets are labelled as 1 while clutter and noises are labelled as 0.

To train a network, the five inputs are presented to the input layer of the network and the error vectors are calculated. The maximum acceptable error is set within 5 percent of the desire value, i.e. 0.05. If the sum squared error for all the training vectors is less than the error goal then training stops and the corresponding vectors will be presented to the output layer. If the error goal is not reached then the error vectors are calculated and back-propagated through the network. Finally the weights are updated using the back-propagation learning rule, i.e.

$$\Delta W(i,j) = \beta E(i) I(j) \qquad \& \qquad \Delta B(i) = \beta E(i)$$

where ΔW is the weight change, I is the input vector E is the error vector and β is the learning rate.

The learning rate specifies the size of changes that are made in the weights and biases at each training sequence. Small learning rates result in long training times but guarantee that the learning process will not jump over valleys in the error surface. If a set of vectors from a radar waveform, which is not in the set of input training vectors, is presented to a well trained network, the network will try to exhibit generalisation in identifying whether the input vectors belong to a target or clutter. To prevent the network from getting stuck in shallow minimum, a term of 'momentum' is added into the network parameters. It allows the network to respond not

only to the local gradient but also to recent trends in the error surface. The effect of momentum is achieved by making weight changes equal to the sum of a fraction of the last weight change and the new change as given by the back-propagation rule. The mathematical term is:

$$\Delta W(i,j) = m\Delta W^{*}(i,j) + (1-m)\beta I(j)$$

where W* is the last weight and m is the momentum constant. The effect of the last weight change is allowed to be mediated by a momentum constant. When the momentum constant is 0, the present weight change is based only on the gradient. When the momentum constant is 1, the new weight change is equal to the last weight change and the gradient is simply ignored. Typically the momentum constant is set to 0.95 which will be used initially for this implementation (Demuth and Beale, 1993).

In order to detect any targets that may be constrained within each sweep, the 50 sample window needs to be shifted along the complete sweep and analysis performed at each window. During the shift, there are samples being overlapped. Excess overlap across samples will increase the number of windows to be processed and the measure processing time. Insufficient overlap could cause a target to me spread across different windows and reduce the chance of detection. If 25 overlapping samples are chosen, assuming that short pulse is used, the period for each sweep is 416.67 microsecond and the sampling rate is 25 MHz. This means that approximately 20,800 windows have to be analysed in each sweep. The number of overlapping samples is determined by trial and this is discussed in the next chapter.

6.6 Conclusion

A general purpose marine radar is used in the implementation. The objective of the detection system is trying to identify targets from the radar returns that are received from such radar equipment. As a complete set of data acquisition system is not available, a continuous recording

of radar videos cannot be performed. By using the storage oscilloscope, a number of sweeps can be recorded at one time. The number of recorded sweeps depend on the pulse width used, the sampling rate and the record length selected. In order to compare the recorded sweep with the image shown on the display, the heading marker signal is used as threshold for initiating the data acquisition by the oscilloscope. A time delay circuit is added to delay the heading marker signal so that the data recorded is in the region of interest. A neural network, that has been trained using back-propagation, then provides the essential part of the detection system. A simple three layer network is adopted for the initial implementation. The criteria for determining the initial setting, e.g. window size, overlapping samples, initial condition, learning rate and momentum constant are discussed. To prepare the training samples, hundreds of sweeps of radar returns are recorded at different times under different environment e.g. rainy or stormy weather. Also, different types of targets such as fishing boat, sailing yacht, cargo vessel and passenger liners are recorded. Hundreds of representative windows are extracted from these sweeps and various statistical characteristics of these windows are calculated. These values provide the training data for the neural network. The training, testing and verification of the detection system will be discussed in the next chapter.

CHAPTER SEVEN

TRAINING, TESTING AND VERIFICATION OF THE RADAR DETECTION SYSTEM

7.1 Introduction

Over two hundred sweeps of radar data were recorded using the data acquisition system as described in the previous chapter. Windows containing targets and clutters were extracted from these signals for training purposes. Initially, the mean amplitude, mean amplitude deviation, mean period, mean period deviation and maximum period are evaluated from the windows. The distribution of these parameters for both target and noise are discussed. Then the neural detection system was formulated using the backpropagation techniques. The training algorithm calculated and minimized the cost function or error value. The anticipated performance of the system can be considered to be improved if the error function has a reduced value. The error is computed in each training cycle of the data set and is summed at the end of each pass through the patterns in the training set. When the detection system has been trained, new sweeps of data are used to ascertain whether the network can detect a target with the unseen data. The author used Matlab together with the neural network tool box (from Math Works Inc.) to develop the software for the implementation.

7.2 Feature Extraction from Radar Sweeps

To formulate the detection system, the first step is to obtain samples of targets, noise and clutter in a 2 microsecond window, which consists of 50 samples at a sampling frequency of 25 MHz. Targets close to the heading marker were first identified on the radar display. When the target just passed the marker, the digital scope would be triggered to acquire the sweep and the range of the target from the radar transmitter was measured. The target would then be identified from

the data recorded and the window extracted as one of the samples. Noise was also present in all the returns and this was extracted from the same sweep when targets were recorded. Rain clutter was recorded when heavy rain was observed in the region of the heading marker. There were a number of occasions which gale force winds were encountered in the Plymouth area during the data recording periods. Sea clutters were observed in closed ranges of the radar and the scope was triggered to acquire such signals in the vicinity of the heading marker. To ensure that no targets existed in the recording of noise and clutter by chance, the gain, sea clutter and rain clutter control of the radar display unit were adjusted to see if targets were presented in the vicinity from the radar screen. Also, the record was carefully checked for any targets that were embedded in the noise. Initially, 100 samples for targets, 50 samples for noise, 50 samples for rain clutter and 50 samples for sea clutter were recorded, i.e. a total of 250 samples. A Matlab program was written to calculate the five parameters from these samples. These include mean amplitude, mean amplitude deviation, mean period, mean period deviation and maximum period. The distribution of these parameters for targets, noise and clutter (rain and sea) is plotted (figures 7.1 to 7.5).

Traditional radar detection system has been using amplitude as a discrimination feature. From the distribution on mean amplitude (Fig.7.1), a large overlap between target, noise and clutter is observed. There were instances where the clutter had a very large amplitude, especially during the rain clutter environment. If a threshold is determined based on this amplitude distribution, large false alarm rate and low detection probability would result. Distribution of amplitude deviation (fig 7.2) shows a better discrimination feature. The majority of the noise and clutter had a very low amplitude deviation from the mean and is independent of the type of clutter. This is due to the fact that the amplitude of noise and clutter tend to be more evenly spread in the window, whereas, for targets, a sharp rise in amplitude usually occurs. A variation of the

window size would have an impact on the value of the amplitude deviation. The selection of the window size will be discussed in section 7.3.

Figures 7.3 to 7.5 show the parameters related to the period of return signals. The noise signals are mainly spikes with a very fast rise and fall time. They consist of large high frequency components that cause the width of the pulse to be much narrower than those of the targets. The system detects the period between the consecutive negative extremes as an indication of the width of the pulse. The mean period of each window was evaluated and shown in fig. 7.3. The use of negative extremes (described in section 6.4 of Chapter 6) as detection criteria is a very effective way of determining the pulse width of individual pulses in a radar return. An ideal target would be one which has only two negative extremes, i.e. at the beginning and the ending of the pulse. However, not all targets belong to this category. The width of the pulse would be reduced if the number of detected negative extremes is increased. As such, some overlap still exists in the distribution of the mean period, the period deviation and the maximum period. The majority of the noise and clutters have a narrow pulse width and their deviation from the mean is small, as shown in fig. 7.4. The maximum period signifies the width of a specific pulse which has a maximum value in a window. This is useful in the identification and classification of a possible target in the window.

Form the graphs provided, it is observed that it would be a difficult task to discriminate the target from noise and clutter based on any one of the statistical characteristics. However, it is important to note that redundancies may spread across more than one parameter but such redundancies will seldom spread across all the five parameters to a degree that may be inseparable by computational techniques. The spread of these five parameters for three targets and three noise samples is shown in fig. 7.6. Examination of these distributions and spreads

show that targets normally have a larger amplitude and period than noise. However, there are occasions where noise may also have similar characteristics in either amplitude or period, e.g. noise 2 has similar features to target 3 in both mean period and period deviation. Yet, they can still be discriminated by the amplitude parameters as well as the maximum period. Noise 3 has a larger mean amplitude than targets 1, 2 and 3, however its amplitude deviation is much smaller than those of the targets. Therefore, it is necessary to include both amplitude and period parameters for feature discrimination in the detection system.

Fig.7.1 Distribution of Mean Amplitude

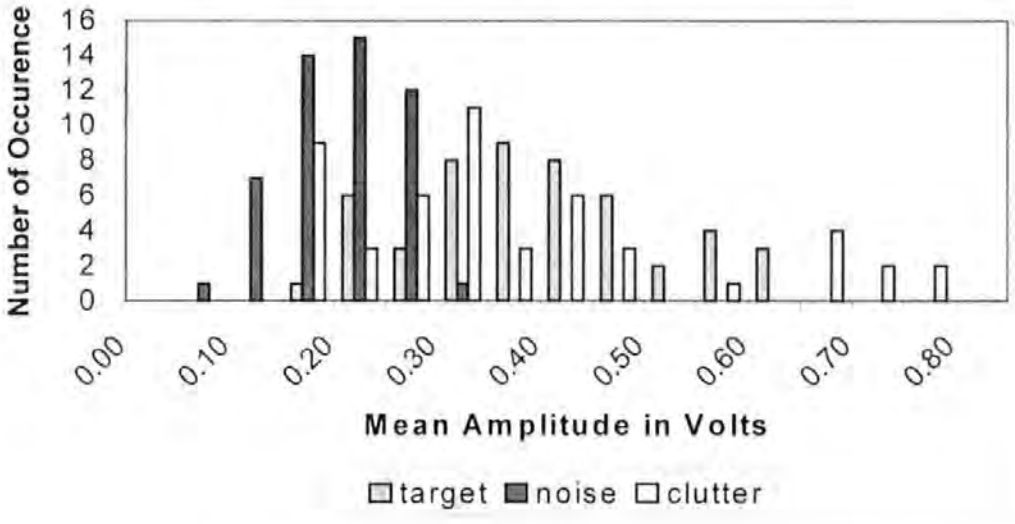

Fig. 7.2 Distribution of Amplitude Deviation

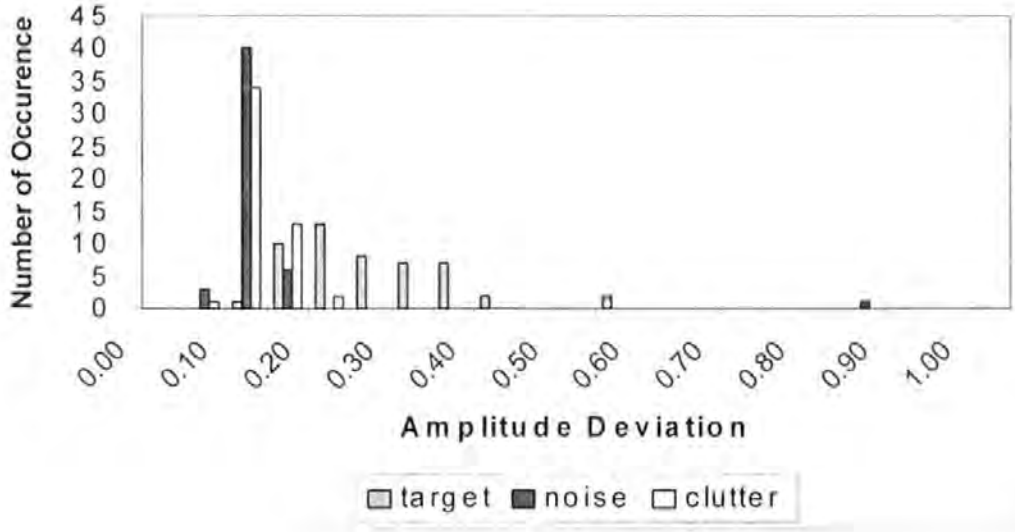

Fig. 7.3 Distribution of Mean Period

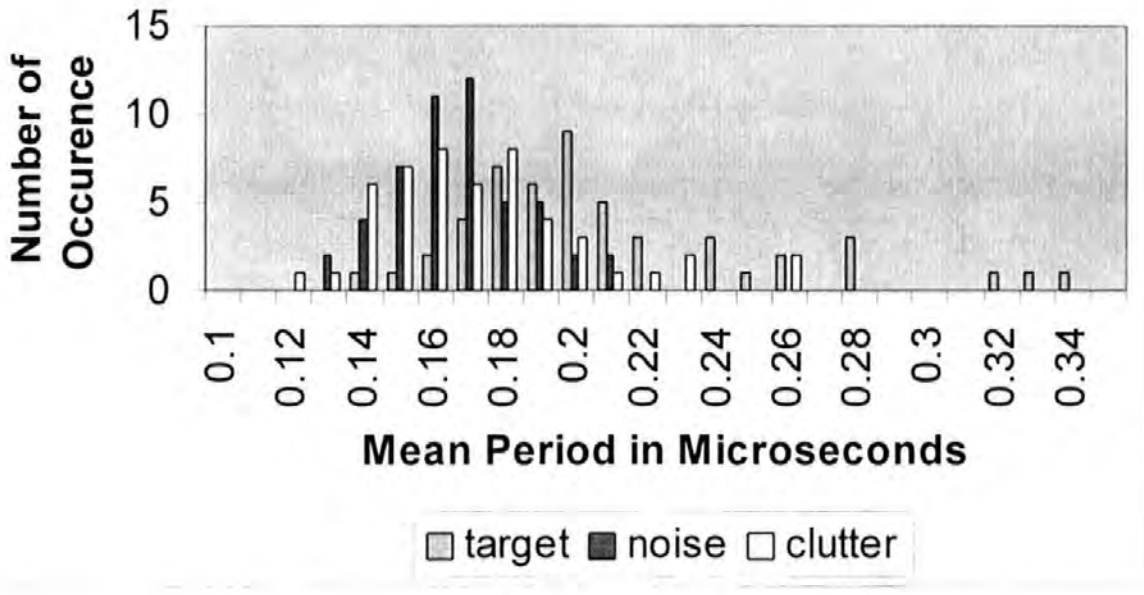

Fig.7.4 Distribution of Period Deviation

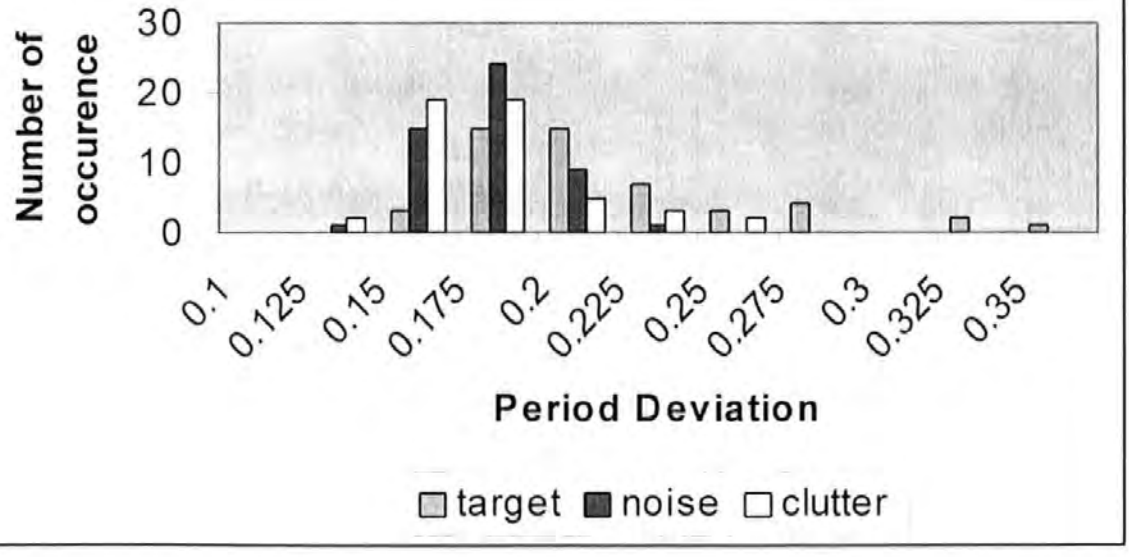

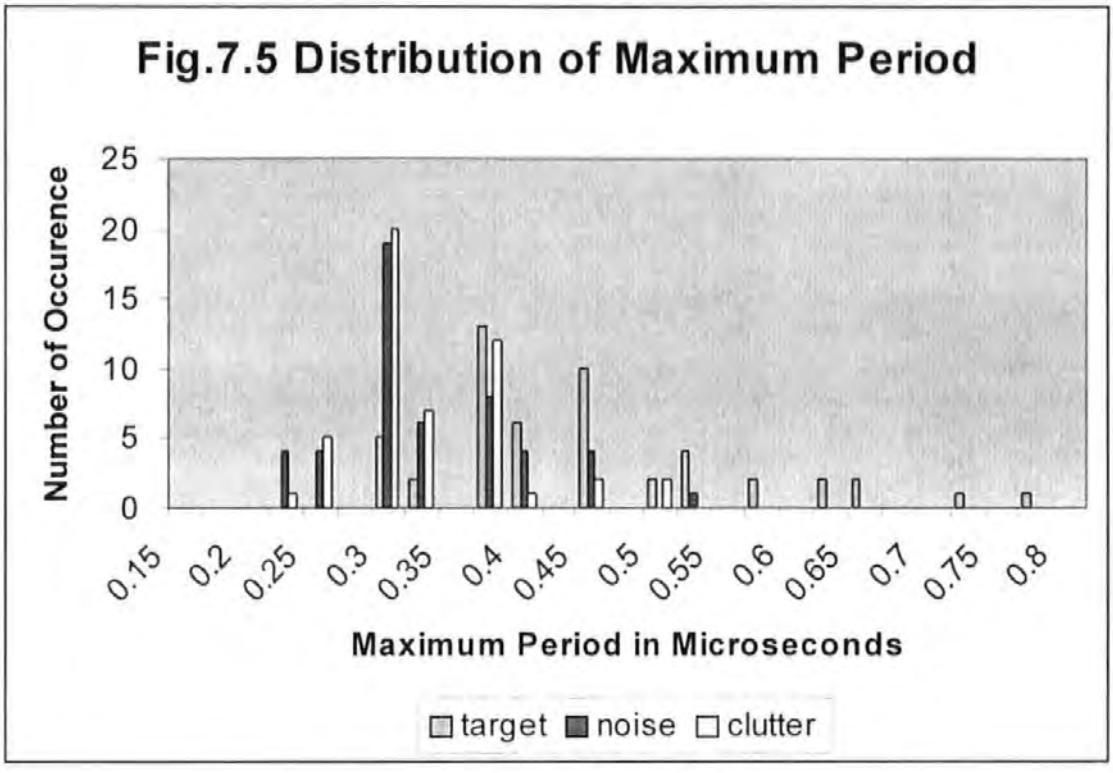

Fig.7.6. Spread of the Five Parameters

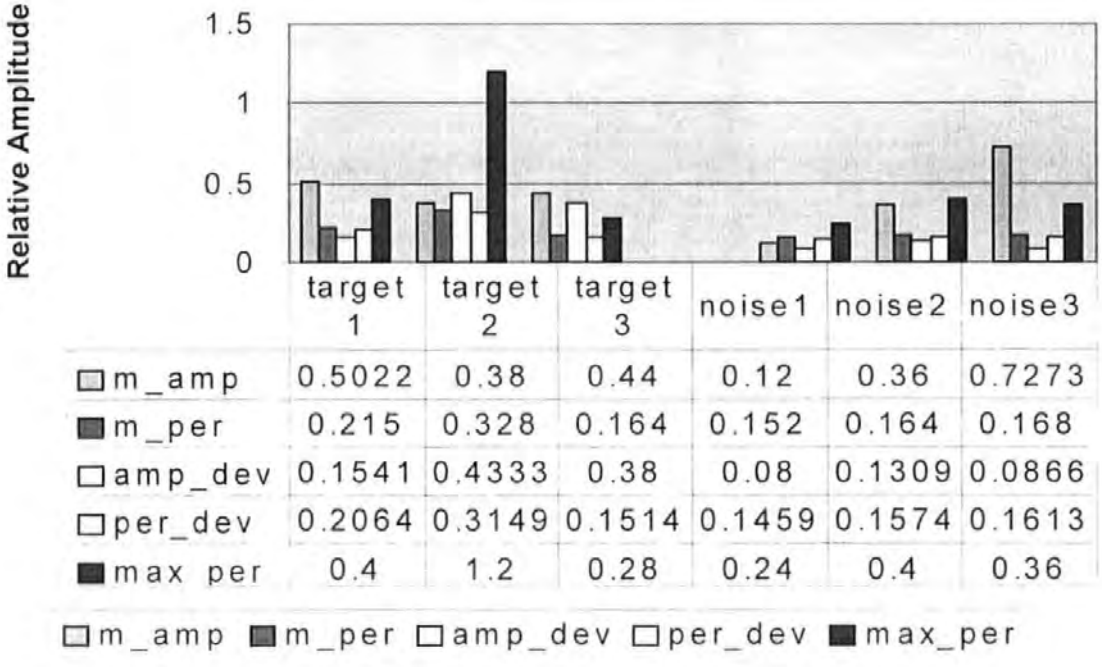

	target 1	target 2	target 3	noise1	noise2	noise3
m_amp	0.5022	0.38	0.44	0.12	0.36	0.7273
m_per	0.215	0.328	0.164	0.152	0.164	0.168
amp_dev	0.1541	0.4333	0.38	0.08	0.1309	0.0866
per_dev	0.2064	0.3149	0.1514	0.1459	0.1574	0.1613
max per	0.4	1.2	0.28	0.24	0.4	0.36

7.3 Size of Moving Windows

A moving window is required to shift along the complete sweep so that the statistical characterisation at specific time frame of the sweep can be evaluated. The effect of the window size on the discrimination performance was also studied. Window sizes of 1.6, 2.0, 2.4 and 2.8 microseconds for both large and small targets were investigated, their waveforms and spreads are plotted in figures 7.7 to fig 7.10. As shown in fig. 7.8, a width of 1.6 microsecond gives maximum relative amplitudes of the spread (for the five parameters of both large and small targets). The changes in relative amplitude with respect to the window sizes were more distinct between 1.6 microseconds and 2 microseconds for large targets, however the changes were not so obvious for the small target. The smaller the window size, the larger the number of computations required to calculate the five sets of parameter. For example, to compute the parameters for 12 nautical miles of radar range with a window size of 1.6 microseconds, it would require (assuming no overlapping window is used)

(12 x 1852 x 5)/(150 x 1.6) = 463 computations

If 2 microseconds window size were used, it would require

(12 x 1852 x 5)/(150 x 2) =370 computations.

[1 nm = 1.852 km, 1 microsecond = 150 meters]

From figures 7.7 to 7.10, a window size of 2 microseconds (150 meters) gives a suitable discrimination against noise.

7.4 Formulation of the Neural Detection System

The following sections describe the methods used to formulate a neural detection system for radar targets. Different network topologies with various training parameters were investigated to

obtain the best performance for target detection. When the network was fully trained, it was implemented in selected sets of test data to allow system verification.

7.4.1 Setting up the Initial Network

The training data required for the neural detection system was obtained from a series of recorded sweeps (around 250) using the method as described in Chapter Six. Sampled targets, sea/rain clutter and noise were picked up from the return radar signals. The five parameters of statistical characterisation, i.e. mean amplitude, mean period, mean amplitude deviation, mean period deviation and maximum period, were calculated for each sampled window with two microseconds duration. A total number of 250 sets of data from these samples (100 samples of targets, 50 samples of noise, 50 samples of rain clutter and 50 samples of sea clutter) were used to train the network. The signal to noise ratio of the targets ranged from 1.45dB to 24.5dB. During the training process, the targets were identified as 1 and clutters/noise as 0.

The number of hidden layers for the initial network was one with two neurons and there were five inputs. The required output was the decision on whether a target was present, i.e. a 1 or 0. To initialise the weights in the network, each weight was set to a small random number initially. These numbers were obtained from a random number generator that utilised a fixed range. The initial weights were made close to zero otherwise the learning rate, which adapts the changes in the weight, would be slow. The changes in weights are dependent on the error terms after each training sequence. The magnitude of the weight changes is controlled by the learning rate constant, ξ. When ξ is large, the changes in weight value will be large and this causes the training process of the network becoming faster. However, a high value of ξ will increase the risk of oscillation, i.e. the network keeps jumping over the error minimum without converging. In order to decide the learning rate to be used, tests were performed to compare the error values

for varying ξ. Six values of ξ were used for this test and the results were plotted in figs. 7.11a to 7.11f. The performance of the network was assessed by the sum square error of the output vectors. When the learning rate is low, it requires a long overall learning time. As the learning rate increases, oscillations are introduced into the training time of the network. If the learning rate is made too large, it will cause the network to become unstable with the error value not converging. From the results obtained, a value of ξ between 0.05 and 0.1 will be a suitable choice for the implementation.

The momentum constant, α, can be used to damp the oscillation to facilitate the fast learning rates. Figures 7.12a to 7.12f show the performance of the network using different momentum values, i.e. 0.1, 0.5, 1, 0.9, 0.98 and 0.95. With low values of momentum, less oscillation was induced but longer training time was required as shown in figures 7.12a and & 7.12b. A high value of momentum will cause the network to become unstable and convergence of the error cannot be achieved. Fig. 7.12c shows the performance with a momentum of 1 and the error is maintained at 100. By slightly reducing the momentum from 1 the network converges again and, on the basis of this result, a value of 0.95 was employed for the network.

To obtain an efficient neural detection system, efforts must be made to determine the optimum network topology. The input layers and the output layers were fixed by the application of the system, i.e. 5 inputs and 1 output. However, the number of the neurons in the hidden layers and the number of hidden layers had to be defined. If the number of neurons in the hidden layers is too large, the network work may take a long time to train. Also, the additional neurons increase the chance that even a local minimum will yield a low error. On the other hand, if there are not enough neurons in the hidden layer, the network may not be trained at all. There is no rule to derive the number of hidden layer neurons to achieve the optimum performance.

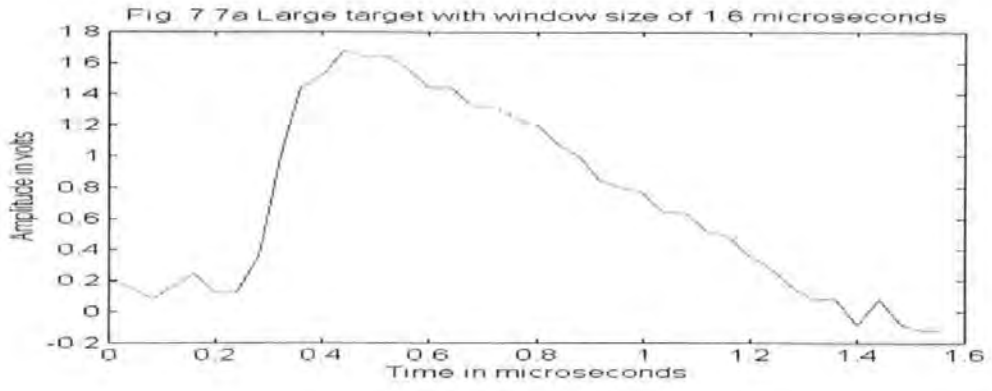
Fig 7 7a Large target with window size of 1 6 microseconds
Amplitude in volts
Time in microseconds

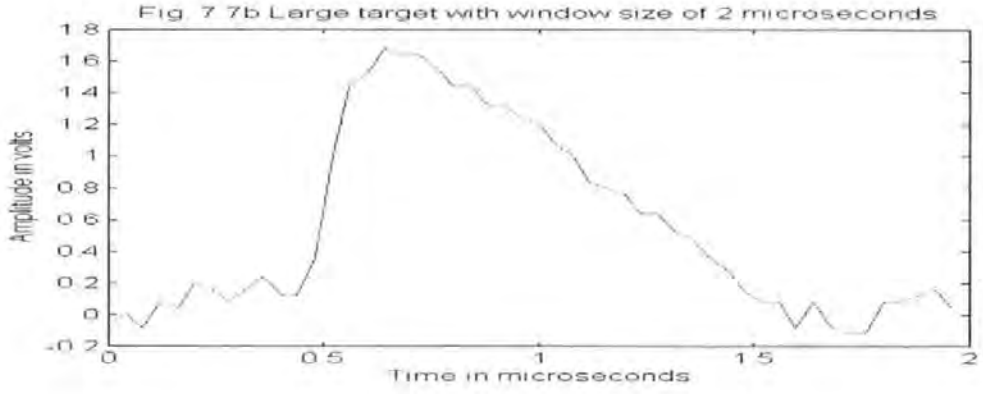
Fig 7 7b Large target with window size of 2 microseconds
Amplitude in volts
Time in microseconds

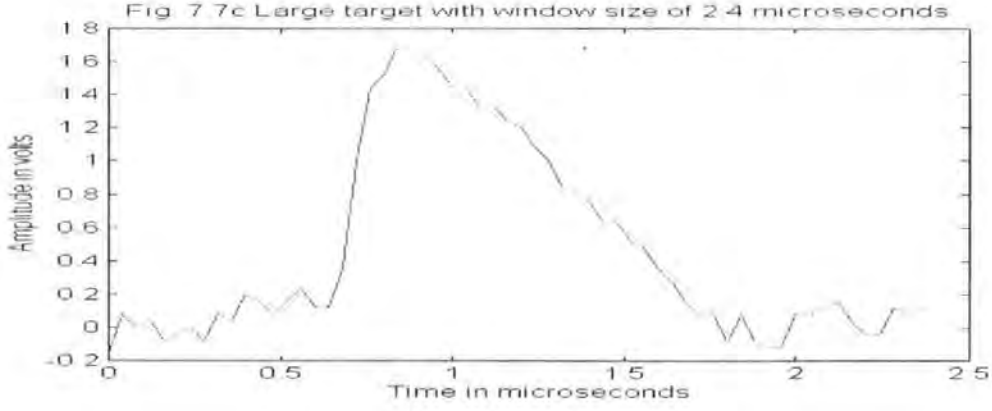
Fig 7 7c Large target with window size of 2 4 microseconds
Amplitude in volts
Time in microseconds

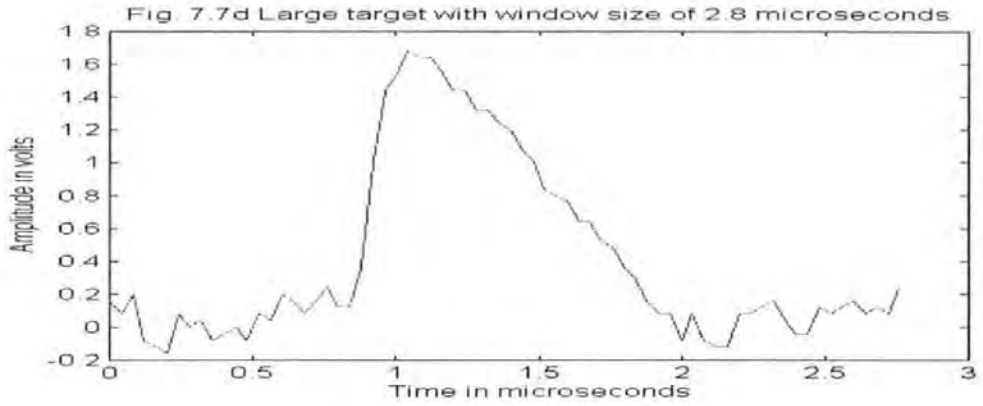

Fig.7.8 Spread with Different Window Size (Large Target)

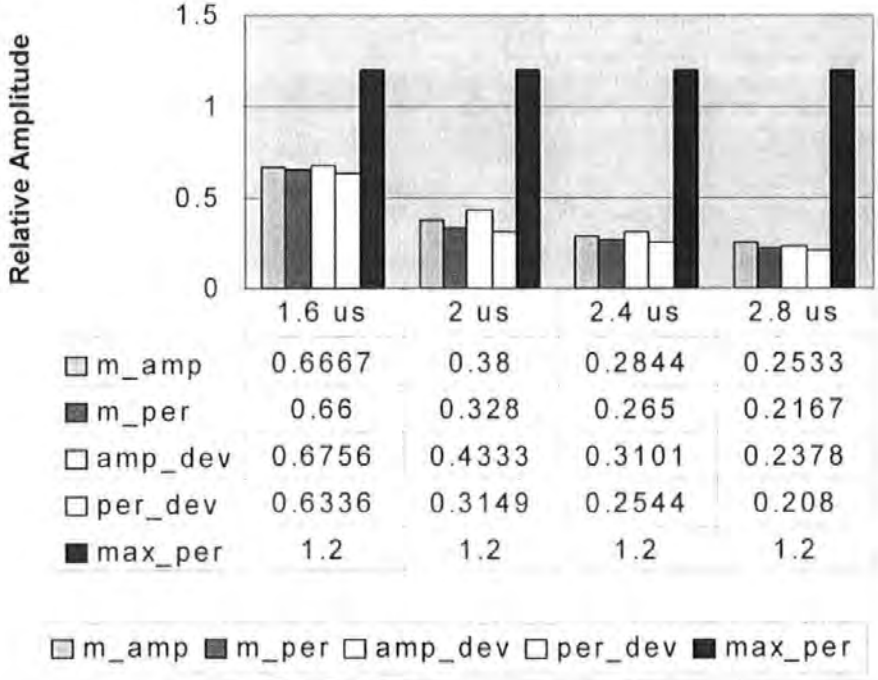

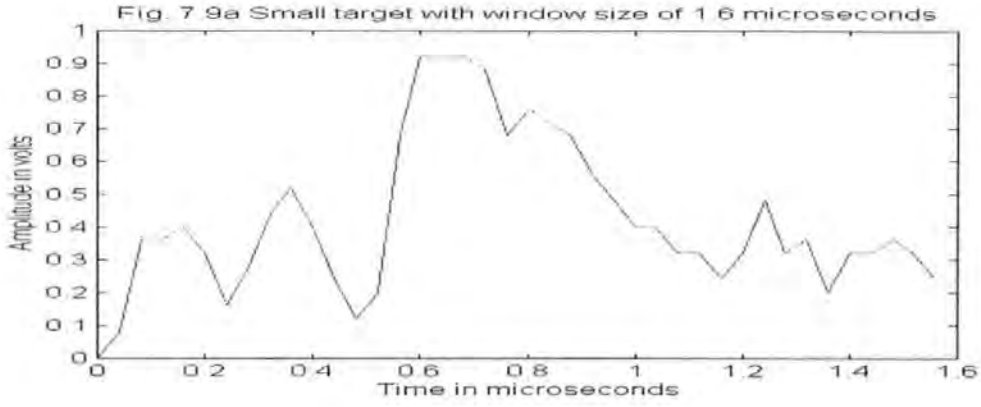

Fig. 7.9a Small target with window size of 1.6 microseconds

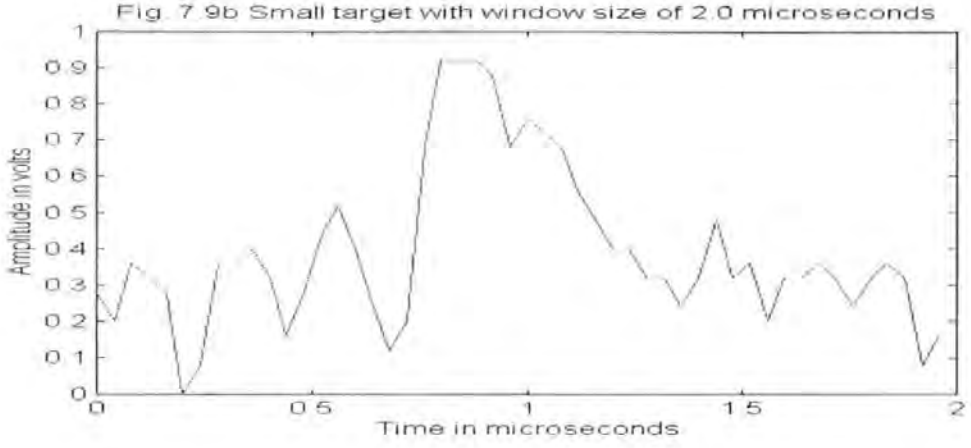

Fig. 7.9b Small target with window size of 2.0 microseconds

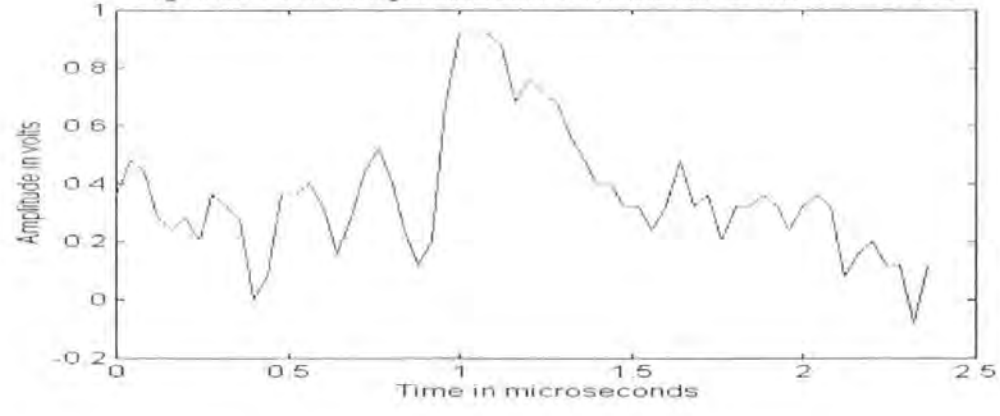

Fig. 7.9c Small target with window size of 2.4 microseconds

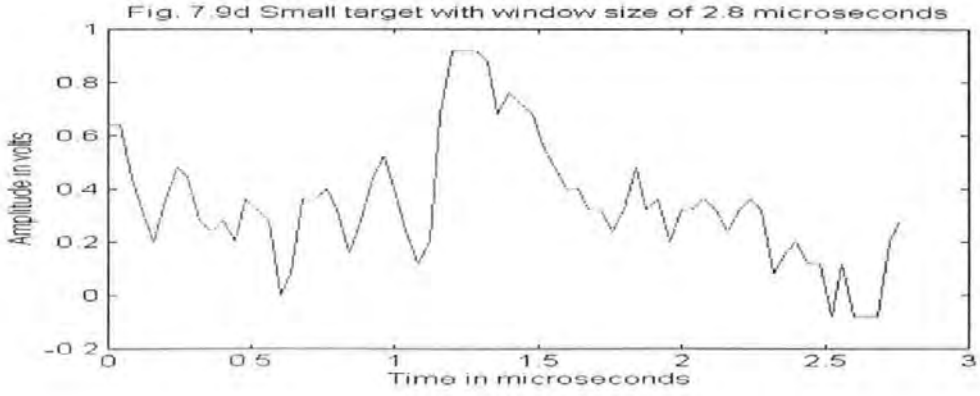

Fig.7.10 Spread with different window size (small target)

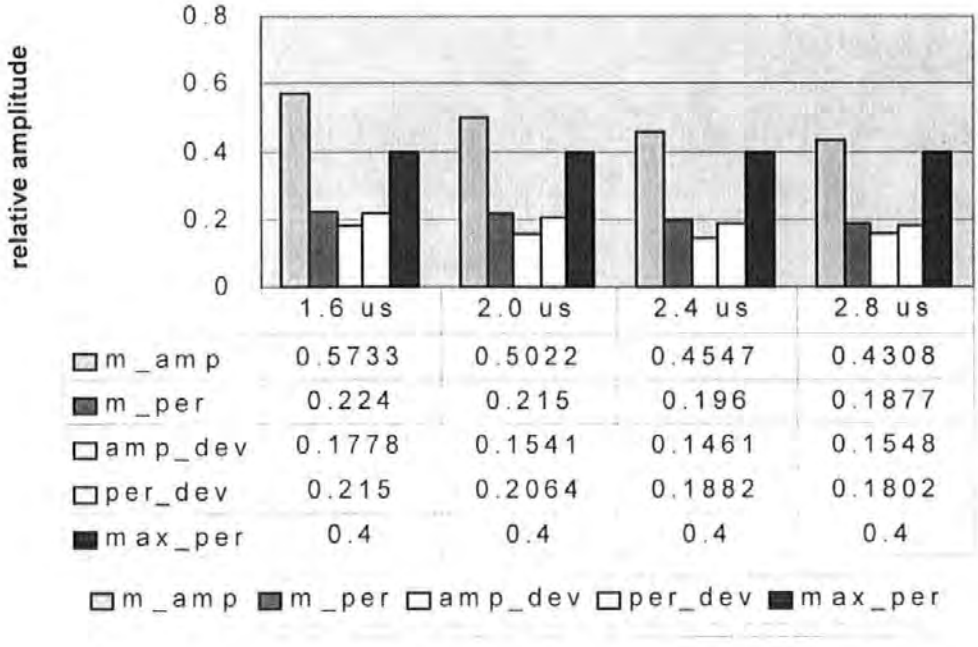

Fig.7.11a Performance of training with learning rate=0.001, SSE=3.7596

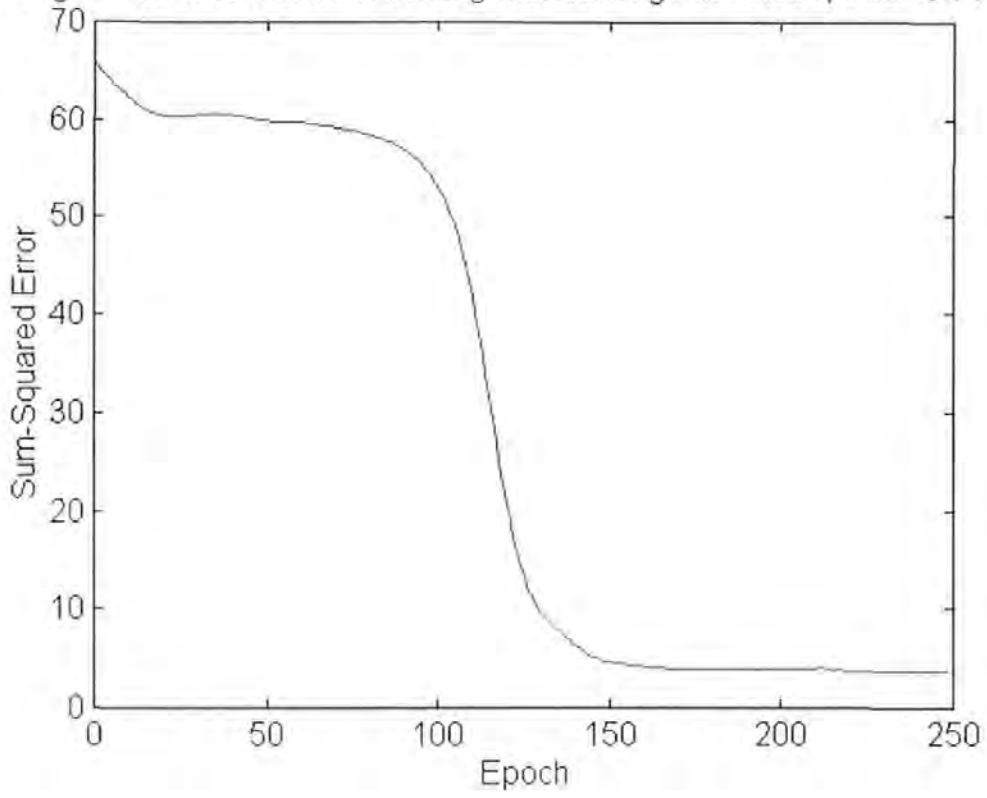

Fig.7.11b Performance of training with learning rate=0.005, SSE=3.7606

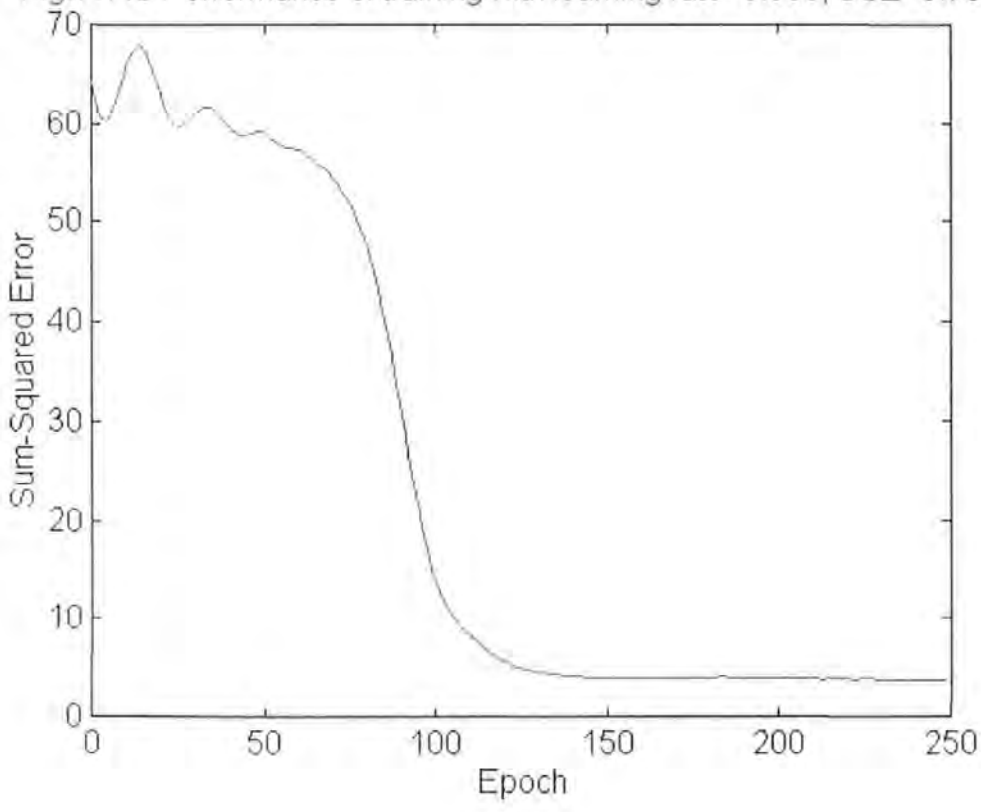

Fig.7.11c Performance of training with learning rate=0.01, SSE=3.7845

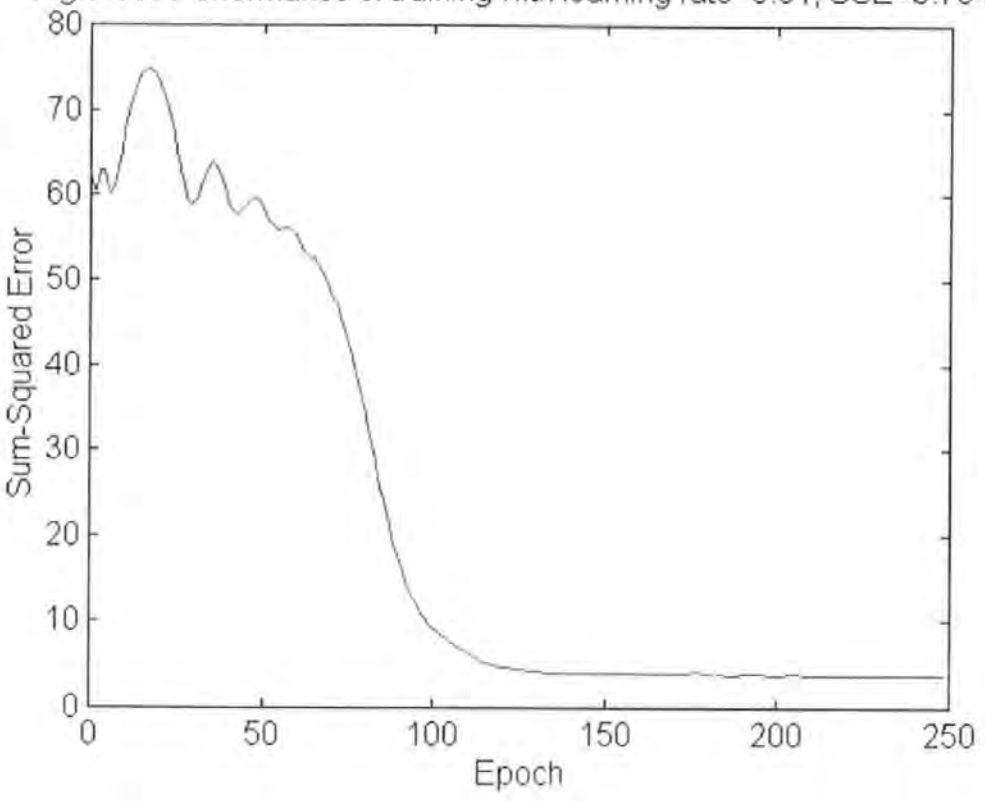

Fig.7.11d Performance of training with learning rate=0.05, SSE=3.6720

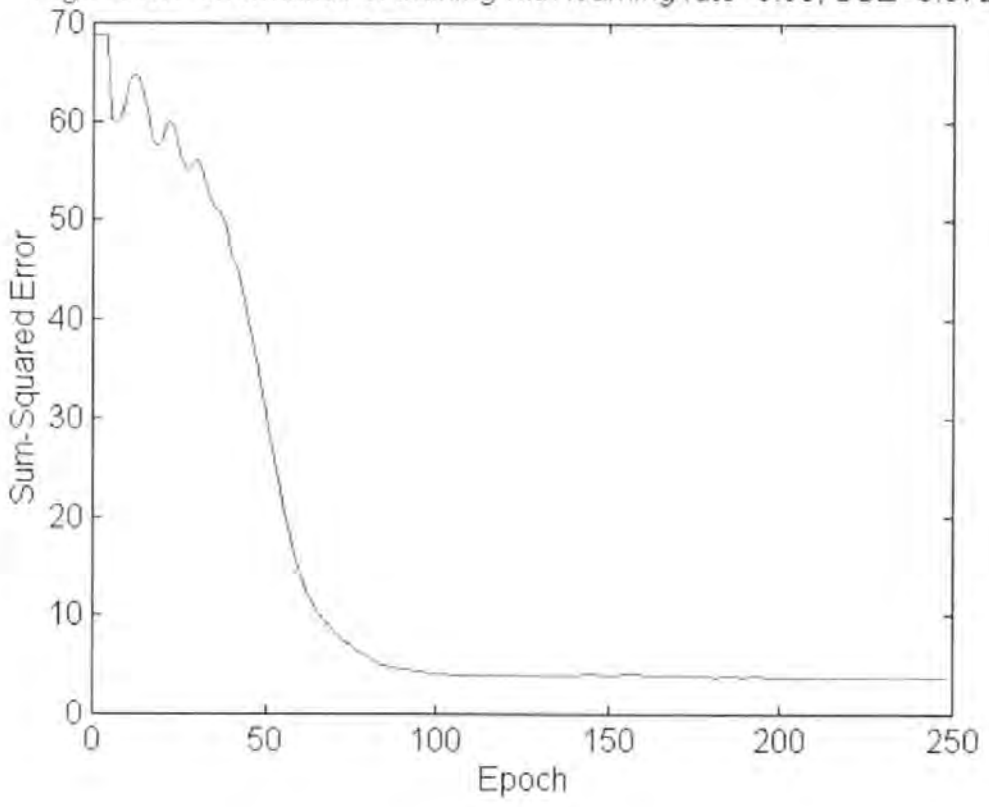

Fig.7.11e Performance of training with learning rate=0.1, SSE=3.7314

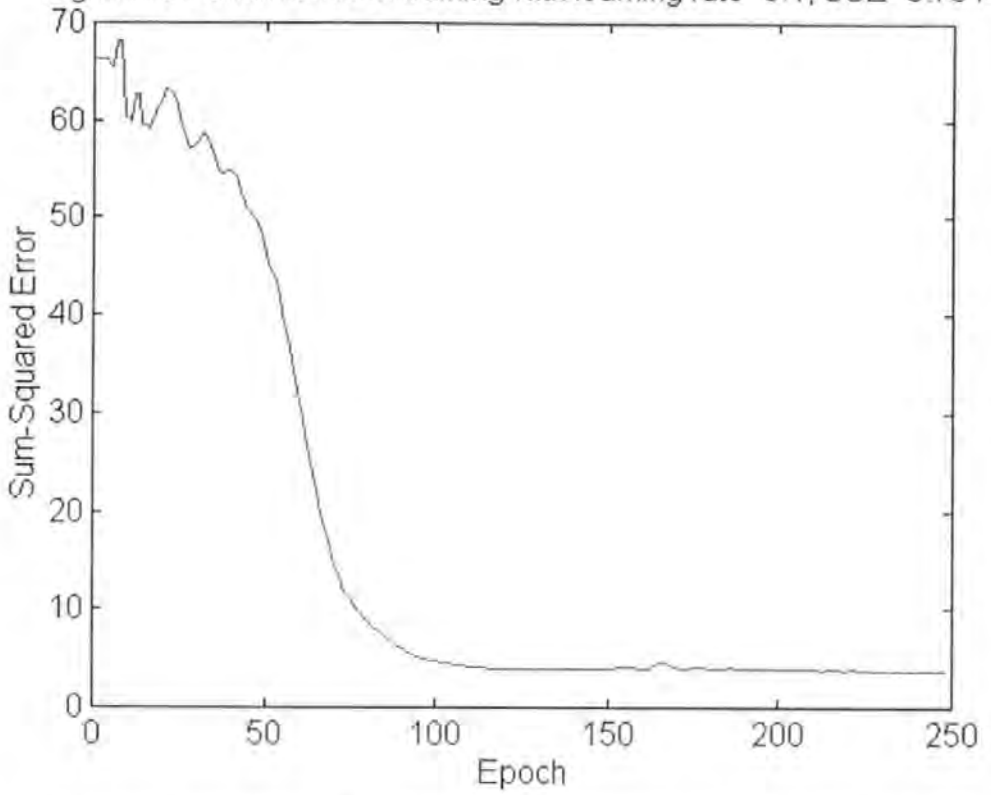

Fig.7.11f Performance of the training with learning rate=0.3, SSE=3.7445

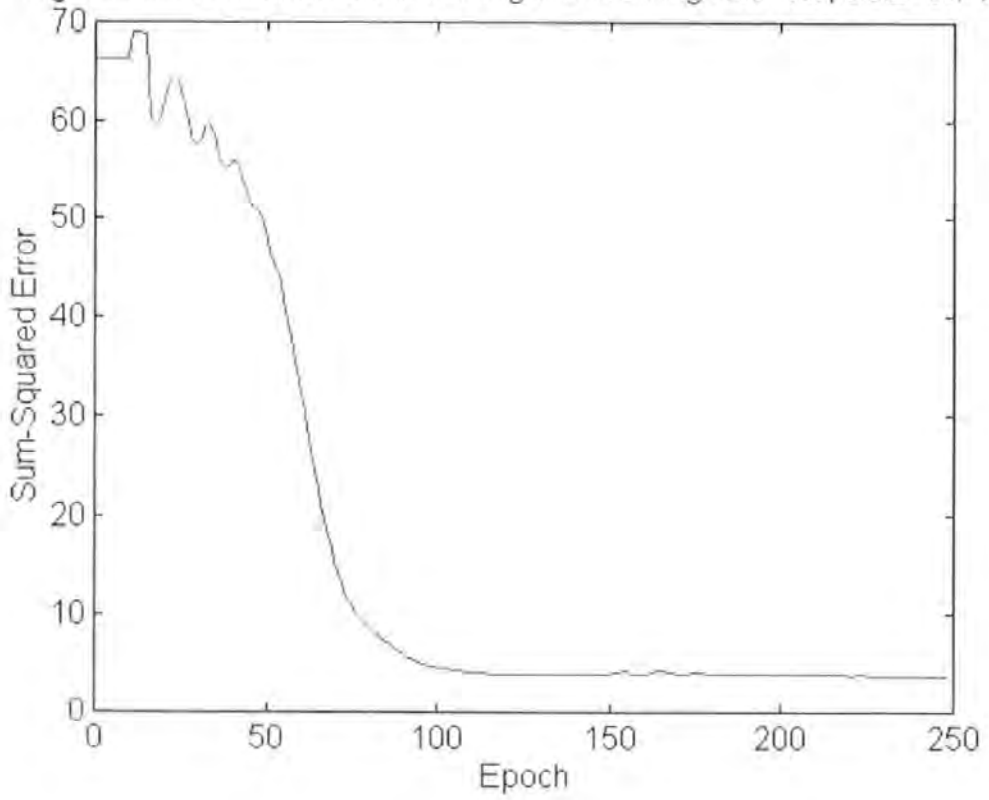

Fig.7.12a Performance of training with momentum=0.1, SSE=7.8479

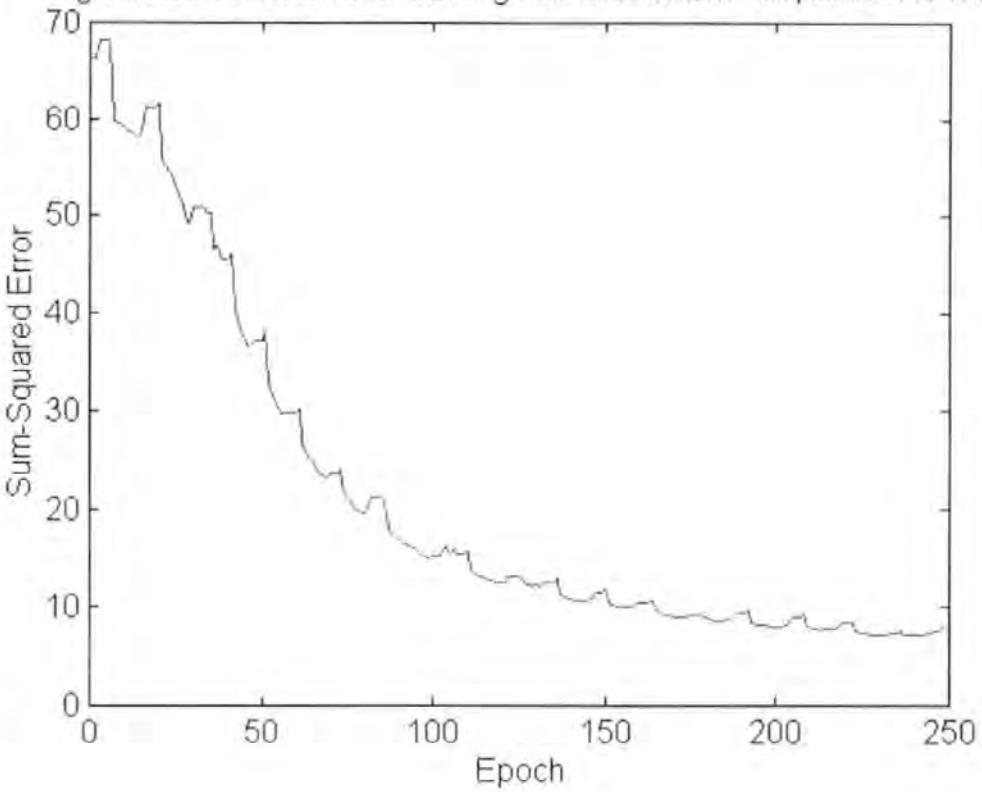

Fig.7.12b Performance of training with momentum=0.5, SSE=4.9738

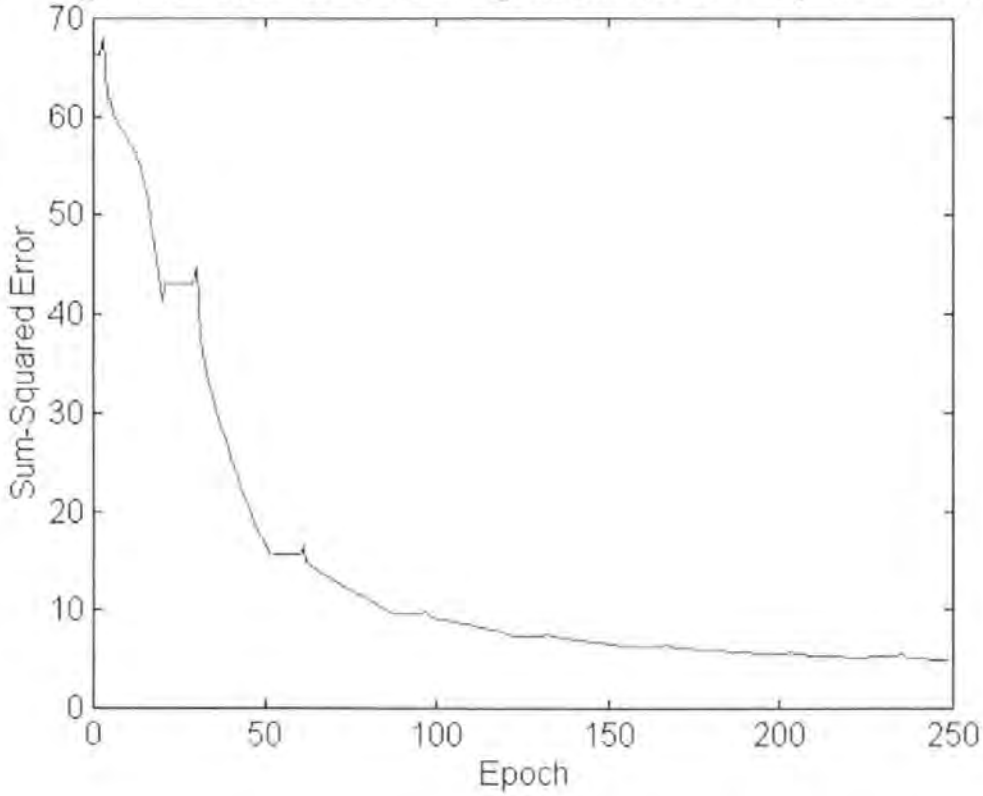

Fig.7.12c Performance of the training with momentum=1, SSE=100

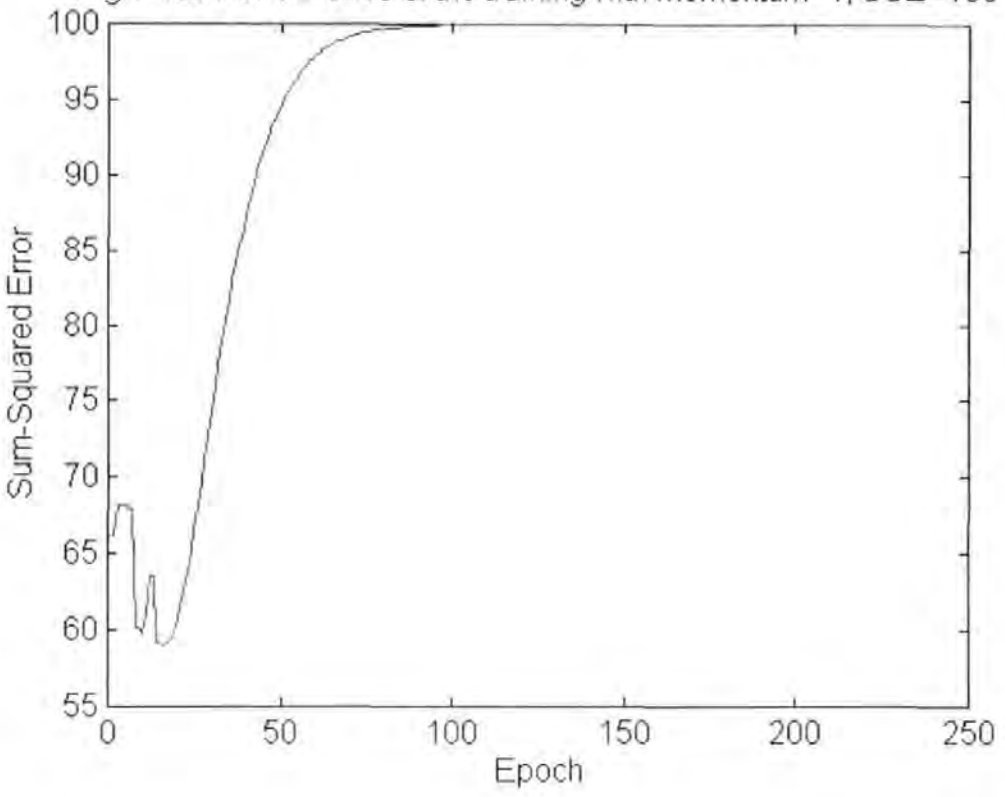

Fig.7.12d Performance of training with momentum=0.9, SSE=3.9437

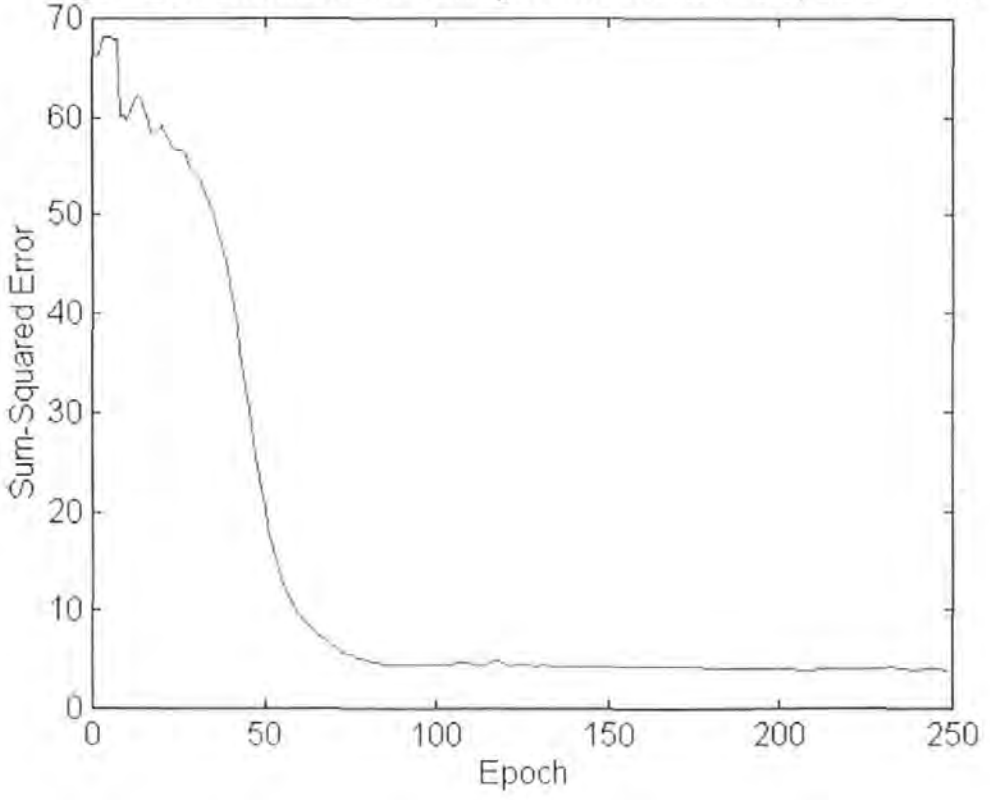

Fig.7.12e Performance of training with momentum=0.98, SSE=4.5261

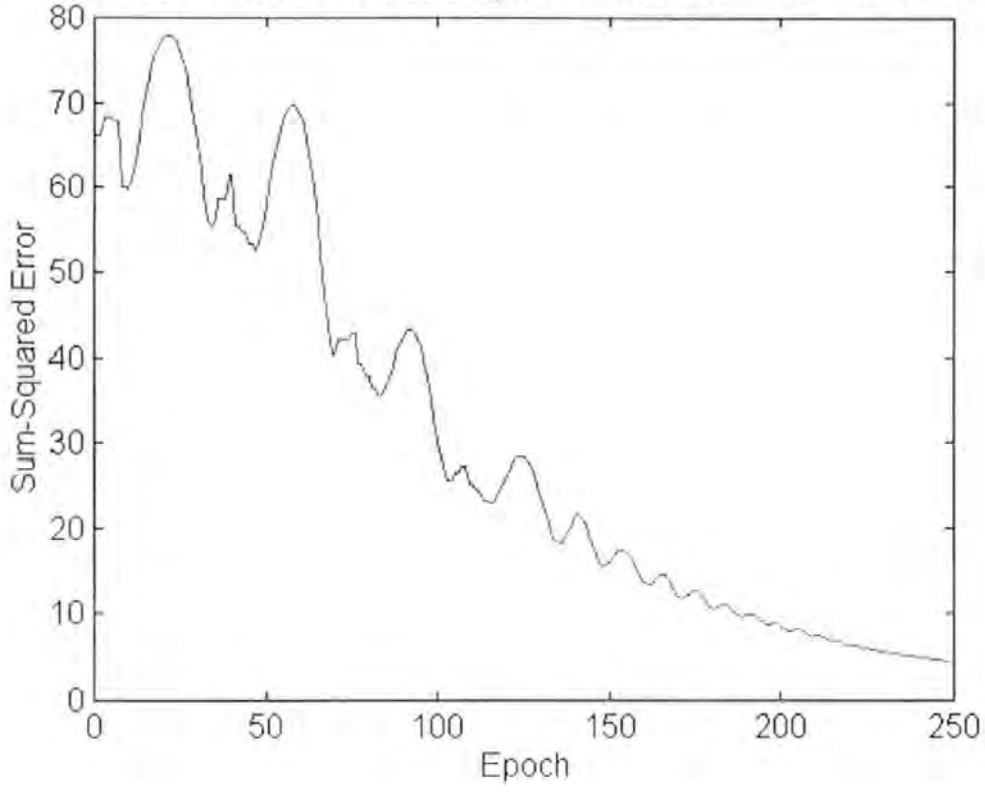

Fig.7.12f Performance of training with momentum=0.95, SSE=3.6789

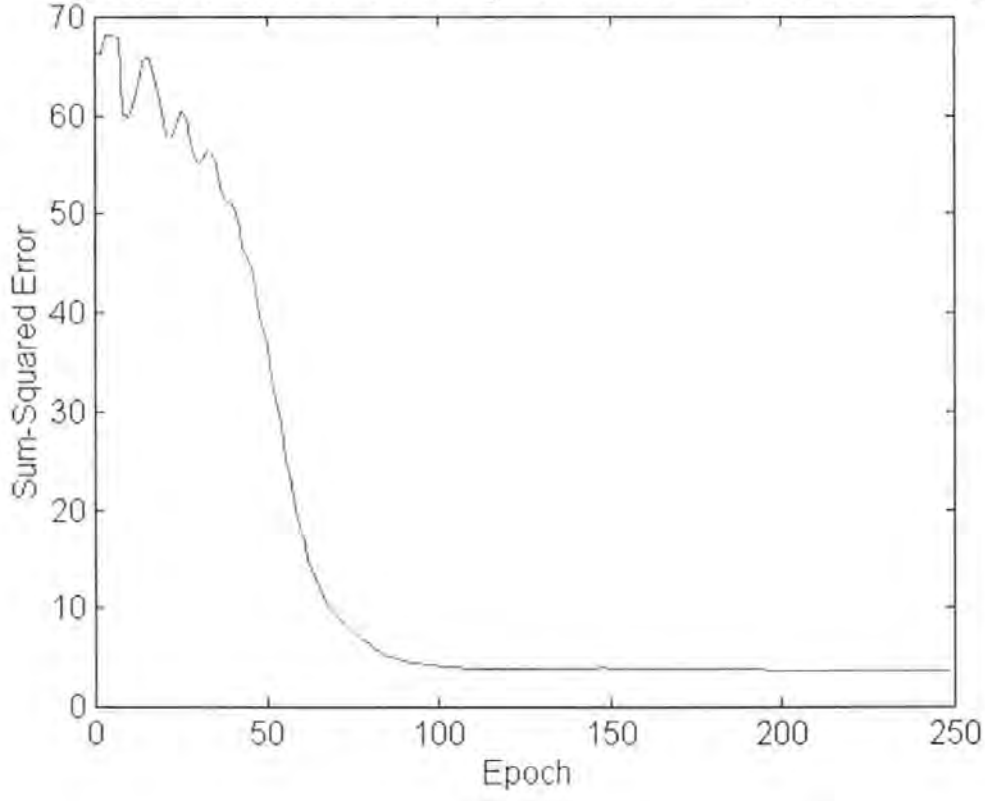

To define the topology of the network, a series of tests were performed using different combinations. These included networks with none, one and two hidden layers, the results with 250 iterations are shown in figures 7.13a to 7.13f, which show the initial response of the network under different topologies. Table 7.1 shows their sum-squared errors after 30,000 iterations.

Table 7.1 Training errors of the network after 30,000 iterations

Topology	Sum Squared Error
No hidden layer	3.0180
One hidden layer with one neuron	3.0231
One hidden layer with two neurons	3.0007
One hidden layer with three neurons	3.0497
Two hidden layers with one neurons	3.4937
Two hidden layers with two neurons	3.4942

Higher training errors were obtained when the network had none or two hidden layers. The optimum performance with least training error was found when the network had a single hidden layer with two neurons and this was chosen for the implementation.

7.4.2 Application of the training algorithm

The developed network with 5 inputs, 1 hidden layer (with two neurons) and 1 output layer was trained with the 250 sets of data. During each epoch, the five parameters of statistical characterisation were presented to the input layers of the network. For each set of parameters, the error was calculated by comparing the network output with the desired output. When the

entire training set, i.e. 250 sets of input data, had been presented to the network, the error was summed to update the values of the weights.

In the training algorithm, the training process was terminated by one of two criteria. The first was to identify a maximum error value to ensure that the network would perform to an acceptable level. However, as the error value might not be reduced to the specified limit with the data available, then under this condition alone training may never be terminated. So, in addition to this rule, an upper limit was placed on the number of training epochs. The training will then stop when this maximum specified number is reached. Under this condition, the training time can be estimated but the performance of the network cannot be guaranteed. In this implementation, the maximum error of 0.05 was used as the limit for the training, and it took 3 million training epochs to reduce the error to this value. The first and the last 300,000 iterations are shown in figures 7.14a and 7.14b. Training was terminated on the performance rule, when the error reduced to 0.05.

Fig. 7.13a Network with a single layer, SSE=4.009

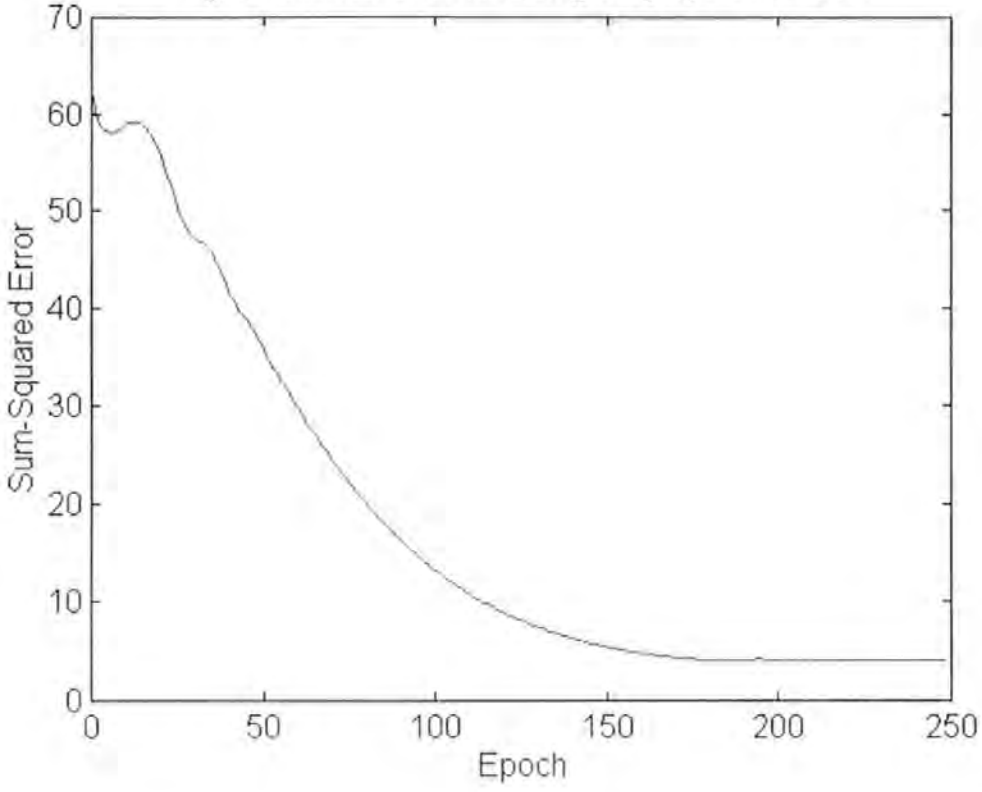

Fig.7.13b Network with one neuron in hidden layer, SSE=4.0675

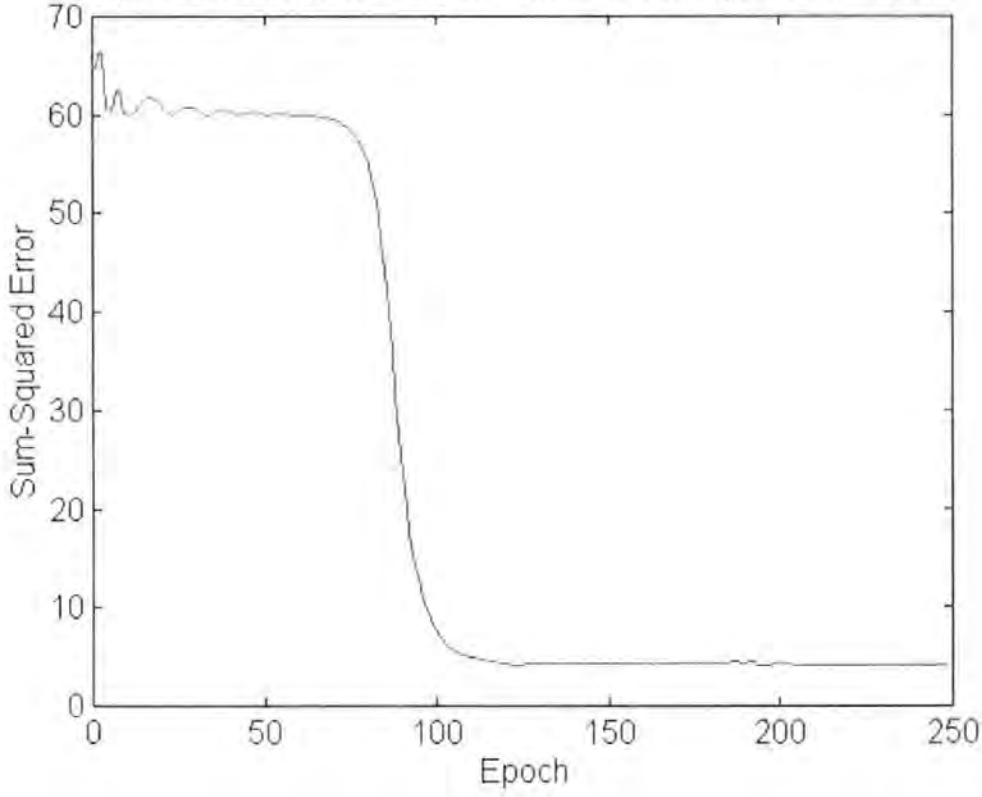

Fig.7.13c Network with two neurons in hidden layer, SSE=3.5629

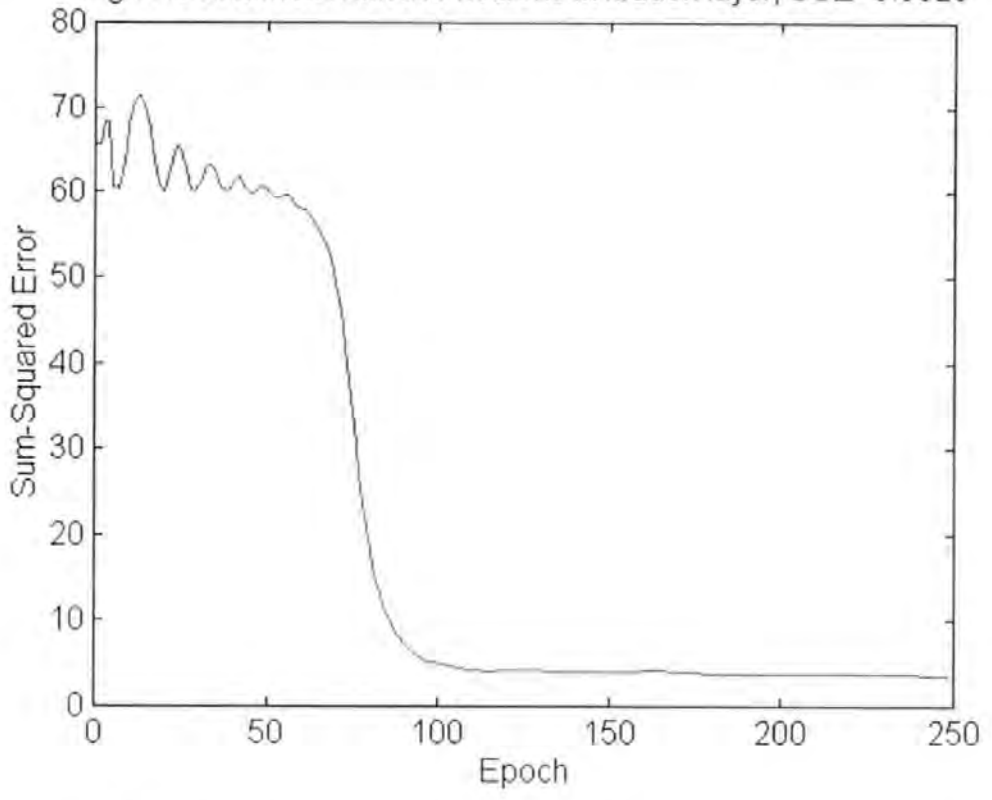

Fig.7.13d Network with three neurons in hidden layer, SSE=4.4272

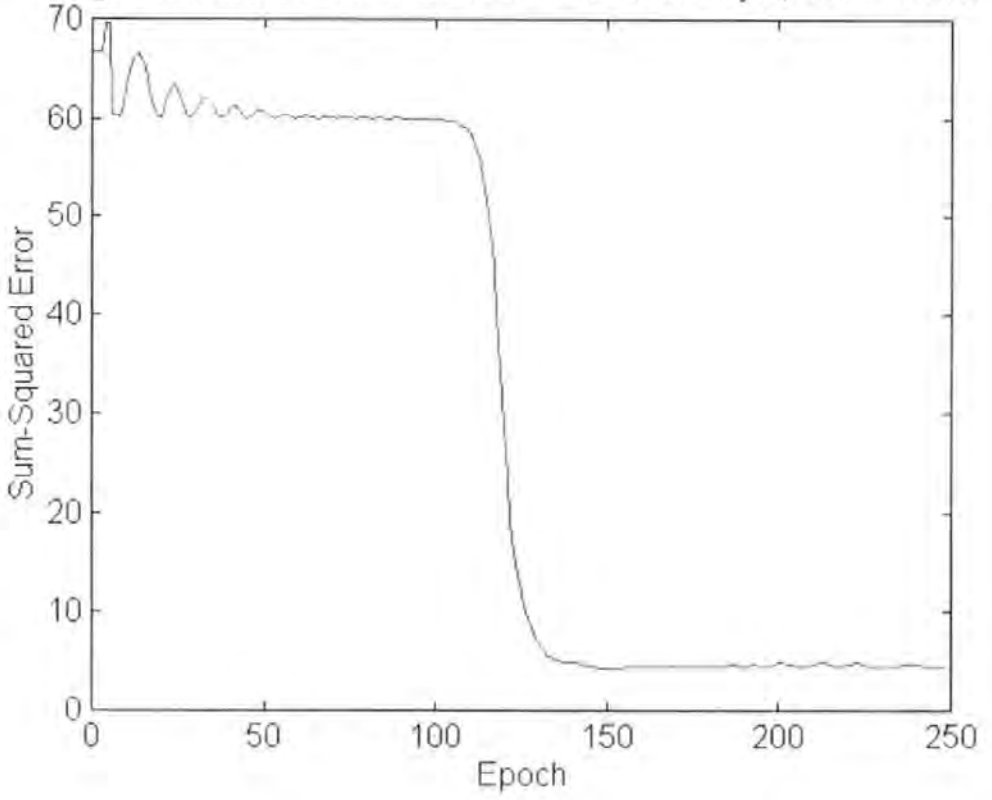

Fig.7.13e Network with 2 hidden layers, each with 2 neurons, SSE=4.4288

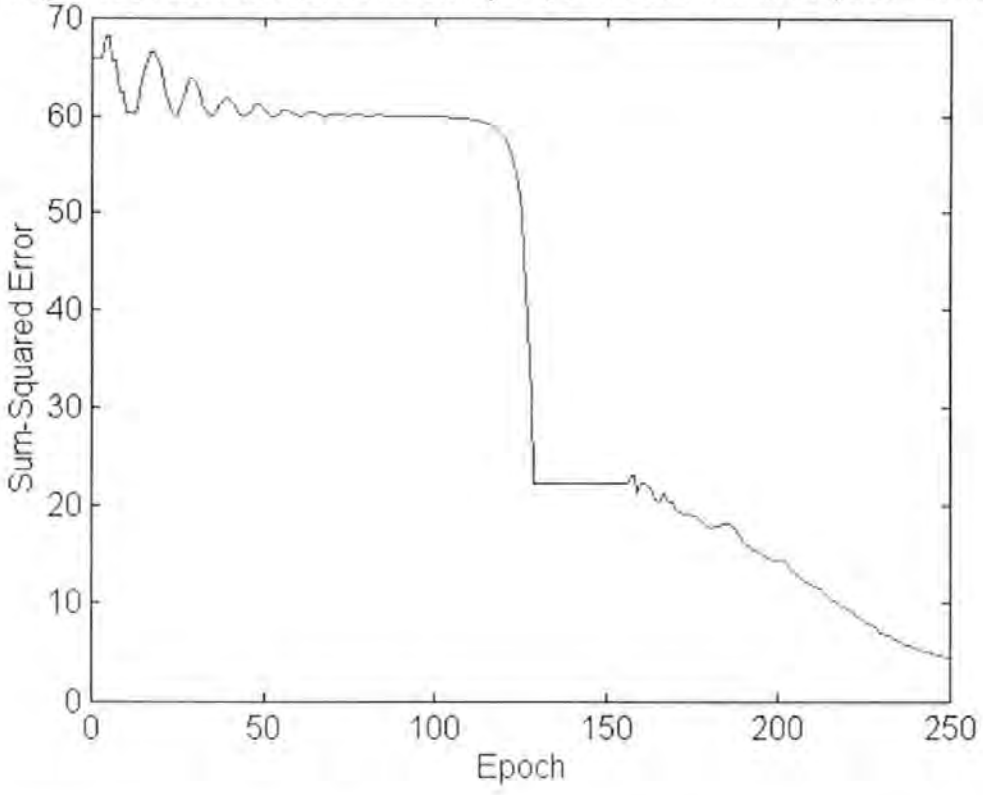

Fig.7.13f Network with 2 hidden layers, each with 1 neuron, SSE=4.0626

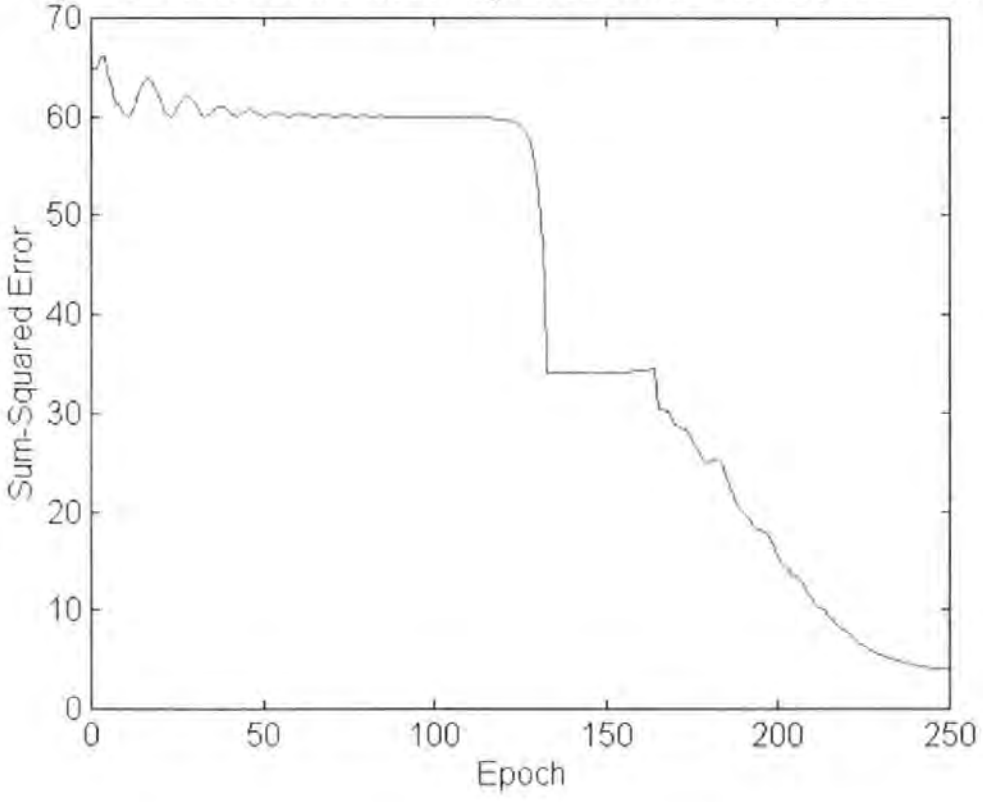

Fig.7.14a 2-Layer Backpropagation with Adaptive LR & Momentum, first 300,000 runs

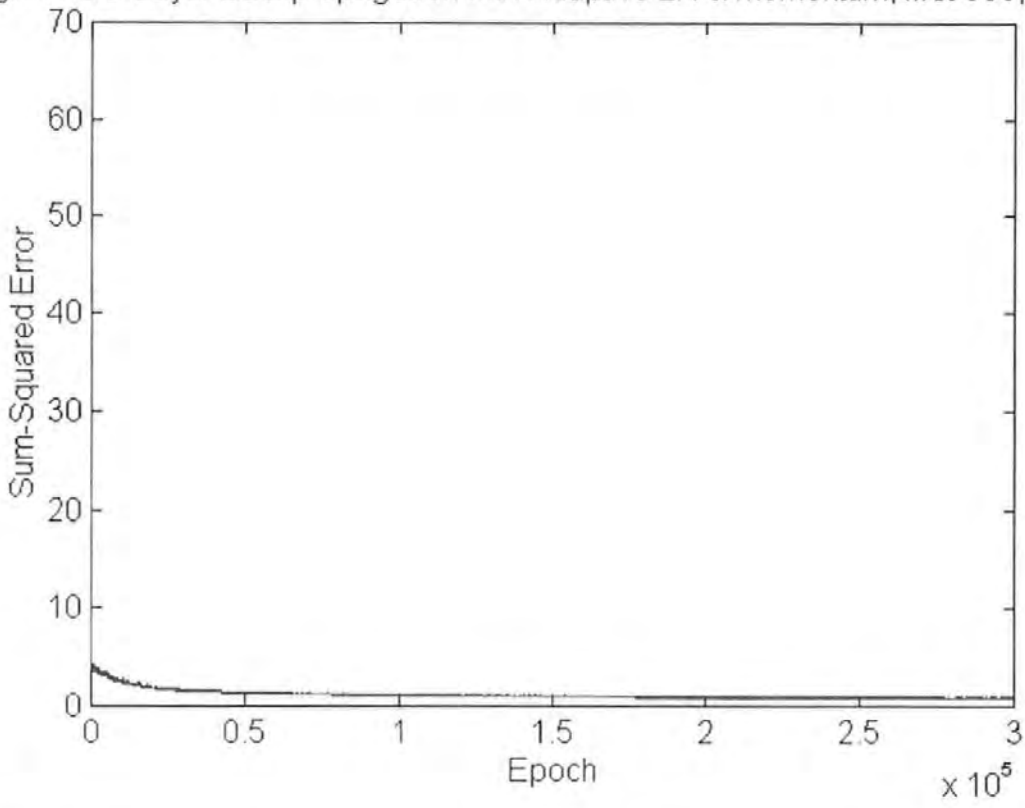

Fig.7.14b 2-Layer Backpropagation with Adaptive LR & Momentum, last 300,000 runs

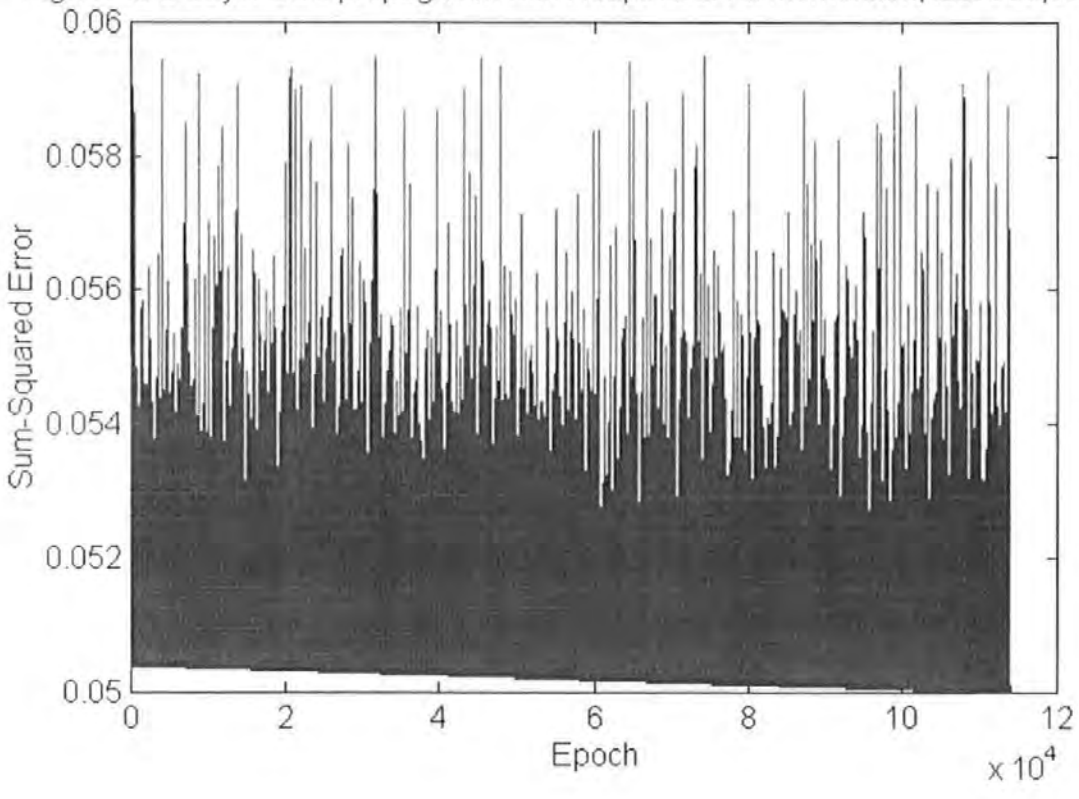

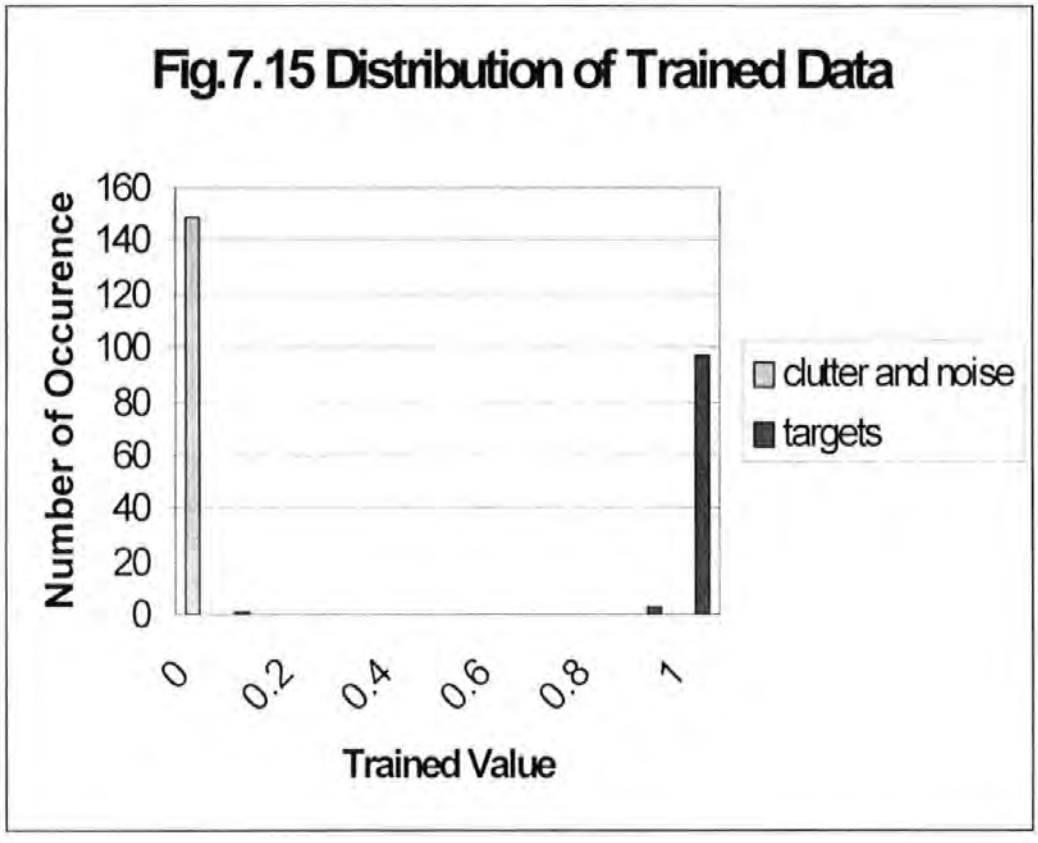
Fig.7.15 Distribution of Trained Data
Number of Occurence
160
140
120
100
80
60
40
20
0
0
0.2
0.4
0.6
0.8
1
Trained Value
clutter and noise
targets

7.4.3 Testing the Trained Network

When the training process was terminated, it was necessary to assess the performance of the trained network with the final values of the weights. Figures 7.14a and 7.14b show the plot of errors against the number of epochs. The rate of change of error reduces as the number of training cycles increase. Figure 7.15 shows the final result after the training exercises. The majority of the targets have a value of one while majority of the noise has a value of zero. There is no overlap between these two values and discrimination can thus be achieved.

A testing process is necessary to verify that the neural network is able to identify targets from data that was not used in the training exercise. The process was undertaken by using 40 further samples of data with different signal to noise ratio and noise background. Each data set consisted of a window of 50 samples and the five statistical characterization parameters were extracted from these data and input to the trained network. The value at the output determined when the data is a target or noise. Figures 7.16a to 7.16d show targets with signal to noise ratio of 3.7dB, 12.6 dB, 6.6dB and 10dB respectively. Figures 7.17a to 7.17d shows part of the sampled noise used for the testing. The testing results are shown in fig. 7.18, where it can be seen that all the noise samples have an output value of 0 while the targets have an output value ranging from 0.76 to 1. No overlap of the output for targets and noise occurs. Fig. 19 shows the distribution of signal to noise ratio for targets used in the testing, which ranges from 1.45dB to 24.5dB

Fig.7.16a Plot of Test Data 1, S/N=3.7dB, Output value=0.9986

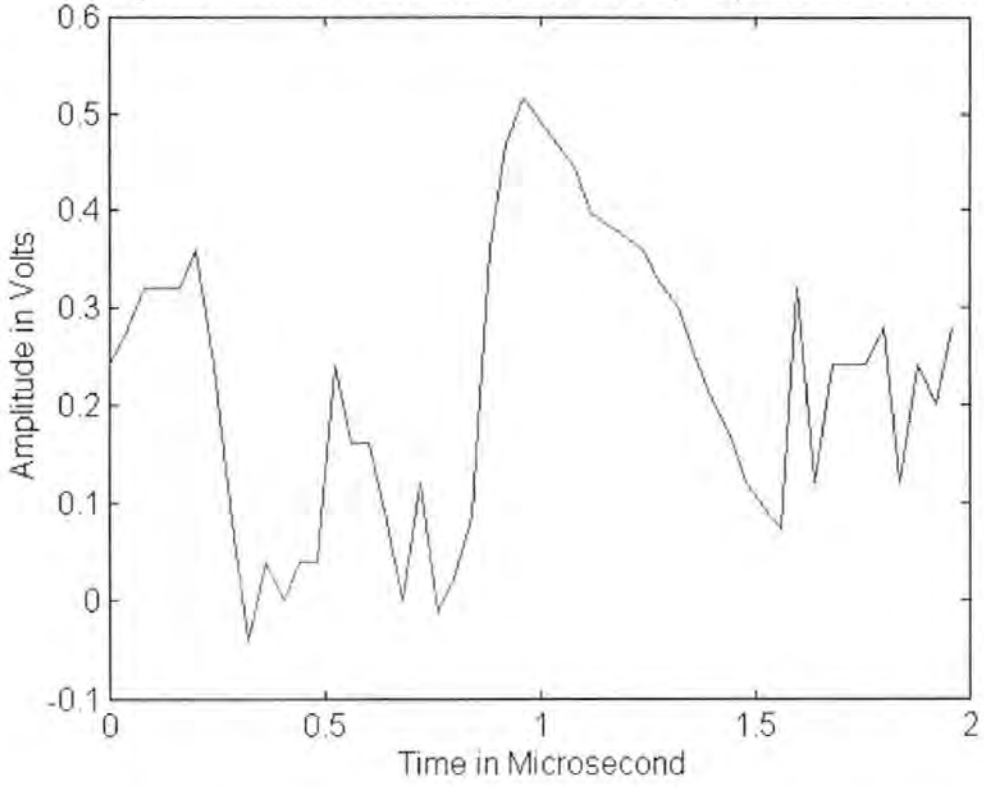

Fig.7.16b Plot of Test Data 2, S/N=12.6dB, output value=0.9964

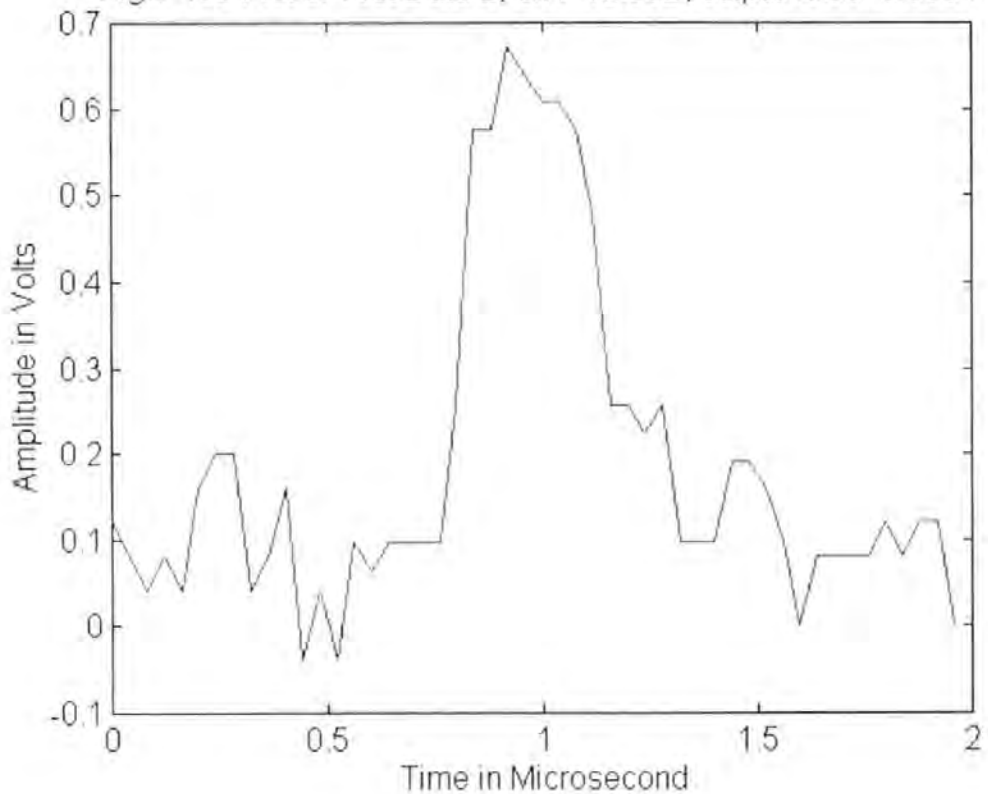

Fig.7.16c Plot of Test Data 3, S/N=6.6dB, output value=0.7732

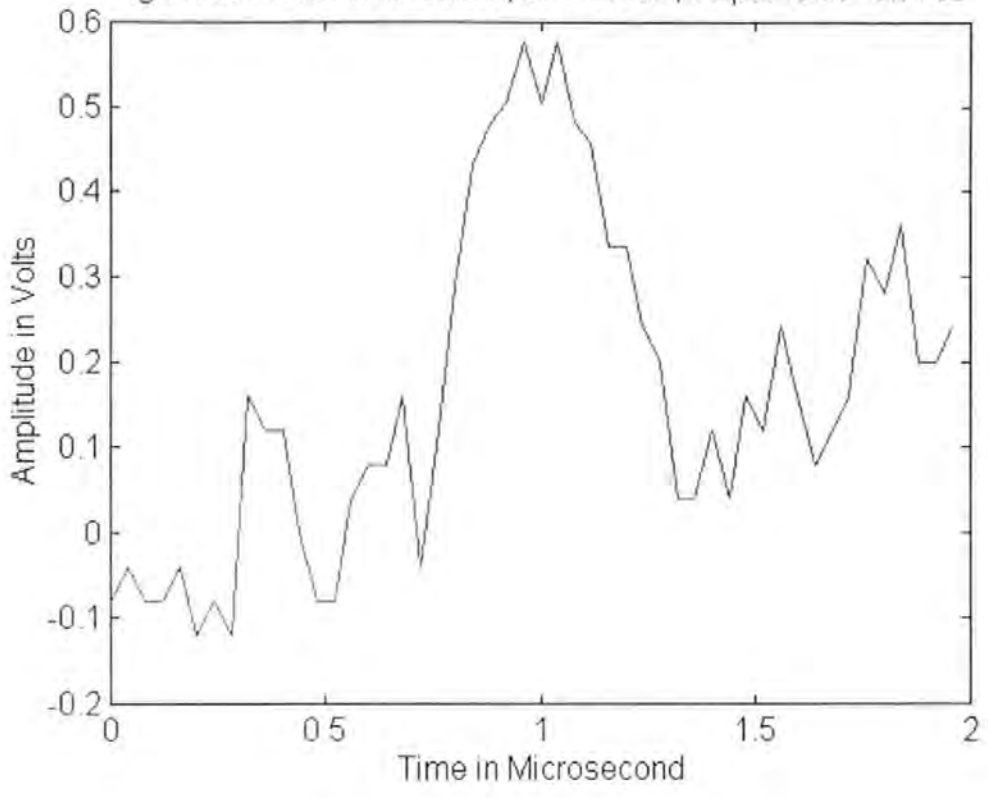

Fig.7.16d Plot of Test Data 4, S/N=10dB, output value=0.9745

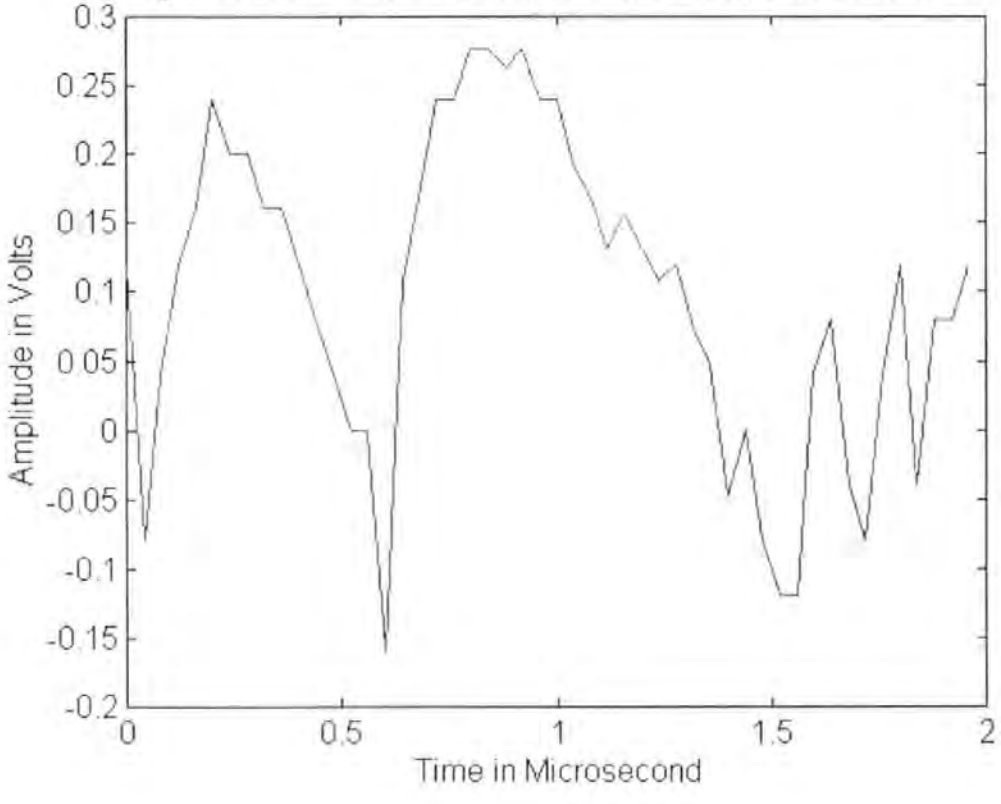

Fig.7.17a Plot of Test Data 5 (noise), output value=0

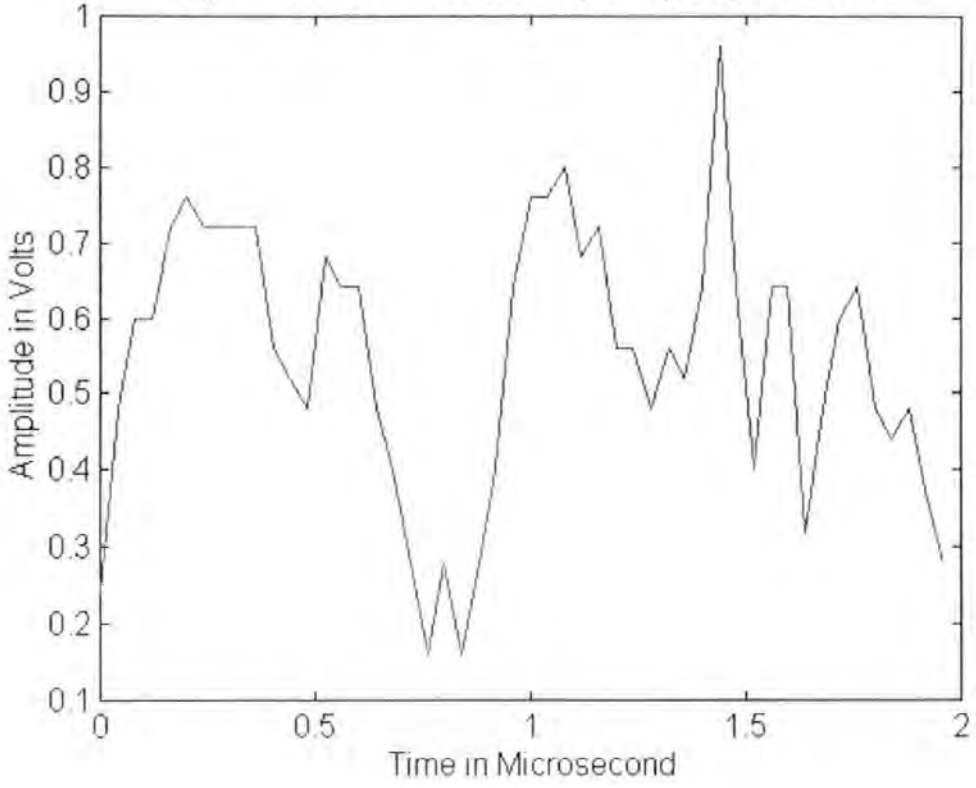

Fig.7.17b Plot of Test Data 6 (noise), output value=0

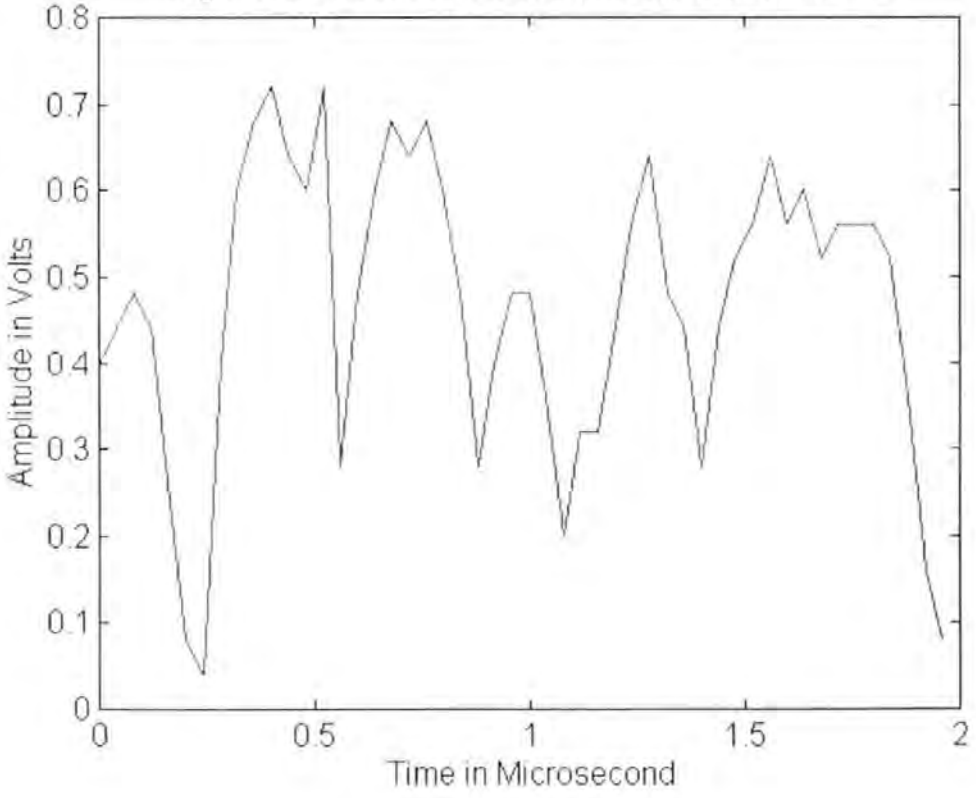

Fig.7.17c Plot of Test Data 7 (noise), output value=0

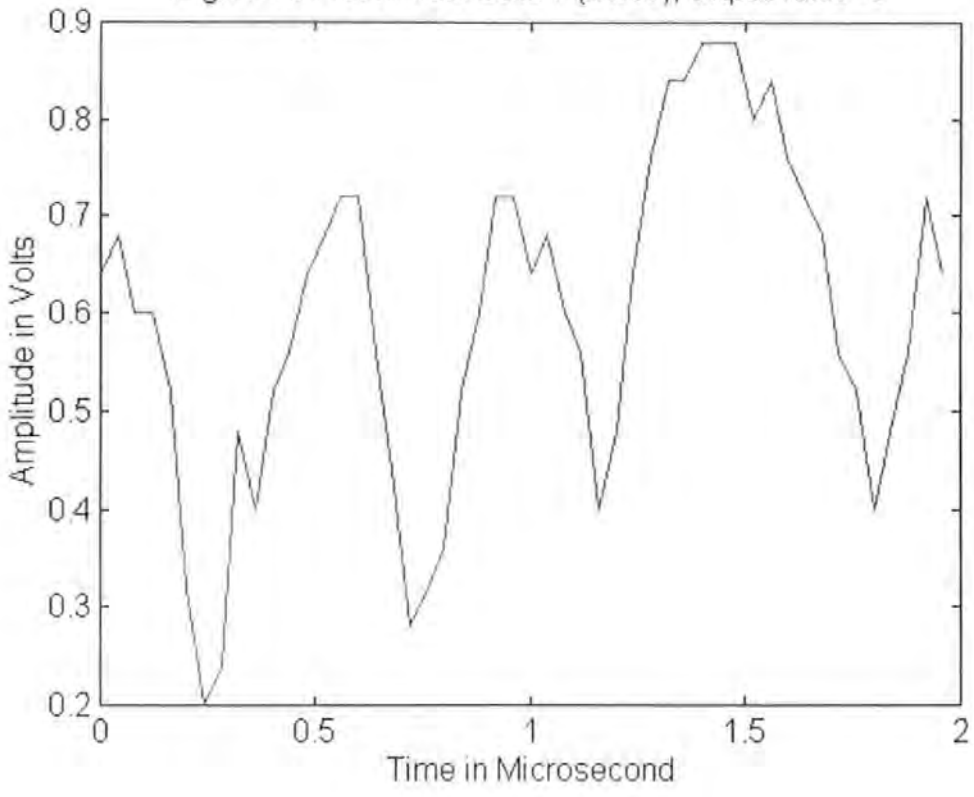

Fig.7.17d Plot of Test Data 8 (noise), output value=0

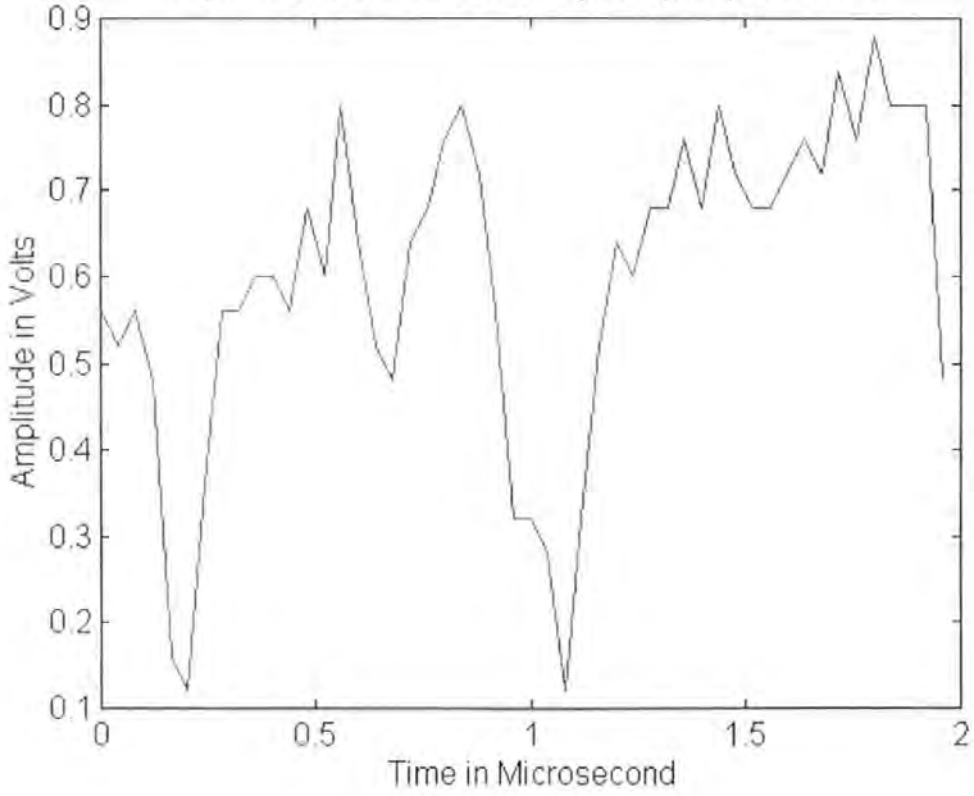

Fig.7.18 Output values for target and noise

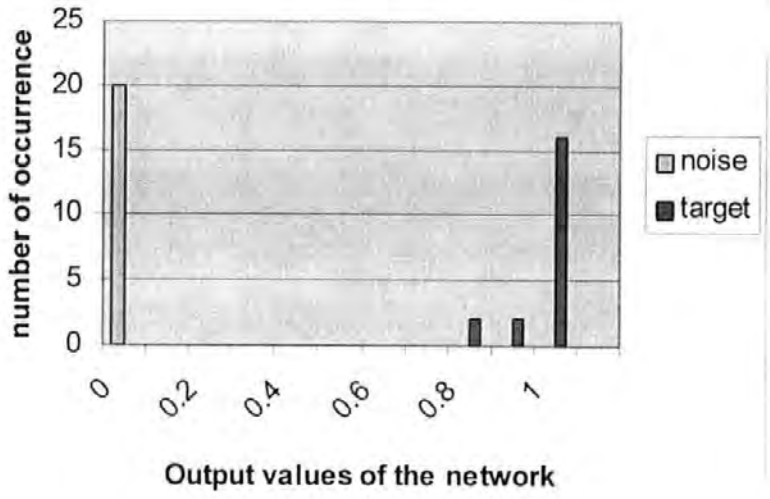

Fig. 7.19. Distribution of S/N Ratio

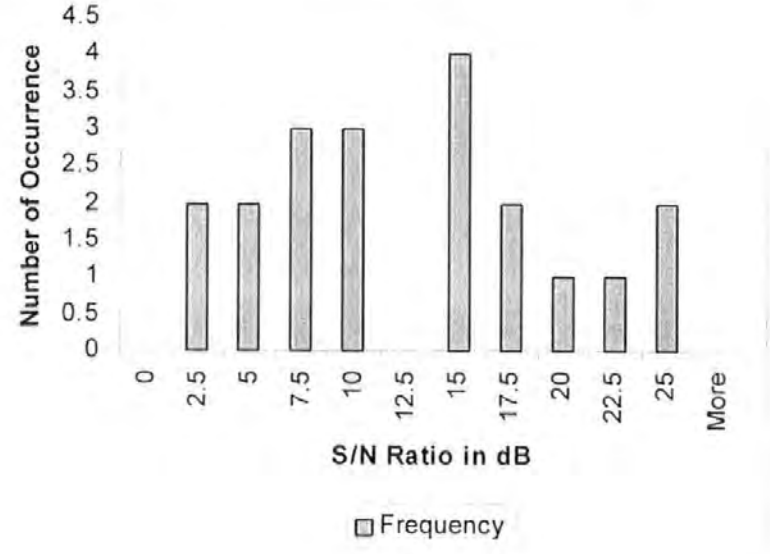

7.5 Investigation of applying the network to a trace of radar of return

The network has been developed to identify whether the window (with 50 samples) is a target or noise. It has already been shown that there is large discrimination at the output of the network between target and noise. The next step was to enhance the network to perform the discrimination in a trace of radar return, which contained more than 50 samples of data. Fig.20a shows a trace of 100 samples (4 microseconds) of radar returns with a target present. To detect the target in this trace, the 50 sample (2 microseconds) window has to be shifted in time from 0 to 4 microseconds. At first, the window was shifted by 1 sample each time and the corresponding output of the network was recorded, Fig. 20b shows the result. The output has a result of 1 when the window starts from 7^{th} sample and this output is maintained until the window exceeds 85^{th} sample. The output is zero for the rest of the trace. If the window is set to act as a filter that allows only the samples contained in windows which have an output of one to pass through the detection system, then the resulting output is shown in fig.20c. The detection system employing this approach would have the following drawbacks.

1. The process will take 52 cycles of calculating the statistical characterization and obtaining output from the network.
2. Part of the noise in the vicinity of the target is also accepted by the detection system as shown in fig 20c.

To overcome these problems, the number of overlapping cells between each window has to be reduced. However, the smaller the number of the overlapping cells, the less information is fed to the detection system. If the number of overlapping cells is made too small, there will be high chance that a target is missed, in particular the smaller targets that are contained within just a few samples. In the example of fig.20a, the target would not be detected if the overlap between windows is less than 10 samples. By testing the detection system with different amounts of

overlap, it was found that an overlap of around 20 samples gave reasonable results for this particular target. With this value, only 2 computer cycles were required to obtain the final result that is shown in fig. 7.20d. The overlap of 20 samples was tested with targets of different sizes and the result was found capable of discrimination in all cases, on each occasion the target could be detected with only two computations. The result of using this overlap in the detection a large target is shown in figures 7.20e and 7.20f.

The detection system with this configuration was then applied to a longer trace as shown in figure 7.21a. The following methods were used to ensure that the target was correctly identified from the trace to evaluate the performance of the detection system.

1. The potential targets were confirmed by checking against the radar display. The gain, rain clutter and sea clutter controls were adjusted to obtain the optimum settings.
2. If the targets did not appear on the radar display, successful scans of the radar sweeps were checked to ensure that the target appeared in the radar trace for more than one scan.
3. It the target was in close range, visual confirmation by means of binoculars was used.
4. The radar trace was carefully examined to observe any signs of targets.

As found during the testing stage, there were occasions when the output of the network for some targets had a value less than 1 but larger than 0.76. To cater for these types of target, the detection system was set to accept signals with an output value of 0.7 or more. This would still allow sufficient discrimination from the noise as described in the early sections. The signal that is retained after passing through the detection system is shown in fig.7.21b and all targets are detected correctly. For comparison purposes, the same trace was applied to a detection system using TM-CFAR, which has the best quality of thresholds as indicated in Chapter 2. Again, the

comparison was based on the assumption that no false alarm would occur. The result is shown in fig. 7.21c. The TM-CFAR detection algorithm uses only the amplitude information and it is unable to identify weak targets that are embedded in the noise. If the threshold were lowered for better probability of detection, then it would accept strong noise and clutters and an excessive false alarm rate would occur. Part of these unwanted signals can be removed by scan to scan correlation and sweep to sweep correlation. However, under such circumstances the existence of a target can only be confirmed after a few scans and the worst case is that such algorithms cannot reject correlated noise and clutters. It is important to note that the developed detection system can detect weak targets as well as retain the shape of the waveform for further use in pattern recognition processes.

Ten traces of live radar returns, which were not used in the training process, were used to test the developed system. Weak targets with low signal to noise ratio were added to the clutter edges in some traces. The results showed that the system was able to discriminate weak echoes from strong clutters by using the five statistical parameters, i.e. mean amplitude, mean amplitude deviation, mean pulse width, mean pulse width deviation and maximum pulse width. The results of some of the tests are shown in figures 7.22 and 7.23 where the performance of the TM-CFAR detection for these two traces is also shown for comparison. In fig. 7.22a, the return signal consists of rain clutters with a weak target at the clutter edge. The signal to noise ratio at the edge of the rain clutter is –4.97dB. Fig. 7.22b shows that all targets are detected by the neural network. The TM-CFAR system (fig. 7.22c) is not able to adapt to the clutter edge and detect the weak echo. In fig. 7.23a, targets are detected from a radar trace with strong sea clutters. The signal to noise ratio of the weakest target is 5.19dB. Again, the result from TM-CFAR in such clutter environment is not satisfactory (fig. 7.23c).

Fig.7.20a A Trace of Radar Return with 100 Samples

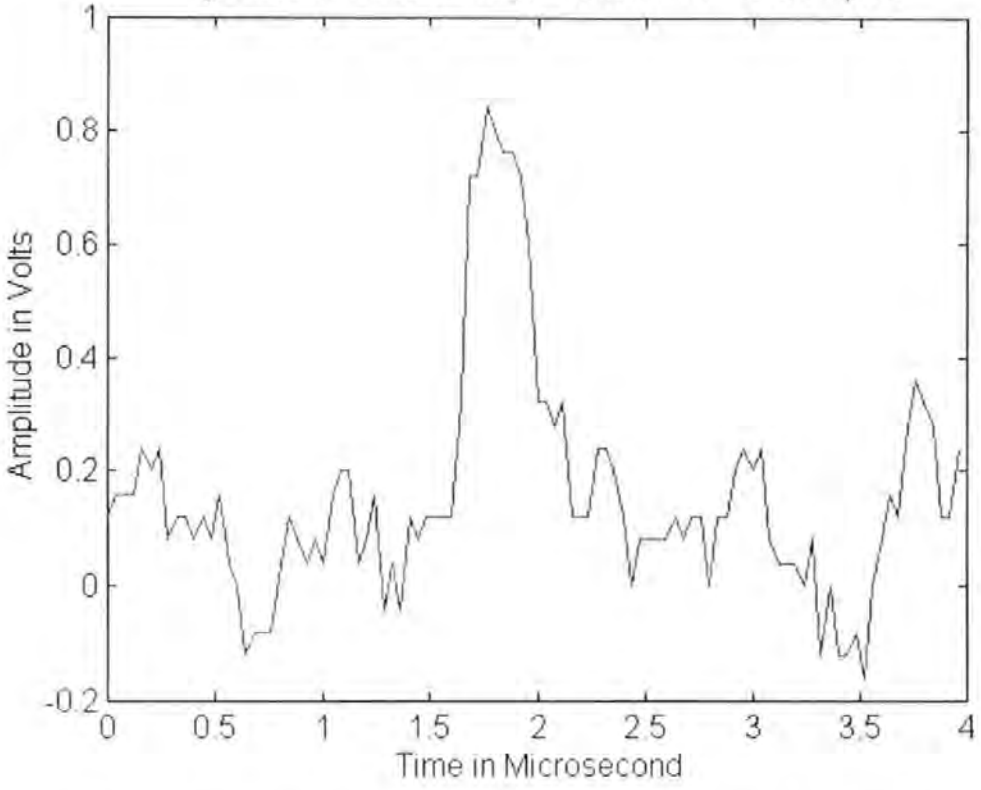

Fig.7.20b Output of the Network for the trace in Fig.7.20a

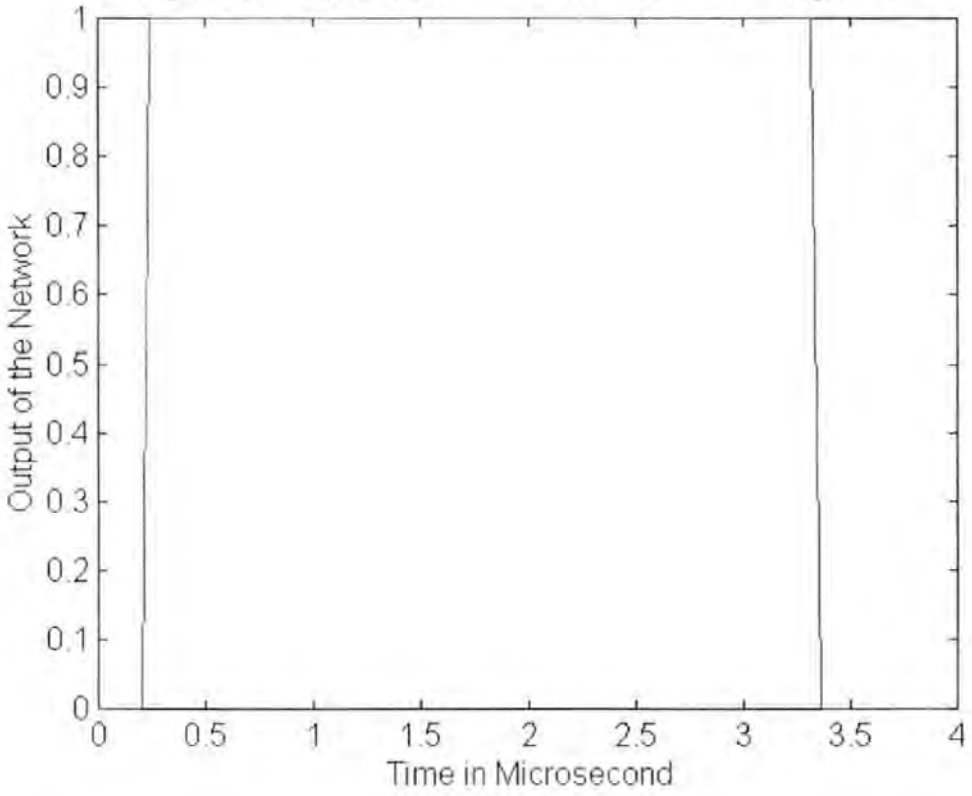

Fig.7.20c Output of the detection system with a shift of one sample

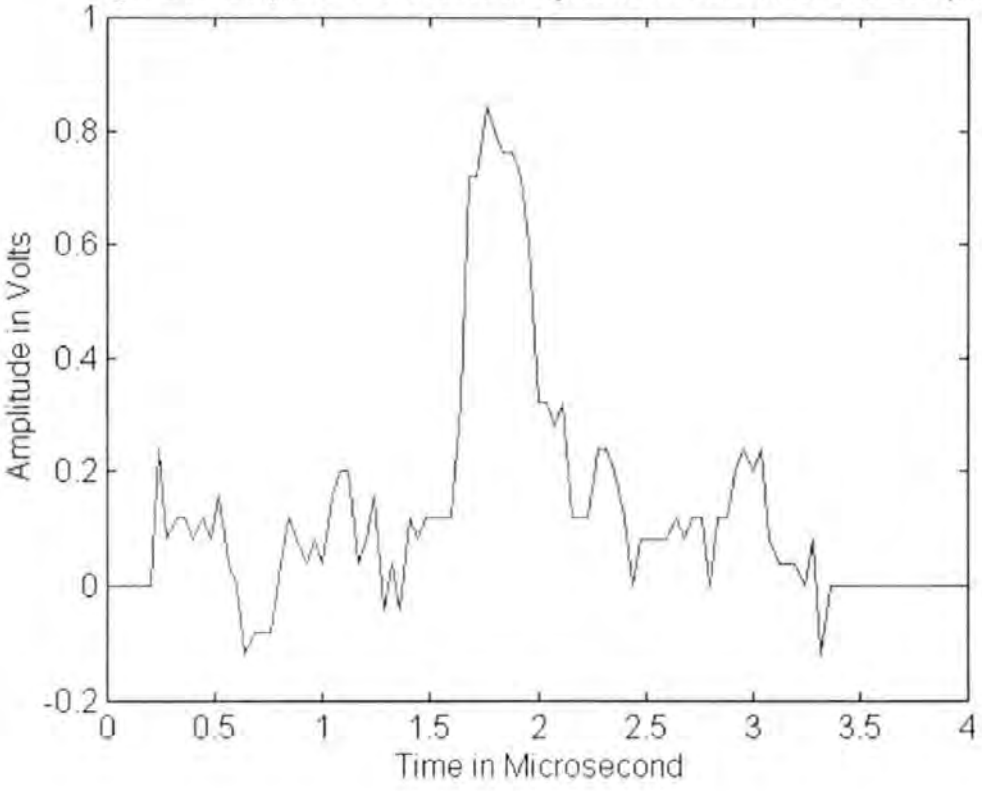

Fig.7.20d Output of the detection system with an overlapping of 20 samples

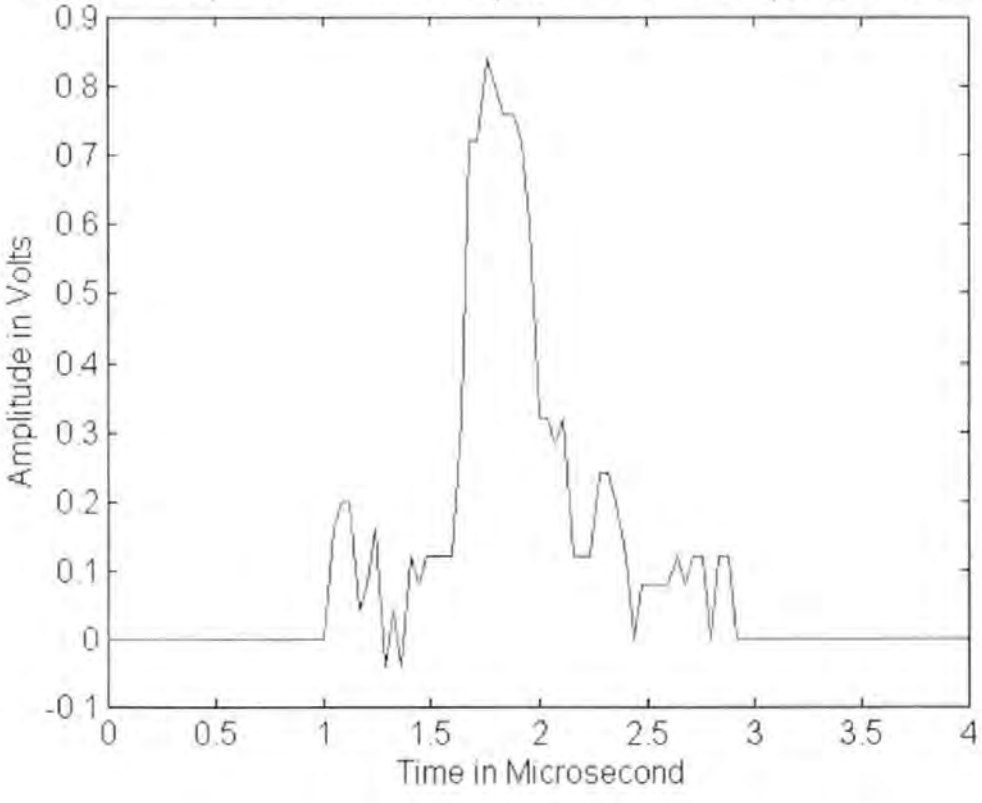

Fig.7.20e A Trace of Radar Return with 100 Samples (large target)

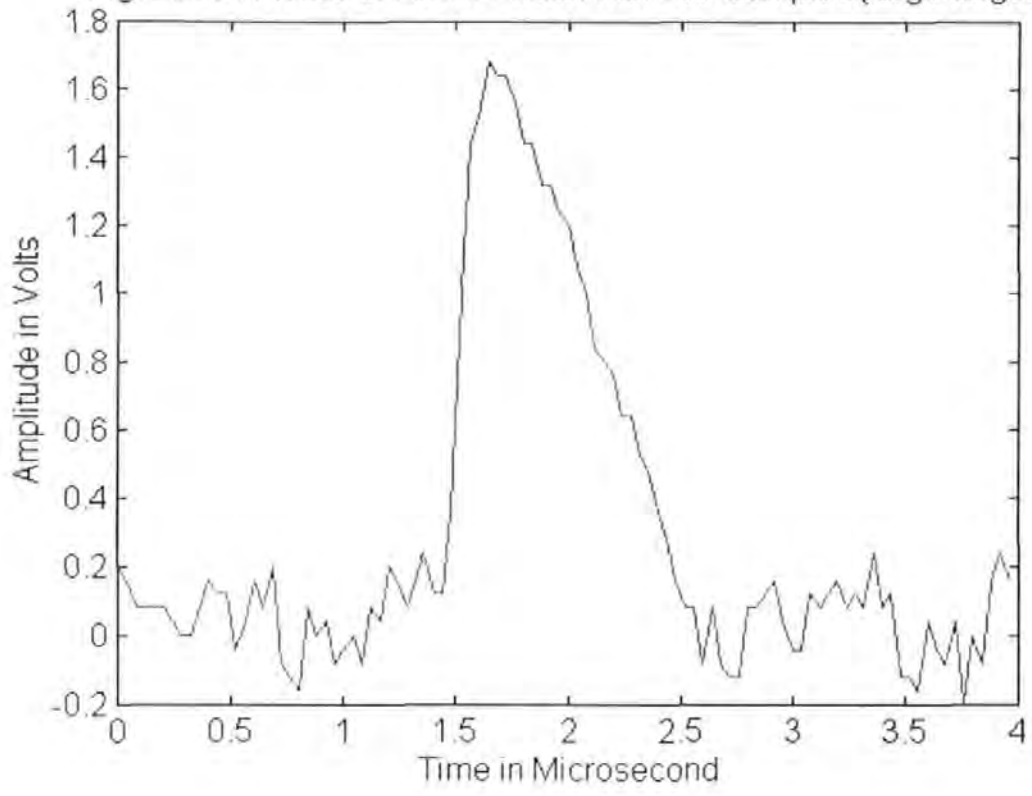

Fig.7.20fOutput of the detection system with an overlapping of 20 samples (large target)

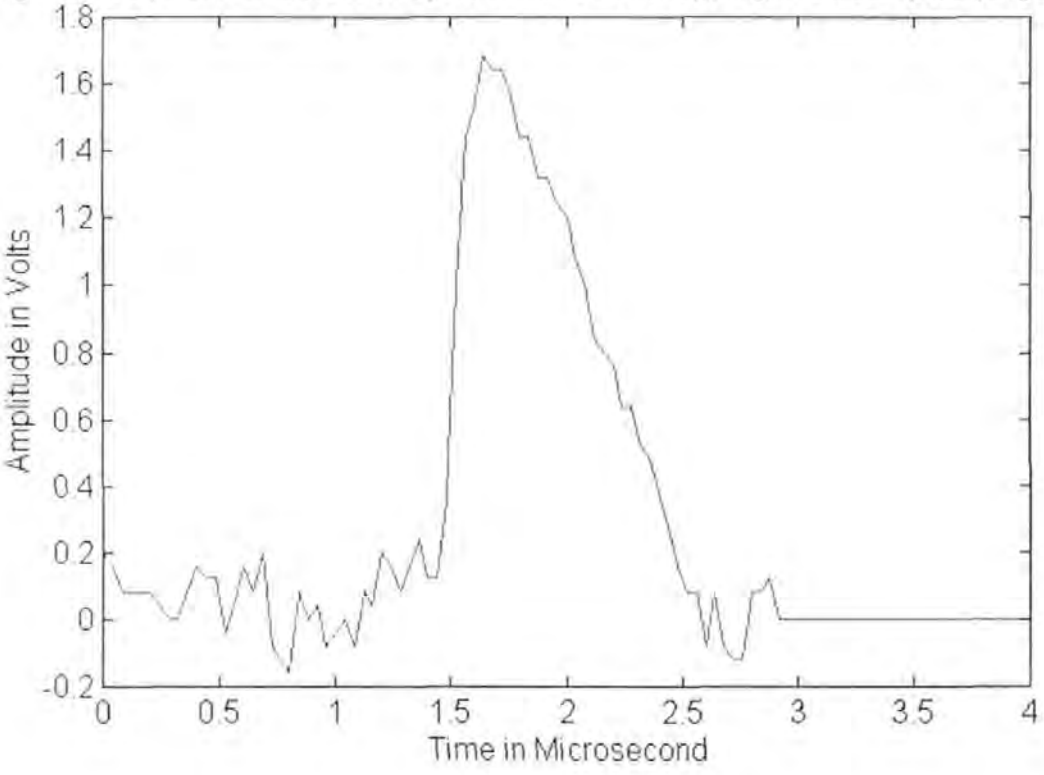

Fig.7.21a A Radar trace with 2000 Samples

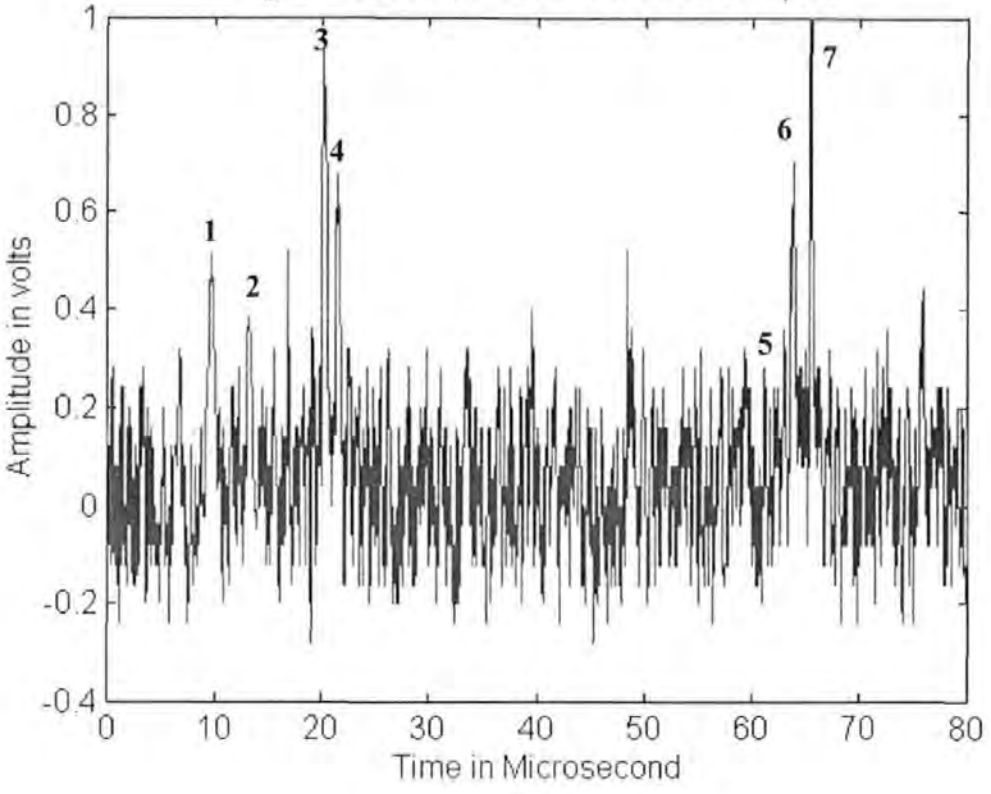

Fig.7.21b Output of the detection system

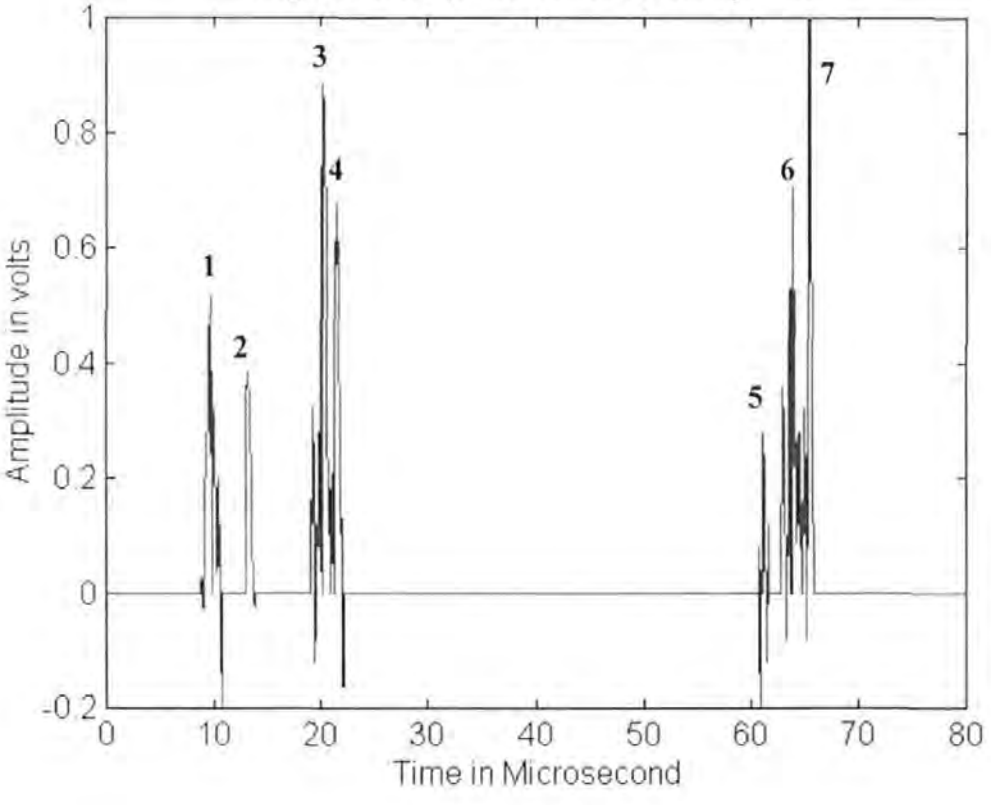

Fig.7.21c Sea Target Signal with TM-CFAR Threshold, T1=40,T2=40)

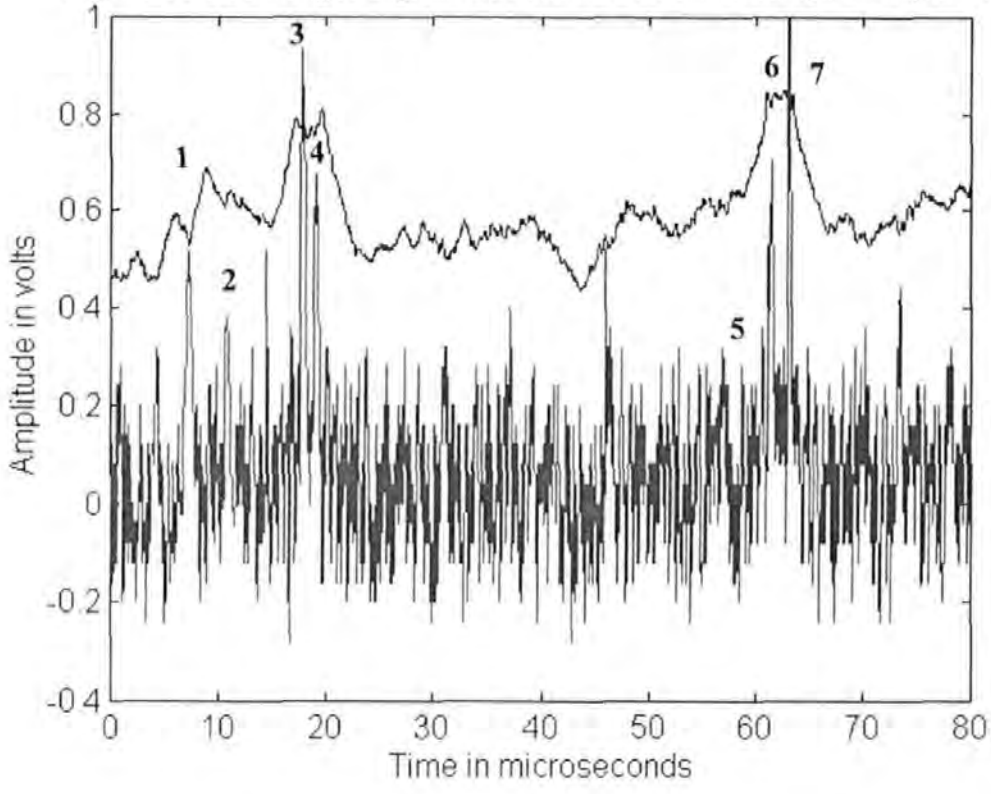

Fig.7.21d Signals accepted by TM-CFAR

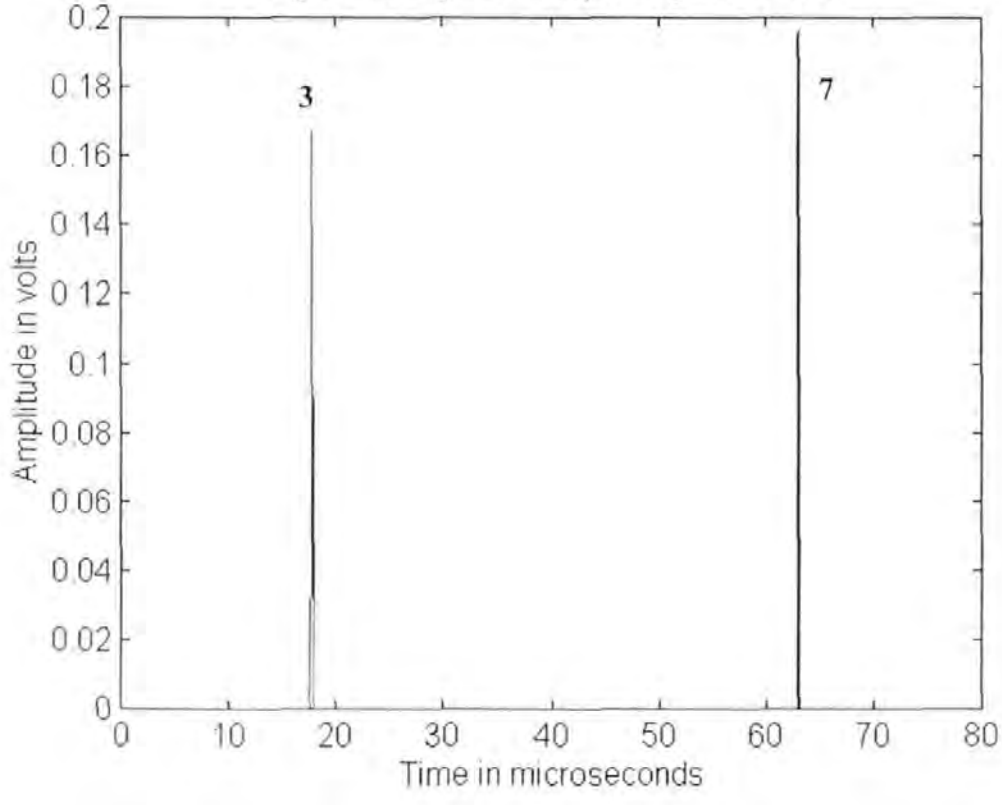

Fig.7.22a Radar trace with rain clutters

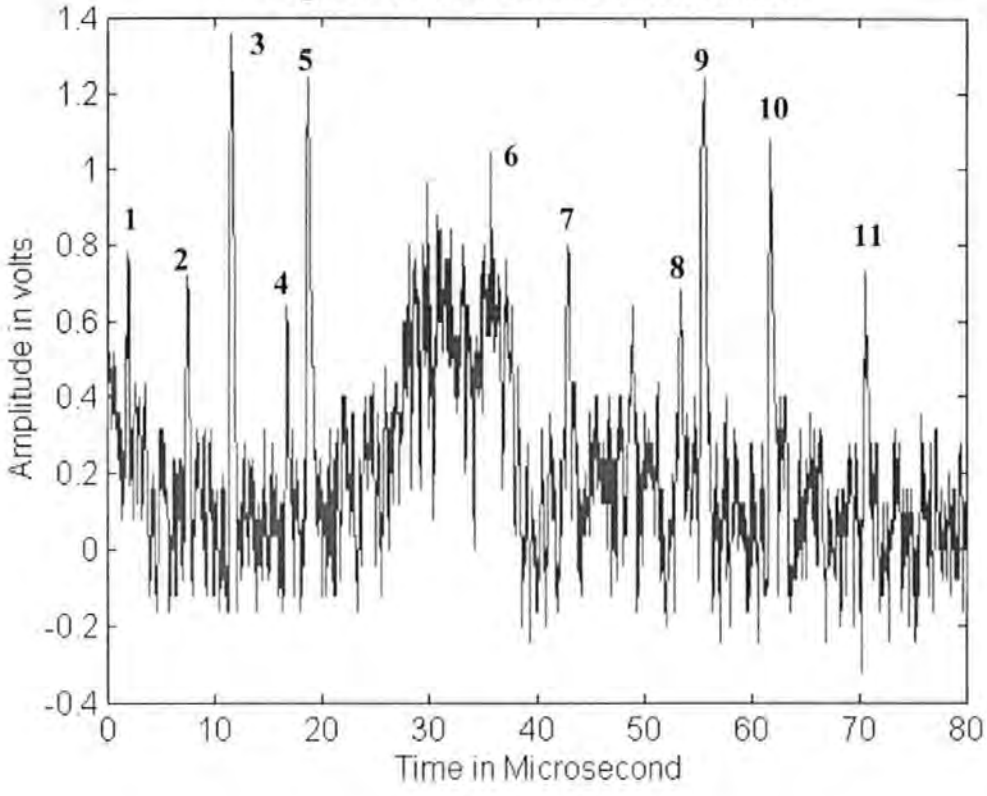

Fig.7.22b Output of the detection system

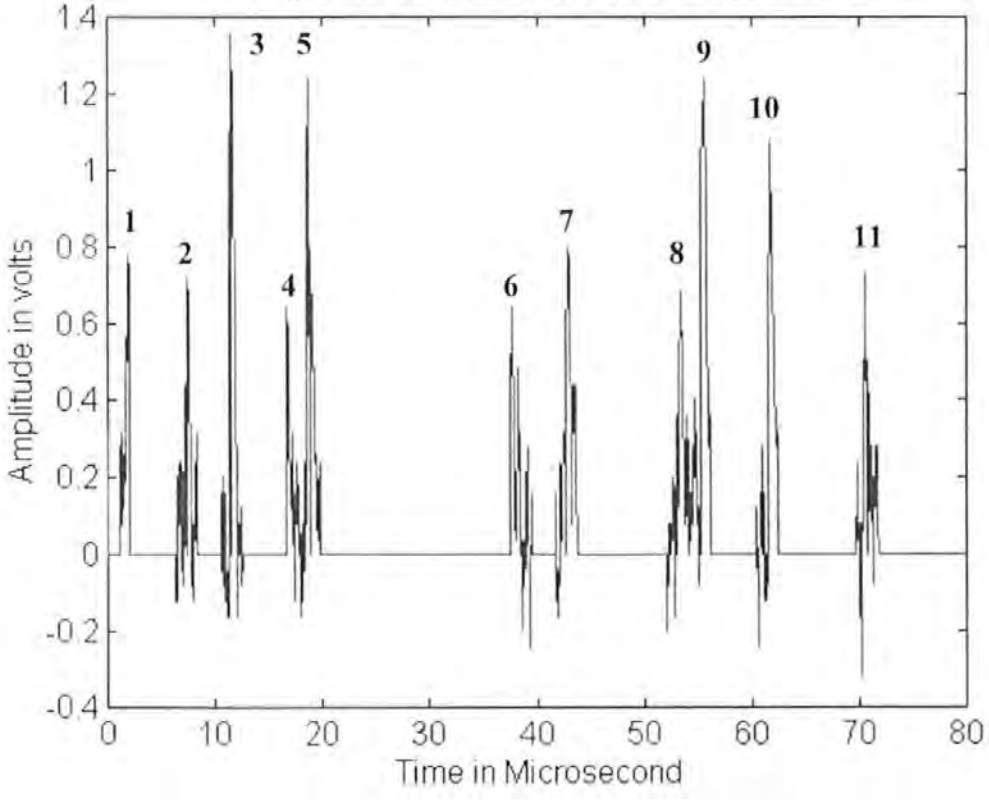

Fig.7.22c Sea Target Signal with TM-CFAR Threshold, T1=40,T2=40)

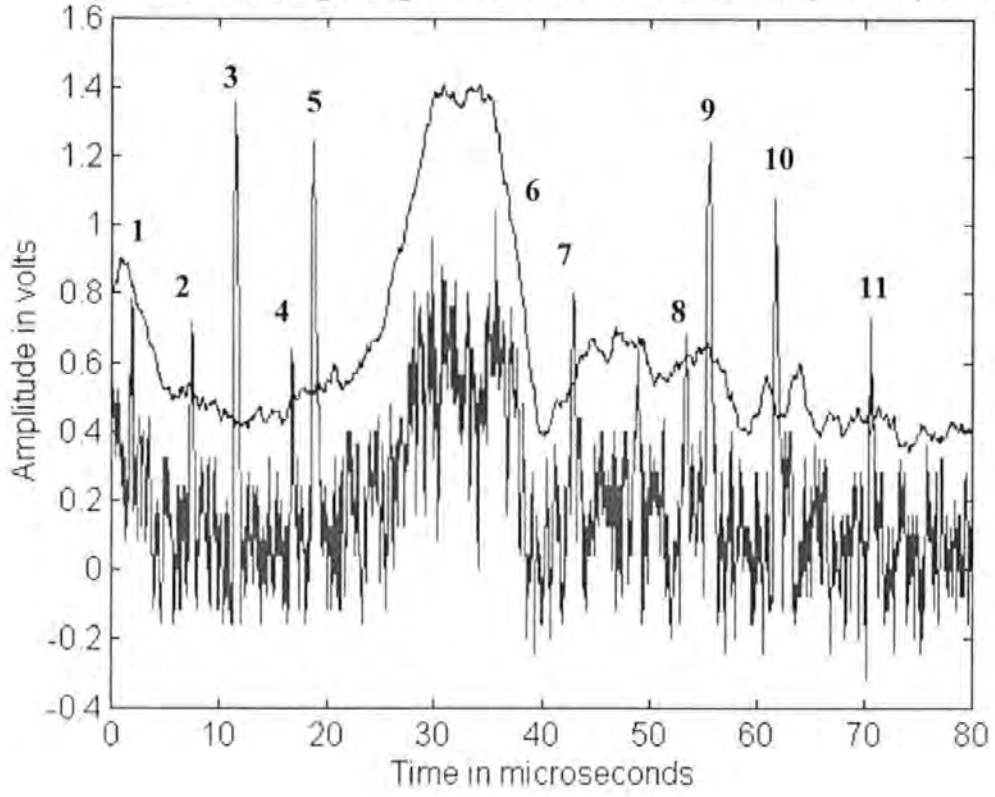

Fig.7.22d Signals accepted by TM-CFAR

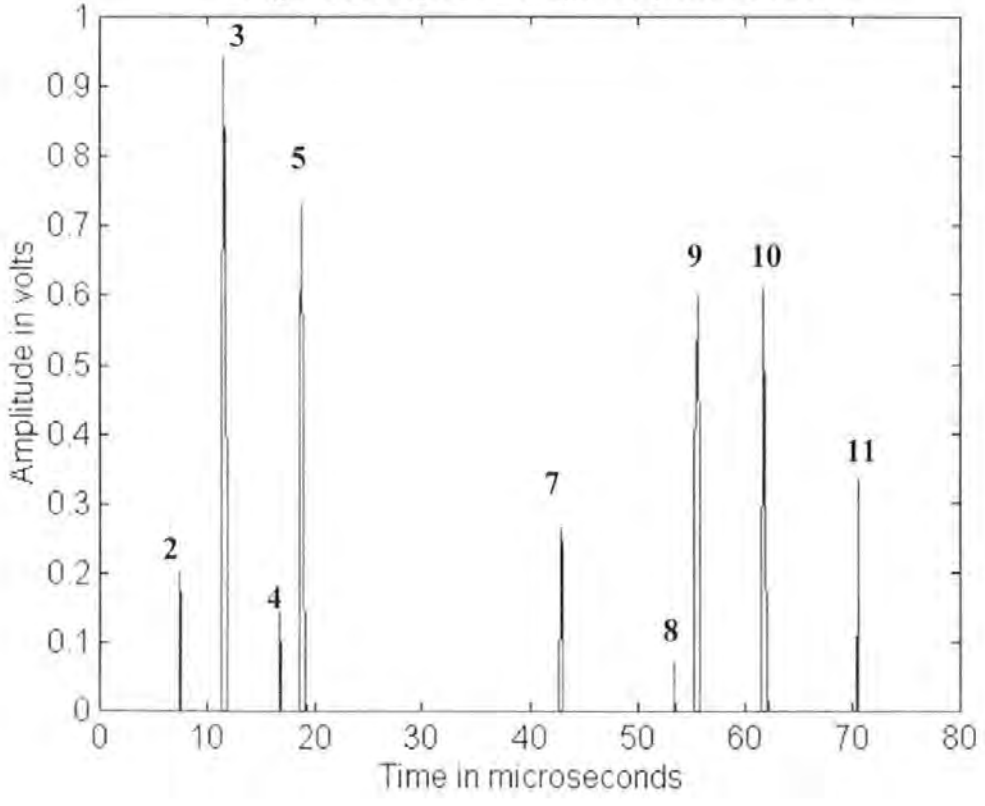

Fig.7.23a Radar trace with sea clutters

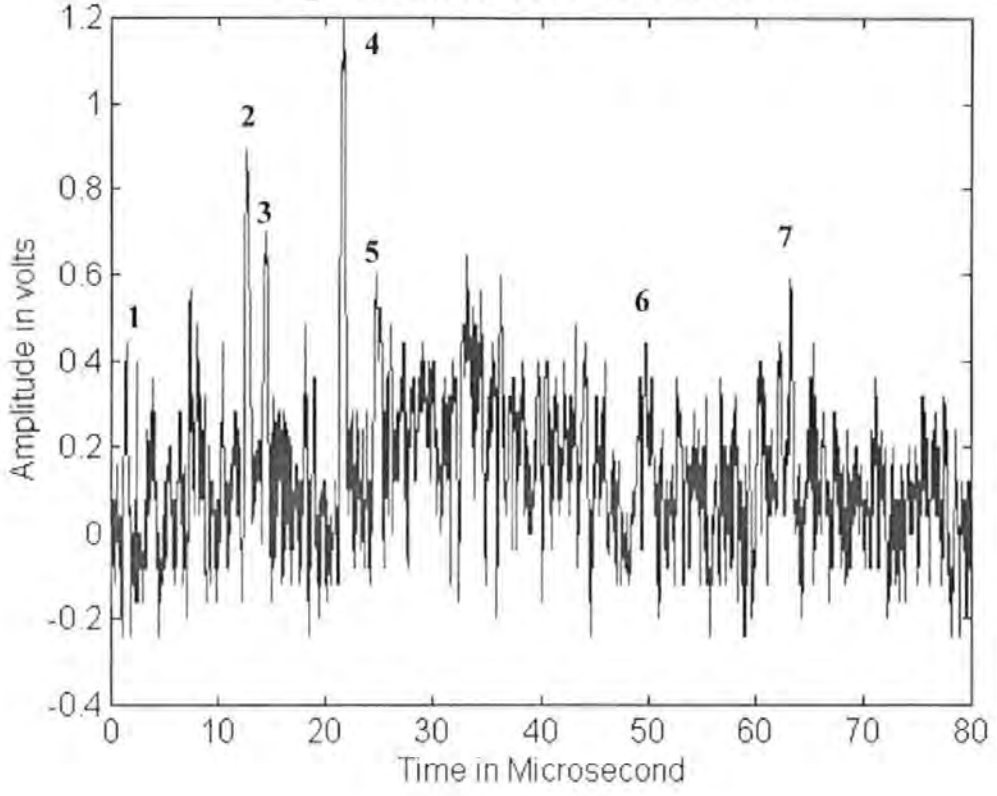

Fig.7.23b Output of the detection system

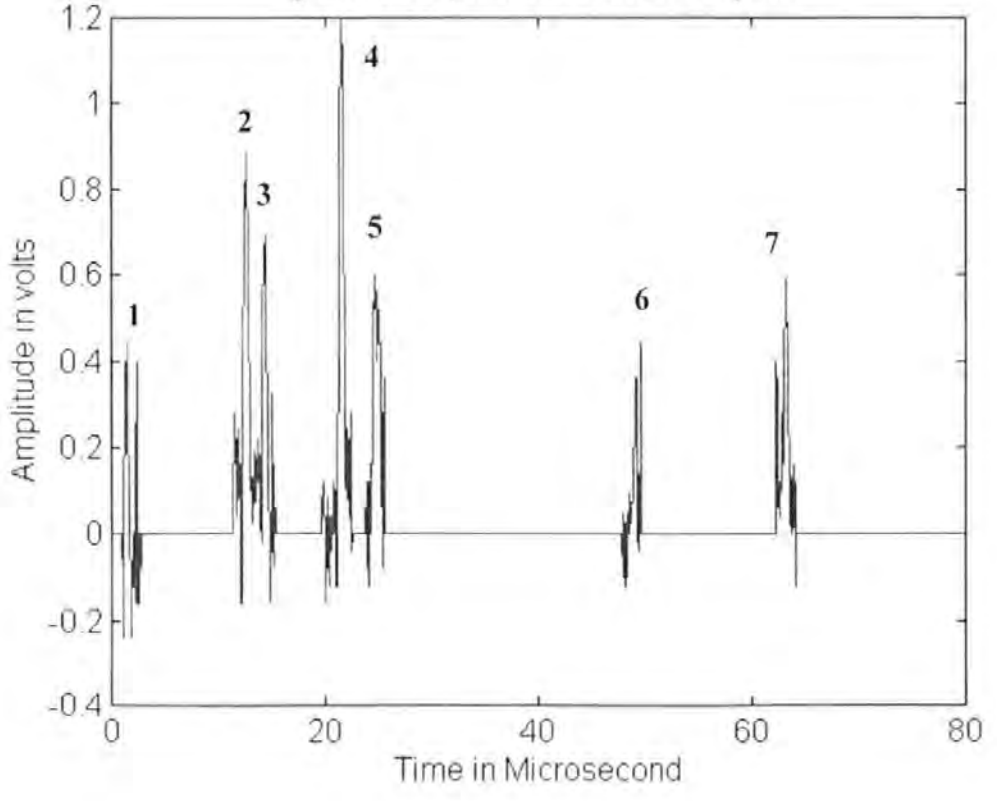

Fig.7.23c Sea Target Signal with TM-CFAR Threshold, T1=40,T2=40)

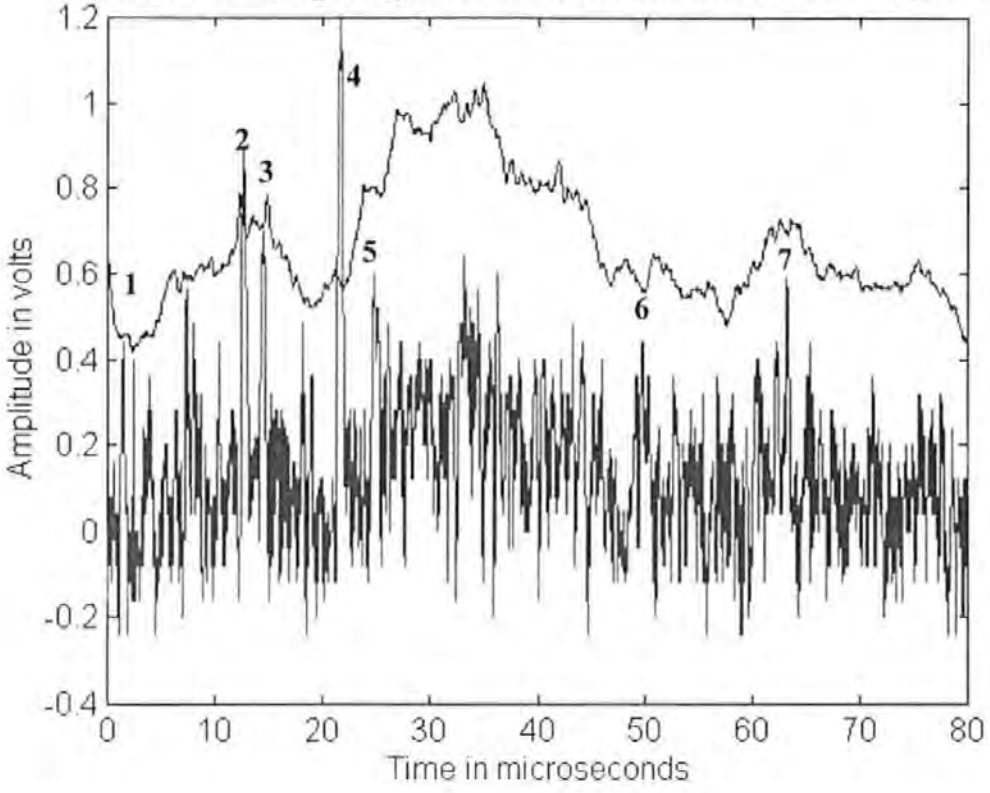

Fig.7.23d Signals accepted by TM-CFAR

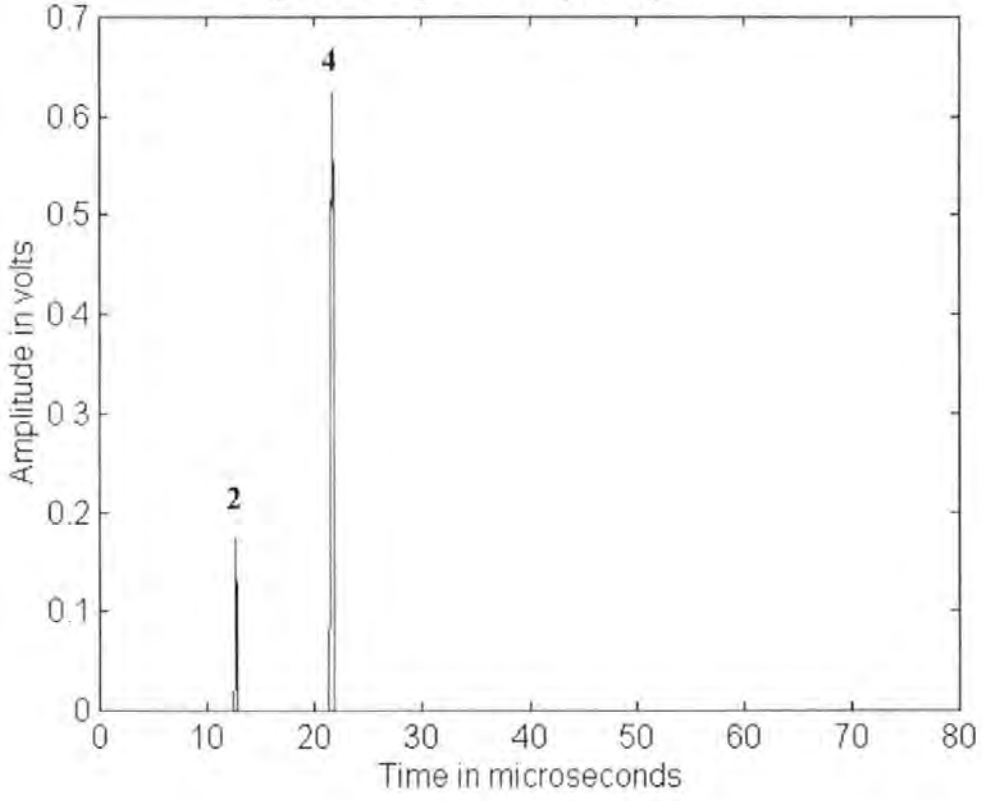

7.6 Investigation of parameters required for target classification

Radar systems transform complex information from the targets into a one-dimensional waveform, which only presents the amplitude information of the target at different times. The earlier sections show how the five statistical parameters (extracted from these waveforms) may be used in the detection of marine targets. To develop the study further, it would be necessary to see if the extracted features can also be used in the target classification process. In general cases, radar observers would first classify the targets into two types, i.e. large and small vessels. Large vessels refer to bulk carriers, warships, tankers, general cargo ships and so on. Small vessels include pleasure craft, tugboats, fishing boats.... etc. After this preliminary classification, a follow up detailed classification could be carried out for further pattern recognition to identify specific types/groups of targets. In order to reach the second stage, it is critical that the preliminary classification is efficient and accurate. The objective was to develop the technology further and investigate the potential for a system that can classify the targets into the two primary groups. The accuracy of a target recognition system depends on the certainty of their extracted features. The extracted feature should have the characteristics of the targets only and should not be affected by other external parameters such as range and the clutter environment. These features or their regular changing patterns can be observed at different time intervals.

Two groups of vessels, large and small were extracted from the radar traces. These are distinguished by visual observation of the vessels as well as by manual inspection of the return signals. Most of the aspects of viewing were from the broad side however, on some occasions echoes from the front side of the vessels were recorded.

To determine the features required in the target classification process, it is necessary to look at the discrimination properties of the five parameters for these two classes of vessels. The results

are shown in figures 7.24a to 7.24e. It can be seen that there is less discrimination in the period parameters than the amplitude parameters and there is noticeable discrimination in the amplitude deviation. Despite the fact that period parameter will give some indications about frequency components of the return wave, the simplified method that has been adopted to date, in order to reduce the computation time, might not be able to provide the necessary details of the frequency distribution. As such, the immediate frequency method as described in Chapter 5 can be adopted in analyzing the target waveform in the frequency domain. The immediate frequency of each target was calculated. The discrimination in the immediate frequency between these two types of target is plotted in fig. 7.24f and shows that effective discrimination may be achieved with inclusion of this parameter. Therefore, these two parameters, i.e. the amplitude deviation and the instant frequency were used to set up the target classification system.

The one-dimensional return from the same target would vary from sweep to sweep as well as from scan to scan. It is difficult to specify a definite value about the parameter describing the class of targets, instead it is really a fuzzy pattern classification process. Figure 7.25a and 7.25b show the variation of the amplitude parameters and the period parameters between the two types of targets for 5 consecutive scans. The immediate frequencies and the amplitude deviation of these two target types vary from scan to scan and their variations are shown in table 7.2.

Table 7.2 Variation of Immediate Frequency and Amplitude Deviation between 5 scans

Scan	1	2	3	4	5
Imme. Freq. (large vessel)	2.6370	2.6762	2.8950	2.7366	2.5336
Amp. Dev. (large vessel)	0.3375	0.2539	0.2519	0.3224	0.3127
Imme. Freq. (small vessel)	2.0327	1.8309	2.4602	1.8631	1.9675
Amp. Dev. (small vessel)	0.2900	0.6104	0.3517	0.4200	0.1772

In view of the variations of the two parameters between scans, a fuzzy approach would be required to deal with the input data to the classification system. To maintain the performance of the neural network in the detection system, a neuro-fuzzy technique was used to classify these two types of targets. This approach has the benefit of handling the two parameters in fuzzy terms as well as training a suitable network to achieve the task of classification. The block diagram of the neuro-fuzzy approach is shown in fig. 7.26.

The input parameters were first fuzzified by means of the membership functions in fig 7.27. The functions were derived from the statistical distributions of the 100 samples, i.e. 50 samples of large vessel and 50 samples of small vessel. The fuzzified data was then used as input for training the network with four input layers, two hidden layers and one output layer.

A similar neural network approach to that adopted in the detection was used to recognise specific targets from the radar returns. The network was trained using 100 samples to classify targets into large vessels (0) and small vessels (1). The output from the neural network system for the 20 test targets is shown in table 7.3.

Table 7.3 Testing set for the neural network

TARGETS	OUTPUTS FROM THE NEURAL NETWORK				
Small (1 to 5)	1	1	0.5987	0.5468	0.55
Small (6 to 10)	1	1	1	1	1
Large (1 to 5)	0.0321	0	0	0	0
Large (6 to 10)	0	0	0	0	0

It can be seen that there is no overlap between the outputs for the two types of targets, and by using a threshold of 0.5, the network classifies the targets into large and small vessels.

Fig. 7.24a Discrimination in Mean Amplitude

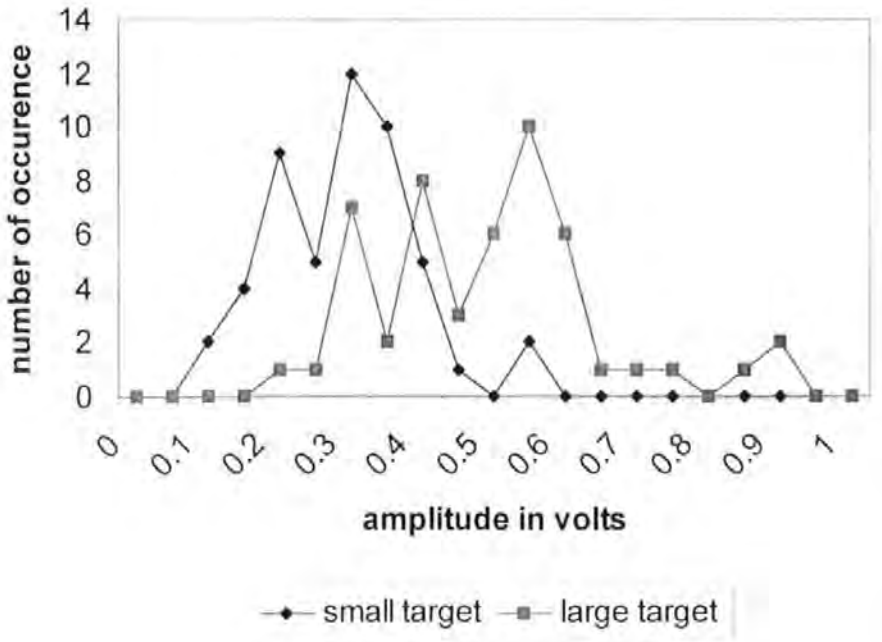

Fig.7.24b Discrimination in Amplitude Deviation

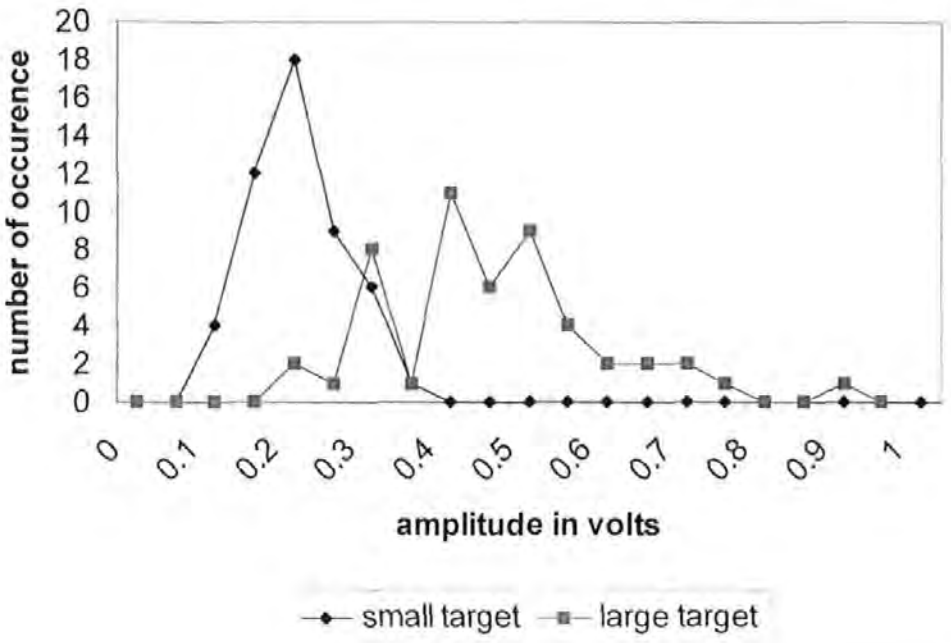

Fig.7.24c Discrimination in Mean Period

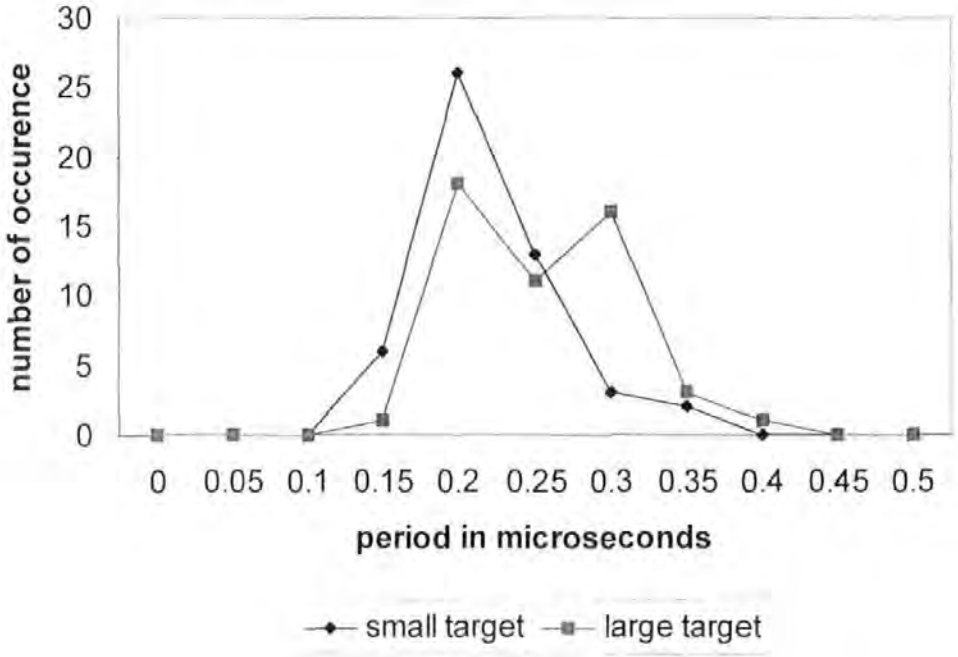

Fig. 7.24d Discrimination in maximum period

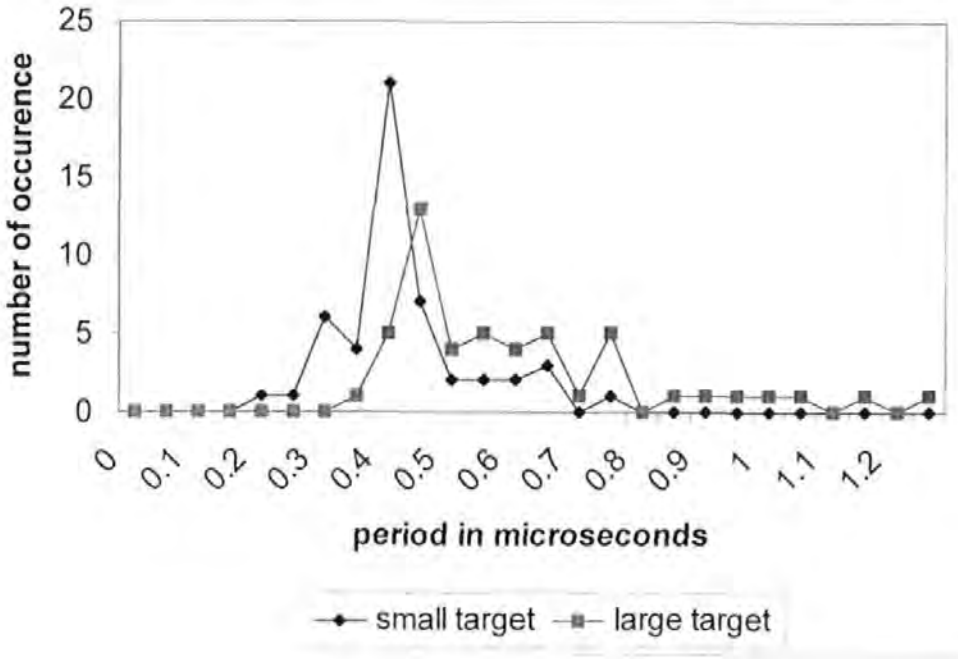

Fig7.24e Discrimination in Period Deviation

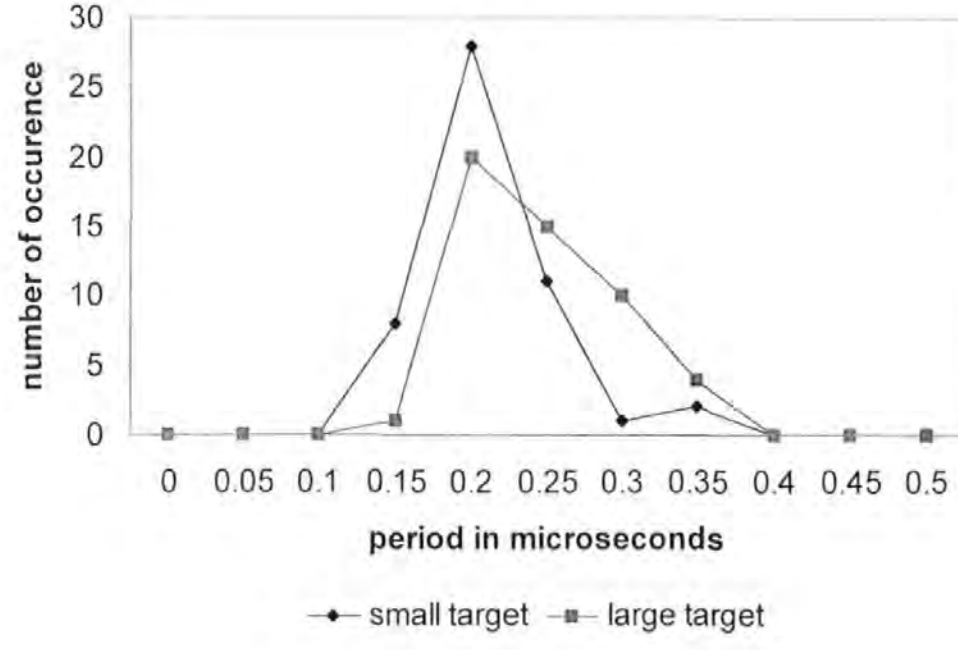

Fig.7.24f Discrimination in Instant Frequency

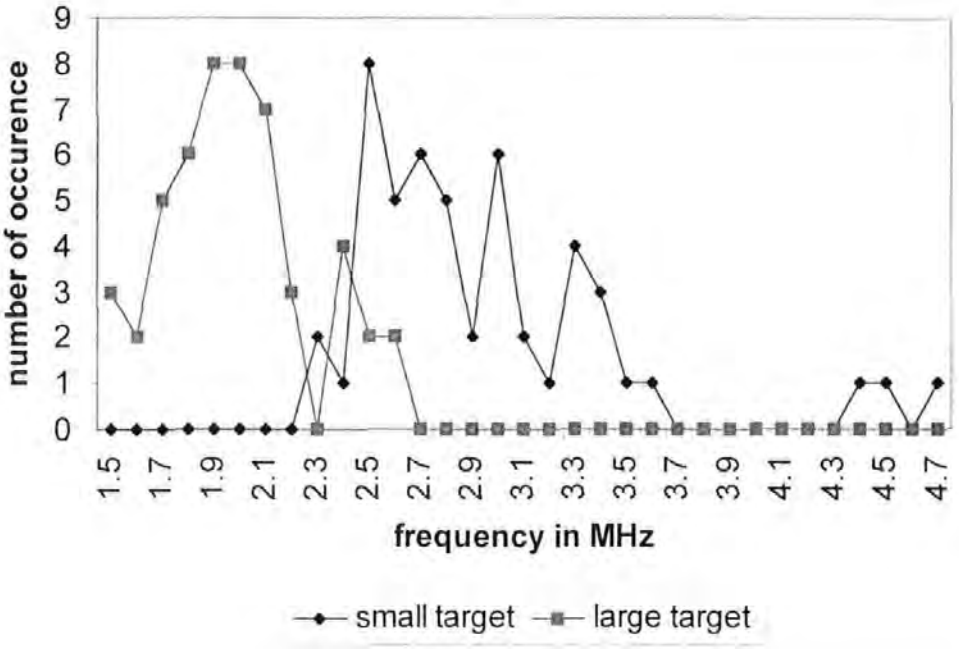

Fig. 7.25a Radar Return Sequence of Large Target

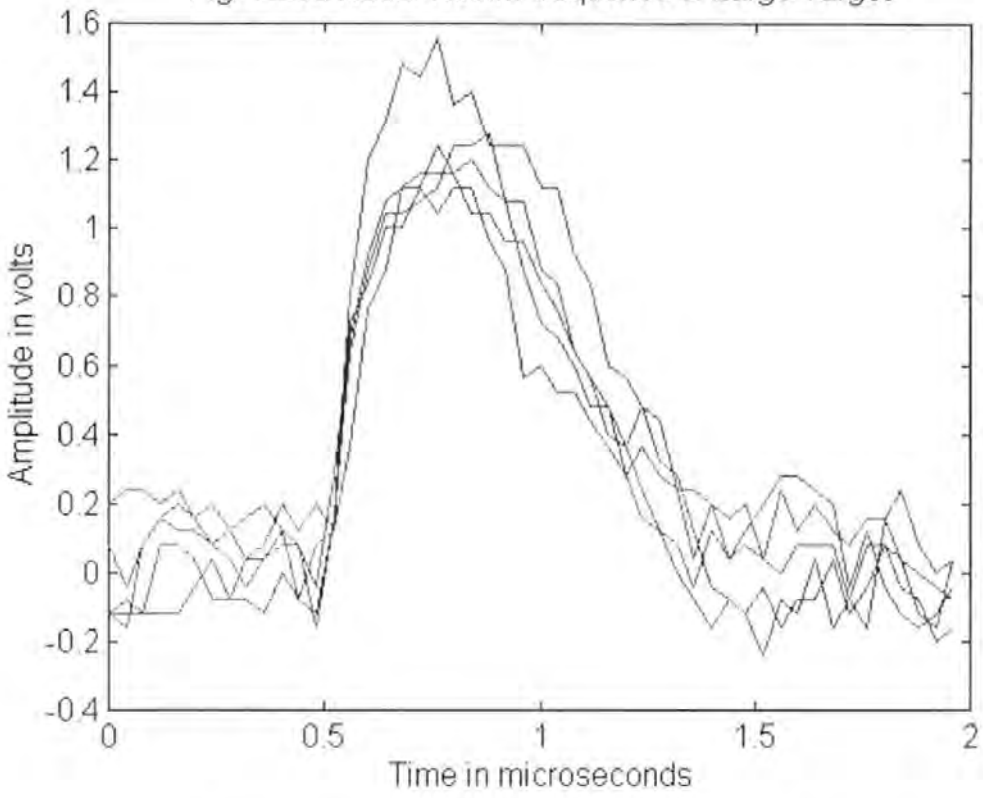

Fig. 7.25b Radar Return Sequence of a Small Target

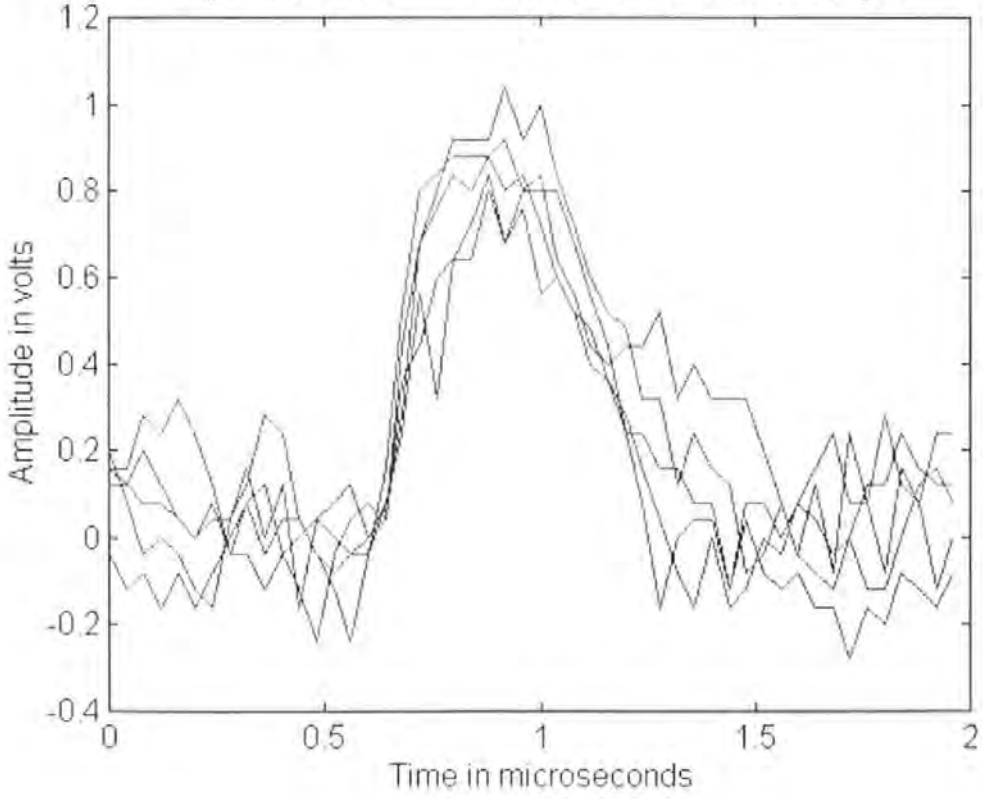

Fig. 7.26 A three layer backpropagation network with fuzzifier

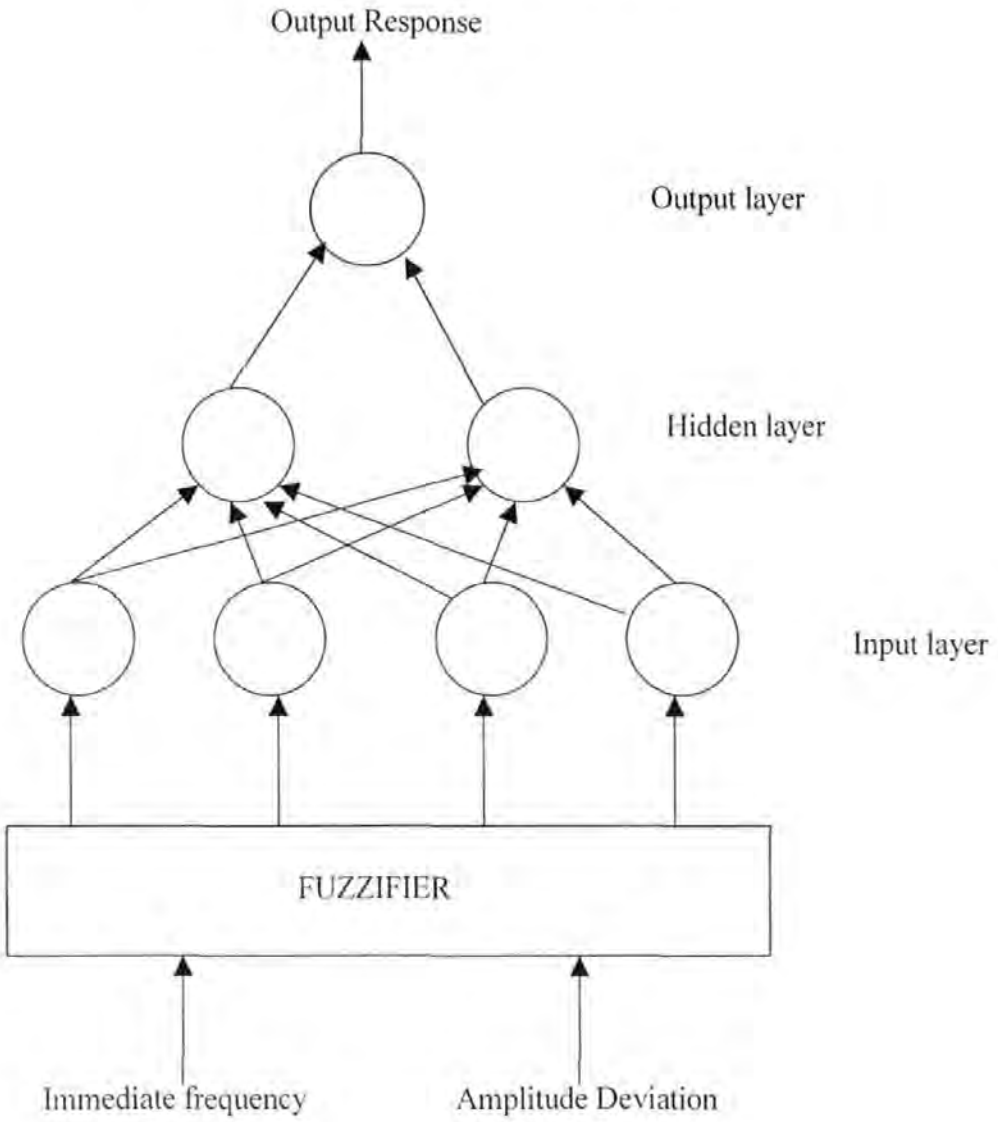

Fig. 7.27a Membership Function of Amplitude Deviation

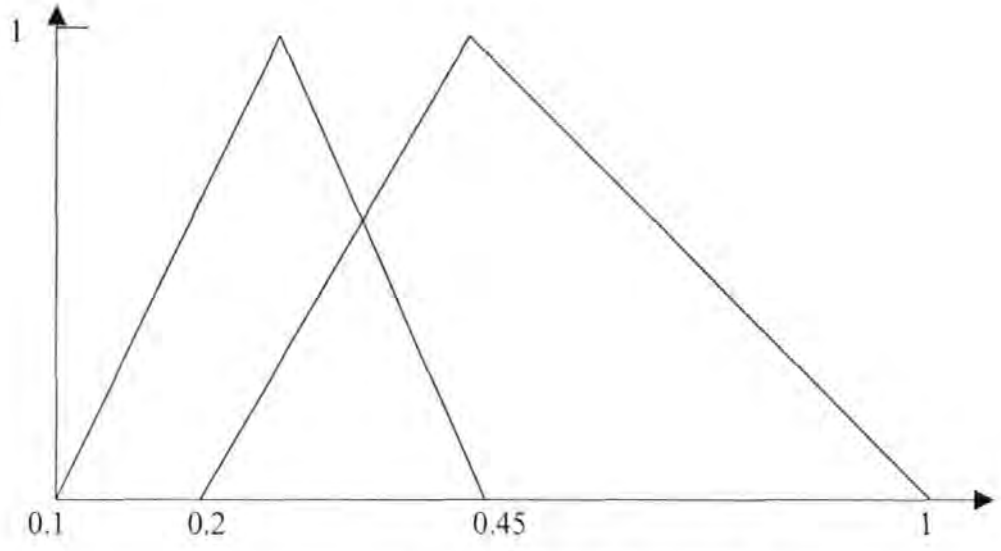

Amplitude Deviation in volts

Fig.7.27b Membership Function of Immediate Frequency

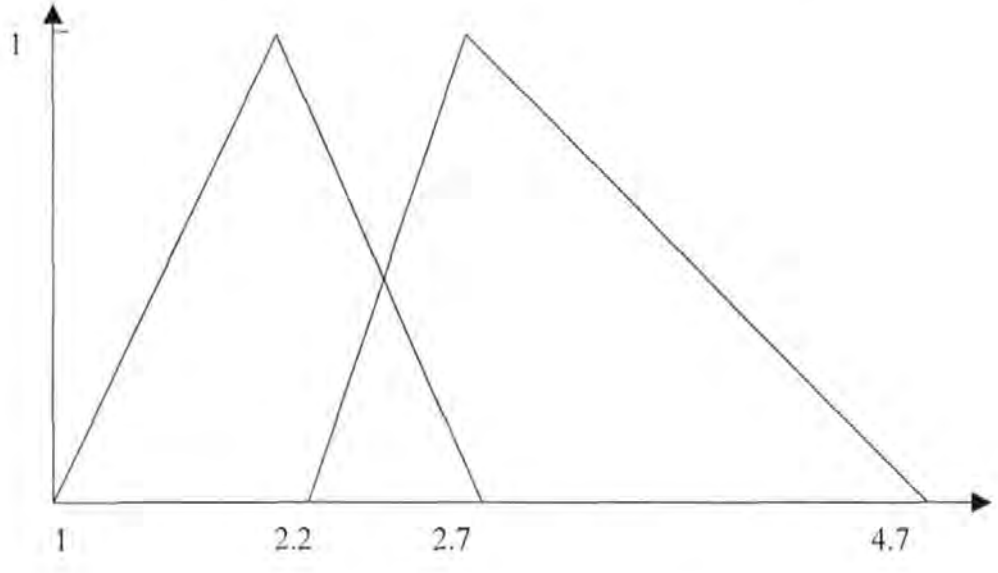

Immediate Frequency in MHz

7.7 Conclusion

The neural network has been developed and optimised for use with the target detection system and enhanced to cater for a basic classification capability. Initially, studies were made to define the network topology as well as formulating the network parameters. The system was trained on 250 waveforms that were extracted from live radar recordings on a system that is located at the University of Plymouth. The waveforms consisted of different targets, noise background, sea clutter and rain clutter. After the training process was completed, the developed system was tested to assess performance. The performance of the detection system was compared with the TM-CFAR system and the result showed that the neural network based system has a much better capability for detecting targets amongst the variation in noise backgrounds presented. It can detect the targets correctly and retain the waveform of the return signals after the detection process.

The testing waveforms have included a variety of situations which have not been met by the system during the training process. Out of the 20 radar traces used in the training, two extreme cases with strong rain clutters and sea clutters were shown. The results of the testing process showed that the network had learnt to identify targets from clutters under all test situations presented to it.

There were difficulties in obtaining sufficient samples to build up the database for both training and testing. As such, a lot of time has been spent in recording the return signals from vessels passing the harbour, and waiting for opportunity to record these under the varying backgrounds including sea clutters and rain clutters. Despite the fact that there were errors in the network output after the training, there were still enough discriminating space between the target and the clutters for the detection process to give the appropriate response. The same philosophy, with the

addition of a fuzzier to match the uncertainties, was used in performing target classification. It proved that the system could classify the targets presented into large and small vessels effectively. To further recognise the vessels to specific types, e.g. destroyer, cruiser, cargo ship ...etc, more samples would be required to train the neuro-fuzzy identifier. A comprehensive simulation environment with different models would be desirable to provide the wide variety of samples that are required for training.

The results from the trials have proved to be encouraging. Simple processing techniques were able to provide valuable information from the radar signal and further computer methods were then able to detect the targets based on this information. The feature extraction process involved only simple mathematics. The objective was to avoid the use of complicated algorithms that require significant computation time. This would limit the application of the system in real time environment where speed of the process is essential. The speed could further be improved if all or part of the tasks were to be performed under parallel hardware implementation.

The developed system is designed for radar target detection and classification purposes. However, the same design concept can also be applied to other signal detection process, such as medical imaging and pattern recognition.

CHAPTER 8

CONCLUSIONS AND FURTHER WORK

8.1 Introduction

The aim of this study was to adopt an artificial intelligence approach to the processing of radar return signals for target detection. The programme of work has involved the evaluation of artificial intelligence and the use of neural networks in this application. The research work was divided into a subset of major tasks:

a. Survey of existing detection algorithms;

b. Investigating the feature extraction techniques;

c. Studying the possibilities of employing neural networks in target detection ;

d. Developing software and hardware for acquiring radar signals for use in the research;

e. Formulating the neural network based detection system;

f. Considering the extension of these methods for the classification of targets.

Recent research into radar target detection has concentrated on the improvement of the existing CFAR algorithms. This study has used a new approach in which detection is based on features extracted from the raw radar data.

This chapter summaries the key findings, draws conclusions from the results of this investigation and considers the possibilities for future developments.

8.2 Approach to the solution of problems in target detection

In the design and evaluation of an intelligent target detection system, the following related problems have been considered.

8.2.1 Drawback of commonly used detection algorithms

Various current methods for target detection in radar have been discussed in chapter one. In a marine radar environment, both ground clutter and sea clutter can cause difficulties in detecting target vessels. These clutters often have sufficient magnitude to mask targets in a region. Clutter changes dramatically as the radar antenna turns. In one location of a single scan, clutter returns from a calm sea may be observed which behave as Rayleigh distributed random variable. In other locations, clutter returns from coastal waters, where land sea interface is situated, are observed. This clutter often behaves as a K-distributed random variable and the detection process in the clutter edge is very unpredictable. Under such a variety of circumstances, a simple detection method employing threshold techniques alone cannot meet the challenge and excessive false alarms or failed detections will be encountered. A comprehensive range of variations on the CFAR detection algorithm has been discussed. Each these aims to tackle a specific problem in detection, e.g. GO CFAR is appropriate for improving performance near clutter edges, SO CFAR was developed to detect closely spaced targets, OS CFAR is considered as a processor to deal with interfering targets. It is concluded in chapter 1 that no single CFAR algorithm, where the decision is made only from the amplitude information of the return echoes, is adequate to solve problems in a complex detection environment.

Research into alternative methods of target detection was reviewed. Papers reporting the success of application of fuzzy logic in signal detection has instigated the application of artificial intelligence in the area of target detection in radar. Fuzzy logic has a distinct advantage over other algorithms in handling information that has a high degree of uncertainty. The membership functions are assigned to the prior probabilities, the cost function and the received signal amplitude. Based on a particular situation and the corresponding statistics of the noise under each hypothesis, the processing mechanism works with this fuzzy information to determine the desired threshold. However, the final threshold depends on the shape of membership functions of the input parameters. It is necessary to ensure that the assignment of the membership is appropriate to the operating environment of the radar system. Also, the selection of rules plays an important role in the performance of the final system. The rules should be formulated to cover all the aspects that the radar will encounter. As such, it is difficult to achieve the optimum state when a fuzzy approach is adopted.

8.2.2. Extraction of features from radar signals

The primary limitation of traditional information processing techniques is their static processing methods which employs only the magnitude of the signals. With recent development in the processing speed of computers, more information can be handled in real time. Important information from radar returns, such as spatial components, amplitude deviations and so on, can be extracted to assist in deciding if a target is present. Theoretical analysis and experimental results provided in chapter 3 on one dimensional space of the radar waveforms show that characteristics of radar targets and clutters are different within a certain degree. Such differences were observed on

signals recorded from a general purpose marine radar and compared with expected values from knowledge/data bases to make a decision regarding the presence of a target. However, it is necessary to identify the amount of information required to make decision process in target detection efficient, bearing in mind the requirement to solve the problem in a computer in real time. For the purposes of this investigation, a number of characteristics of the return signal were identified. Conventional waveform analysis techniques such as Fourier transform and correlation were evaluated. These involve complex computational sequences, which did not prove to be practical for real time processing. Statistical signal characterization involves the division of the waveform into segments, which are bound by positive and negative extreme conditions. Eventually, five waveform parameters namely; amplitude mean, amplitude deviation, period mean, period deviation and maximum period were identified as the primary measures appropriate to this application. The use of these measures can achieve similar objectives to spectral analysis and correlation, but they need significantly fewer computer operations. Each set of waveform parameters is unique to a particular waveform. In very complex situations (e.g. heavy clutter), a redundancy may spread across more than one parameter between target and noise, but it does not spread across all the five parameters to a degree which is beyond the computational capabilities in discriminating the features.

8.2.3. Data acquisition of radar signals

The radar equipment used within this investigation is a general purpose marine radar, which looks out across Plymouth harbour. Ideally, the research required a data acquisition system that is able to record the radar signal continuously for a number of scans and incorporate bearing identification in each sweep. Such a recording system

was not available on the market during the research period, however it was at the development stage. This demonstrates the industrial drive towards further digital methods in the processing of radar return signals and the imminent possibility of implementation of this research. In order to progress with the original objectives, it was decided that a simple system should be designed to acquire the radar signals and transfer the data into a computer for analysis. The system consisted of a digitized oscilloscope with a maximum sampling frequency of 100MHz which was able to record the signal for a number of sweeps, depending on the sampling rate used. The heading marker was employed as a trigger signal to initiate the recording and any targets passing the heading marker region could be recorded. As the existing heading marker of the radar at the University of Plymouth was in a radar blinding sector, a simple hardware circuit with variable delay was designed and built. This enabled the heading to be shifted by around 10 degrees and facilitated the acquisition of returns from targets over a sector that looked across Plymouth Sound and beyond. The recording system proved to be satisfactory and was used to record over 300 sweeps from the radar transceiver to form a database of digital radar return signals. This included a variety of targets, sea clutter, rain clutter, land clutter and noise. A substantial amount of time was spent recording these returns, and it was also essential to maintain visual observation to verify and catalogue targets that were observed passing the heading marker region.

8.3 The application of neural networks to radar detection

The information fusion techniques using neural network have been discussed in chapter four. The strategies were based on a multi-layer perceptron network with backpropagation learning algorithms. The research concentrated on the application of

neural networks to improve the target detection and did not intend to develop new neural theories or revolutionary learning. Research into applications is a relevant subject of interest. The topology, structure, training requirements and input parameters are application dependent and the theory has not yet been developed to provide a rule base for design. By studying the performance of various topologies, a 3 layer network with 5 inputs and 1 output was formulated to investigate the use of neural networks in solving complex detection problems. The five statistical characteristics were extracted from 250 samples of radar signals. The 250 samples were chosen to represent a wide variety of signals that would encompass the range of conditions that a radar system is likely to encounter in a complex port environment. Test runs were performed to determine the optimum parameters for use in the learning process, such as learning rates, momentum values and network structures.

The integrated system and the results have been described in Chapter 6 and Chapter 7 respectively. The resulting neural detection system was able to identify targets from samples of radar signals even at low signal to noise ratios. The performance of the network was found to be similar under both training and testing conditions and the maximum error of 0.05, chosen in the training process, allowed sufficient margin for the discrimination between targets and noise. In applying the detection system to the real time situation, a moving window was shifted along the complete sweep. The effect on the number of overlapping samples in the window was studied to obtain the optimum setting. Sweeps containing strong rain clutters and sea clutters were used in testing the system and the results showed that the network is able to discriminate targets that are embedded in the clutter edge. For the purpose of comparison, a TM-

CFAR algorithm was tested with the same sweeps of radar signals and was unable to perform satisfactorily under such adverse conditions.

The neural detection system was further extended to include a fuzzifier to investigate the potential for classification of targets. The inclusion of fuzzy logic, and with immediate frequency as an additional input, the process was able to handle the uncertainties of the parameters between scans/sweeps. The combined neural-fuzzy system was able to classify the targets into large and small vessels by using only two parameters, i.e. amplitude deviation and immediate frequency, with satisfactory results.

8.4 Contribution of this study to radar detection system

The result of this study is considered to be a break through in the existing technology of radar detection. The developed technique does not use the conventional CFAR algorithms to determine the thresholding level of the amplitudes. Instead, important features from the raw radar videos are extracted to determine the presence of a target. The features are not limited to the amplitude parameter, information such as amplitude/period deviation from the mean, mean period and maximum period are also used in the task of detection. The study introduced the concept of adopting data fusion in the detection stage of the radar signal processing to combine the extracted features. Live video was used in training the neural network to facilitate the developed system to handle the real radar data. The result showed that the system is efficient and is able to detect targets even when the amplitude is lower than that of clutters and background noise. The existing detection algorithms only accept the part of waveform that is above the threshold amplitude. As such, some valuable information in the

waveform will be lost. With the neural detection system, a large section of the target waveform was retained after the detection process and this information is available for use in subsequent processing such as target identification, as well as the tracking stage. This can further be used to improve the tracking reliability of present radar systems. The introduction of a neural-fuzzy system has demonstrated that the system was able to handle fuzzy data and classify the targets into small and large vessels. This neural-fuzzy approach can form a framework for any future sophisticated radar target identification processes.

8.5 Future developments

The work produced by this research has established an intelligent target detection system that can be used as a basis for the development of future detection methods in radar or other areas, such as recognition of patterns from medical instrumentation. To implement the developed system in pattern recognition, similar parameters can be extracted from incoming signals. Provided that redundancies do not appear in all the five parameters, then an individual database for different types of signals can be formulated to meet the requirements of the specific application.

To further develop the system, it is suggested that the following improvements and future research are necessary.

- Additional outputs and inputs to the system
- The use of more sophisticated data recording system
- Using high speed parallel processor
- The investigation of alternative intelligent algorithms
- The use of additional features in the classification of radar targets

8.5.1 Additional inputs and outputs to the system

The system has five inputs to the neural networks and these are mean amplitude, mean amplitude deviation, mean period, mean period deviation and maximum period. The neural network has only one output that is the weight to determine if a target is present in the window. The system could be enhanced if the environmental condition could be used as further inputs. The information on the sea-state or wind speed will provide the system with information regarding the amount of sea clutter that the radar is likely to receive. The database can then contain sea clutter signals at different sea states and this will assist the system to discriminate targets from heavy sea clutters. Similarly, the precipitation condition will provide important information about the expected magnitude of the rain clutters.

The system could also be improved by producing outputs that are able to classify the input waveform into different categories. To achieve this requirement, the system would require a comprehensive database of different signals, which would in turn require a sophisticated data recording system. Also, the measurement of simulated targets in a controlled environment with different models of targets, such as could be provided in an anechoic chamber, may be necessary. This classification would enable the radar tracking system to process interesting signal/targets only. This would greatly reduce the processing time needed by the computer.

8.5.2 The use of sophisticated data recording system

The present recording system employed a digital oscilloscope which is limited to the size of memory in the equipment and hence can only record a few sweeps of radar signals at one time. As such, it is necessary to transfer the data between the

oscilloscope and the computer after each recording. This procedure caused difficulty in building up a long history of radar returns from specific targets. The ideal system should integrate the digitizer with a computer so that data can be transferred automatically when the buffer memory is full. The recording system should also be able to identify the bearing of each sweep uniquely so the targets at specific sectors can be searched quickly; however they would still need to be identified and catalogued visually. With this type of system, the radar returns from different types of targets could be recorded at various ranges and an extensive database constructed. Further training of the neural network with more extensive data would improve the probability of detecting and identifying individual types of targets. It is understood that a company based in Russia is designing a digital acquisition system to work with its radar systems. Unfortunately, there is no indication as to when such recording system will be available in the market, or of the facilities that will be available to extract digital data from their dedicated hardware. This is a requirement for the purposes of further research into methods for integrating this detection system with the radar tracking processes to enhance the capability of the tracker.

8.5.3 Using high speed parallel processor

The detection system has to extract the features from windows of radar signal sequentially, then the features have to input to the neural network to decide the output value. This will take up considerable amount of computational time and induce delays in the detection system. For practical implementation, the delay can be improved by employing parallel high speed signal processing chips, e.g. TMS 320 family, to perform feature extraction of the radar returns. The duty of inference can then be performed by a fast speed PC, e.g. with a P3 family CPU. This arrangement will

enable better efficiency in the real time implementation of the target detection and recognition process.

8.5.4 The implementation of alternative artificial intelligence methods

The detection algorithms that have been studied are CFAR, fuzzy logic and neural network. The CFAR algorithms could not achieve the detection capability in adverse conditions due to their decision being based on amplitude information only. The fuzzy approach has many successful applications in engineering fields, but it requires the definition of a reliable rule base. In the area of target detection, the application of fuzzy algorithms alone will be difficult due to the requirement for the compilation of a comprehensive rule base that covers the different environments that are likely to be encountered by the radar. The neural network based detection system has the ability to learn, and the learning can be performed off-line. However, it requires the collection of training data, and the definition of suitable topology and various training parameters. More importantly, for the purposes of real time operation, a consideration is that neural work approach is relatively slow when operated in software. With the development of the neural network chips in the market, it is feasible that the system can be implemented in hardware to achieve the speed required in radar signal processing.

There are other techniques that may prove to be suitable for further investigation into target detection, such as Wavelet Transforms and neurofuzzy methods. The Wavelet Transform decomposes the radar return into signal bands that are orthogonal to one another, reducing the redundancy and increasing the chance of revealing the useful feature (Lu, Yu and Guo (1993), and Chan (1995)). Further studies can be performed

on the application of hybrid intelligent system, which combines two intelligent techniques to meet specific requirements, such as the fuzzy-decision neural networks (Taur and Kung, 1993, and Jang (1993)). Such hybrid system could be applicable to target detection and recognition with fuzzy decision system or other intelligent algorithms to optimize the performance of the neural network.

8.5.5 The use of additional features in the classification of radar targets

The proposed neural fuzzy network system can classify radar returns into large and small targets. To determine the type of vessels within the same category with minimum error, e.g. discrimination between a tanker and a general cargo ship, a yacht and a small fishing boat, more distinct features have to be extracted from the signals. A method of target recognition using image processing techniques has been described by Nebabin (1984). The image of the target is formed by a number of consecutive sweeps of the radar signal. The range width of the two dimensional image is contributed by the length of the vessel, that may reach 400 meters for ships with displacements of several hundred thousand tons. The azimuth width of the image depends on the angular spread of the target. Additional features from these images, such as the area of the target, the intensity mean, intensity variance, and centroid of the image will further facilitate the classification process. It is necessary that a database of different classes of targets of interest be created by observing similar models under laboratory conditions, with measurements being taken at various aspect angles. This database can then be searched to select an appropriate class to match with the target to be identified.

8.6 Conclusion

The research work has shown the possibility of using an intelligent approach to detect targets in a clutter environment. The methodology used in developing the neural network has proved that this technique can produce better results in target detection when compared with conventional CFAR algorithms. However, in order to implement such improvements a more sophisticated digital data acquisition system is initially required. The data record will form a valuable tool to enhance the detection and tracking capability of a radar system for vessel traffic management, or shipboard use.

This research has proved that neural networks can be used in radar target detection, and that they can provide an improvement in performance over conventional CFAR methods. The limitation of using a neural network is in the time required in both training and processing. A further consideration might be that the neural network has no tunable parameters to allow controllability by the operator through the man machine interface. It would therefore not be easy for the operator to perform any online adjustment to the target detection system. At present CFAR algorithms are commonly used in marine radar equipment because of their simplicity. All the CFAR components can be constructed in hardware and as such they do not cause any delays to the detection process. If radar manufacturers decide to take up the option of using artificial intelligent algorithms such as neural networks within the detection system, then the speed of the algorithms and the controller interface would be prime considerations. With the advancement of technology, special chips for the application of artificial intelligence are already available on the market, which offer the prospect of suiting such needs. It will therefore not be long before all radar system are equipped with artificial intelligence networks that are able to perform target detection and recognition in an efficient manner.

APPENDIX A

PUBLISHED PAPERS

---

1. Target Detection in Radar: Current Status and Future possibilities, Li YFV and Miller KM, Journal of Navigation, Royal Institute of Navigation, May 1997.

2. Radar Target Detection Using Feature Extraction, Li YFV and Miller KM, IRS98, Proceedings of an International Radar Symposium, German Institute of Navigation, Munich, September 1998.

Target Detection in Radar: Current Status and Future Possibilities

Vincent Y. F. Li

(Hong Kong University of Science and Technology)

and Keith M. Miller

(Institute of Marine Studies, University of Plymouth)

Most of the radar systems used in operating marine vessel traffic management services experience problems, such as track loss and track swap, which may cause confusion to the traffic regulators and lead to potential hazards in the harbour operation. The reason is mainly due to the limited adaptive capabilities of the algorithms used in the detection process. The decision on whether a target is present is usually based on the amplitude information of the returning echoes. Such method has a low efficiency in discriminating between the target and clutter, especially when the signal-to-noise ratio is low. With modern signal processing techniques more information can be extracted from the radar return signals and the tracking parameters of the previous scan. The objectives of this paper are to review the methods which are currently adopted in radar target identification, identify techniques for extracting additional information and consider means of data analysis for deciding the presence of a target. Instead of employing traditional two-state logic, it is suggested that the radar signal should be allocated in terms of threshold levels into fuzzy sets with its membership functions being related to the information extracted and the environment. Additional signal processing techniques are also suggested to explore pattern recognition aspects and discriminate features which are associated with a return signal from those of clutter.

1. INTRODUCTION. Vessel traffic management systems extract data from the raster of the incoming radar signal. This data is further processed to generate target tracks which are then displayed for traffic control. In a dense harbour situation where vessels are usually manoeuvring in very close proximity to each other, targets may be swapped giving the controller a false impression of ships manoeuvres and intentions. Furthermore, reflections from land based objects such as buildings increase the level of interference to the received signals and provide further confusion to the tracking algorithms employed. When the weather is bad, clutter due to sea waves and fog will also affect the quality of the signals. All these restrictions limit the detection/tracking capability of the vessel traffic management to a great extent. Any resulting target loss or swap which may occur will create a burden for the safety operation of managing traffic in the harbour. There is a need to review the radar signal processing technique with the objective of making the processing more adaptive to dynamic changes of the environment.

The initial step in radar signal processing can be regarded as the task of removing all the non-useful data. The returned radar information from the

receiver must be reduced to a few signals which represent the known and new targets. The key operation to achieve this data reduction is the thresholding process, where the data are compared with a reference level. Only those signals with magnitudes exceeding the threshold level are processed further. However, the radar signal from a target is usually embedded in both thermal noise and clutter. The magnitude of the noise and clutter will vary in different sweeps, ranges and scans. To achieve a low false alarm rate and a high probability of detection, the setting of a threshold with a constant amplitude is not feasible.

The constant false alarm rate (CFAR) processing technique has been developed to adjust the threshold value according to the noise power of the return signal at specific times. The threshold of individual cells is decided based on the signal strength of a group of reference cells nearby. In the conventional cell averaging constant false alarm rate (CA-CFAR) detector,[1] digitized radar video is clocked through a moving window (delay line). For each range cell, which corresponds to a given range on some bearing, the mean video levels of the 'N' preceding cells and of the 'N' following cells are calculated. The threshold comparator calculates the average of these two mean levels, and the resulting threshold is compared with the radar signal. Those which are above the threshold level, will be processed as targets for the following stages. Otherwise, they are treated as noise. The probability of detection of the CA-CFAR detector depends on the threshold multiplier (which is a function of the probability of false alarm), the signal to noise ratio and the number of range cells in the window.[2]

CA-CFAR provides optimum detection in a homogeneous environment where the noise power in the range cells is such that the observations are independent and identically distributed.[3] However, this assumption frequently fails due to the environment in which the radar system is operating. A reference window may contain cells with large sudden changes in the noise power due to some other phenomena providing a reflection which appears as clutter on the system. If the target is embedded in the test cell, this transition will unnecessarily increase the threshold to a high level and lower the detection probability. Yet, if the test cell contains the clutter, the threshold value may not be high enough to reject the clutter because cells with low noise level are also contributing to the calculation of the mean value. As a result, an excessive false alarm rate will occur. Also, when multiple targets are very close in range and appear in the same window, the noise associated with these targets may cause the threshold to increase. Such an effect will allow only the strongest target in the window to be detected.

In view of the above drawbacks of CA-CFAR, alternative solutions have been proposed to improve the effect of non-homogeneous noise backgrounds to the CFAR detector. A 'greatest of ' logic selection (GO-CFAR) was proposed by Hansen and Sawyers[4] to reduce the number of excessive false alarms at clutter transitions. Two reference windows are formed in the leading and lagging sides of the test cell and a target is declared if the amplitude of the test cell exceeds the greater of the two windows. A slight reduction in detection probability may be expected when the leading window contains signals with low noise power while the lagging window contains clutter with large magnitude. However, the use of greatest selection will not allow the CFAR detector to efficiently detect

closely spaced targets. Also, the detection probability will be greatly affected when interfering targets appear in the leading and lagging windows.[5,6]

It has been shown[7] that the use of 'smallest of' (SO-CFAR) selection method is able to resolve targets which are closely spaced in range. The smaller value of the leading or the lagging windows will be used to estimate the noise power.[7] Again, the performance of the SO-CFAR detector will be degraded if interfering targets are found in the leading and lagging windows. The SO-CFAR detector is not able to limit the false alarm rates during the clutter transitions. For example, if there is a clutter transition in the window, and the clear background contributes to a low magnitude of estimated noise level, this will cause the threshold to go low and increase the false alarm rate.

2. ADVANCED CFAR ALGORITHMS. In view of drawbacks of the simple CFAR algorithms as described, a lot of research has been performed to provide adaptive CFAR algorithms which are able to handle radar detection in a non-homogeneous environment.

Ordered statistics (OS) CFAR has been developed to reject transient noise.[8] In this algorithm, the range cells (c(1)...c(N)) in a window are first ordered according to their magnitudes to yield the ordered samples, $c(1) < c(2) < \ldots c(N)$, where N is the window size. The noise power is then estimated by selecting the nth largest cell to work out the threshold. To choose the order n, analysis has been performed by plotting the required signal-to-noise ratio as a function of n.[9] The plot was based on a window (N) of 20 cells, with constant probability of detection (Pd) and false alarm (Fa). The broad minimum in the required signal-to-noise ratio was found to be from $n = 14$ to $n = 19$. This agrees with the general assumption[10] that n approximately equals to $3N/4$. As n increases from a low value, Pd improves until n reaches this optimum value, further increases in n degrade Pd. The detection performance does not depend on the position of the interfering targets in the window. Since OS CFAR ranks the full range of cells in the window, the order of an interfering target will not be affected by its location. For optimization of the false alarm rate, OS CFAR has the best performance when $n = N$. However, this is the highest order sample and it cannot be used in practice as it will suppress the targets. For n less than N, OS CFAR can discriminate the target from $N-n$ interfering targets without degradation in detection. The performance of OS CFAR in clutter edges is good when the clutter returns have constant/slow varying amplitude characteristics. However, OS CFAR suffers serious degradation if the clutter returns are fluctuating independently.

Trimmed mean filtering has been used in signal and image restoration processes.[9] The noise power of the trimmed mean CFAR[10] is estimated by combining the ordered samples linearly. It firstly ranks the samples according to their magnitude and then filters T_1 samples from the lower end and T_2 samples from the higher end. The remaining samples are summed to work out the threshold. As the trimming increases, the threshold multiplier has to be increased to maintain the false alarm rate. When T_1 reaches $n-1$ and T_2 reaches $N-n$, the detector becomes an OS-CFAR. It corresponds to a CA-CFAR when there is no trimming at all ($T_1 = T_2 = 0$). Symmetric trimming that is $T_1 = T_2$, limits

the performance of the detector in the clutter boundaries, especially when the leading window contains the clutter and noise, and the lagging window has a clear background. The symmetric trimming technique may develop a threshold which will not be high enough to reduce the false alarm rate when the test cell contains a sample with clutter in the background. For asymmetric trimming, it is necessary to determine optimum trimming parameters T1 and T2. The value of T2 should correspond to the number of interfering targets in the window. For better performance in detection, T1 should be kept as small as possible. Yet, for reducing false alarm rates in clutter boundaries, T1 should be large and T2 should be small. Optimization of such an algorithm is then a matter of fine tuning these parameters and is dependent on the amount of clutter and number of targets.

Another CFAR, which is proposed to deal with interfering targets, is the censored mean level (CML) CFAR.[11] The outputs from the range cells are ranked according to their magnitude and the largest n samples are censored. The remaining $N-n$ samples are used to estimate the noise level (c) of the cell under test. This estimate (c) is multiplied by a threshold multiplier (M) which is based on the desired false alarm rate (Fa). If the magnitude of the strength of the signal return in a cell exceeds Mc then a target is assumed to be present. Ideally, if the samples to be censored are equal to the number of the interfering targets in the window, the performance of CML will be optimal. However, it will be degraded if the censorship does not include all the interfering targets. This may be the case when the number of interfering targets is unknown. Thus, if an interfering target is included in the process of noise estimation, the threshold will be unnecessarily high and will lower the probability of detection. However, if we overestimate the number of interfering targets, this will cause the threshold to be low and will increase the false alarm rate.

The generalized censored mean-level (GCML) CFAR does not require an exact knowledge of numbers of interfering targets.[11] The samples of both the leading and the lagging windows are ordered independently. The returning signals in the cells, which are considered as interfering targets, will be censored. To decide whether the cell should be censored or not, the higher ordered samples are compared with the lower ones in sequence. A scaling multiplier (M), which is a function of the desired false alarm rate, will be introduced to the lower ordered samples. If $c(k)$ is greater than $Mc(k-1)$, then samples $c(k)\,(k, k+1, \ldots, N)$ are regarded as echoes from interfering targets and they will be censored. The noise estimate is processed based on the magnitude of the remaining samples. The performance of the GCML CFAR is optimum when the interfering targets appear in both the leading and lagging window. The performance will be slightly degraded when the interfering targets fall in one of the windows only. The number of range cells in a window will also affect the performance, the higher the number the better the performance.

The 'greatest of order statistics estimator' CFAR (GOOSE-CFAR)[10] takes the nth ordered samples from both the leading and the lagging windows. It compares these two samples and takes the larger one to estimate the threshold. Since n is less than $N/2$ (the number of samples in each window), GOOSE-CFAR can handle interfering targets in both windows and such targets will normally appear in

samples from $n+1$ to $N/2$. When a clutter boundary appears in the window, the worst case occurs when the cell under test is in the heavy clutter. With the larger of the two ordered samples being taken for threshold estimation, the threshold will be high enough to prevent excessive false alarms. GO-CFAR has demonstrated its good performance in clutter boundaries when interfering targets are not present. However, with GOOSE-CFAR, targets with magnitude larger than the nth samples in both windows will be filtered. This will prevent the masking of multiple targets in the window and improve the detection capability in the clutter boundary.

'Censored greater-of' (CGO) CFAR[13] filters n largest range cells from both leading and the lagging windows. The remaining samples of each window are summed. The larger of the two will be multiplied by a threshold multiplier to give the required threshold. The choice of the numbers of cells to be censored depends on the likelihood of the number of interfering targets in the windows. When the number of interfering targets exceeds the number of samples to be censored, the performance of CGO CFAR will be degraded. However, the detection loss of CGO CFAR will be less than the OS and GOOSE CFAR because CGO CFAR takes the mean of the magnitude of the interfering targets and the noise samples, while OS and GOOSE CFAR will use the ordered magnitude alone. Both GOOSE and CGO CFAR have the greatest-of logic which is able to reduce the sharp rise of false alarm rate at the clutter boundary.

MEMO CFAR[14] combines both median and morphological filtering[15] to decide the threshold level. The first median filter transforms the input into a new series of samples in which those samples less than the mean power of the clutter will be replaced by this mean value. As such, it changes the smaller values of clutter to the estimate of the mean noise power. Any samples with a magnitude greater than a fixed multiple of the mean power will also be replaced by the mean value. The objective is to reduce the effect caused by interfering targets. The second median filter will be used to smooth out the samples from the first filter and gives an unbiased estimate of the original samples. Then the output from the second filter is processed by a morphological filter using an open-closing technique.[16] 'Open' breaks small targets and smoothes boundary while 'close' fills up narrow gaps between targets. MEMO CFAR detectors have superior performance in the presence of interfering targets since they give a mean estimate of noise power with minimum bias and smaller variance. They are able to overcome problems due to masking of targets by clutter boundaries. However, they require much more computer execution time to process the samples than other CFAR detectors.

3. INTELLIGENT METHODS IN RADAR DETECTION. Fuzzy logic has the capability of addressing the imprecise information from a physical system and is becoming a valuable tool in practical engineering applications. It applies rule-based algorithms to resemble the flexibility of the human decision making process. Successful applications of fuzzy logic in various fields have been reported.[17,18,19,20] Recently, a fuzzy approach to signal detection has also been addressed.[21,22,23]

Radar detection uses probability theory to decide on the presence of a target. A two state binary logic is usually used to define the state of the signal, that is

a threshold is applied to the signal. Signals above the threshold level will be accepted as targets and others will be rejected. Since the target in a radar return is not always clearly defined (for example if it is embedded in clutter or noise), uncertainty can appear in every task of the detection stage. Any premature decision based on limited information made at an early task of the radar processing will have an large impact on the following stages, such as tracking and feature extraction. Such processing techniques using binary logic quantize the input signal and cause incomplete information to be processed. With the aid of fuzzy logic, radar detection will not be only limited to the likelihood of detection/false alarm, it can also be expressed in degrees to which an event is likely to happen. Instead of offering a combination on conditional probabilities, the membership functions used in fuzzy logic theory combine inexact information. The fuzzy associative memories function defines the degree of likelihood of the returned signal being a target and its exact value is of no absolute important. When the magnitude of the returned signal is increasing, it is more likely that the signal will be detected as target and the false alarm rate will be decreased. Such a model provides explicit features to represent uncertainty in the radar detection process.

In binary hypothesis testing, Bayes Theory[24] formulates the minimization of the expected cost, called the Bayes risk, and leads to the likelihood ratio test (LRT).

$$LR = \exp\{0{\cdot}5[R^2 - (R-X)^2]\}$$

where LR is the likelihood ratio; R is the observed data; X is a positive mean of the signal amplitude.

To model the uncertainties of the received radar signals, binary hypothesis testing can be reformulated using fuzzy set theory.[25]

$$H_1 : R = X + N$$
$$H_0 : R = N$$

where N is the standardized Gaussian noise.

Now x is a fuzzy parameter, $x = \{[X, u_X(X)]\}$, in which X is an element of set R and u_X is the membership function of X. For convenience, a triangular membership function is adopted, this is centred about a nominal amplitude value X_0 and extending between X_1 and X_2, such that $u_X(X_0) = 1$. The likelihood ratio (LR) becomes a fuzzy set. As shown by Saade,[26] the fuzzy threshold of the likelihood ratio can be determined from prior probabilities and cost functions, which are again fuzzy in nature. In order to compute the fuzzy decision on the optimum threshold of the detection, it is necessary to order the fuzzy sets over the real line and obtain the expression for the utility ranking index of LR, which has been described in.[27] The performance of the fuzzy algorithms may be evaluated using the probability of error technique,[28] where it was shown that the method provided a better result in treating the false alarms and misses in decision making process for radar detection.

Cross validation of wakes against bright spots has been adopted to reject false targets. This performs fuzzy decisions which associate a confidence level for each

entity based with suitable fuzzification functions.[29] In order to define a membership function for a fuzzy set of radar echoes, a set of vessels features which will not be critically affected by speckle noise, such as mean grey level and elongation, need to be selected. Ship classes are selected according to the area of the target, for example class 1 for areas less than 60 pixels, class 2 for areas less than 120 pixels and so on. Each potential ship echo is compared with prototypes of true ships using a weighted distance method. The classifier, referred to the weighted results, associates a high fuzzy index (approximately 1) to a true ship and a low fuzzy index (less than 0·5) to a false ship. Information with respect to the ship/wake relation is processed to give a coupling coefficient which is worked out based on the distance between the centroid of the ship and its closest extreme of wake. This coefficient, between 0 and 1, defines the position of a ship with respect to its wake in the radar image. The coefficient will finally be multiplied by the fuzzy index from the classifier to give a global value that measures the reliability of the detected ship-wake couple. It has been demonstrated[29] that this method provides advantages with respect to the classical method of wake detection using Hough transforms on noisy images.

Edge detection has been used as a means of classification for radar images. However, the decision on whether it is the edge or not possesses ambiguity. A fuzzy reasoning technique, as proposed by Cho,[30] detects the transition on intensity changes. Both the brightness and contrast measures of the pixel intensity are processed as fuzzy input, then fuzzy rules are applied to determine the threshold decision, which will be in the form of a membership function. To defuzzify the threshold decision, the centroid of the calculated membership function is derived by summing the confidence level of the function multiplied by the individual measurement value. Such techniques are effective in extracting edge features because various types of objects and regions have different grey level ranges within a single image. This same phenomena makes it difficult for a global threshold method to identify such features.

In recent years, with the improvement of methods in signal processing, more attention has been paid to the waveform recognition of the radar returns as a detection technique. The amplitude information of radar videos will no longer be the only component for processing a threshold decision. Valuable information is contained in a radar return which can be processed for effective detection. Such information includes symmetry/spread and width of waveform, correlation of special features, shape and gradient of waveform and so on. To extract such features from ship radar returns, Guo[31] proposed a ship target recognition algorithm using various transform techniques, for example:

$$F(X) = F_3(F_2(F_1(X))),$$

where F_1 is the Fourier transformation or maximum entropy spectral transformation; F_2 is the Mellin transformation; F_3 is coding transformation and selection of the events; X is a one dimensional digitized waveform. To enable the transformation to be done effectively, a suitable width and shift for the calculation window should be selected for sampling. The width should be slightly larger than the radar pulse width and the shift should be smaller than half the

radar pulse width. It was shown by Guo that spikes in the signal due to sea clutter have narrower and sharper features than those of weak targets. A threshold in the width will be able to remove obvious sea spikes.

Feature extraction techniques in dynamic processing, such as radar detection, can be regarded as an information fusion system to estimate, screen and combine the features in a complex waveform. However, an intelligent radar detection system should not only rely on the features themselves and the interrelationships between them, but also on the *a priori* information about the ships targets, such as speed and course of a ship, wind situation, distance of the ship from the radar centre and so on. Rules that incorporate this information are stored in a data base. Such detection systems require high speed signal processing hardware to cater for the needs of target detection in real time and will be able to detect weak targets under strong sea clutter.[32]

4. CONCLUSION. Various methods for the detection of targets in marine radar have been discussed in this paper. In a vessel traffic management system, both ground clutter and sea clutter cause difficulties for detecting target vessels. This clutter is often of sufficient magnitude to mask the targets in the region. Clutter changes dramatically as the radar antenna rotates. In one sector of a single scan, we may observe clutter returns from a calm sea, which behave as Rayleigh distributed random variable. In other sectors, clutter returns from coastal waters, where the land sea interface is situated, may be observed. This clutter often behaves as a K-distributed random variable[33] and the detection process at this clutter edge is very unpredictable. It is obvious that a simple thresholding detection method cannot meet such a challenge and excessive false alarms or misses will be encountered. A comprehensive selection of CFAR algorithms, including those for non-homogeneous clutter environment, has been discussed. Each algorithm aims to tackle a specific problem in detection, for example GO CFAR is appropriate for improving performance near clutter edges, SO CFAR was developed to detect closely spaced targets, OS CFAR is considered as an appropriate processor to deal with interfering targets. It is obvious that no single CFAR algorithm is adequate to solve problems in a complex detection environment, such as a VTS system. Another drawback on the CFAR algorithm is that the decision is made only from the amplitude information of the return echoes.

Research has been undertaken using approaches other than the CFAR technique. Papers reporting success of the application of fuzzy logic in signal detection have enlightened the development in the area of radar detection. Fuzzy logic has a distinct advantage over other algorithms in terms of its ability to handle information which has a high degree of uncertainty. It is shown by Saade[26] that, in order to apply fuzzy logic in radar detection, it is necessary to establish the specific regime in which the radar is to be operated. This allows the assignment of membership functions to the prior probabilities, the cost function and the received signal amplitude. Based on a particular situation and the corresponding statistics of the noise under each hypothesis, the processing mechanism works with this fuzzy information to determine the desired threshold. However, the final threshold depends on the shape of membership functions of the input

parameters. It is necessary to ensure that the assignment of the membership is appropriate to the operating environment of the radar system. Also, since the amplitude information is fuzzy, the implication is that the signal-to-noise is also fuzzy and so is the minimum detectable signal. As such, it is difficult to predict the range of a radar system if a fuzzy approach is adopted.

Pattern recognition has already been used as an interesting tool for radar detection. Potential ship targets and their elongated wakes are examined to obtain a higher reliability in detection. A fuzzy ship wake coupling coefficient, together with a fuzzy index of the ship, give a final reliability index of the result. As edges in radar images involve abrupt changes in amplitude, extracting this feature will enhance the accuracy of target detection. A method of using a contrast measure and a brightness measure as input parameters in edge detection is described. It is suggested that an edge detector could be applied to a wide class of returns ranging from clear to vague images.

With the recent development in the processing speed of computers, more information can be handled in real time. Important information from radar returns, such as spatial components, correlation features and so on, can be extracted to assist in deciding if a target is present. A vast number of algorithms for estimating unknown signal parameters from the measured output of a sensor system are now available to deal with signal extraction[34,35,36] which can be applied in radar, radio/microwave communication, underwater acoustics, and geophysics. Research has been undertaken to develop the tool of artificial intelligence for application to the radar detection problem. The concept develops inference machines which process data from various knowledge/data bases to evaluate the situation and provide a final decision. Initial work undertaken in this area has been described in this paper and the results appear to be promising. It is clear that future technology in radar signal processing will be moving towards artificial intelligence with required information from the returns being extracted by modern adaptive algorithms. The next step in the development of this technology is to identify the minimum amount of information which will be required to optimize the efficiency of the decision process in target detection, bearing in mind the limitation in the processing speed of the computers in real time. Also, the identification of methods which relate the available/extracted information to a final decision remains a challenge in the task of intelligent radar detection.

REFERENCES

[1] Barkat, M. (1996). CFAR detection for multiple target situations, *IEE Proceedings*, vol. 136, no. 5, October, 193–209.

[2] Steenson, B. O. (1968). Detection performance of a mean-level threshold, *IEEE transactions on Aerospace and Electronic Systems*, AES-4, July, 529–534.

[3] Kassam, S. A. (1988). Analysis of CFAR Processors in Nonhomogeneous background, *IEEE Transactions on Aerospace and Electronic Systems*, vol. 24, July, 427–444.

[4] Hansen, V. G. and Sawyers, X. (1980). Detectability loss due to greatest of selection in a cell averaging CFAR, *IEEE transactions on Aerospace and Electronic Systems*, AES-16, 115–118.

[5] Al-Hussaini. (1988). Performance of the greater-of and censored greater-of detectors in multiple target environments, *IEE proceedings*, vol. 135, June, 193–198.

[6] Weiss, M. (1982). Analysis of some modified cell-averaging CFAR processors in multiple-target situations, *IEEE Transactions on Aerospace and Electronic Systems*, AES-18, January, 102–103.

[7] Trunk, G. V. (1983). Range resolution of targets using automatic detectors, *IEEE Transactions on Aerospace and Electronic Systems*, AES-19, July, 750–755.

[8] Rohling, H. (1983). Radar CFAR thresholding in clutter and multiple target situations, *IEEE Transactions on Aerospace and Electronics System*, AES-19, 608–612.

[9] Bovik, A. C., Huang, T. S. and Munson, D. C., Jr. (1983). A generalization of median filtering using linear combinations of order statistics, *IEEE Transactions on Acoustic, Speech and Signal Processing*, ASSP-31, 1342–1350.

[10] Wilson, S. I. (1993). Two CFAR algorithms for interfering targets and nonhomogeneous clutter, *IEEE Transactions on Aerospace and Electronic Systems*, vol. 29, 57–71.

[11] Rickard, J. T. and Dillard, G. M. (1971). Adaptive detection algorithms for multiple target situations, *EEE Trans.*, AES-13 (4), 338–343.

[12] Ritcey, J. A. (1986). Performance analysis of the censored mean level detector, *IEEE Trans*, AES-22, 443–454.

[13] Al-Hussaini, E. K. (1988). Performance of the greater-of and censored greater-of detectors in multiple target environments, *IEE Proceedings*, vol. 135, 193–198.

[14] Vassilis Anastassopoulos and Lampropoulos, G. A. (1992). A new and robust CFAR detection algorithm, *IEEE Transactions on aerospace and electronic systems*, vol. 28, 420–427.

[15] Jain, A. K. (1989). *Fundamentals of Digital Image Processing*, Prentice-Hall International Editions.

[16] Stevenson, R. L. and Arce, G. R. (1987). Morphological filters: statistics and further syntactic properties, *IEEE Transactions on Circuits and System*, November, 1292–1305.

[17] Kosko, B. (1992). *Neural networks and fuzzy systems*, Prentice-Hall, Inc.

[18] Russo, F. and Ramponi, G. (1992). Fuzzy operator for sharpening of noisy images, *IEE Electronics Letters*, August, 1571–1717.

[19] Russo, F. (1992). *A fuzzy approach to digital signal processing: concepts and applications*, IEEE, 640–645.

[20] Li, Y. F. and Lau, C. C. (1989). Development of fuzzy algorithms for servo systems. *IEEE Control Systems Magazine*, April, 65–71.

[21] Boston, J. R. (1993). *A fuzzy model of signal detection incorporating uncertainty*, IEEE, 1107–1112.

[22] Russo, F. (1994). *A totally fuzzy approach to multisensor instrumentation: pre-processing techniques*, IEEE, 1143–1146.

[23] Son, J. C., Song, I. and Kim, S. (1991). *A fuzzy set theoretic approach to signal detection*, IEEE, 150–153.

[24] Van Trees, H. L. (1968). *Detection, Estimation, and Modulation Theory, Part 1*, John Wiley and Sons, New York.

[25] Zadeh, L. A. (1965). *Fuzzy sets, Inform. and Control 8*, 338–353.

[26] Saade, J. J. (1994). Towards intelligent radar systems, *Fuzzy Sets and Systems 63*, 141–157.

[27] Saade, J. J. (1992). Ordering fuzzy sets over the real line: An approach based on decision making under uncertainty, *Fuzzy Sets and Systems 50*, 237–246.

[28] Saade, J. J. (1990). Fuzzy hypothesis testing with hybrid data, *Fuzzy Sets and Systems 35*, 197–212.

[29] Benelli, G., Garzelli, A. and Mecocci, A. (1994). Complete processing system that uses fuzzy logic for ship detection in SAR images, *IEE Pro.-Radar, Sonar Navig.*, vol. 141, 181–186.

[30] Cho, S. M. and Cho, J. H. (1994). Thresholding for edge detection using fuzzy reasoning technique, *Singapore ICCS*, 1121–1124.

[31] Guirong, Guo (1989). *An intelligence recognition method of ship targets*, IEEE, 1088–1096.

[32] Guirong, Guo (1992). *Target detection and recognition based on dynamic processing techniques*, *IEEE* 171–181.

[33] Baldygo, W. (1993). *Artificial intelligence applications to constant false alarm rate processing*, *IEEE* 275–280.

[34] Kaveh, M. and Barabell, A. J. (1986). The statistical performance of the MUSIC and the

minimum-norm algorithms in resolving plane waves in noise, *IEEE Trans. Acoust. Speech. Signal Processing*, vol. ASSP-34, 331–341.

[35] Roy, R. and Kailath, T. (1989). ESPRIT – estimation of signal parameters *via* rotation invariance techniques, *IEEE Trans. Acoust., Speech, Signal processing*, vol. ASSP-37, 984–995.

[36] Wax, M. and Kailth, T. (1985). Detection of signals by information theoretic criteria, *IEEE Tran. Acoust. Speech. Signal Processing*, vol. ASSP-33, 387–392.

KEY WORDS

1. Radar. 2. Signal processing. 3. Target detection.

RADAR TARGET DETECTION USING FEATURE EXTRACTION

Vincent Y.F. Li and Keith M. Miller
Institute of Marine Studies, University of Plymouth,
Drake Circus , Plymouth, Devon PL4 8AA,
United Kingdom

Abstract

Target detection based on magnitude of the amplitude information alone has a very low efficiency in discriminating between targets and clutter, performance depends on the signal-to noise ratio environment. Conventional detectors that rely on these techniques can produce high false-alarm rates when they are operating in adverse conditions. However, valuable information is contained in a radar return that can be processed for effective detection. The methods of extracting this critical information from sequenced sweeps of a radar signal and the integration of such data have been a challenging problem. The objective of this paper is to study the characteristics of radar return signals and identify the features that can improve the detection capability of the radar system. Methods of extracting this information to identify the presence of targets are also discussed.

Introduction

Radar target detection has been a difficult task due to the presence of clutter. These unwanted signals are often of sufficient amplitude to mask any weak targets in the region. The statistical nature of radar signals changes dramatically as the radar antenna rotates and does not always conform to the established distributions. The constant false alarm rate (CFAR) processing technique has been developed to adjust the threshold value according to the noise power of the return signal at specific times and various CFAR algorithms have been reported [1, 2, 3]. However, each algorithm aims to tackle a specific problem in detection; Greatest of (GO) CFAR is appropriate for improving performance near clutter edges, Smallest of (SO) CFAR was developed to detect closely space targets, Ordered Statistics (OS) CFAR is considered as a processor to deal with interfering targets. It appears that no single CFAR algorithm, in which a decision is made only from the magnitude of amplitude information, is adequate to solve problems in a complex detection environment [4].

The performance of radar target detection depends on the features that can be used to discriminate between clutter and targets. To have a significant improvement in the detection of weak targets, more obvious discriminating features must be identified. The detection system can give a better performance when the characteristics of target and clutter are in line with some predicted values. A wide range of targets and clutters will be received by radar systems and it is necessary to formulate descriptions about these signals at specific times. To decide whether a target is present, there are factors other than the magnitude of the return signal to be considered. The echo from reflecting objects may consist of many components of energy scattered from points over the surface. Their time-frequency and correlation characteristics will vary as a function of time, angle of incidence and transmitting frequency. The interaction of these components will affect the radar detection process. With the recent development in the processing speed of computers, more information can be handled in real time. The statistical nature of the clutter returns can be calculated using the probability distribution function of a

random variable in sequential windows. Time-frequency and correlation characteristics from radar returns can be extracted to assist in deciding if a target is present.

Section 1 of this paper describes the statistical characterization of different radar returns and shows how such information can be extracted in target identification. The various correlation characteristics of radar signals are discussed in Section 2. Section 3 shows the time frequency characteristics of a radar return. All data presented has been acquired by the authors using a radar system operating at X band that looks out across the city and then the harbor at Plymouth, UK.

1. Statistical Characterization

Most of the random noise arises in the initial stages of the radar receiver. The behavior of the noise during the period that the return signal from the target is being received cannot be predicted. However, the statistical distribution of random noise at the input to the intermediate amplifier can be assumed as Gaussian, with zero mean. This is mainly due to the thermal motion of electrons in the early amplification stages.

Most targets and clutters have a very complicated relationship to the cross section area seen by the radar, and it is difficult to format equations based on the physical dimensions. Swerling summarized these targets in statistical form and established four statistical models based on probability density function [5]. It was reported that class 1 targets (constant amplitude on any one scan) and class 2 targets (rapidly fluctuating target) are Rayleigh type model and corresponds to targets which many scattering sources are added. Basically, all targets received by the radar equipment are very close to this model.

The Rayleigh model can also apply to sea clutter if the sea is calm and the range cells are fairly large. However, when considering a short pulse radar of high resolution, the range cells at which the system discriminates are relatively small. The size of individual sea waves may often be comparable with a range cell, especially in a rough sea. The distribution then departs from the Rayleigh model, with sharp peaks at the larger wave tops. Other forms of distributions, e.g. Weibull and Log-normal have been used to model sea clutter received by marine radar systems. These types of function have a longer 'tail' than the Rayleigh distribution. The decision on which distribution is applicable depends on the sea state at that time.

Volume clutter is usually caused by particles in the atmosphere such as rain and cloud droplets. The systems performance is then influenced by weather conditions. The reflectivity of volume clutter is quantified in effective radar cross-section per unit volume. The unit volume is calculated using the pulse length, horizontal beamwidth and vertical beamwidth. The rain and cloud droplets are usually very small compared with the radar wavelength. Their effect, in terms of noise characteristics, can normally be described by the Rayleigh distribution. However, the radar cross section of droplets for cloud and rain is proportional to the fourth power of the transmitter frequency. This causes high frequency radars to be more susceptible to effects on clutter caused by the weather. For shorter wavelength systems the scattering properties may cause the noise characteristics to depart from the pure Rayleigh distribution.

Figures 1 to 4 show the recorded noise, target, sea clutter and rain clutter, and their statistical distribution in a 4 microsecond time window, which contains 100 samples of the radar return signal corresponding to a distance of 600 meters.

Despite the fact that the magnitude of the random noise, sea clutter and rain clutter of these signals are similar, their distributions show that each type of return has its unique features. To characterize the difference in amplitude between these signals, their mean value and standard deviation in the 4 microsecond windows are evaluated. It can be seen that the width of echoes from clutters and noise are usually narrow and sharp. Such characteristics can be extracted by calculating the time differences, i.e. the period between the negative extremes of the signals inside the window. Also, the maximum period in each window is evaluated. The details are shown in the following table.

	Target	Sea Clutter	Rain Clutter	Noise
Mean (amplitude in volts)	0.1952	0.2340	0.5880	0.0584
S. Deviation (amplitude)	0.2296	0.2014	0.1960	0.1060
Maximum (period in microseconds)	0.8	0.44	0.36	0.48
Mean (period in microseconds)	0.1704	0.1508	0.1584	0.1523
S. Deviation (period)	0.1550	0.1026	0.0905	0.9799

By comparison, the noise has a low mean amplitude. This is because the noise is fluctuating randomly around zero and the sum of these amplitudes will be close to zero. The rain clutter has a high mean amplitude, caused by high peaks in the radar receiver. The period mean of sea clutter is small, most of these return signals are sharp and spiky. The period mean of the window containing target(s) is large, which signifies that targets have a wider pulse width when compared with noise and clutters. Such statistical characterization may form the basis for a discrimination system for target detection.

2. Correlation

According to the Cauchy-Schwartz Inequality [6], the maximum value of signal to noise ratio can be obtained by choosing $h(\tau)$ proportional to $u(\tau+(\tau_d-t))$ and $h(\tau)$ is a reversed and shifted copy of $u(\tau)$. τ_d is the time delay, hence,

$$y(t)=\int_{t-\tau_d}^{\tau} u(\tau)u(\tau+\tau_d-t)d\tau$$

where $u(\tau)$ is the incoming signal

$u(\tau+\tau_d-t)$ is a copy of $u(\tau)$ shifted to a duration of $t-\tau_d$.

The product of the signal and its shifted version is integrated over the ranges for which the integral is not equal to zero. y(t) has the same shape as the autocorrelation function of u(t). As t varies, the shifted $u(t)$ will come to align with the incoming signal and then out of alignment again. When they are fully align, i.e. $t=\tau_d$, the maximum signal to noise ratio will occur and the amplitude is given by:

$$y(t)=\int_{0}^{\tau} u^2(\tau)d\tau$$

Fig. 5a shows a radar return with a target (at 18 microsecond) being contaminated by noise. Since the transmitting pulse is rectangular in shape with a pulse width of 0.05 microseconds, the return echo will be stretched. The width of the integrating pulse can be determined by trials,

and it has been found that the best result can be obtained when it is around 10 times the width of the transmitting pulse. Fig. 5b shows the result of integrating the product of a 0.4 micro second rectangular pulse by the radar return. It is obvious that the signal to noise ratio is much improved and this will facilitate the target to be detected more easily.

Due to the beam width of the radar antenna, the target will appear in more than one sweep and there exists correlation of such target between different sweeps. The degree of correlation will depend on the size and type of targets. Targets that present a large cross section to the radar will be correlated in a greater number of consecutive sweeps than smaller ones. The speed of a vessel is relatively slow when compared with the time between sweeps and can be ignored in calculating the correlation. For example, the vessel is moving at a speed of 15 knots (27.78 km/hr) and the Pulse Repetition Frequency (PRF) is 1300Hz (short/medium pulse).,i.e. one sweep takes 769.2 microsecond, then the vessel only travels 0.463 mm between sweeps. The correlation between the targets within consecutive sweeps can be determined by:-

$$C_{s_n s_{n+1}}(v) = \sum_{m=0}^{m=l} v_{s_n l_m} v_{s_{n+1} l_m}$$

where $C_{s_n s_{n+1}}(v)$ is the correlation of target points between n, and n+1 sweeps

$V_{s_n l_m}$ is the amplitude of nth sweep at time m

l is the size of the correlation window

Random noise is usually uncorrelated and thus can be removed after the correlation process. Figures 6a, 6b and 6c show three consecutive sweeps of a radar return with a time frame of 10 microseconds. The correlation of N/N+1 and N+1/N+2 are shown in figures 7a and 7b respectively. Despite the fact that most of the uncorrelated noise is removed, there is still some correlated noise apparent which may affect the target detection process. The use of a high order correlation technique [7] can provide a better capability for discrimination between clutter and noise. This is achieved by correlating the correlated results of N/N+1 and N+1/N+2 to generated a new sequence of radar signals and the result is shown fig. 8. The noise is suppressed and the targets can be discriminated from the trace easily.

3. Time Frequency Characteristics

Radar targets have distinct features in the frequency domain compared with clutter and noise. Targets appear at some specific time of the radar sweep and the corresponding changes in the immediate frequencies throughout the time sweep are of interest in the detection theory. Armstrong and Ahmed [10] have modeled the immediate frequency function for a broadband signal by considering an input of n frequency varying spectral components.

$$x(t) = \sum_{i=1}^{n} A_i \cos[\phi_i(t)]$$

By taking the square of the time derivative of the signal x(t), we have

$$[x'(t)]^2 = \sum_{i=1}^{n} \frac{1}{2} A_i^2 w_i^2(t)\{1-\cos[2\phi_i(t)]\}$$

+ other cross-multiplied terms

where $w_i(t)$ denotes the time frequency function

If a low pass filter is applied to the signal $[x'(t)]^2$, it will suppress the terms associated with $\cos[2\phi_i(t)]$ and the other cross multiplied terms.

$$[x'(t)]^2 |_{LPF} = \sum_{i=1}^{n} \frac{1}{2} A_i^2 \omega_i^2(t)$$

The low pass filter output of the square of the input is also calculated as follows:

$$[x(t)]^2 |_{LPF} = \sum_{i=1}^{n} \frac{1}{2} A_i^2$$

The immediate frequency function $\omega(t)$ can then be estimated as:-

$$[\omega(t)^2] = [x'(t)^2]/[x(t)^2] = \sum_{i=1}^{n} A_i^2 \omega_i(t) / \sum_{i=1}^{n} A_i^2$$

The normalization element provides the weights of the individual spectral components to calculate a reasonable estimate of the immediate frequency.

The detection of radar targets in the frequency domain requires the instantaneous frequency at each time slot to be estimated. A moving window of a fixed number of range cells is shifted through the entire sweep. The immediate frequency for each window is calculated using the normalization technique as described. If the window size is made too large, frequency changes for small targets may be missed. However, a window that is too small will involve additional computation time as well as producing unwanted fluctuation of the frequency function due to random noise. A window consisting of 20 samples is currently used.

The slope of the distribution of the instant frequency will also be significant in detecting targets. A large slope will imply that there is a target embedded in the high frequency noise, or that there has been an abrupt change in the frequency of the noise. To remove any sharp slopes caused by random noise, the immediate frequency is averaged over several samples so that short duration changes of slope can be filtered out. So, in addition to considering the frequency response of returned signals, the presence of target may be confirmed by examining the rate of change of the instant frequency. This can be achieved by differentiating the immediate frequency function and detecting the slope change.

The respective time frequency characteristics of the signal returned by a radar target and that of clutter are different on the return sweep. The targets have a lower frequency component and this characteristic can easily be identified and extracted in the instantaneous frequency

distribution. Figure 9a shows a radar return in which targets are embedded in a series of rain clutters. Their time frequency representation is shown in figure 9b, in which the targets are displayed with lower frequency components.

Conclusion

Various methods for the extraction of features in the time domain have been discussed. During a full rotation of the radar antenna, a variety of return characteristics may be observed. For example, when operating in coastal regions, very low clutter may be seen in the seaward sector and significant clutters due to the land sea interface and reflections may be received in other sectors. The research presented in this paper has been based on the acquisition and processing of digitized live radar signals, and has shown that targets and clutters have unique features in their statistical characterization over a finite window. These can be extracted for discrimination purposes. Radar return signals, which have been reflected by different objects, possess unique features when correlated with other waveforms. When the received signal is correlated with a square pules of similar pulse width, the signal to noise ratio is much improved. Radar pulses are transmitted at fixed time intervals and correlation of the targets between different sweeps reduces the amplitude of random noise. This is easily removed by the sweep to sweep correlation process. The use of high order correlation, which performs the correlation between correlated results of two consecutive sweeps, further suppresses the partially correlated clutters. The time frequency characteristics can also be used to achieve effective target detection. To study such characteristics, the instant frequency value of the signal at any specific time of the sweep is estimated using a normalization technique.

The statistical characterization, correlation, and time-frequency characteristics can be extracted from radar waveforms to determine if a target is present. In a very complicated environment, e.g. boundaries between the sea and land, the sea clutter may have certain similar characteristics when compared with the targets. However, it is unlikely to have similarities in all these parameters. These parameters themselves are extracted from moving windows along the radar return and can be fed into an information fusion process for making the final decision. Thus, the detection process is not based solely on the magnitude of the radar echoes and will provide a more reliable technique for discrimination in target identification and tracking algorithms.

References:

1. Bracket M (1996). CFAR detection for multiple target situations, IEE Proceedings, vol. 136, no. 5, October,

2. Kasumi, S.A. (1988). Analysis of CFAR. Processors in Nonhomogeneous background, IEEE Transactions on Aerospace and electronic Systems, vol. 24, July,

3. Wilson, S.I. (1993). Two CFAR algorithms for interfering targets and nonhomogeneous clutter, EEEE Transactions on Aerospace and Electronic Systems, vol. 29,

4. Li and Miller (1997), Target Detection in Radar: Current Status and Future Possibilities, Journal of Navigation, May

5. Pa

6. Un

7. B.J
   Tra

8. Gu
   Tec

9. H

10. Ar

5. Paul A. Lynn, Radar System, Macmillan New Electronics Series

6. Understanding Radar Systems, Simon Kingsley and Shaun Quegan, Mcgraw-hill

7. B.J. Liou, Dim Target Detection Using High Order Correlation Method, IEEE Transactions on Aerospace and Electronic Systems, Vol. 29, No.3, July, 1993.

8. Guirong, Guo, Target Detection and Recognition Based on Dynamic Processing Techniques, IEEE, 1992

9. Herbert Hirsch, Statistcal Signal Characterization, Artech House

10. Armstrong and Ahmed, Detection of Broadband Dispersive Signals, IEEE 1989

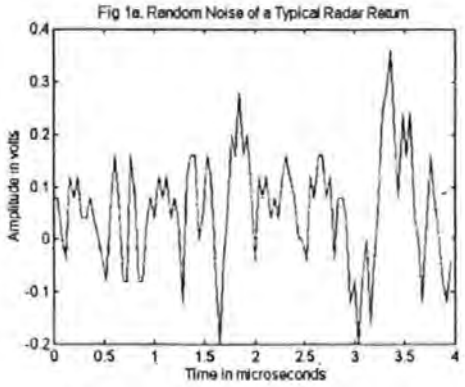
Fig 1a. Random Noise of a Typical Radar Return
Amplitude in volts
Time in microseconds

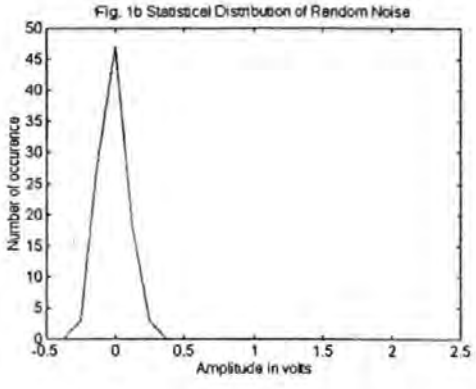
Fig. 1b Statistical Distribution of Random Noise
Number of occurance
Amplitude in volts

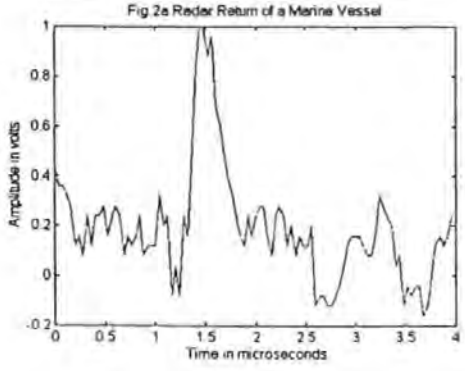
Fig 2a Radar Return of a Marine Vessel
Amplitude in volts
Time in microseconds

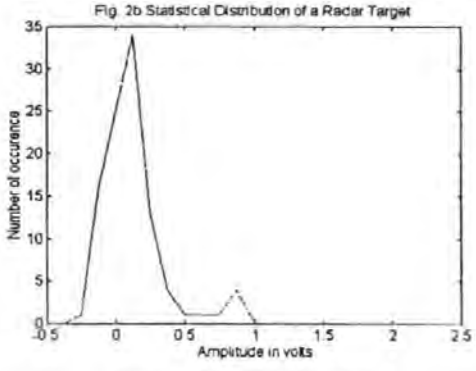
Fig. 2b Statistical Distribution of a Radar Target
Number of occurance
Amplitude in volts

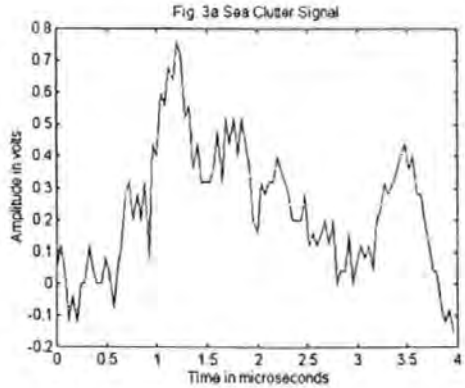
Fig. 3a Sea Clutter Signal
Amplitude in volts
Time in microseconds

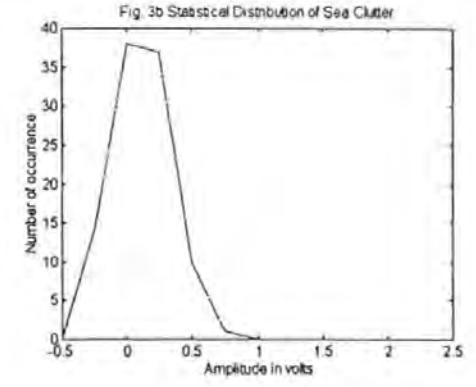
Fig. 3b Statistical Distribution of Sea Clutter
Number of occurance
Amplitude in volts

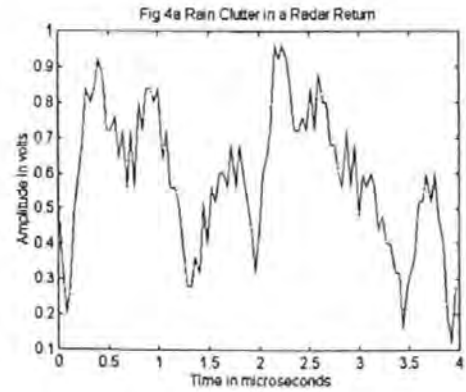
Fig 4a Rain Clutter in a Radar Return
Amplitude in volts
Time in microseconds

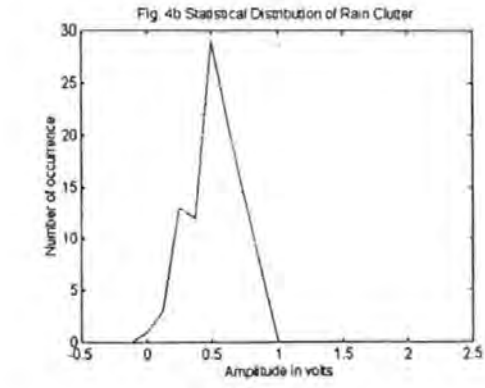
Fig. 4b Statistical Distribution of Rain Clutter
Number of occurrence
Amplitude in volts

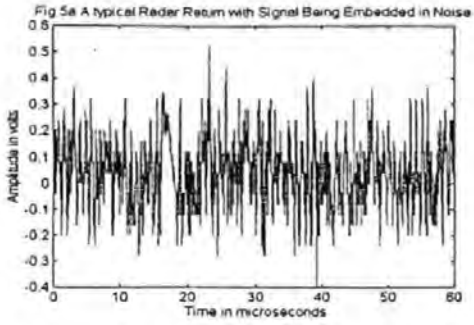
Fig 5a A typical Radar Return with Signal Being Embedded in Noise
Amplitude in volts
Time in microseconds

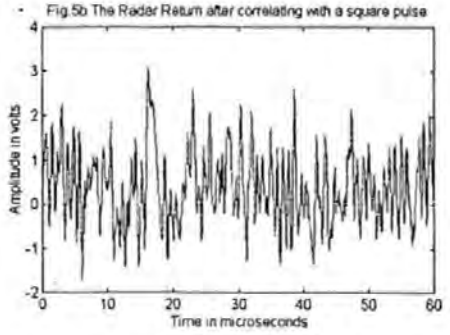
Fig 5b The Radar Return after correlating with a square pulse
Amplitude in volts
Time in microseconds

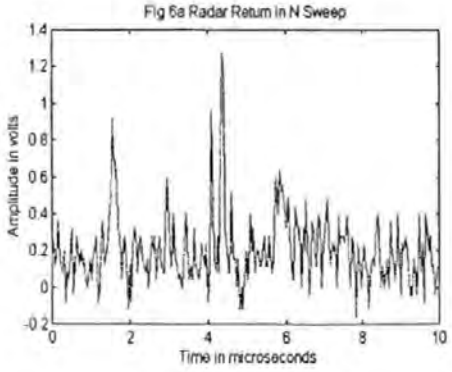
Fig 6a Radar Return in N Sweep
Amplitude in volts
Time in microseconds

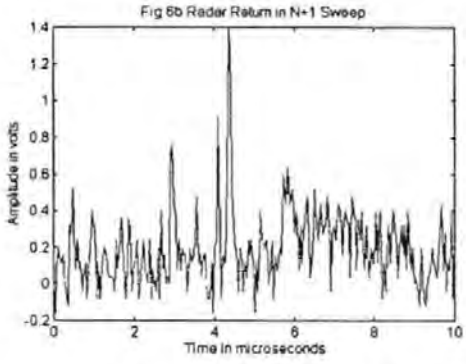
Fig 6b Radar Return in N+1 Sweep
Amplitude in volts
Time in microseconds

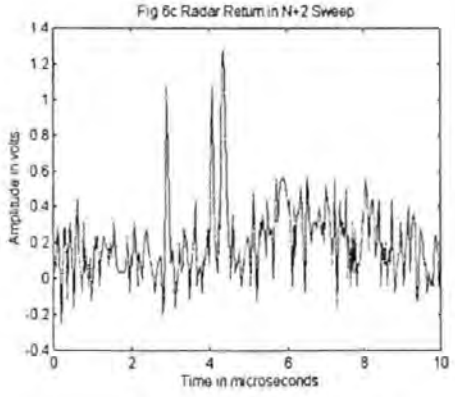
Fig 6c Radar Return in N+2 Sweep
Amplitude in volts
Time in microseconds

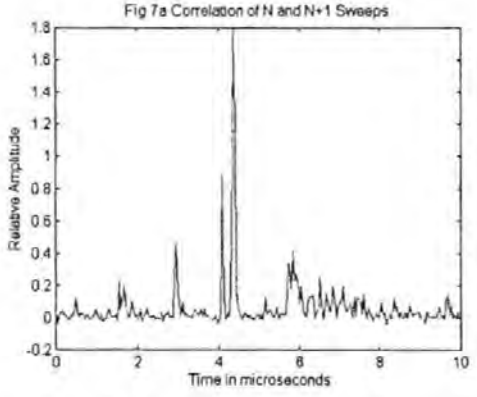
Fig 7a Correlation of N and N+1 Sweeps
Relative Amplitude
Time in microseconds

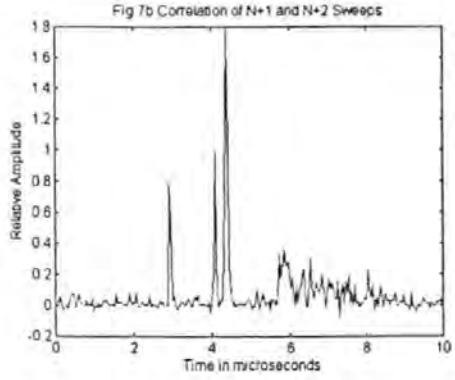
Fig 7b Correlation of N+1 and N+2 Sweeps
Relative Amplitude
Time in microseconds

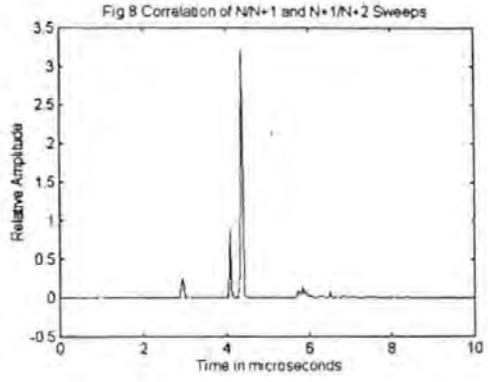
Fig 8 Correlation of N/N+1 and N+1/N+2 Sweeps
Relative Amplitude
Time in microseconds

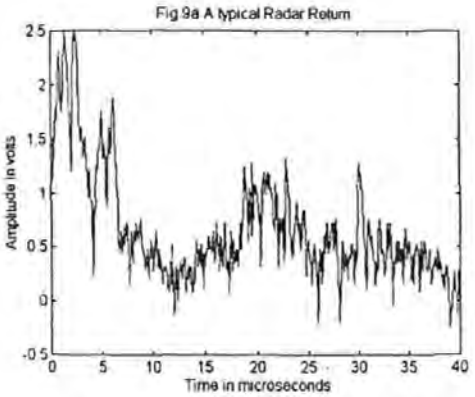

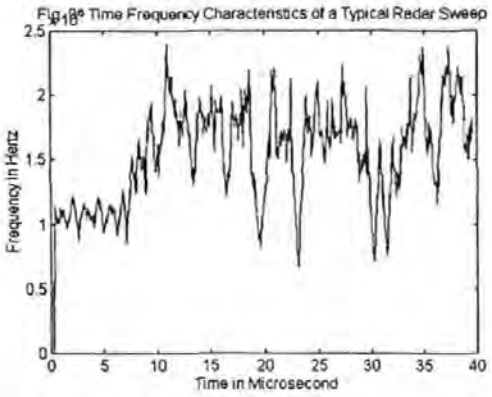

For sophist
increasing
more efficie
of time/en
when diffic

By using int
and based
consider th
for track m
idea up to v
of a single,
standard te

Key Word
Multiple Mc

1 Intr

For multiple
like the dat
detection th
While offeri
increased nu
sensor mana
Bayesian tec
radar the cu
the correct
algorithm. E
the general
well be explc

In military a
targets will n
(sudden turn